Mucus and Gut Barrier in Health and Disease

Bruno Sovran

Mucus and Gut Barrier in Health and Disease

Bruno Sovran

Thesis committee

Promotors
Prof. Dr Jerry M. Wells
Professor of Host-Microbe Interactomics
Wageningen University

Prof. Dr Paul de Vos
Professor of Immunoendocrinology
University Medical Center Groningen

Co-promotor
Dr Jan Dekker
Expert Nutrition, Department Exploration and Development
Avebe, Veendam

Other members
Prof. Dr Joost van Neerven, Wageningen University
Dr Philippe Langella, Institut National de la Recherche Agronomique, Jouy-en-Josas, France
Prof. Dr Dirk Haller, Technical University of Munich, Germany
Dr. Malin Johansson, Gothenburg University, Sweden

Mucus and Gut Barrier
in Health and Disease

Bruno Sovran

Thesis
Submitted in fulfilment of the requierement for the degree of doctor
at Wageningen University
by the authority of the Rector Magnificus
Prof. Dr A.P.J. Mol
in the presence of the
Thesis Committee appointed by the Academic Board
to be defended in public
on Friday 23 October 2015
at 4 p.m. in the Aula

A ma famille

Table of Contents

Chapter 1

General Introduction

Bruno Sovran

1.1 Overview of the mammalian gastrointestinal tract and its cellular architecture

The mammalian gastrointestinal (GI) tract consists of the stomach, small intestine and large intestine all of which have distinct anatomical features and physiological roles in the digestion and absorption of nutrients and retention of water and electrolytes. The small intestine, which includes the duodenum, jejunum, and ileum, is the major organ for the absorption of nutrients. The large intestine or colon comprises the ascending, transcending, and descending colon and functions to reabsorb water and salts from indigested food matter, and to excrete waste material from the body (Fig. 1A). The intestinal wall consists of 4 tissues layers enveloping the lumen. The inner-most layer, is the mucosa comprising of a single layer of epithelial cells and a thin layer of loose connective tissue called the lamina propria (LP) beneath the epithelium. The epithelium forms physical barrier between the intestinal lumen (topologically the outside of the body) and the inside of the body. The second layer is the *muscularis mucosae* comprising two layers of muscle (one longitudinal and one circular) that enables peristalsis to move intestinal contents through the GI tract. Surrounding this is the submucosa, a highly vascular layer of loose connective tissue, including lymph vessels and nerves. The outer tissue is a layer of loose connective tissue known as the serosa or adventitia (Fig. 1B and C). In humans, the epithelium is renewed in approximately 5 days by proliferation and differentiation of pluripotent stem cells at the base of each crypt. The epithelium of the human and rodent small intestine contains four different cell lineages; absorptive cells (enterocytes) and secretory cells (enteroendocrine, Paneth, and goblet cells), which are in direct contact with the lumen. These cell types are also present in the epithelium of the mammalian large intestine with the exception of Paneth cells. The huge surface area of the intestine (approximately 200 m^2 in humans) is exposed to (potentially) harmful substances in the lumen as well as the large number of commensal bacteria, collectively known as microbiota. The total number of bacteria inhabiting the human GI tract is around 10^{13}-10^{14}, which exceeds the number of cells in the human body by a factor 10. The concentration of intestinal bacteria progressively increases from the duodenum to the colon: from 10^2-10^3 per gram of luminal content, in the duodenum and jejunum, to 10^7-10^8 in the ileum and 10^{11}-10^{12} in the colon [1] (Fig. 1A).

This microbial ecosystem contains at least 500 to 1000 species of eukarya, archea, and bacteria [2] that vary in composition and abundance along the GI tract. In healthy adults, the intestinal microbiota is dominated by two phyla, the Bacteroidetes and the Firmicutes [3]. Other phyla that are present but less abundant are Proteobacteria, Verrucomicrobia, Tenericutes, Deferribacteres and Fusobacteria [3][4]. Despite high species diversity and differences between individuals there appears to be a common "functional core" of bacteria, which is shared among most of the human population [5][6]. The bacteria reside in the lumen, some of which are in proximity to the mucosa, and enzymatically degrade glycans and use

the breakdown products as nutrients. *Akkermansia muciniphila* is one of the few mucin-degrading bacterial species that has been cultured and characterised in detail [7].
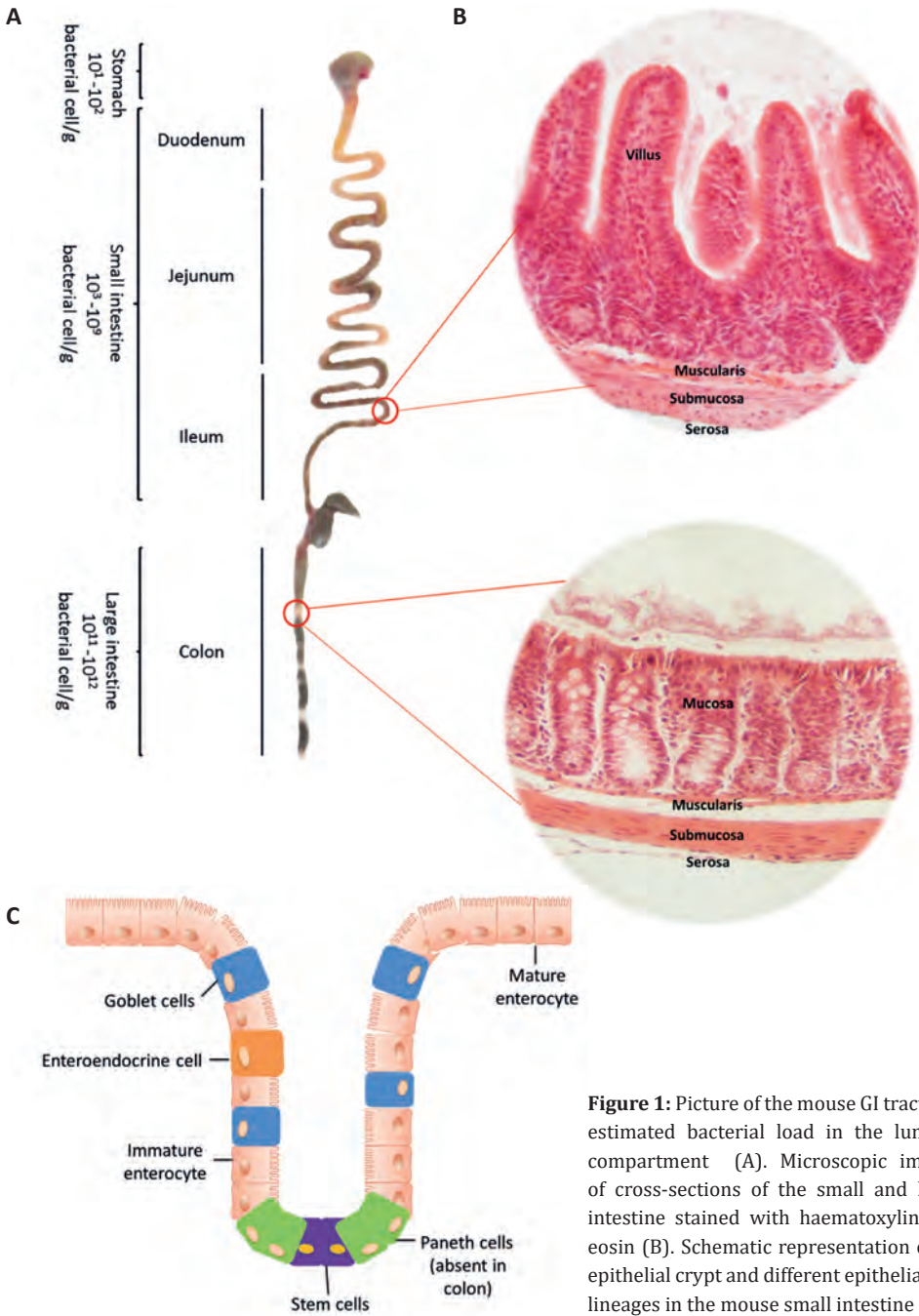

Figure 1: Picture of the mouse GI tract and estimated bacterial load in the luminal compartment (A). Microscopic images of cross-sections of the small and large intestine stained with haematoxylin and eosin (B). Schematic representation of an epithelial crypt and different epithelial cell lineages in the mouse small intestine (C).

The intestinal microbiota is often referred to as a metabolic 'organ' due to its role in harvesting energy for the host from the fermentation complex carbohydrates that cannot otherwise be digested. It is also recognized that the microbiota plays an important role in shaping aspects of host physiology and immune function [8] [9]. Although the microbiota is an important part of our lives, it also brings certain risks and may harbour opportunistic pathogens. When micro-organisms penetrate our tissues, serious diseases, like chronic inflammation, and even death by sepsis, might follow. To avoid this several mechanical, physical, chemical, and immunological mechanisms have evolved to help maintain intestinal homeostasis and the symbiotic relationship between host and microbiota [10].

1.2 The gut barrier principle

The gut barrier principle can be defined as the collective mechanisms that allow physiological process of digestion and uptake of nutrients to occur, while preventing bacterial colonization of tissues, entry of potentially inflammatory or of harmful antigens and bacteria into tissues. The gut barrier consists of multi-layered defences (Fig. 2). The first layer of defence comprises all the physical barriers and the different tissue layers of the intestine (including tight junctions (TJ)), which separate the systemic compartment from the outside (described above). This includes the epithelial cell barrier, which is reinforced by the mucus layer and a range of antimicrobial peptides, and proteins that prevent intimate contact with the commensal and pathogenic bacteria.

Paneth cells in the small intestinal epithelium secrete a diverse range of peptides and proteins with antimicrobial properties, referred to as antimicrobial peptides (AMPs). A major group of these AMPs in mammals are defensins, which are highly basic, small antimicrobial peptides of 2-6 kDa with a β-sheet structure and six cysteine residues, which are disulphide linked [11] [12]. Defensins show antimicrobial activity against Gram-positive and Gram-negative bacteria, certain fungi, protozoa and enveloped viruses [13] [14]. There are 3 subgroups of defensins: α-defensins, β-defensins and θ-defensins, based on structural features of the gene, such as the connectivity of three cysteine linkages, precursor and mature peptides [15] [16]. Humans produce 2 known Paneth cell α-defensins, HD5 and HD6 as well as 6 β-defensins (HBD), produced by epithelial cells in the intestine. Human β-defensin-1 is constitutively expressed in enterocytes, whereas the expression of human β-defensin-2 (HBD2) and human β-defensin-3 (HBD-3) are induced by microbial products and inflammatory cytokines [17]. Inducible expression of HBD-2 in enterocytes has been shown to be dependent on Toll-like receptor (TLR) or MyD88-dependent signalling [22] [23]. The bactericidal activity of defensins is obtained through interaction with the bacterial membrane. Initially the defensins are attracted to the membrane by electrostatic interactions, and through their amphipathic properties

they associate and displace lipids to cause pores in the membrane . This is called the "carpet wormhole" mechanism and eventually leads to the loss of membrane integrity and cell death [13] [15] [14].

Other antimicrobial factors produced by Paneth cells include lysozyme, secretory phospholipase A2, angiogenin-4, and hepatocarcinoma-intestine-pancreas/pancreatic-associated protein (HIP/HAP) [11] [12]. The latter, the orthologue of Reg3γ (Regenerating gene 3 gamma) in mice, belongs to the C-type lectin superfamily based on cDNA sequence homologies [24] [25], and shows inducible expression in the pancreas and intestine [26]. Reg proteins, more specifically Reg3 proteins, have shown great relevance in homeostasis and disease, both in humans and animal models [27].

Non-specific secretory immunoglobulin A (sIgA) is also produced by activated B cells and is transcytosed across epithelial enterocytes into the lumen via the polymeric IgA transporter. Secretory IgA limits bacterial association and penetration with the intestinal epithelial cells by causing agglutination of bacteria in the intestinal lumen [28-29]. Secretory IgA can also interfere with assembly of intracellular viruses in the Golgi apparatus during transcytosis and remove potential inflammatory antigen complexes from the lamina propria by binding during transport via the polymeric IgG receptor. Humans secrete several grams per day of sIgA into the intestinal lumen highlighting its importance to mucosal protection [30].
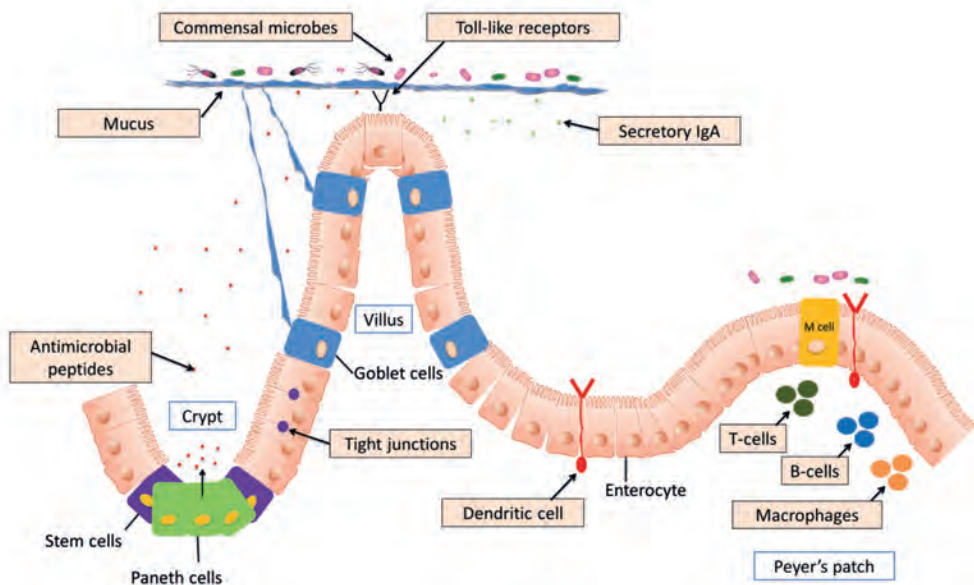

Figure 2: Schematic representation of the gut barrier principle in the small intestine.

The second layer of gut defence is composed mainly of innate myeloid and lymphoid cells and includes the gut-associated lymphoid tissue (GALT). Along the intestine, specialized lymphoid structures, including Peyer's patches (PPs) and isolated lymphoid follicles permit the sampling of luminal antigens via specialized M cells in the follicular epithelium [31]. Dentritic cells (DCs) play a key role in the induction of tolerance and immunity. Different subsets of DCs reside in PPs and in the lamina propria (LP) where they can sample luminal antigens by extending dendrites through the epithelial tight junctions into the intestinal lumen [32]. Epithelial and immune cells such as DCs in the LP recognize microbes through common structures on microorganisms often referred to as pathogen-associated molecular patterns (PAMPs) or microbe-associated molecular patterns (MAMPs) via pathogen recognition receptors (PRRs). The best-characterized family of PRRs is the Toll-like receptor (TLR) family, which are expressed on cells of the myeloid and lymphoid lineages as well as on non-immune cells such as enterocytes and fibroblasts. Innate recognition of microbes and MAMPs by host PRRs plays a pivotal role in the maintenance of intestinal homeostasis. These families of receptors are involved in immune cell activation, production of cytokines and chemokines as well as regulation of production of components of the gut barrier such as antimicrobials, mucins, and TJ proteins [33].

1.3 Homeostasis of the intestinal barrier

The intestinal barrier is essential for maintaining intestinal homeostasis and health and impairment increases the risk of development of inflammatory and other gut diseases.

Mucosal inflammation may be a key driver for the abnormal composition and decreased complexity and richness of the microbiota that are common features in inflammatory bowel diseases (IBD) patients and mouse models of colitis [34] [35] [36]. Many studies have described changes in the microbiota of IBD patients, the majority of which have been in Crohn's disease (CD) cases. Collectively, these studies have shown that in both CD and ulcerative colitis (UC) there is a lower proportion of Firmicutes, an increase in Gamma-proteobacteria including the Enterobacteriaceae, and an overall decrease in biodiversity. In CD patients the *Clostridia* are altered due to decreased abundance of the *Roseburia* and *Faecalibacterium* genera of the *Lachnospiracae* and *Ruminococcaceae* families, an exception being *Ruminococcus gnavus,* which increases in abundance [37] [38] [39]. The inflammatory processes in the intestine may enable the Enterobacteriaceae to gain an advantage over other commensals as they can use products of the host inflammation such as tetrathionate and nitrate as electron acceptors for anaerobic respiration and growth [40] [41] [42]. *E. coli* symbionts exhibiting pathogen-like behaviours such as adhesion and invasiveness (AIEC) are more frequently cultured from IBD patients [43].

The inherent property of the gut to act as a semipermeable barrier is crucial for the maintenance of health. As an example of failing barrier function, between 12% and 50% of patients with irritable bowel syndrome (IBS) have been reported to have altered intestinal permeability in research studies [44], using various methods to reflect gut permeability at different parts of the gastrointestinal tract [45][46], and both post infectious IBS as well as non-selected groups of patients with IBS have been investigated. An acute bacterial infection results in a transient increase in intestinal permeability [47][48]. This phenomenon seems to be highly persistent in patients who develop post infectious IBS [48][49], but altered intestinal permeability does not seem to be confined to post infectious IBS alone, as the different subtypes of IBS all seem to have a proportion of patients with increased gut permeability [50].

The mechanisms underlying increased permeability in IBS have not been fully established, but the impaired expression of epithelial tight junctions and adherence-junction-associated proteins is probably involved. For example, studies demonstrating low expression of the tight junction protein zonula occludens 1 junctional adhesion molecule A (JAMA) and E cadherin in IBS imply a dysfunctional mucosal epithelium in these individuals [51][52]. However, whether the alteration in permeability precedes onset of IBS, maybe as a result of luminal or host factors, or whether it merely reflects alterations associated with the disorder is unknown.

Celiac disease constitutes a unique model of auto immunity; in contrast to most other autoimmune diseases, a close genetic association with HLA genes, a highly specific humoral auto immune response against tissue transglutaminase. Early in the development of celiac disease, tight juctions (TJs) are opened [53][54] and severe intestinal damage ensues [54]. The up-regulation of the zonulin innate immunity pathway is directly induced by exposure to the disease's antigenic trigger, gliadin [55]. Gliadin has been shown to also be a potent stimulus for macrophage proinflammatory gene expression and for cytokine release [56].

1.4 Mucus is a key component of the intestinal barrier

1.4.1 Structure and function

Intestinal mucus is the term given to the translucent gel-like substance forming a lubricant and physical barrier between the lumen content and the epithelium. Mucus is formed by the N- and C-terminal polymerization of MUC2, a large mucin polypeptide (around 500 kDa) that is highly O-glycosylated in the Golgi apparatus [57][58]. The proline, threonine, serine-dominated (PTS) domains of Muc2 are covalently modified with GalNAc (N-acetylgalactosamine) and further extended and branched by a series of other glycosyltransferases [59][60], resulting in a voluminous and brush-like structure of complex glycans [61][62]. Substantial, co-translationally added N-glycosylation helps to structure the N-

and *C*-terminus of the polypeptide. The polymerization of MUC2 occurs after glycosylation to form the large net-like polymers secreted by epithelial goblet cells (Fig. 3).
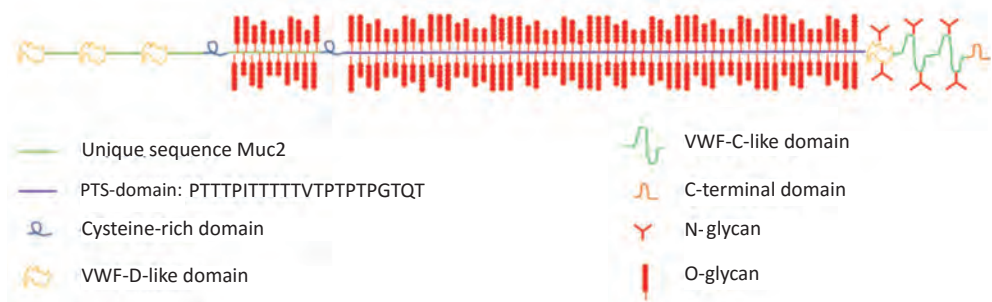
1

——	Unique sequence Muc2	⎍	VWF-C-like domain
——	PTS-domain: PTTTPITTTTTVTPTPTPGTQT	⎍	C-terminal domain
℧	Cysteine-rich domain	Y	N-glycan
⌘	VWF-D-like domain	▮	O-glycan

Figure 3: Schematic representation of a MUC2 molecule re-drawn from Dekker *et al.* 2002 [63].

When mucus is released from the goblet cells, it attracts and binds water; forming a gel [64]. Approximately 95% of the weight of this gel comprises of water [65]. The colonic mucus forms 2 layers, a dense inner layer closest to the epithelium, and a loose outer layer. The inner layer contains few if at all bacteria compared to the loose outer layer of mucus [64] [66]. The conversion of mucus from the dense to the loose structure is based on limited proteolytic action of host enzymes, possibly complemented by microbial enzymatic activity [64]. The molecular details of this process remain unknown, but it also occurs in the absence of microbiota in germ-free mice. Proteolytic cleavage of the cysteine-rich region of MUC2 is considered to be the most likely explanation for conversion of dense mucus to loose mucus [66].

In the small intestine (SI), the mucus layer is thinner, and consists of only one layer, which similar in properties and components to the outer layer found in the colon. However, the SI mucus layer becomes thicker and more visible towards the end of the small intestine [67].

The viscous mucus, also contains sIgA, AMPs, including defensins, C-type lectins (such as Reg3 proteins), cathelicidins [68] and lipocalins to reinforce its protective function against microbes. The AMPs are secreted by Paneth cells and/or other intestinal epithelial cells as part of the innate immune system [10]. Some are produced constitutively, while others are induced by cytokines or activation of innate pattern recognition receptors such as the TLRs by MAMPs [69]. Studies have shown that these antimicrobial peptides are essential for maintaining an efficient small intestinal mucus layer. Loonen *et al.* described that Reg3γ-deficient mice have altered mucus distribution and increased mucosal inflammatory responses to the microbiota and enteric pathogens in the ileum [70]. Moreover, Reg3β plays a protective role against intestinal translocation of the Gram-negative bacterium *S. enteritidis* in mice [71] [72].

Another important component of the gut barrier is the epithelial glycocalyx comprising of several non-secreted transmembrane mucins including MUC1, MUC3, MUC4, MUC13, and MUC17. These membrane-tethered mucins extend at least 100 nm from the enterocytes into the lumen and associate with the extracellular mucus, especially in the colon and stomach [73]. The membrane-tethered mucins contain an extensively *O*-glycosylated extracellular domain [74], forming known ligands for specific microbial adhesins [75] [76]. The membrane-associated mucins are normally shed and replaced, but this process can be sped up upon bacterial adhesion, helping to protect the epithelium from microbial invasion. Apart from their barrier function against potential pathogens, specific membrane- tethered mucins have also been shown to modulate responses to inflammatory cytokines [74].

1.4.2 Mucus morphology within the GI tract

1.4.2.1 Small intestine

In the SI mucus forms a thin layer covering the epithelial surface from the bottom of the crypt to the villus tips to facilitate nutrient-uptake while limiting contact with microrganisms and particulate matter [1] [77]. The protection of the crypts and the epithelial stem cells at the crypt base is most important, as they are essential for the renewal of the tissue. Protection of stems cells is largely mediated by mucus production by goblet cells and secretion of antimicrobial peptides by Paneth cells. Antimicrobial products secreted from the epithelial cells diffuse into the mucus thereby inhibiting growth and colonization of the mucus layer with microorganisms (Fig. 4) [22]. The transit time through the SI is shorter than the colon which is also considered an important mechanism to minimize exposure of the epithelial cells to potential threats [78].

Along the GI tract, specialized structures called mucosal lymphoid follicles facilitate the interaction between luminal antigens including microorganisms, epithelial cells, and cells of the immune system [79]. There are both isolated and aggregated lymphoid follicles in the gut. Lymphoid follicles consist of a B cell germinal centre, a marginal zone, where B cells and macrophages reside, and the sub-epithelial dome, where can be found T cells, B cells, macrophages, and dendritic cells. Large aggregates of lymphoid follicles form structures known as PPs, the inductive sites of mucosal immune responses [80]. The domes of PPs are covered by a single layer of epithelial cells, the follicle-associated epithelium (FAE), consisting of enterocyte-like cells and membranous cells commonly called M cells [81] [82]. The M cells have a specific role in transepithelial transport, more specifically the ability to transcytose soluble molecules as well as adherent antigens and particles such as bacteria from the apical membrane to basolateral membrane, where they are released in the sub-epithelial dome of the patch to encounter antigen presenting cells [83] [84] [85].

There has been some controversy in the literature concerning the number of goblet cells on the domes and whether the PPs are covered by a mucus layer [86] [87] [74] [88]. Recently Ermund *et al.,* proposed that PPs of mice are covered by a mucus layer based on mucus production by ileal tissue mounted in a horizontal Ussing-type chamber [89]. However such a set up does not exclude the possibility that the mucus flows over the dome from neighbouring epithelium. Around 5% of epithelial cells in the FAE of ileum tissue sections from mice were identified as mucin producing goblet cells using Periodic Acid Schiff (PAS)/Alcian blue staining but their distribution over the entire dome FAE was not discussed. Thus it remains a possibility that the dome is not completely covered by mucus *in vivo*.
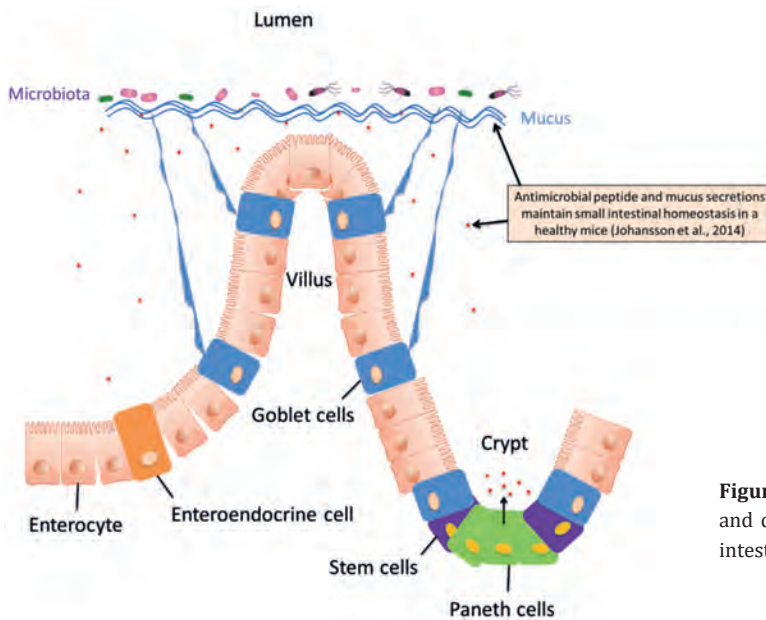
Figure 4: Mucus morphology and distribution in the small intestine.

1.4.2.2 Large intestine

In the colon, water is absorbed, together with salts and short chain fatty acids (SCFAs), increasing the hardness of the undigested matter, thereby creating mechanical stress on the epithelium. In this respect mucus acts as a lubricant and protective sheet by covering the epithelium [1] [77]. The majority of our gut microbiota reside in the colon and provide a number of functions beneficial to the host, such as recovering energy from digestion of complex carbohydrates and mucus, and providing us with several vitamins [4].

The large bacterial population in the colon has potential to trigger chronic inflammatory immune response as demonstrated in IBD. However, direct exposure of the epithelium to luminal bacteria is avoided through a mucus barrier composed of a dense inner layer and loose outer layer [66] [90] [91] (Fig. 5).

The colon is covered by a stratified inner mucus layer restricting bacteria to reach the epithelium. The bacteria reside in the outer mucus (Johansson et al., 2014).

Figure 5: Mucus morphology and distribution in the large intestine.
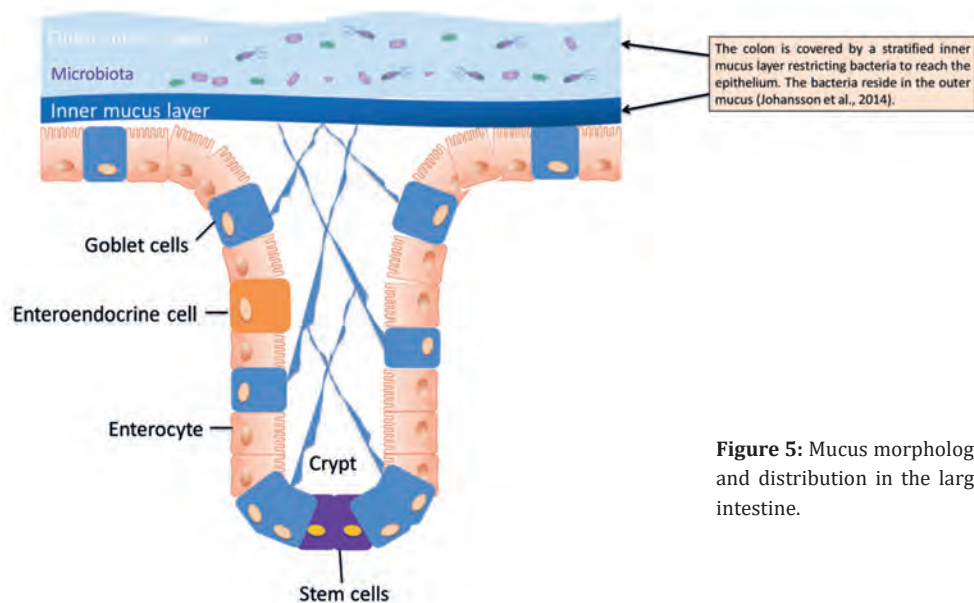
1.4.3 Role of goblet cells and mucins in signalling and immunomodulation

Glycans of MUC2 were recently shown to confer tolerogenic properties to LP DCs through interaction with a galectin 3-dectin 1 receptor complex [92]. Muc2 also enhances epithelial expression of B cell cytokines and trypsin-like serine protease, promoting development of tolerogenic DCs and anti-inflammatory mechanisms contributing to gut homeostasis, possibly through the same receptor-complex [92].

MUC1 is the most extensively studied membrane-associated mucin and is the most ubiquitously expressed across all mucosal epithelia. MUC1 has been estimated to be 200 – 500 nm in length (depending on the number of tandem repeats), suggesting it will tower above other molecules attached to the plasma membrane [93]. MUC1 is composed of an external domain, a transmembrane domain and a cytoplasmic tail. The cytoplasmic tail appears to interact with the cytoskeleton and secondary signalling molecules [94]. Importantly, there is also evidence that interaction with bacteria can induce phosphorylation of MUC1 *in vitro* [98]. Signalling by the cytoplasmic domains of cell-surface mucins is complex and much remains to be elucidated about their mode of action. However, the evidence to date suggests that these domains are involved in cellular programs regulating growth and apoptosis in mucosal cells perhaps in response to microbes and / or their toxins.

1.4.4 Mucus dysfunction and pathophysiology

There are two main forms of IBD, UC, which is restricted to the colon and CD, which can affect the entire GI tract [99]. These two types of IBD also differ in goblet cell and secreted mucus phenotypes. In CD, there is typically an increase in goblet cells and a thicker mucus layer [100] [101], whereas in UC there is a reduction in goblet cells, MUC2 production and sulphation, mucus secretion and [102] [103] [104] an accumulation of the MUC2 precursor [104]. Although it remains unclear whether changes in mucus are causative or secondary to inflammation [105], the lack of these changes in CD indicate they are not a universal consequence of intestinal inflammation. Reduced mucus synthesis and secretion [102], and altered *O*-glycosylation [106] [107] [108] contribute to the penetration of mucus barrier by bacteria [109], and are suggested to be involved in other gut pathologies.

In murine colitis models such as *IL-10*^{-/-}, *TLR5*^{-/-}, and *Agr2*^{-/-} the development of pathology was associated with a shrinkage (or even absence) of the mucus layer, indicative of a compromised barrier function [110] [111]. Additionally the mucus in different mouse colitis models has been shown to be more penetrable to fluorescent beads and bacteria than in healthy mice [66] [110] [112]. The reasons for these changes in mucus thickness and permeability are not fully understood, but may result from the structural changes in the glycoprotein core and/or the sulphation and sialylation of mucins oligosaccharide residues, as reported in IBD patients [113]. Indeed, studies performed on mice conditionally lacking core-1-derived *O*-glycans such as C1galt1 (C1galt1^{-/-} mice) showed a severely impaired establishment of the mucus layer in the colon [114]. The impaired mucus barrier was characterized by dramatic thinning of the inner mucus layer and breaches in its structure compared to wild-type mice. Loss of core 1-derived O-glycans also led to a rapid induction of severe spontaneous colitis by two weeks after birth [115]. However, Sommer *et al.* found that TM-IEC C1galt^{-/-} mice lacked any sign of colon inflammation, but were more susceptible to experimentally induced Dextran Sulfate Sodium (DSS) colitis [116]. In contrast Fu *et al.* found that ten days after induced loss of core 1-derived *O*-glycans the TM-IEC C1galt^{-/-} mice spontaneously developed intestinal inflammation. As these mice were housed in a different animal facility, colitis development might be dependent on the microbiota [114]. Moreover, aberrant mucin assembly due to endoplasmic reticulum stress in goblet cells and activation of the unfolded protein response may be an important component of some types of chronic inflammation including diseases like IBD [117].
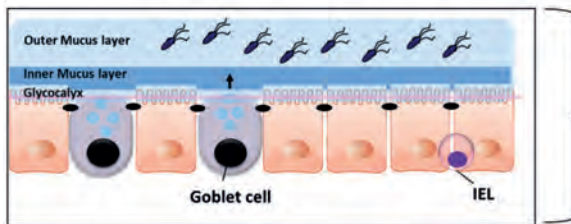
1.5 The Muc2 knockout mouse model as a tool to study the role of mucus in the intestine

To evaluate the importance of secreted mucus in the intestine, Velcich *et al.* generated a mouse which does not express MUC2, the glycosylated protein component of the most abundant secreted gastrointestinal mucin [118] [119] [120]. *Muc2* knockout mice (*Muc2-/-*) were generated by substituting a genomic fragment spanning exons 2 to 4 of Muc2 with a phosphoglycerate kinase-neomycin (PGK-Neo) cassette [118]. Staining of intestinal tissue sections from *Muc2-/-* mice with Alcian blue (staining of acidic mucins) showed absence of morphologically recognizable goblet cells along the entire length of the intestine of *Muc2-/-* mice [118]. *Muc2-/-* mice developed GI tumours by 6 months which spontaneously progressed to invasive carcinoma [118].

Van der Sluis *et al.*, showed that Muc2-deficient mice develop spontaneous colitis after weaning, suggesting that Muc2 mucin is crucial for colonic protection [121]. Colitis was characterised by mucosal thickening, increased proliferation, and superficial erosions, which become more severe with age. Later, Johansson *et al.*, described that in *Muc2-/-* mice the bacteria are in close contact with the colonic epithelium and enter into the crypts and epithelial cells [66].

Micro-array analysis of gene expression in *Muc2-/-* and wild type (WT) mice around weaning time (week 3), showed that Muc2-deficiency altered genes involved in inflammatory response and was associated with decreased epithelial functions (TJ expression) and increased epithelial proliferation (cell growth expression) (Fig. 6) [122].
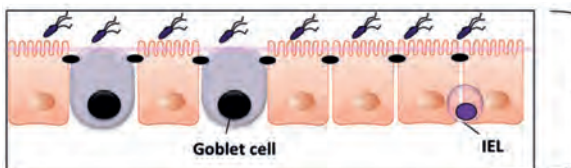

Figure 6: Schematic figure of WT and *Muc2-/-* mice, summarising the key findings from studies using the *Muc2* knockout mouse model. Prior to this thesis only the effects of mucus deficiency in the colon were investigated. IEL: intraepithelial lymphocyte.

1.6 Models to study mucus morphology and properties

The nature of the mucus gel layers covering the gastrointestinal tract makes it difficult to study outside its natural position attached to the mucosa. The past decade, several techniques (*in vitro* and *ex vivo*) were developed to study the mucus morphology and properties, while minimising alteration of its structure.

1.6.1 In vitro techniques

Histological and cell culture techniques have been developed to study mucus morphology and properties. Johansson *et al.* published a protocol in 2012 for staining both secreted mucus and luminal microbiota on Carnoy's-fixed tissue sections, by combining the use of immunohistochemistry and fluorescent *in situ* hybridization (FISH) [123]. The use of Carnoy's solution (60% water-free methanol, 30% chloroform, 10% glacial acetic acid) and the presence of an *in situ* faecal pellet in the lumen were essential for preserving the colonic mucus layers. This *in vitro* technique is useful to localize bacteria in the lumen and visualize the morphology and the quality of the mucus barrier. However, the use of water-free fixatives such as Carnoy's solution may alter mucus structure and properties and induce some shrinkage of the mucus layer.

Cell culture models have been developed to resemble the mucus-covered epithelium. For example, Navabi *et al.*, showed that some gastrointestinal cell lines produce an adherent mucus layer when cultured as polarised monolayers in semi-wet interfaces with mechanical stimulation [124]. In fact, a semi-wet interface culture in combination with mechanical stimulation and presence of DAPT (3,5-Difluorophenacetyl)-L-alanyl]-S-phenylglycine t-butyl ester), a γ secretase inhibitor, caused HT29 MTX-P8, HT29 MTX-E12, and LS513 cells to polarize, form functional TJs, a three-dimensional architecture resembling colonic crypts, and produce an adherent mucus layer. The limitations of this model are that it does not include all the epithelial cells normally present in the intestine, e.g., stem cells and Paneth cells and the secreted mucin produced is not MUC2 but stomach-type mucins such as MUC5AC and MUC6 [125]. Furthermore, these cell lines were all derived from carcinomas and have many well-recognized limitations including prolonged time to attain mature monolayers aneuploidy, and the presence of numerous undefined DNA mutations.

Multiple tissue culture systems have been described [126] [127], but only recently long-term culture systems became available that maintain basic crypt physiology. Two different protocols were published that allow long-term expansion of murine small intestinal epithelium. Ootani *et al.* showed long-term growth of small fragments containing epithelial as well as stromal elements in a growth factor–independent fashion [128]. Sato *et al.* designed a culture system for single intestinal stem cells by combining previously defined insights in the growth requirements of intestinal epithelium [129]. Based on these

insights, Sato *et al.* have established culture systems that allow the outgrowth of single mouse or human intestinal stem cells into continuously-expanding mini-gut 'organoids', which contain all the functional cells of the gut (stem cells, Paneth cells, enterocytes, and goblet cells) [129]. These organoids grow as 3D irregular-shaped closed structures of polarized cells and secrete mucus into the lumen. Although substances can be injected into individual organoids it is not convenient or easy system to study mucus properties and the interactions between mucus and commensals. Moreover, injecting substances into the lumen of the organoids or spheroids is laborious and has practical limitations for assays.

However, the production of 2D monolayers derived from the 3D organoids would help in getting a monolayer of fully developed intestinal epithelial cells with a mucus-layer on top, and therefore solve the issues mentioned above [130] [130]. Such a model would be of great interest to study *in vitro* interactions of pathogens or commensals with mucus and epithelium.

1.6.2 *In vivo* and *ex vivo* techniques

A technique for intra-vital microscopy studies of the mucus gel layer from the stomach to the colon in anesthetized rats and mice have been reported [131]. Mucus thickness and accumulation rate in each segment of the gastrointestinal tract is measured with a micropipette technique under observation through a stereomicroscope. In this way, the nature of the mucus gel *in vivo* is readily studied, and effects of interventions or disease on the mucus can be determined in longitudinal studies or by comparing animals. Using this technique, Holm and Phillipson have been able to demonstrate that there are two forms of mucus gel adherent to the stomach and colon mucosa: one layer which is removable by suction and an underlying firm adherent gel layer, whereas in the small intestine, all mucus adhering to the mucosa can easily be removed [131].

An *ex vivo* tissue explant culture method has been developed to be able to analyse human mucus secretion in an experimental system [132]. This method utilises, colon biopsies or tissues mounted in a horizontal perfusion chamber with the apical surface facing upward. The secreted mucus thickness is microscopically visualized by sprinkling of powdered charcoal on top of the layer. The viability of the explants is monitored by recording potential difference across the mucosal layer and typically measurements of mucus thickness or permeability can be performed for up to 2 hours after mounting. This allows for measurements of the mucus thickness and functionality (e.g., with fluorescent beads), as well as manipulation with pharmacological and other reagents. However, these techniques are too labour intensive to perform on multiple experimental animals in intervention or challenge studies.

1.7 Ageing and the intestinal barrier

Ageing is defined as "the regression of physiological function accompanied by the development of age" [133]. It is an ill-defined process involving changes in various body systems, which progressively convert a mature, healthy person into an increasingly infirm one. With the passage of time, individuals show a lower degree of adaptation with consequent increase in mortality, due to increased incidence of cancer and infectious disease [134] [135], as well as a decline of mental health, wellbeing, and cognitive abilities [136] [137]. Ageing is characterized by a progressive impairment of multiple metabolic processes and physiological functions of most body systems including the systemic immune system, heart, brain, and skeletal muscles [138].

Ageing process is due to cellular aging processes described by Hayflick and Moorhead in 1961 [139]. It was shown that human cells in culture do not divide indefinitely but reach a limit (called the Hayflick limit) of replication. Cells approach this limit by slowing their divisions and entering cellular senescence, a dormant stage. Recently, for damaged cells, this pathway of cellular progression has been considered an alternative to apoptosis (cell suicide). Both DNA damage and insufficient telomere replication are common signals leading to these events. When the cell does not trigger either of these pathways, it can become cancerous [140] [141].

Aging significantly increases the vulnerability to GI disorders with approximately 40% of geriatric patients reporting at least one GI complaint during routine physical examination [142]. Despite the need to further understand age-associated factors that increase the susceptibility to GI dysfunction, there is a paucity of studies investigating the key factors in aging that affect the GI tract. To date studies in rodents have demonstrated that aging alters intestinal smooth muscle contractility [143], as well as the neural innervations of the GI tract musculature [144]. Several studies in rodents have also reported an increase in intestinal permeability to macromolecules with age [145] [146]. Specifically, advancing age was shown to correlate with an enhanced transepithelial permeability of D-mannitol, indicating that there may be an age-associated decline in barrier function [147].

With a global impact on the physiology of the GI tract, the ageing process can seriously affect the composition of the human gut microbiota. The decreased intestinal motility results in a slower intestinal transit that affects defecation and leads to constipation [148]. Immune functions are also known to deteriorate with age in several species. In humans, the elderly are at a higher risk for infections, especially severe infections, as well as for certain autoimmune diseases and cancer, and their immune responses to vaccination are diminished [149]. It has been accepted that aged humans exhibit a loss of naive T cells and a more restricted T cell repertoire [150]. Furthermore, aging results in decreased human CD8+ cytotoxic T lymphocyte responses, restricted B cell clonal diversity, failure to produce

high-affinity antibodies, and an increase in memory T cells [151] [152]. It has been suggested that although certain DC populations are fully functional in ageing [153] [154], both foreign and self-antigens induce enhanced proinflammatory cytokines [155] [155]. This enhancement of inflammation can be detrimental. However, very old individuals with a more balanced pro- and anti-inflammatory phenotype may be the most fortunate [156] [157]. The association of inflammation in ageing has been termed 'inflammageing' [158].

Human microbiome analyses have revealed significant changes in the intestinal micobiota specifically with an increase of Bacteroides ssp in the elderly (<65 years) [159] [160]. However, others have shown that the change in the microbiota was seen only in centenarians with increased inflammatory cytokine responses, but not in the elderly (average age 70 ± 3 years) [161]. In centenarians, the microbiota differs significantly from the adult-like pattern, by having a low diversity in terms of species composition. Bacteroidetes and Firmicutes still dominate the gut microbiota of extremely old people (representing over 93% of the total bacteria). However, in comparison to younger adults, specific changes in the relative proportion of Firmicutes subgroups were observed, with a decrease in the contributing Clostridium cluster XIVa, an increase in Bacilli, and a rearrangement of the Clostridium cluster IV composition [161]. Moreover, the gut microbiota of centenarians is enriched in Proteobacteria, a group containing "pathobionts", shown to cause harm in a compromised or susceptible host [162] [163].

The intestinal barrier function is compromised by aging, causing an increased susceptibility to infection in elderly individuals [164]. The decline in barrier function is a combination of (1) a decline in the amount of antimicrobial peptides due to a decrease in number and secretory function of the Paneth cells [165], (2) a decline in the IgA mediated mucosal immunity [166], and (3) increased permeability of epithelial tight junctions due to an increased concentration of IL-1β and other pro-inflammatory cytokines in the ageing gut [167]. These studies suggest that the integrity of the gut epithelium (innate and adaptive immunity, TJs etc.) can be strongly compromised in the process of ageing. As the first-line of defence of the gut, it is interesting to look into the effects of ageing on the mucus layer and how this relates to other processes of ageing. Previous research has shown that in healthy subjects there is no correlation between age and the thickness of the mucus layer of the stomach and duodenum [168]. To date nothing has been published on the effects of aging on the mucus layer of the epithelium of the small intestine and colon.

Studying the effects of ageing in mouse is quite time-consuming due to the time needed to get old mice with a defined microbiota (18 to 24 months). To solve this problem, a fast aging Ercc1$^{-/\Delta7}$ hypomorphic mouse model has been described by Dollé *et al.* [169]. This fast-ageing mouse is a hemizygote, carrying one mutated allele *Ercc1* lacking seven amino acids. As Ercc1 encodes a DNA endonuclease, which is essential for DNA repair, mechanisms, *Ercc1*$^{-/\Delta7}$ mice accumulate DNA damage at a faster rate than normal mice.

1

The fast-aging *Ercc1*$^{-/\Delta7}$ mice have a significantly reduced median life span of 19/21 weeks for males/females, respectively (compared to 111/119 weeks for WT). Moreover, multiple signs and symptoms of aging were found to occur at an accelerated rate in the *Ercc1*$^{-/\Delta7}$ mice as compared to WT controls, including a decline in weight of whole body and various organs, numerous histopathological lesions, and immune parameters [169]. However, it is not known whether the intestinal barrier of fast-ageing mouse resembles a naturally aged mouse, and how this might affect microbiota composition.

1.8 Sexual dimorphism and the intestinal barrier

During the initial phase of embryonic development, differences between males and females are already detectable [170] [171]. After 10.5 to 12 days *post coitum*, male expression of the Y chromosome *Sry* gene initiates molecular and cellular cascades in the undifferentiated gonads of males leading to differentiation of the testes and divergent conversion of the male and female development [172]. Further phenotypic differences between males and females also occur post-puberty in response to increasing circulating hormone levels.

Until now, sexually dimorphic effects in the intestine have only been marginally described. Oestrogen-mediated effects on visceral pain in the intestine have been reported [173] [174], and gender-specific differences in gene expression of metabolic pathways in the SI has been described for adult mice [175]. Despite extensive information regarding the effects of sex hormones on immune cells, our knowledge is limited regarding the effects of gender on the function of the gut mucosal immune system [176] [177].

Although the GALT is the largest lymphoid organ in the body and is an important site for host-microbe interactions, most investigations on gender and immunity have focused on the analysis of the peripheral blood mononuclear cells. The involvement of the GI tract is well documented in several inflammatory and autoimmune disorders, including CD, UC, and celiac disease. Gender distribution in IBD is dependent on the disease subtype, CD, or UC. In CD there is a greater prevalence of females, while in UC population-based studies have shown no significant differences [178]. However, it is not known whether the regulation of intestinal inflammatory response is influenced by sex differences [179]. Differences in immune cell infiltration of the colonic mucosa such as mast cells have been shown to correlate with symptomatic differences between the sexes in IBS [180]. However, no differences were observed in young healthy controls [180].

These differences might be enhanced with advancing age particularly when females go into menopause. While female mice do not have the equivalent of a menopause, they do undergo reproductive senescence, becoming essentially acyclic by 11-16 months of age [181] [182]. Therefore, ovariectomy is necessary to simulate the effects of human menopause

in mouse models. Studies in female mammals (rats) indicated that ovariectomy is associated with a shortened life span [183], and that the pathological deficiency or loss of ovarian function is associated with the derangement of energy metabolism and immune function (rodents and humans) [184]. These data suggest that the ovaries and their endocrine activity may have a positive effect on longevity in mammals. Supporting this theory, it has been reported that women had greater longevity after elective hysterectomy compared with those who received ovariectomy and hysterectomy [185]. In addition, menopause is associated with metabolic dysfunction [184] and pathologies involving inflammation (e.g., osteoporosis and metabolic disorders, including diabetes, atherosclerosis, joint diseases and even neurodegeneration) [186] [187].

There is growing recognition that males and females differ with respect to basic physiology, body composition and susceptibility to and progression of a broad variety of non-communicable diseases, as well as in the response to pharmacological treatment. However, the intestinal physiological mechanisms underlying these sexually dimorphic phenotypes are currently largely unresolved. Increased knowledge on these mechanisms might contribute significantly to disease prevention and treatment, for instance by optimizing dietary recommendations and pharmacological protocols in a gender-specific way.

1.9 Aims and outline of this thesis

The work presented in this thesis was embedded in a larger Top Institute of Food and Nutrition (TIFN) funded project (GH002) on "Food-induced modulation of the intestinal immune barrier", with the major goal of investigating whether food components can affect the intestinal immune barrier and if so, the mechanisms involved.

The overarching goal of this thesis was to investigate the role of mucus in the maintenance of the intestinal immune barrier in health and disease. The specific objectives were to study the effects of mucus deficiency, which is a feature of IBD, and the effects of ageing and gender differences on mucus production and other aspects of intestinal homeostasis using different mice models and a multidisciplinary approach (Fig. 7).

$Muc2^{-/-}$ mice were used to investigate the effect of reduced mucus (i.e. $Muc2^{+/-}$), or mucus absence (i.e. $Muc2^{-/-}$) on the small intestinal barrier. None of the previous published studies in $Muc2^{-/-}$ mice investigated the effects of Muc2-deficiency in the small intestine in any detail. Here we performed transcriptomics, histology, and 16S rRNA microbiota profiling on ileal samples from WT, $Muc2^{-/-}$, and $Muc2^{+/-}$ mice at 2, 4, and 8 weeks after birth with the aim of gaining a better understanding of homeostatic mechanisms, early indicators of gut barrier dysfunction, and the impact of mucus on diversity and composition of microbiota in the ileum (**Chapter 2**).

A detailed understanding of the temporal changes in microbiota and their relationship to intestinal gene expression prior to and during the development of colitis is currently lacking. Such knowledge might provide new insights into the dynamics of the interplay between the host and microbiota in IBD and have implications for future therapies, for example by manipulation of the microbiota. However, prospective studies requiring repeated biopsy sampling are difficult to perform in humans and the data will be complex to statistically analyse and interpret due to genetic diversity and variability in environmental exposures of the subjects. To address these problems we took advantage of the *Muc2*$^{-/-}$ mouse experimental model of colitis, which provides an opportunity to identify microbiota changes and host gene expression before and after the onset of colitis (**Chapter 3**). Although heterozygote (*Muc2*$^{+/-}$) mice do not develop spontaneous colitis we hypothesized there would be decreased mucus production and a mild mucus barrier dysfunction, which might lead to altered microbiota-host interactions. Microbiota composition was determined using a diagnostic 16S rRNA array for the mouse intestinal microbiota and transcriptomics data was obtained from colonic tissue. Furthermore, histology and FISH techniques were performed on mouse colonic tissue to obtain temporal data on morphological changes, mucus production, mucosal gene expression, and spatial compartmentalization of bacteria in the lumen.

Knowledge of the impact of ageing on the GI tract mucus layer is incomplete and limited to reports of altered gastric mucus layer. None of the previous studies in mice have deeply investigated the effects of ageing in the physiology of the small and large intestine. Such knowledge might provide new insights into the dynamics of the interplay between the host and microbiota in elderly and have implications for future interventions, for example by manipulation of the microbiota. The effects of natural ageing on the intestinal homeostasis, barrier functions, microbiota in the ileum and the colon, were studied in mice (**Chapter 4**) separately taking into account the influence of gender (**Chapter 5**). There is growing recognition that males and females differ with respect to basic physiology, body composition and susceptibility to and progression of a broad variety of non-communicable diseases, as well as in the response to pharmacological treatment. However, the intestinal physiological, including gut barrier, mechanisms underlying these sexually dimorphic effects are currently largely unresolved. Increased knowledge on these mechanisms might contribute significantly to disease prevention and treatment, for instance by optimizing gender-specific dietary and pharmacological requirements for females and males. The reason for observed gender differences has been attributed to sex hormones, but little is known regarding their effect on the intestinal physiology and the gut barrier.

The results obtained in naturally aged mice were compared to those obtained in a fast-ageing (*Ercc1*$^{-/\Delta7}$) mouse model (**Chapter 6**). An intervention with different bacterial strains (*Lactobacillus casei*, *Bifidobacterium breve* and *Lactobacillus plantarum*) was

performed to investigate potential beneficial effects on the process of intestinal ageing and the mucus barrier.

Methods for studying the mucus structure and permeability in living tissue, while allowing host factors or treatments to be included are limited to short-term measurements in explants and are too laborious to be performed on more than 10 samples per day. Therefore in **Chapter 7**, we assessed different histological techniques for quantifying the thickness and location of the mucus in both the SI and colon of gnotobiotic, conventional and germ-free mice. Additionally we developed a simple and versatile *ex vivo* method to assess mucus permeability in living tissue that can be easily performed on multiple tissue samples in one day. In Chapter 7 we also studied the immune sampling of a model lactobacillus strain in gnotobiotic mice in the lymphoid tissue, including PPs and mesenteric lymph nodes (MLNs).

Chapter 8 completes this thesis with a general discussion and conclusions on the obtained results, with recommendations and perspectives for future studies.
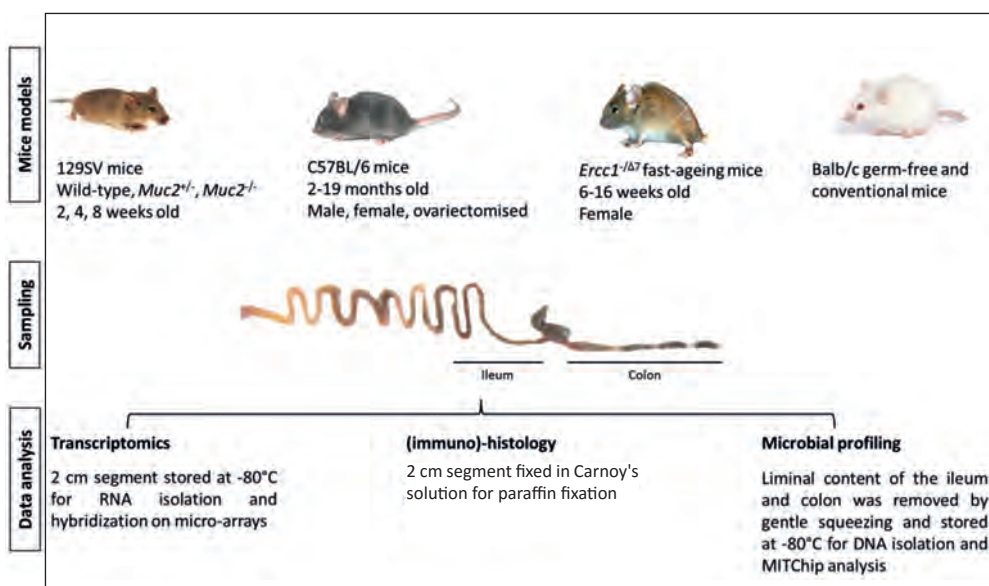
Figure 7: Outline of the animal experiments performed in this thesis.

Chapter 2

The IL-22-STAT3 pathway plays a key role in the maintenance of ileal homeostasis in mice lacking secreted mucus barrier

Bruno Sovran,[1,2*] Linda MP Loonen,[1,2*] Peng Lu,[8,9] Floor Hugenholtz,[1,4] Clara Belzer,[1,4] Ellen H Stolte,[2] Mark V Boekschoten,[1,3] Peter van Baarlen,[2] Michiel Kleerebezem,[1,2,5] Paul de Vos,[1,6] Jan Dekker,[1] Ingrid B Renes,[7,8] and Jerry M Wells[1,2]

* These authors contributed equally to this study
[1] Top Institute Food and Nutrition, Wageningen, the Netherlands
[2] Host-Microbe Interactomics Group, Animal Sciences Department, Wageningen University and Research Center, Wageningen, the Netherlands
[3] Division of Human Nutrition, Wageningen University and Research Center, Wageningen, the Netherlands
[4] Laboratory of Microbiology, Wageningen University and Research Center, the Netherlands
[5] NIZO food research, Ede, the Netherlands
[6] University Medical Center of Groningen, Groningen, the Netherlands
[7] Nutricia Research, Utrecht, the Netherlands
[8] Department of Pediatrics, Erasmus MC-Sophia, Rotterdam, the Netherlands
[9] Department of Pediatrics, Academic Medical Center, Amsterdam, the Netherlands

Abstact

Background: Muc2-deficient mice show no signs of ileal pathology, but the mechanisms remained unknown.

Methods: Wild-type (WT), *Muc2$^{+/-}$* and *Muc2$^{-/-}$* mice were sacrificed at 2, 4, and 8 weeks of age. Total RNA from ileum was used for full genome transcriptome analysis and qPCR. Microbiota composition was determined using a mouse intestinal chip (MITChip). Morphological and immunohistological studies were performed on segments of ileum.

Results: The ileum was colonized by more diverse microbiota in young (week 4) WT than in *Muc2$^{-/-}$* mice and composition was influenced by genotype. Weaning was associated with major changes in the transcriptome of all mice, and highest number of differentially expressed genes compared to adults, reflecting temporal changes in microbiota. Although the spatial compartmentalization of bacteria was compromised in *Muc2$^{-/-}$* mice, gene set enrichment analysis revealed a down-regulation of TLR, immune, and chemokine signalling pathways compared to WT mice. The predicted effects of enhanced IL-22 signalling were identified in the *Muc2$^{-/-}$* transcriptome, as the up-regulation of epithelial cell proliferation, altered expression of mitosis and cell cycle control pathways. This is consistent with increased villus length and number of Ki67 positive epithelial cells in *Muc2$^{-/-}$* mice. Additionally, expression of the network of IL-22 regulated defence genes, including *Fut2*, *Reg3β*, *Reg3γ*, *Relmb* and the Defensin *Defb46* were increased in *Muc2$^{-/-}$* mice.

Conclusions: These findings highlight a role for the IL-22-STAT3 pathway in maintaining ileal homeostasis when the mucus barrier is compromised and its potential as a target for novel therapeutic strategies in IBD.

Keywords: Muc2, Reg3 proteins, intestinal homeostasis, ileum, microbiota, interleukin 22

Introduction

Secreted mucus, antimicrobial proteins, and IgA in the lumen play a key role in maintaining intestinal homeostasis by regulating contact between host cells and potentially harmful antigens and microbes [29][188]. Intestinal mucus is primarily composed of mucin 2 (MUC2), secreted by goblet cells in the epithelium [57][119]. Glycans of Muc2 were recently shown to confer tolerogenic properties to lamina propria (LP) dendritic cells (DCs) through interaction with a galectin 3-dectin 1-FcγRIIB receptor complex [92]. MUC2 also enhances epithelial expression of B cell cytokines and trypsin-like serine protease, promoting development of tolerogenic DCs and anti-inflammatory mechanisms contributing to gut homeostasis, possibly through the same receptor-complex [92]. Mouse colonic mucus is composed of an inner layer, which is attached to the epithelium and largely devoid of bacteria, and a less-dense outer layer, containing commensal bacteria and luminal contents [66]. Both mucus sub-layers have essentially the same composition, suggesting the outer layer arises from limited, specific proteolytic cleavage, and volumetric expansion of the inner layer in combination with (partial) consumption by bacteria [189]. The density and stratified organization of the inner mucus layer is proposed to prevent penetration by bacteria, minimizing contact of bacteria and ingesta with the epithelium. The structure and function of small intestinal mucus is less well understood, and it is noticeably thinner than in the colon [66].

Defects in barrier properties of mucus are considered to be contributing factors in inflammatory bowel disease (IBD) patients with Crohn's disease (CD) or ulcerative colitis (UC). In both forms of IBD the intestinal mucus harbours higher numbers of bacteria than healthy subjects [109] and in UC patients the colonic mucus layer is thinner, with a 70% reduction of MUC2 production in active periods of disease [102,190]. Recently, colonic mucus in an experimental rodent model of colitis and in biopsy samples from UC patients, appeared highly penetrable to fluorescent beads compared to healthy tissue [110]. The diminished barrier functionality of mucus in colitis may be due to structural changes in the sulfation and sialylation of MUC2 oligosaccharides, as was reported in IBD patients [191]. A consequence of defective barrier function is increased contact of bacteria with the epithelium which triggers inflammatory responses through recognition of microbe-associated molecular patterns (MAMPs), by pattern recognition receptors (PRRs) of the innate immune system, including Toll-like receptors (TLRs) and NOD-like receptors (NLRs), resulting in inflammatory mucosal cytokine production and increased epithelial permeability (15). In IBD, a dysfunctional mucus barrier will increase influx of luminal antigens into the lamina propria, leading to innate and adaptive responses to luminal antigens and a perpetuating cycle of inflammation and barrier dysfunction that may be difficult to resolve without therapy (13).

An abnormal composition and decreased diversity of (specific subgroups of) the microbiota is associated with chronic inflammatory conditions such as IBD [112] [34]. This may be due to the selective targeting of members of the resident microbiota by antimicrobial factors induced by the host inflammatory response, leading to increased abundance of potentially pathogenic bacterial pathobionts in the microbiota [192].

Muc2^{-/-} mice lack an intestinal mucus layer and develop spontaneous colitis from 4 weeks of age onwards [121]. In these mice, bacteria are found in colonic crypts and in direct contact with epithelial cells [66]. The inflammatory responses in *Muc2*^{-/-} mice prior to development of colitis have been previously studied in the colon of 2- and 4-week-old mice [193] [122]. Distinct phases were observed in colitis development, which might be related to the expansion of the microbiota after weaning, and/or loss of protective factors in mother's milk. The most notable changes observed in *Muc2*^{-/-} mice were the exacerbation of inflammatory gene expression after weaning and a decline in the number of regulatory T cells [193]. None of the previous studies in *Muc2*^{-/-} mice have deeply investigated the effects of MUC2-deficiency in the ileum. Here we performed transcriptomics, histology, and 16S microbiota profiling on ileal samples from wild-type (WT), *Muc2*^{-/-}, and *Muc2*^{+/-} mice at 2, 4, and 8 weeks after birth with the aim of gaining a better understanding of homeostatic mechanisms, early indicators of gut barrier dysfunction, and the impact of mucus on diversity and composition of microbiota in the ileum.

Materials and Methods

Animals

Muc2^{-/-} mice with a 129SV background were bred as previously described [118]. Mice were generated from interbreeding *Muc2*^{+/-} mice and genotyped [118]. Mice were housed in a specific pathogen-free environment with *ad libitum* access to AIN93 diet (Special Diets Services, Witham, Essex, England), and acidified tap water in a 12-hour light/dark cycle. The Erasmus MC Animal Ethics Committee (Rotterdam, the Netherlands) approved the animal experiments.

Experimental set up

Groups of WT, *Muc2*^{+/-}, and *Muc2*^{-/-} (n=5 in each group) littermates were housed together with their respective birth mothers until weaning at 21 days, and sacrificed at 14, 28, and 56 days postnatal. Ileal tissues were excised and fixed in 4% (w/v) paraformaldehyde (PFA) in phosphate-buffered saline (PBS), stored in RNAlater® (Qiagen, Venlo, the Netherlands) at -20°C, or frozen in liquid nitrogen and stored at -80°C. Additionally, colonic tissue was collected, fixed in 4% PFA in PBS and embedded in paraffin.

Histology

Paraffin sections (5 μm) of ileum were attached to poly-L-lysine-coated glass slides (Thermo scientific, Germany). After overnight incubation at 37°C, slides were de-waxed and hydrated step-wise using 100% xylene followed by several solutions of distilled water containing decreasing amounts of ethanol. Sections were stained with haematoxylin and eosin (H&E) and Periodic Acid Schiff (PAS)/Alcian blue [194]. Ten morphologically well-oriented crypt-villus regions were randomly chosen per ileal segment and their length was measured using ImageJ software (NIH, Maryland, USA).

Immunohistochemistry

The slides were deparaffinised and antigen retrieval was performed by heating the sections for 20 min in 0.01 M sodium citrate (pH 6.0) at 100°C. Sections were washed for 3 h with 3 changes of PBS. Non-specific binding was reduced using 10% (v/v) goat serum (Invitrogen, Life technologies Ltd, Paisley, UK) in PBS for 30 min at room temperature. Cell proliferation marker Ki67 was detected by incubating the sections with anti-Ki67 antibody (Abcam, Cambridge Science Park, Cambridge, UK) diluted 1:200 in PBS, 90 min at room temperature. Apoptotic cells were identified by staining for cleaved-Caspase 3 expression using an anti-Caspase-3 antibody (Abcam) diluted 1:200 in PBS, overnight at 4°C.

Detection of bacteria using fluorescent *in situ* hybridization (FISH)

The slides were deparaffinised with xylene and washed twice in 100% ethanol. The tissue sections were incubated with the universal bacterial probe EUB338 (5'-GCTGCCTCCCGTAGGAGT-3') (Isogen Bioscience BV, De Meern, the Netherlands) conjugated to Alexa Fluor488. A 'non-sense' probe (5'-CGACGGAGGGCATCCTCA-3') conjugated to Cy3, was used as a negative control. Tissue sections were incubated overnight with 0.5 μg of probe in 50 μL of hybridization solution (20 mmol/L Tris-HCl (pH 7.4), 0.9 mol/L NaCl, 0.1% (w/v) SDS) at 50°C in a humid environment using a coverslip to prevent drying of the sample. The sections were washed with (20 mmol/L Tris-HCl (pH 7.4), 0.9 mol/L NaCl) at 50°C for 20 min and then washed 2 times in PBS for 10 min in the dark and incubated with DRAQ5 (Invitrogen) (1:1000) for 1 h at 4°C to stain nuclei. Sections were washed 2 times in PBS for 10 min, mounted in Fluoromount G (SouthernBiotec, Alabama, USA) and stored at 4°C.

RNA isolation, cDNA synthesis, and qPCR

Total RNA was isolated using the RNeasy® kit (Qiagen) with a DNase digestion step according to the manufacturer's protocol. One μg of RNA was reverse transcribed using a qScript® cDNA synthesis kit (Quanta Biosciences, Gaithersburg, MD) according to the manufacturer's protocol. QPCR was performed on a Rotorgene 2000 real-time cycler

(Qiagen) (see Table 1 for qPCR primer sequences). For qPCR 5 µL cDNA (1:20 diluted from cDNA synthesis mixture) was used, together with 300 nmol/L forward and reverse primer, 6.25 µL 2x Rotor-Gene SYBR Green PCR kit (Qiagen), and demineralized water up to a volume of 12.5 µL. QPCR was performed (2 min 95℃, 40 cycles of 15 s at 95℃, 1 min at 60℃, and 2 min at 60℃) on a Rotorgene 2000 real-time cycler (Qiagen).

Raw QPCR data were analysed using Rotorgene Analysis Software V5.0. Changes in transcript levels were calculated relative to the glyceraldehyde-3-phosphate dehydrogenase (Gapdh) and hypoxanthine phosphoribosyl transferase (Hprt) genes that were expressed at the same level in WT, Muc2$^{+/-}$ and Muc2$^{-/-}$ mice. Reactions lacking reverse transcriptase or template were included as controls in all experiments and no amplification above background levels was observed. The melting temperature and profile of each melting curve was checked to ensure specificity of the amplification product. For each PCR reaction, amplification of the correct amplicon was verified by sequencing.

Statistics were performed using GraphPad Prism® 5.0 software (GraphPad, San Diego, CA, USA). Data shown are the means and the standard errors of the means (SEM), analysed with the non-parametric Mann-Whitney test. Differences were considered statistically significant when $p < 0.05$.

Table 1: QPCR primer sequences (5' to 3', left to right)
Legend: *Gapdh*: Glyceraldehyde 3-phosphate dehydrogenase ; *Hprt*: Hypoxanthine guanine phosphoribosyl transferase ; *Muc2*: Mucin 2; *Reg3γ*: Regenerating islet-derived protein 3 gamma; *Fut2*: fucosyltransferase 2 ; *IL-1β*: Interleukin-1β.

	Forward primer	Reverse primer
Gapdh	GGTGAAGGTCGGTGTGAACT	CTCGCTCCTGGAAGATGGTG
Hprt	GTTAAGCAGTACAGCCCCAAA	AGGGCATATCCAACAACAAACTT
Muc2	ACCTGGGGTGACTTCCACT	CCTTGGTGTAGGCATCGTTC
Reg3g	TTCCTGTCCTCCATGATCAAAA	CATCCACCTCTGTTGGGTTCA
Reg3b	ATGCTGCTCTCCTGCCTGATG	CTAATGCGTGCGGAGGGTATATTC
Fut2	AGTCTTCGTGGTTACAAGCAAC	TGGCTGGTGAGCCCTCAATA
IL-1β	AGTTGACGGACCCCAAAAG	CACGGGAAAGACACAGGTAG

Transcriptome analysis

Quantity and quality of ileal RNA (5 arrays of individual mice per group) was assessed using spectrophotometry (ND-1000, NanoDrop Technologies, Wilmington, NC, USA), and Bionanalyzer 2100 (Agilent, Santa Clara, CA, USA), respectively. RNA was only used to generate cDNA and perform microarray hybridisation when there was no evidence of RNA degradation (RNA Integrity Number > 8). 100 ng of total RNA was labelled using

the Ambion WT Expression kit (Life Technologies Ltd, Paisley, UK) together with the Affymetrix GeneChip WT Terminal Labelling kit (Affymetrix, Santa Clara, CA, USA). Labelled samples were hybridised to Affymetrix GeneChip Mouse Gene 1.1 ST arrays. Hybridisation, washing, and scanning of the array plates were performed on an Affymetrix GeneTitan Instrument, according to the manufacturer's recommendations.

Quality control of the datasets obtained from the scanned Affymetrix arrays was performed using Bioconductor [195] packages integrated in an on-line pipeline [196]. Probe sets were redefined according to Dai *et al.* [197] utilising current genome information. In this study, probes were reorganised based on the Entrez Gene database (remapped CDF v14.1.1). Normalised expression estimates were obtained from the raw intensity values using the Robust Multiarray Analysis (RMA) pre-processing algorithm available in the Bioconductor library affyPLM using default settings [198].

Differentially expressed probe sets were identified using linear models, applying moderated t-statistics that implemented empirical Bayes regularization of standard errors [199]. A Bayesian hierarchical model was used to define an intensity-based moderated T-statistic (IBMT), which takes into account the degree of independence of variances relative to the degree of identity and the relationship between variance and signal intensity [200]. Only probe sets with a fold-change (FC) of at least 1.2 (up/down) and p value < 0.05 were considered to be significantly different. Pathway analysis was performed by Gene Set Enrichment Analysis (GSEA) [201] [202] and visualized in Cytoscape (http://www.ncbi.nlm.nih.gov/pubmed/20656902).

Bacterial DNA extraction and microbiota profiling

Except for 2-week-old mice, which appeared to lack sufficient luminal content to allow sampling, the contents of the ileum could be recovered by gently squeezing and the DNA extracted using PowerSoil® DNA extraction kit (MO BIO Laboratories, Carlsbad, CA, USA). Microbiota composition was analysed by Mouse Intestinal Tract Chip (MITChip), a diagnostic 16S rRNA array that consists of 3,580 unique probes especially designed to profile mouse intestine microbiota [203]. 16S rRNA gene amplification, *in vitro* transcription and labelling, and hybridization were carried out as described previously [204]. The data was normalized and analysed using a set of R-based scripts in combination with a custom-designed relational database, which operates under the MySQL database management system. For the microbial profiling the Robust Probabilistic Averaging (RPA) signal intensities of 2667 specific probes for the 94 genus-level bacterial groups detected on the MITChip were used [205]. Diversity calculations were performed using a microbiome R-script package (https://github.com/microbiome). Multivariate statistics, redundancy analysis (RDA) and Principal Response Curves (PRC), were performed in Canoco 5.0, and visualized in triplots or a PRC plot [206].

Ethical considerations

Animal care and procedures were in compliance with the guidelines of the Animal Ethics Committee, Erasmus MC (Rotterdam, the Netherlands).

Results

Muc2$^{-/-}$ mice lack secreted mucus and Muc2-positive goblet cells

From 4 weeks of age, colitis was observed in proximal colon in *Muc2*$^{-/-}$ mice (Fig. 1A). Alcian blue staining was used to identify acidic carbohydrates like Muc2, and PAS for neutral carbohydrates. PAS-positive and combined PAS-Alcian blue-positive goblet cells were observed in the ileum of WT and *Muc2*$^{+/-}$ mice. In contrast, goblet cells in *Muc2*$^{-/-}$ mice only stained positive for PAS (Fig. 1B).

Immunohistochemistry revealed presence of Muc2-positive goblet cells in WT as well as *Muc2*$^{+/-}$ mice, and absence of such cells in *Muc2*$^{-/-}$ mice (Fig. 1B). Ileal *Muc2* mRNA expression was absent in *Muc2*$^{-/-}$ mice, but was not significantly different between WT and *Muc2*$^{+/-}$ (Fig. 1C). Similar numbers of MUC2-stained goblet cells were detected in *Muc2*$^{+/-}$ and WT mice (Fig. 1B). These observations confirm the *Muc2* mutation phenotype in the ileal region of the intestine.

Increased epithelial cell proliferation is observed in *Muc2*$^{-/-}$ but not *Muc2*$^{+/-}$ mice

Muc2$^{-/-}$ mice developed colitis after about 4 weeks, but the ileum lacked any signs of mucosal damage, such as superficial erosions. In the ileum, there were no apparent differences in overall morphology of the epithelium in *Muc2*$^{-/-}$, *Muc2*$^{+/-}$, and WT mice at 2 weeks, but from 4 weeks the villi of *Muc2*$^{-/-}$ mice were significantly ($p < 0.05$) longer (but not the crypts) (260 ± 6.6 µm compared to WT and *Muc2*$^{+/-}$, 200± 6.2 µm) (Fig. 2A). Ki67-staining revealed epithelial hyper-proliferation in ileal crypts of *Muc2*$^{-/-}$ compared to WT mice at week 2 (Fig. 2B).

There were no apparent differences in numbers of caspase 3-stained epithelial cells in ileum from *Muc2*$^{-/-}$ and WT mice (Fig. 2B). Taken together this indicates that the elongated villi observed at week 4 and 8 in *Muc2*$^{-/-}$ mice were due to increased epithelial cell proliferation.
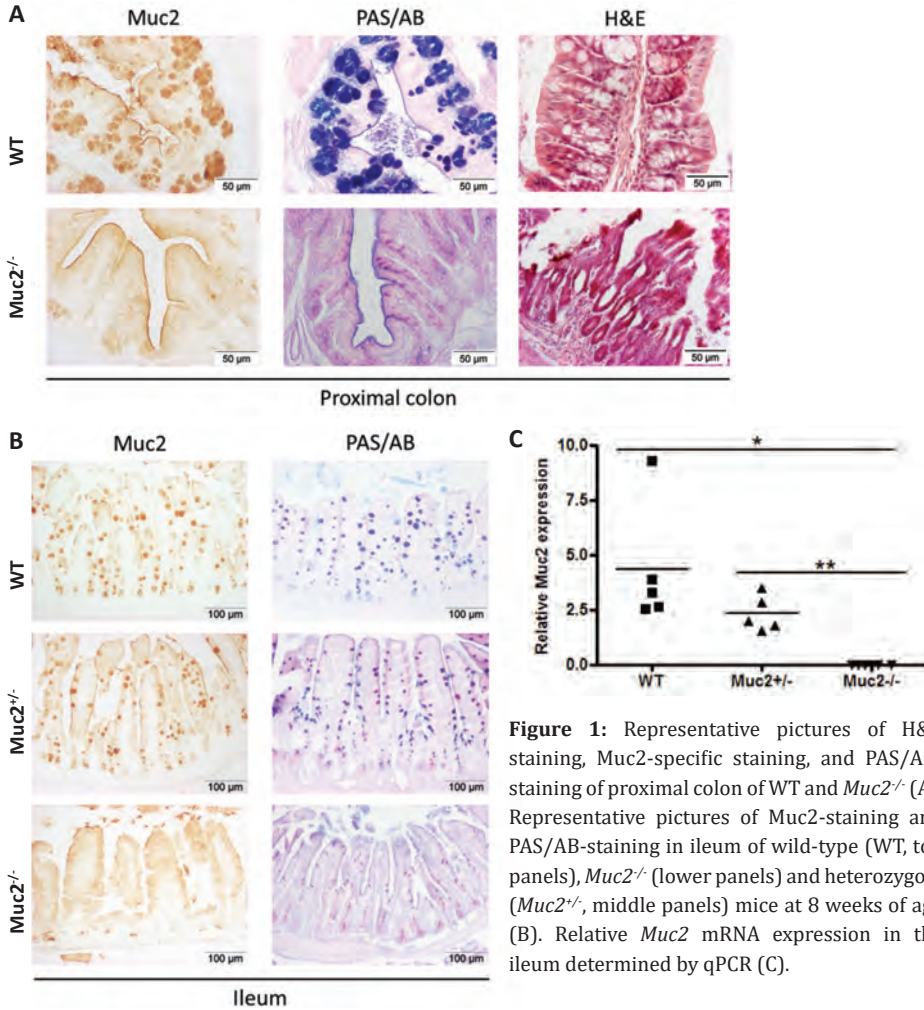
Figure 1: Representative pictures of H&E staining, Muc2-specific staining, and PAS/AB-staining of proximal colon of WT and *Muc2⁻/⁻* (A). Representative pictures of Muc2-staining and PAS/AB-staining in ileum of wild-type (WT, top panels), *Muc2⁻/⁻* (lower panels) and heterozygote (*Muc2⁺/⁻*, middle panels) mice at 8 weeks of age (B). Relative *Muc2* mRNA expression in the ileum determined by qPCR (C).
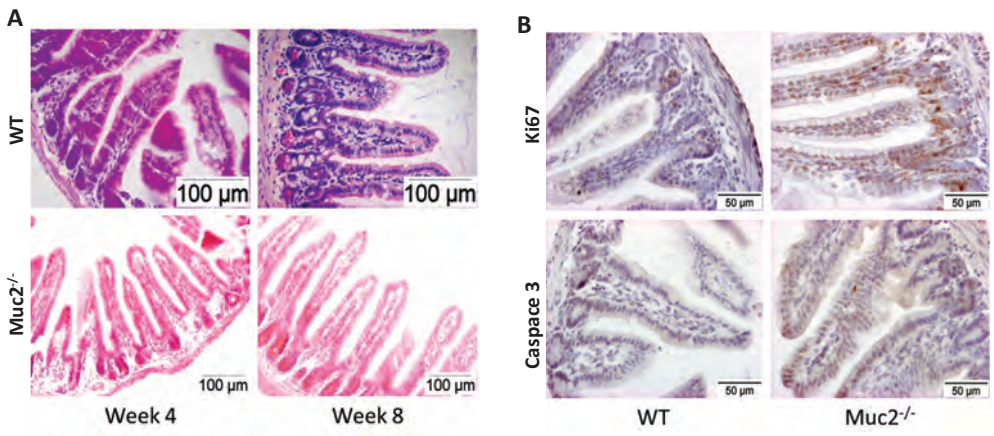
Figure 2: H&E staining of ileum of wild-type (WT) and *Muc2⁻/⁻* mice at 4 weeks and 8 weeks of age (A). Ki67 and Caspase 3 staining of ileum in wild-type (WT) and *Muc2⁻/⁻* mice (B).

Muc2 limits contact of bacteria with ileal epithelium

As the mucus barrier has been proposed to play a role in restricting direct contact between the microbiota and the mucosa, we stained bacteria *in situ* using FISH and measuring the average distance between bacterial cells and the mucosal surface. In WT mice a distance of approximately 50 µm was measured between the microbiota and the top of the ileal villi (Fig. 3A), corresponding to the thickness and position of the mucus layer in healthy Carnoy's-fixed ileal tissue (not shown). In the ileum of *Muc2^-/-* mice the microbiota are more frequently observed in contact with epithelial surfaces than in WT (Fig. 3B), confirming the microbiota barrier function of *Muc2* expression in the ileum.
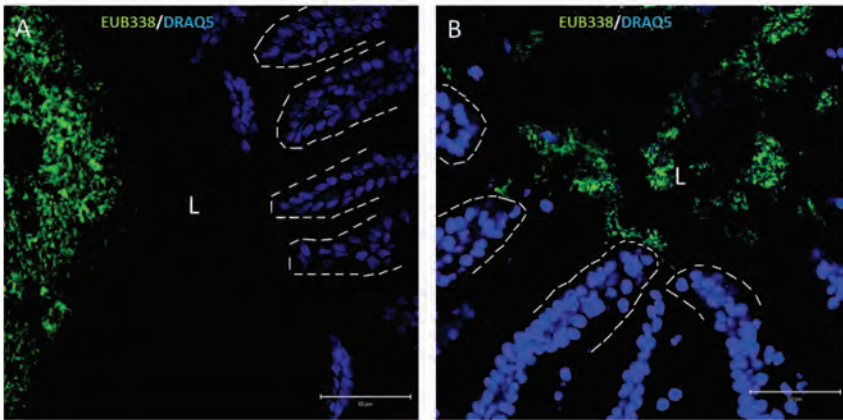

Figure 3: FISH analysis of the distal ileum of WT (A) and *Muc2^-/-* (B) using the general bacterial probe EUB338-Alexa Fluor 488 (green) and nuclei staining DRAQ5 (blue). The apical membranes of the epithelial cells are indicated by a dashed white line. Scale bar, 50 µm; L indicates lumen.

Mucus plays a role in shaping the microbiota composition, diversity and richness

To investigate the impact of Muc2-deficiency on the colonization pattern of the ileum, 16S DNA microbiota profiles of ileal content from 4- and 8 weeks-old WT, *Muc2^+/-*, and *Muc2^-/-* mice were determined using the MITChip microarray [203]. At 4 weeks the ileal content of *Muc2^-/-* mice displayed a significantly higher microbial diversity than WT mice (P<0.05), due to increased richness in bacterial taxonomic units (Fig 4A and B). The richness of the microbiota samples from *Muc2^+/-* mice was also significantly higher than WT mice at 4 weeks (Fig. 4B). However, at week 8 the microbiota diversity and richness was similar in all groups of mice (Fig. 4B). Nevertheless, redundancy analysis clearly established that both at week 4 and 8 the microbiota composition clustered according to the host's genotype (Fig. 4C and D). At week 4 the variance between microbiota of WT and other groups of mice was partly explained by higher abundance of a range of different microbial groups (Fig. 4C). This could be an indication that in WT there is an initial colonization by a more constrained group of bacteria, that reached

higher abundance in the WT mice compared to the other groups of mice. In the *Muc2*^{+/-} and *Muc2*^{-/-} groups, however, there is only one genus-like group, *Bryantella* spp. that was more abundant in the *Muc2*^{-/-} group (Fig. 4C). This lack of multiple microbial groups with higher abundances in the *Muc2*^{+/-} and *Muc2*^{-/-} mice could be an indication of colonization with a higher number of different microbial groups albeit at low relative abundance per group. The idea that *Muc2*^{+/-} and *Muc2*^{-/-} mice are colonized by many, low abundance species at week 4 is supported by the richness calculation showing *Muc2*^{+/-} and *Muc2*^{-/-} have higher bacterial diversity than WT mice (Fig. 4B).

Figure 4: Box-and-whiskers-plot showing the diversity (Shannon index) of microbiota in ileum of WT, *Muc2*^{+/-} and *Muc2*^{-/-} mice (A). Box-and-whiskers-plot showing the richness of microbiota in ileum of WT, *Muc2*^{+/-}, and *Muc2*^{-/-} mice (B). Redundancy Analysis (RDA) representing microbial ecology of *Muc2*^{-/-} , *Muc2*^{+/-}, and WT in the ileum at week 4 (C) and 8 (D).

In adult mice (week 8) the RDA analysis revealed specific differences between the microbiota of WT mice and the *Muc2*^{+/-} and *Muc2*^{-/-} mice, which was mainly associated with higher relative abundances of *Desulfovibrio* spp, *E. coli*, *Lactobacillus salivarius*, and *Turicibacter et rel.* in WT mice, and higher relative abundances of *Lactobacillus plantarum et rel.* and *Akkermansia muciniphila* in *Muc2*^{+/-} and *Muc2*^{-/-} mice (Fig. 4D). In the principal response curves (PRC) over time, the microbiota community displayed more overall similarity in adult animals (week 8) as compared to those at the early weaning stage (week 4) (not shown).

Muc2-deficiency specifically alters expression of numerous immune, metabolic, and cell-cycle control pathways in ileum

The number of differentially expressed genes in ileum of *Muc2*^{-/-}, compared to WT, was around 10-fold higher at 4 weeks than at weeks 2 and 8. Interestingly, a similar pattern is also visible in the *Muc2*^{+/-} mice, although at week 4 the number of differentially regulated genes was less than in the *Muc2*^{-/-} mice (not shown).

Gene Set Enrichment Analysis (GSEA), using the differentially expressed ileal genes as input, was used to identify significantly modulated gene networks in the different genotypes. In the ileum of *Muc2*^{-/-} mice, specific immune-related gene sets were repressed at weeks 2, 4, and 8 compared to their wild-type counterparts, including TLR-, immune-, and chemokine-signalling (Fig. 5A and B).
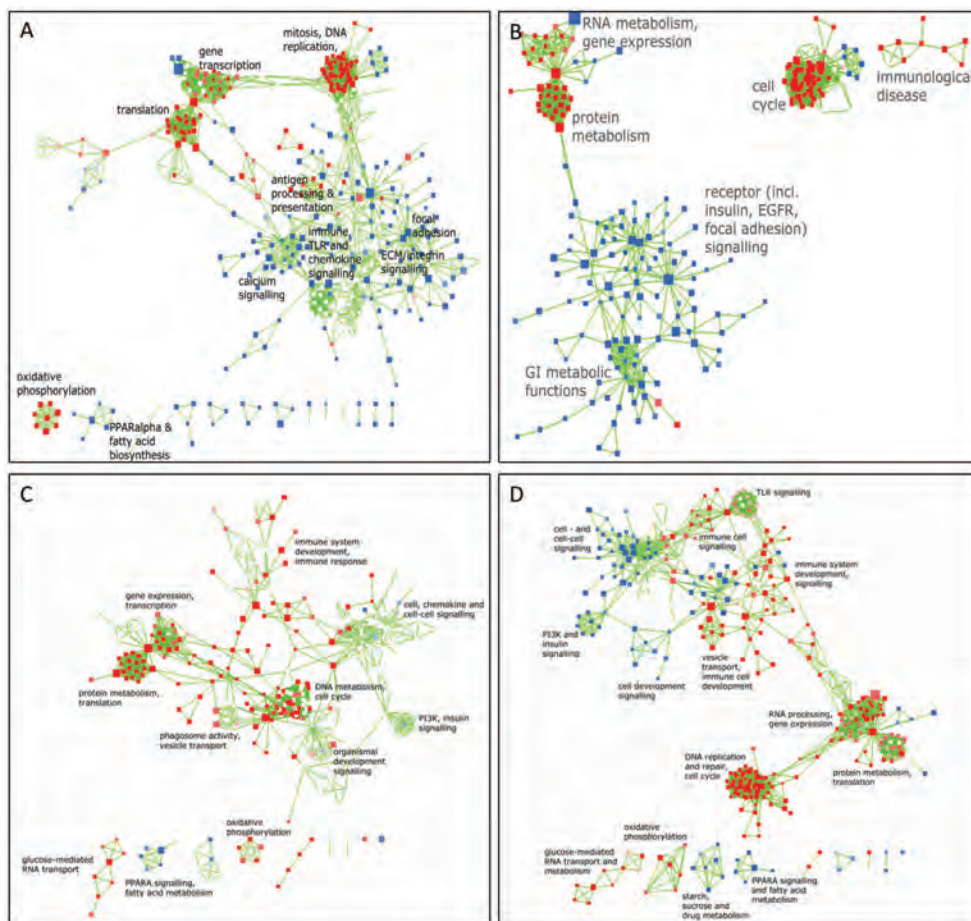

Figure 5: Network representation of gene set enrichment analysis (GSEA) profile of up-regulated (red) or down-regulated (blue) pathways in the ileum of *Muc2*^{-/-} mice compared to wild-type mice at week 4 (A), and week 8 (B). Network representation of gene set enrichment analysis (GSEA) profile of up-regulated (red) or down-regulated (blue) pathways in the ileum of *Muc2*^{+/-} mice compared to wild-type mice at week 4 (C), week 8 (D). The 'geography' of these representations has no implicit meaning.

Conversely, gene sets involved in mitosis, cell cycle control, and oxidative phosphorylation were induced in $Muc2^{-/-}$ compared to WT mice at all time points (Fig. 5A and B). Notably, at week 8, but not week 4, adaptive immune response pathways were repressed in $Muc2^{-/-}$ mice compared to wild type mice (Fig. 5B). At both week 4 and 8, lipid metabolism pathways were repressed in $Muc2^{-/-}$ (Fig. 5A and B).

Further analysis using Ingenuity highlighted that the highest up-regulated genes at week 2 were Fucosyltransferase 2 (*Fut2)*, Metalloproteinase-7 (*Mmp7*) and Reg3γ. Later on, Serum Amyloid A1 (*Saa1*), Fucosyltransferase 2 (*Fut2)*, and Resistin-like β (*Retnlb)*, Beta-1,3-galactosyltransferase 5 (*B3Galt5*) and the IL-22-induced pro-proliferative gene *Pla2g5* were the highest significantly increased genes in $Muc2^{-/-}$ at week 4 and 8 (not shown).

To gain more insights into the processes affected in the heterozygote $Muc2^{+/-}$ mice compared to the WT, we also performed GSEA to identify the most significantly affected processes (Fig. 5C and D). Although $Muc2^{+/-}$ and $Muc2^{-/-}$ mice appeared to have many differentially expressed genes in common. For example, gene sets associated with cell cycle, and metabolic functions were consistently up-regulated and down-regulated, respectively, in both the $Muc2^{+/-}$ and $Muc2^{-/-}$ mice compared to the WT at each time point. However, comparative analysis identified considerable differences between the $Muc2^{+/-}$ and $Muc2^{-/-}$ mice in comparison to the WT, which was clearly exemplified by the immune system related gene sets that were up-regulated at all time points in the $Muc2^{+/-}$ compared to the WT, whereas they were consistently down-regulated in the $Muc2^{-/-}$ relative to the WT (Fig. 5). Interestingly, the heterozygote mice also significantly overexpressed (but with lower fold changes) the genes that were expressed at the highest fold-change levels in the $Muc2^{-/-}$ mice at week 4 and 8, such as *Saa1*, *Fut2* and *Retnlb* (not shown).

Additionally, to confirm the data observed in the trancriptomic analysis, qPCR were done on specific genes involved in inflammation (*IL-1β*), innate immunity (*Reg3β* and *Reg3γ*) and fucosylation (*Fut2*). We showed that *Reg3β* and *Reg3γ* mRNA levels were significantly increased in $Muc2^{-/-}$ at weeks 8, compared to WT and $Muc2^{+/-}$ (Fig. 6A and B). *Fut2* mRNA levels were strongly increased in $Muc2^{-/-}$ at weeks 4 and 8 (Fig. 6C). *IL-1β* mRNA levels were not significantly different in any of the groups at week 8 (Fig. 6D). Those data are in line with the transcriptomics data previously described.
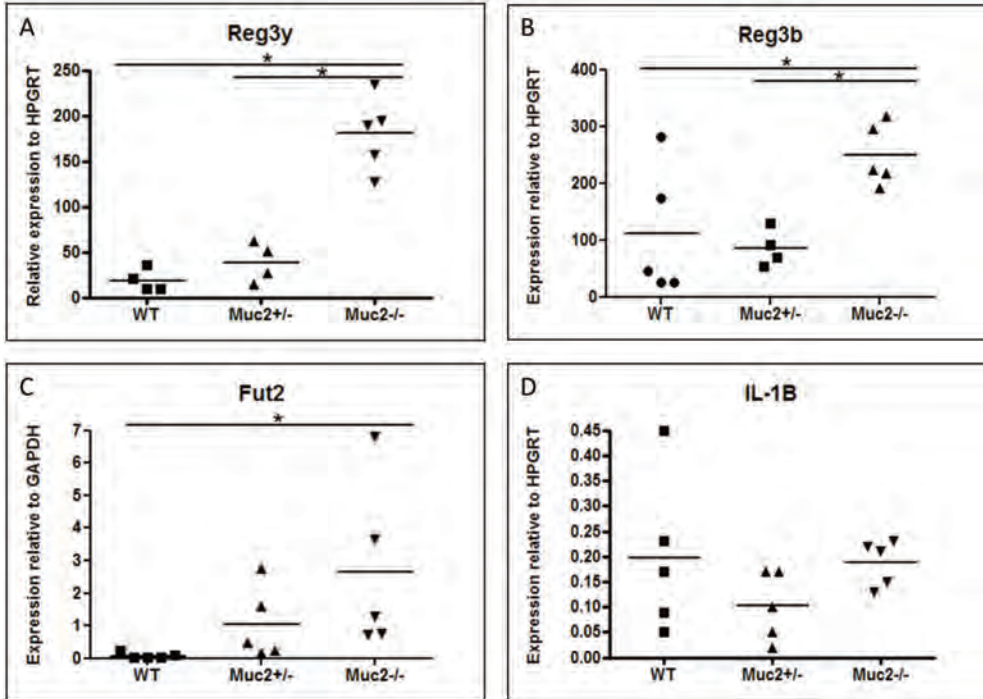
Figure 6: QPCR measurements of *Reg3γ* (A), *Reg3β* (B), *Fut2* (C) and *IL-1β* (D) in ileum of wild-type (WT), *Muc2+/-* and *Muc2-/-* mice at week 8. * p<0.05.

IL-22 pathway plays a key role in maintaining the homeostasis in the ileum of *Muc2-/-* mice

The IPA Upstream Regulator Analytic Analysis enabled us to identify the cascade of upstream transcriptional regulators that can explain the observed gene expression changes in the ileum of *Muc2-/-* mice. Many upstream transcriptional regulators were activated or inhibited in *Muc2-/-* mice at each time point, although only a few were connected to immune responses. Among the upstream regulators, IL-22 was identified as playing a central role in the activation of gene expression at week 2 and 4 in the *Muc2-/-* mice (Fig. 7). Notably, IL-22 is produced by activated DCs and type 3 subset of innate lymphoid cells (ILC3) after sensing bacteria and initiates protective innate immune responses against bacterial pathogens especially in epithelial cells [207]. Therefore, increased IL-22 signalling could explain the up-regulation of innate immunity related genes like *Reg3γ*, *Saa1*, *Fut2* and *Retnlb* at week 2 and 4 in *Muc2-/-* mice (Fig. 7). This is consistent with our finding that expression of IL-22ra2, a secreted, soluble antagonist of IL-22 signalling was decreased in *Muc2-/-* mice. Moreover, pro-proliferative factors such as *Myc* were also potentially controlled by the IL-22 signalling pathway at week 2 in the *Muc2-/-* mice, which correlates with the observed hyperproliferation (Ki67 positive cells) at this time point.
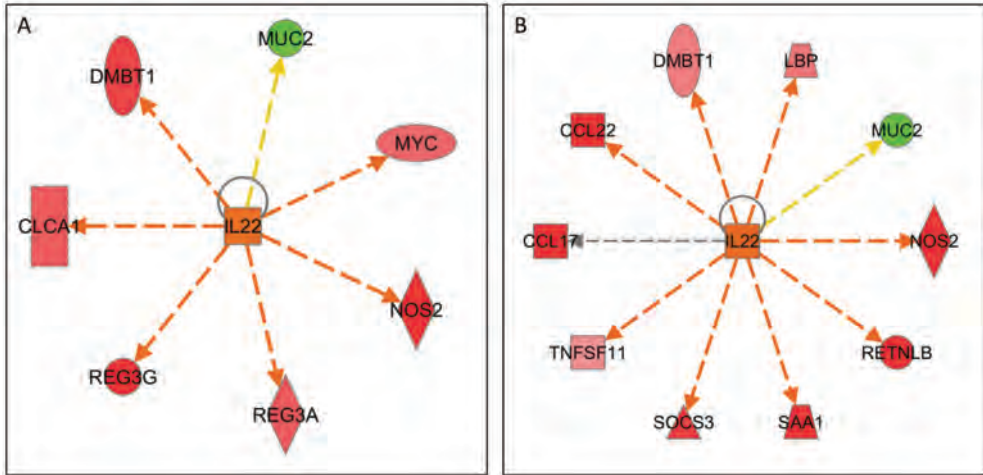
Figure 7: Down-stream genes regulated by IL-22 in the ileum of *Muc2*^{-/-} mice at week 2 (A) and week 4 (B). Up-regulated genes are depicted in shades of red and down-regulated are indicated in green. The colour of the arrow indicates the influence of IL-22 on the respective genes. Brown arrows indicate activation of the gene, yellow arrows indicate that the findings are not consistent with state of downstream molecule, and grey arrows indicate that the effect is not predicted.

Discussion

MUC2 is the major secreted intestinal mucin and in its absence was previously shown to cause colitis in mice [121] [193]. We confirmed that after 4 weeks *Muc2*^{-/-} mice develop colitis evidenced by increased thickness of the mucosa associated with hyper-proliferation, apoptosis in crypts, ulceration accompanied by faecal blood, and weight-loss [121] [193]. These histological changes are characteristic of murine models for IBD and clinical symptoms of IBD in humans. To date the effect of *Muc2*^{-/-} or *Muc2*^{+/-} genotypes on small intestinal physiology and microbiota have not been described in detail. Therefore, our aim was to investigate how the small intestine responds to complete (*Muc2*^{-/-}) or partial (*Muc2*^{+/-}) mucus-barrier defects as it might reveal crucial differences in ileal response with respect to homeostatic mechanisms.

Deletion of *Muc2* was not compensated by expression of other secreted mucins *Muc5B*, *Muc5AC* or *Muc6* in the ileum (results not shown). In contrast to the colon, the ileum of Muc2^{-/-} showed no histological signs of tissue damage, the only noticeable morphological difference being an increased length of the villi (week 4 and 8) in agreement our results showing hyper-proliferation of the intestinal epithelium. The evidence for hyperproliferation comes from increased epithelial staining of Ki-67 but not apoptotic cells, as well as increased expression of genes involved in cell cycle progression and differentiation such as *Myc* and *Pla2g5* were observed in *Muc2*^{-/-} mice (week 2).

Few genes associated with inflammation such as *Mip-1a (Ccl3), Tnf-α,* and *Ccl17* were up-regulated in ileum of *Muc2⁻/⁻* compared to WT. Eight genes of the mouse orthologues of human IBD-related genes i.e. *IL6ra*, *IL22ra1*, *Ccl2*, *Cxcl1*, *Timp1*, *S100a6*, *S100a13* and *Abcb1a* were differentially expressed. In contrast, 12 of the 32 IBD-related genes were up-regulated in colon of both *Muc2⁻/⁻* and *Muc2⁺/⁻* mice at weeks 4 and 8 (not shown). Interestingly, one of the strongly down-regulated genes in the ileum was *Tlr5*, which induces NF-κB activation upon binding of bacterial flagellin. Indeed, down-regulation of *Tlr5* in colitis has been observed and may be a feedback response to low-level inflammation [208]. Furthermore *Nfap*, a transcriptional activator of NF-κB, was down-regulated, whereas *Iκβ*, an NF-κB inhibitor that binds to cytosolic NF-κB to prevent nuclear translocation, was amongst the most strongly up-regulated genes. This apparent repression of innate inflammatory signalling via repression of NF-κB signalling may have contributed to preventing immune-mediated pathology in ileal mucosa of *Muc2⁻/⁻*. In contrast innate defence genes encoding antimicrobial *Defb46*, *Reg3β* and *Reg3γ* were expressed at significantly greater amounts in *Muc2⁻/⁻* than in WT mice.

In contrast to WT, bacteria in the ileum of *Muc2⁻/⁻* mice were frequently found in direct contact with the epithelium. However, the expression of innate gene sets except for Reg3 and defensin genes was less in the *Muc2⁻/⁻* mice than in WT, given the results of our extensive GSEA analysis. This supports the notion that innate responses were suppressed in the ileum of *Muc2⁻/⁻* mice compared to WT, possibly through a regulatory feedback mechanism. One plausible explanation for reduced expression of innate pathway genes could be the relatively high amounts of *Reg3γ* and *Reg3β* expressed in the *Muc2⁻/⁻* mice. Incubation of mucosa from active Crohn's disease with the human orthologue of Reg3β (HIP/PAP) was shown to reduce pro-inflammatory cytokines secretion [209]. Furthermore, HIP/PAP prevented TNF-α-induced NF-κB activation in monocytic, epithelial, and endothelial cells and reduced pro-inflammatory cytokine mRNA levels and adhesion molecule expression [209]. Moreover antisense blocking of HIP/PAP expression in a rat model of acute pancreatitis increases severity of inflammation [210]. In endothelial cells, purified human HIP/PAP decreased expression of surface receptors involved in leukocyte recruitment suggesting that HIP/PAP might dampen inflammatory responses by inhibiting leukocyte recruitment into the intestine [209].

These findings support the idea that Reg3 proteins have anti-inflammatory activity and their up-regulation participates in protection of epithelial cells in response to excessive inflammatory stimuli. Down-regulation of NF-κB and inflammatory pathways in the ileum of *Muc2⁻/⁻* mice, which express high amounts of Reg3β and Reg3γ, is reminiscent of the effects of IL-10, an anti-inflammatory cytokine triggering expression of suppressor of cytokine signalling via the JAK/STAT pathway. This hypothesis is supported by previous studies showing that purified human PAP inhibits the NF-kB pathway via JAK/STAT signalling in epithelial cells [211].

At week 8 both *Reg3* genes were significantly up-regulated in the ileum of *Muc2$^{-/-}$* mice and in the ileum of *Muc2$^{+/-}$* mice at week 4. Expression of Reg3 proteins was also increased in the colon, but the overall amount of transcription in colon was much lower, as shown previously [40]. Expression of Reg3 proteins is induced during infection or inflammation [71], and is dependent on IL-22 signalling [212]. This is consistent with our finding that expression of IL-22ra2, a secreted, soluble antagonist of IL-22 signalling [213] was decreased in *Muc2$^{-/-}$* mice. Apart from its role in stimulation of epithelial cells to produce antibacterial proteins, IL-22 regulates cellular stress response, apoptosis, and wound healing pathways in intestinal epithelial cells (IECs) via the signal transducer and activator of transcription 3 (STAT3) pathway [214]. Notably, STAT3 activation induces expression of IL-6, which promotes epithelial survival and proliferation [215], which may explain the increased proliferation and villus length in the *Muc2$^{-/-}$* ileum. Moreover, mRNA encoding *Pla2g5*, which is induced by Il-22 and stimulates proliferation in IECs was strongly up-regulated in *Muc2$^{+/-}$* and *Muc2$^{-/-}$* at week 4 and 8. Interestingly expression of the IL-6 receptor was also increased in ileum of *Muc2$^{+/-}$*. Another highly up-regulated gene in the ileum at weeks 4 and 8, both in *Muc2$^{+/-}$* and *Muc2$^{-/-}$* was *Fut2*. The *Fut2* gene, encoding an α-1,2-fucosyltransferase responsible for enzymatic linkage of α1,2-linked fucose to cell membrane attached and secretory mucins of the intestinal mucosa [216], *Fut2* was significantly up-regulated in the ileum of *Muc2$^{-/-}$* at week 8. It has been shown that at weaning when the transition toward adult-type colonization by microbiota occurs, *Fut2* mRNA is increased leading to expression of fucosylated epitopes in the colonic epithelium and fucose decoration of mucins [217] [218] [219] [220]. This may be a mechanism to promote colonization by preferred groups of symbionts that produce beneficial short-chain fatty acids and provide colonization resistance against pathogens. Lamina propria ILC3 were recently shown to produce IL-22 through sensing of bacteria via an unknown mechanism [207], leading to increased expression of Fut2 and Reg3 proteins. This is consistent with our observation of increased bacterial contact with the epithelium in *Muc2$^{-/-}$* deficient mice (Fig. 3) and the IL-22 mediated effects on epithelial expression and proliferation reported here.

Mucus directly or indirectly played a role in shaping the microbiota composition, diversity and richness with greatest effect immediately preceding weaning, but becoming more similar to that of WT in adult mice. This may be due to the ability of specific members of the microbiota such as *Akkermansia muciniphila* to colonize the mucus and utilize the mucus-associated glycans as a carbon source for growth [221]. The syntrophic interactions between mucus degraders and other bacteria in the small intestine are poorly understood, but could explain differences in composition between WT and mice lacking MUC2. The significant up-regulation of Reg3 proteins in *Muc2$^{-/-}$* mice could also shape the composition of the microbiota through selective inhibition or killing of specific bacterial species.

In summary, we propose a key role for the IL-22/STAT3 pathway in maintaining homeostasis in the ileum as a consequence of loss of mucus barrier (Fig. 8). This model is consistent with previous studies reporting increased expression of *Reg3β* and *Reg3γ* [212] and stimulation of epithelial regeneration through STAT3 induction of pro-proliferative genes.
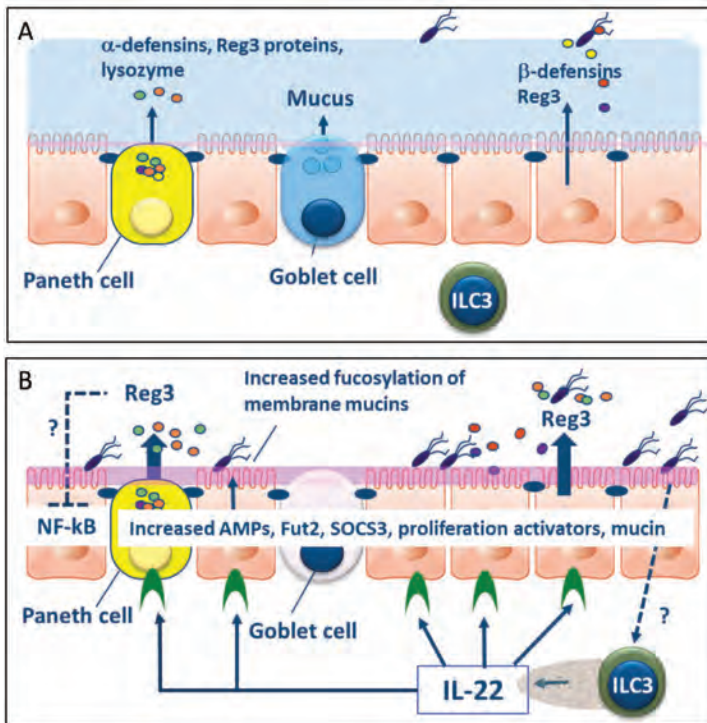

Figure 8: The IL-22-STAT3 pathway plays a key role in the maintenance of ileal homeostasis in Muc2-deficient mice. A: Schematic representation of the small intestine of a wild-type mice. B: Schematic representation of the small intestine of *Muc2⁻/⁻* mice showing known functions of IL-22. The anti-inflammatory mechanism of PAP (Reg3β) on NF-κB driven inflammatory pathways is shown as a dotted line as it has only been described for human colonic tissue and the precise mechanisms are not known. We speculate that IL-22 might also regulate Fut2 (shown as a dotted line). Mucus is indicated in blue, fucosylation is indicated in pink. Legend: IEL: Intra-epithelial Lymphocytes; DC: Dendritic Cell; AMPs: Antimicrobial Peptides; SOCS3: Suppressor of cytokine signalling 3. ILC3: Group 3 Innate Lymphoid Cells.

For example, *Pla2g5*, which is induced by IL-22 and induces proliferation in IECs [222] was strongly up-regulated in *Muc2⁺/⁻* and *Muc2⁻/⁻* mice at week 4 and 8. IL-22 induced STAT3 signalling in epithelial cells may also explain the increased expression of other protective factors such as *Defb46* and *Fut2*. TLR, chemokine and innate pathways were down-regulation of in the ileum of *Muc2⁻/⁻* mice compared to WT which may be due to the protective effects of Reg3 proteins including anti-inflammatory signalling [211], capacity to bind soluble MAMPs and direct antimicrobial activities [27]. IL-22 is

constitutively expressed in the small intestine by innate and adaptive cells including TCRγδ T cells and dendritic cells, which can encounter bacteria at the epithelial surface. These findings support the notion that IL-22 might be an attractive target for therapy of intestinal inflammation.

Acknowledgements

Disclosure

2

Chapter 3

Identification of commensal species positively correlated with early stress responses to a compromised mucus barrier

Bruno Sovran,[1,2] Peng Lu,[8,9*] Linda MP Loonen,[1,2*] Floor Hugenholtz,[1,4] Clara Belzer,[1,4] Ellen H Stolte,[2] Mark V Boekschoten,[1,3] Peter van Baarlen,[2] Hauke Smidt,[4] Michiel Kleerebezem,[1,2,5] Paul de Vos,[1,6] Ingrid B Renes,[7,8] Jerry M Wells,[1,2] and Jan Dekker[1]

* These authors contributed equally to this study
[1] Top Institute Food and Nutrition, Wageningen, the Netherlands
[2] Host-Microbe Interactomics Group, Animal Sciences Department, Wageningen University and Research Center, Wageningen, the Netherlands
[3] Division of Human Nutrition, Wageningen University and Research Center, Wageningen, the Netherlands
[4] Laboratory of Microbiology, Wageningen University and Research Center, the Netherlands
[5] NIZO food research, Ede, the Netherlands
[6] University Medical Center of Groningen, Groningen, the Netherlands
[7] Nutricia Research, Utrecht, the Netherlands
[8] Department of Pediatrics, Erasmus MC-Sophia, Rotterdam, the Netherlands
[9] Department of Pediatrics, Academic Medical Center, Amsterdam, the Netherlands

Abstract

Background: Our aims were (i) to correlate changes in the microbiota to intestinal gene expression prior to and during the development of colitis in *Muc2*^{-/-} mice and (ii) to investigate whether the heterozygote *Muc2*^{+/-} mouse, would reveal host markers of gut barrier stress.

Methods: Colon histology, transcriptomics and microbiota profiling of faecal samples was performed on WT, *Muc2*^{+/-}, and *Muc2*^{-/-} mice at 2, 4, and 8 weeks of age.

Results: *Muc2*^{-/-} mice develop colitis in proximal colon after weaning resulting in inflammatory and adaptive immune responses, and expression of genes associated with human IBD. *Muc2*^{+/-} mice do not develop colitis, but produce a thinner mucus layer. The transcriptome of *Muc2*^{+/-} mice revealed differential expression of genes participating in mucosal stress responses and exacerbation of a transient inflammatory state around the time of weaning. Young WT and *Muc2*^{+/-} mice have a more constrained group of bacteria as compared to the *Muc2*^{-/-} mice, but at 8 weeks the microbiota composition is more similar in all mice. At all ages microbiota composition discriminated the groups of mice according to their genotype. Specific bacterial clusters correlated with altered gene expression responses to stress and bacteria, prior to colitis development, including colitogenic members of the genus Bacteroides.

Conclusions: The abundance of Bacteroides pathobionts increased prior to histological signs of pathology suggesting they play a role in triggering the development of colitis. The heterozygote *Muc2*^{+/-} mouse produces a thinner mucus layer and can be used to study mucus barrier stress in the absence of colitis.

Keywords: Muc2-deficiency, colitis, Bacteroidetes, stress markers

Introduction

A key element of the mammalian strategy for maintaining a microbiota accommodating intestinal homeostasis is to minimize and regulate contact between luminal microorganisms and the intestinal epithelial cell surface. Physical separation of bacteria and the epithelium is largely accomplished by secretion of mucus, antimicrobial proteins and IgA into the lumen [29] [188]. Intestinal mucus is primarily composed of the highly *O*-glycosylated mucin 2 (MUC2), which is secreted by goblet cells in the epithelium. In the mouse colon, two distinct layers can be distinguished; a stratified inner layer which is attached to the epithelium and largely devoid of bacteria, and a less dense outer mucus layer that is accessible to commensal microbes [66]. The protective properties of mucus are evident in *Muc2*^{-/-} mice, which develop spontaneous colitis after weaning, when there is an expansion of the microbiota and loss of protective factors in the mother's milk [121] [193]. This is associated with exacerbation of inflammatory gene expression and a decline in regulatory T cells [122]. In the ileum the IL-22 -regulated network of genes involved in antimicrobial and wound-healing functions play a role in protecting the epithelium from damage due to chronic inflammatory responses to the microbiota (Chapter 2) [223].

Mucosal barrier dysfunction is observed in inflammatory bowel diseases (IBD), and different knockout mouse models of colitis have shown that mucus was more penetrable to fluorescent beads (1-2 μm) and bacteria than their healthy counterparts [66] [110] [112] [109]. The reasons for these changes in mucus permeability are not fully understood, but may result from the structural changes in the glycoprotein core and/or the sulphation and sialylation of mucin oligosaccharide residues, as reported in IBD patients [113]. Excessive and/or altered bacterial contact with the epithelium is known to trigger production of inflammatory cytokines, which increase epithelial permeability [33], leading to an influx of bacteria and their products across the epithelium thereby perpetuating the inflammatory response. In human IBD, clinical pathology is associated with the altered transcription of 32 common genes [224]. Many of which are also differentially expressed in mouse models of colitis.

Mucosal inflammation may be a key driver for the abnormal composition and decreased diversity and richness of the microbiota that are common features in IBD patients and mouse models of colitis [34] [35] [36]. Many studies on the microbiota of IBD patients have shown there is a lower proportion of Firmicutes, an increase in Gammaproteobacteria including the *Enterobacteriaceae*, and an overall decrease in microbiota diversity. Reduced complexity of the phylum Firmicutes is a signature of faecal microbiota of Crohn's disease patients with many studies describing decreased abundance of *Faecalibacterium prausnitzii* [225]. Decreased relative abundance of members of the families *Lachnospiraceae* and *Ruminococcaceae* has been described in some studies, an exception being *Ruminococcus gnavus,* which increases in abundance [37]. *Escherichia coli*

pathobionts exhibiting pathogen-like behaviours such as adhesion and invasiveness (AIEC) are more frequently cultured from IBD patients [43] due to their selective growth advantage in inflammatory conditions [40 41 42 192]. Functional tests of the ability of specific microbes to induce colitis in genetically susceptible mice has led to the identification of other pathobionts including members of the *Bacteroides*, with the two most potent disease inducing isolates belonging to the species *B. thetaiotaomicron* and *B. vulgatus* [226 227]. Changes in the abundance of commensals belonging to the Bacteroidetes have been reported in studies on IBD patients but not all studies are consistent with this finding [34 228 229 230 231].

A detailed understanding of the temporal changes in microbiota outlined above and their relationship to intestinal gene expression prior to and during the development of colitis is currently lacking. Such knowledge might provide new insights into the dynamics of the interplay between the host and microbiota in IBD and have implications for future therapies, for example by manipulation of the microbiota. However, prospective studies requiring repeated biopsy sampling are difficult to perform in humans and the data will be complex to statistically analyse and interpret due to genetic diversity and variability in environmental exposures of the subjects. To address these problems we took advantage of the *Muc2*^{-/-} mouse experimental model of colitis, which provides an opportunity to identify microbiota changes and host gene expression before and after the onset of colitis. Although heterozygote *Muc2*^{+/-} mice do not develop colitis, we hypothesized there would be decreased mucus production and a mild mucus barrier dysfunction, which might lead to altered microbiota-host interactions.

Materials and Methods

Animals

Muc2^{-/-} mice with a 129SV background were bred as previously described [118]. Mice were generated from interbreeding *Muc2*^{+/-} mice and genotyped [118]. Mice were housed in a specific pathogen-free environment with *ad libitum* access to AIN93 diet (Special Diets Services, Witham, Essex, England), and acidified tap water in a 12-hour light/dark cycle. The Erasmus MC Animal Ethics Committee (Rotterdam, the Netherlands) approved the animal experiments.

Experimental set up

Groups of WT, *Muc2*^{+/-}, and *Muc2*^{-/-} (n = 5 in each group) littermates were housed together with their respective birth mothers until weaning at 21 days, and sacrificed at 14, 28, and 56 days postnatal. Proximal colons were excised and fixed in 4% (w/v) paraformaldehyde (PFA) in phosphate-buffered saline (PBS), stored in RNAlater® (Qiagen, Venlo, the Netherlands) at -20°C, or frozen in liquid nitrogen and stored at

-80°C. Additionally, colonic tissue was collected, fixed in 4% PFA in PBS or Carnoy's fixative, and embedded in paraffin.

Histology

Paraffin sections (5 µm) of proximal colon were attached to poly-L-lysine-coated glass slides (Thermo scientific, Germany). After overnight incubation at 37°C, slides were de-waxed and hydrated step-wise using 100% xylene followed by several solutions of distilled water containing decreasing amounts of ethanol. Sections were stained with haematoxylin and eosin (H&E) or Periodic Acid Schiff (PAS)/Alcian blue [194].

Immunohistochemistry

Cell proliferation marker Ki67 was detected by incubating the sections with anti-Ki67 antibody (Abcam, Cambridge Science Park, Cambridge, UK) diluted 1:200 in PBS, 90 min at room temperature. Apoptotic cells were identified by staining for cleaved-Caspase 3 expression, using an anti-Caspase-3 antibody (Abcam) diluted 1:200 in PBS, overnight at 4°C, following described methods.

Detection of bacteria using fluorescent *in situ* hybridization (FISH)

Paraffin sections were deparaffinised with xylene and hybridized with a general bacterial probe, EUB 338 conjugated to Alexa 488 as described previously [223]. Nuclei were stained with DRAQ5 (Invitrogen, Life technologies Ltd, Paisley, UK), mounted in Fluoromount G® (SouthernBiotec, Alabama, USA), and stored at 4°C.

RNA isolation, cDNA synthesis, and qPCR

Total RNA was isolated using the RNeasy® kit (Qiagen) with a DNase digestion step according to the manufacturer's protocol. One µg of RNA was reverse transcribed using a qScript® cDNA synthesis kit (Quanta Biosciences, Gaithersburg, MD, USA) according to the manufacturer's protocol. QPCR was performed on a Rotorgene 2000 real-time cycler (Qiagen). For qPCR, 5 µL cDNA (1:20 diluted from cDNA synthesis mixture) was used, together with 300 nmol/L forward and reverse primer, 6.25 µL 2x Rotor-Gene SYBR Green PCR kit (Qiagen), and demineralized water up to a volume of 12.5 µL. QPCR was performed (2 min 95°C, 40 cycles of 15 s at 95°C, 1 min at 60°C, and 2 min at 60°C) on a Rotorgene 2000 real-time cycler (Qiagen).

Muc2 expression was measured using the primer sequences 5'ACCTGGGGTGACTTCCACT3' and 5' CCTTGGTGTAGGCATCGTTC3'. The relative mRNA expression levels were normalized against *Gapdh* (Forward: 5'GGTGAAGGTCGGTGTGAACT3' ; Reverse: 5'CTCGCTCCTGGAAGATGGTG3'), and *Hprt* (Forward: 5'GTTAAGCAGTACAGCCCCAAA3'; Reverse: 5'AGGGCATATCCAACAACAAACTT3') expression in each mouse.

Raw qPCR data were analysed using Rotorgene Analysis Software V5.0. Changes in transcript levels were calculated relative to the glyceraldehyde-3-phosphate dehydrogenase (*Gapdh*) and hypoxanthine phosphoribosyl transferase (*Hprt*) genes that were expressed at the same level in WT, *Muc2*^{+/-}, and *Muc2*^{-/-} mice. Reactions lacking reverse transcriptase or template were included as controls in all experiments and no amplification above background levels was observed. The melting temperature and profile of each melting curve was checked to ensure specificity of the amplification product. For each PCR reaction, amplification of the correct amplicon was verified by sequencing. Statistics were performed using GraphPad Prism® 5.0 software (GraphPad, San Diego, CA, USA). Data shown are the means and the standard errors of the means (SEM), analysed with the non-parametric Mann-Whitney test. Differences were considered statistically significant when $p < 0.05$.

Transcriptome analysis

Quantity and quality of RNA (5 arrays of individual mice per group) was assessed using spectrophotometry (ND-1000, NanoDrop Technologies, Wilmington, NC, USA), and Bionanalyzer 2100 (Agilent, Santa Clara, CA, USA), respectively. RNA was only used to generate cDNA and perform microarray hybridisation when there was no evidence of RNA degradation (RNA Integrity Number > 8). 100 ng of total RNA was labelled using the Ambion WT Expression kit (Life Technologies Ltd, Paisley, UK) together with the Affymetrix GeneChip WT Terminal Labelling kit (Affymetrix, Santa Clara, CA, USA). Labelled samples were hybridised to Affymetrix GeneChip Mouse Gene 1.1 ST arrays. Hybridisation, washing, and scanning of the array plates were performed on an Affymetrix GeneTitan Instrument, according to the manufacturer's recommendations.

Quality control of the datasets obtained from the scanned Affymetrix arrays was performed using Bioconductor [195] packages integrated in an on-line pipeline [196]. Probe sets were redefined according to Dai *et al.* [197] utilising current genome information. In this study, probes were reorganised based on the Entrez Gene database (remapped CDF v14.1.1). Normalised expression estimates were obtained from the raw intensity values using the Robust Multiarray Analysis (RMA) pre-processing algorithm available in the Bioconductor library affyPLM using default settings [198]. Differentially expressed probe sets were identified using linear models, applying moderated t-statistics that implemented empirical Bayes regularization of standard errors [199]. A Bayesian hierarchical model was used to define an intensity-based moderated T-statistic (IBMT), which takes into account the degree of independence of variances relative to the degree of identity and the relationship between variance and signal intensity [200]. Only probe sets with a fold-change (FC) of at least 1.2 (up/down) and p value < 0.05 were considered to be significantly different. Pathway analysis was performed by Gene Set Enrichment Analysis (GSEA) [201] [202], and visualized in Cytoscape (http://www.ncbi.nlm.nih.gov/pubmed/20656902).

Microbiota profiling and multivariate integration and correlation analysis

Microbiota composition was determined using the Mouse Intestinal Tract Chip (MITChip) as previously described [203], and analysed as described in supplementary methods. To get insight into the interactions between changes in gene expression and microbiota composition, the datasets per time point were combined using the linear multivariate method partial least squares (PLS) [232], as described before [233]. By this integration the different genotypes in the study are not taken into account, but the two datasets were integrated per individual mouse. For 14 mice both gene expression and microbiota composition data was available at 2 weeks. Both datasets were log2 transformed before analysis and the canonical correlation framework of PLS was used [234]. The correlation matrices were visualized in clustered image maps [235]. Analyses were performed in R using the library mixOmics [236].

3

Results

***Muc2*+/- mice have altered mucus properties compared to WT mice, but do not develop histopathological features of colitis**

Alcian blue-staining was used to identify acidic carbohydrates, and Periodic Acid Schiff (PAS) for neutral carbohydrates, both of which occur on the Muc2 glycoprotein. PAS-positive and combined PAS-Alcian blue-positive goblet cells were observed in the colon of WT and *Muc2*+/- mice. In contrast, goblet cells in *Muc2*-/- mice only stained slightly positive for PAS (Fig. 1B). Moreover, these PAS-positive cells did not stain positive for MUC2 and lacked the swollen morphology typical of goblet cells. As expected a secreted mucus layer was absent *Muc2*-/- mice (not shown).

Muc2+/- mice had fewer Muc2-positive goblet cells than WT mice (Fig. 1B). The relative amount of *Muc2* transcript was not significantly different between WT and *Muc2*+/- due to large biological variation (Fig. 1C). Nevertheless, the mucus was significantly thinner in *Muc2*+/- compared to WT mice, supporting the hypothesis that this genotype produces less mucus (Fig. 2).

From 4 weeks of age, colitis was observed in the proximal colon of *Muc2*-/- mice, coinciding with altered crypt architecture, increased crypt length, and mild infiltration of lymphocytes in the lamina propria (Fig. 1A). In *Muc2*-/- there were increased numbers of proliferative enterocytes (Ki67-positive), and Caspase 3-positive apoptotic cells present within the crypt epithelium, compared to WT colon tissue (Fig. 3). In contrast no distinct morphological differences were observed between WT and *Muc2*+/- at 2, 4, and 8 weeks (Fig. 1A).
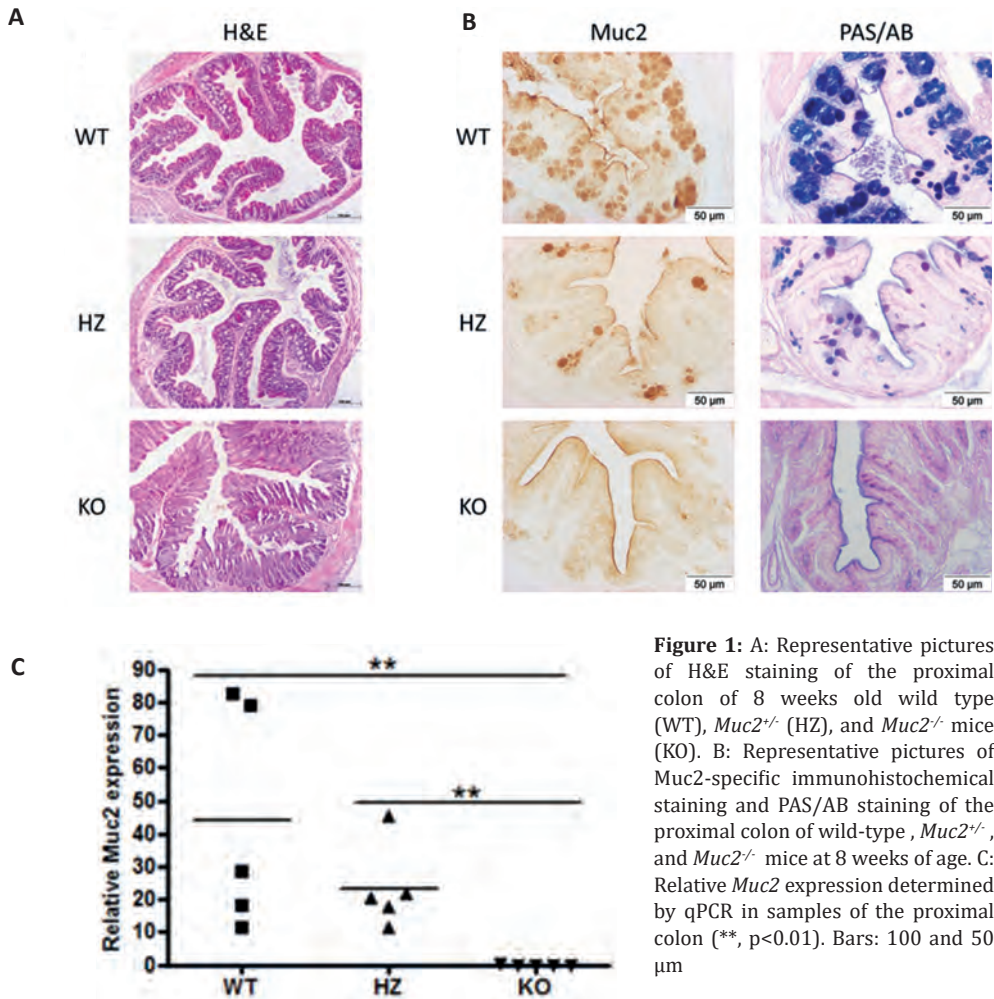
Figure 1: A: Representative pictures of H&E staining of the proximal colon of 8 weeks old wild type (WT), *Muc2*$^{+/-}$ (HZ), and *Muc2*$^{-/-}$ mice (KO). B: Representative pictures of Muc2-specific immunohistochemical staining and PAS/AB staining of the proximal colon of wild-type , *Muc2*$^{+/-}$, and *Muc2*$^{-/-}$ mice at 8 weeks of age. C: Relative *Muc2* expression determined by qPCR in samples of the proximal colon (**, p<0.01). Bars: 100 and 50 µm

In WT mice we observed a clear spatial separation of the microbiota and the epithelium (Fig. 4A). At many locations in the colon of *Muc2*$^{-/-}$ mice the microbiota was observed in direct contact with epithelial surfaces and deep in the crypts (Fig. 4C), which was never observed in the WT. Bacteria were also occasionally seen in direct contact with epithelium of *Muc2*$^{+/-}$ mice (Fig. 4B), presumably due to the thinner colonic mucus layer (Fig. 2).
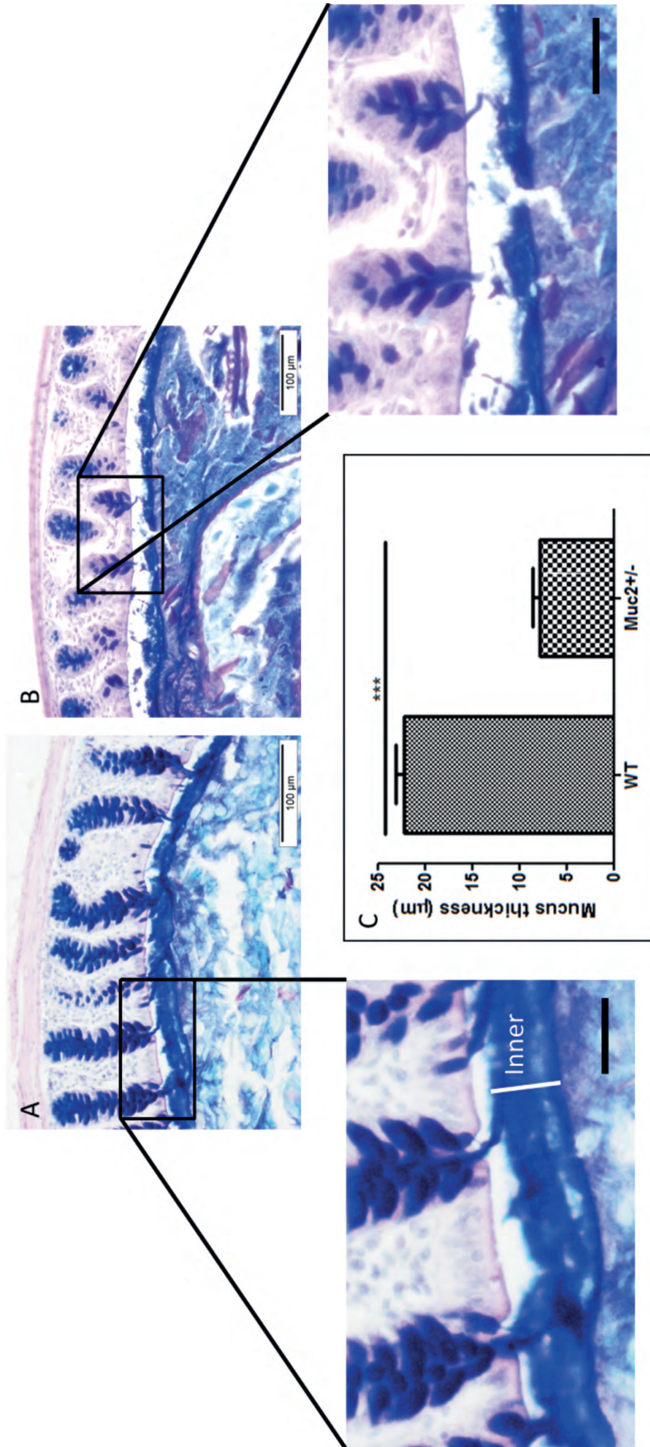
Figure 2: A: Representative pictures of PAS/Alcian blue of the proximal colon of 8 weeks wild type (WT) (A) and *Muc2*$^{+/-}$ mice (B). The inner mucus layer thickness (white bar) has been measured using ImageJ software (***, p<0.001) (C). Scales: 100 μm and 20 μm
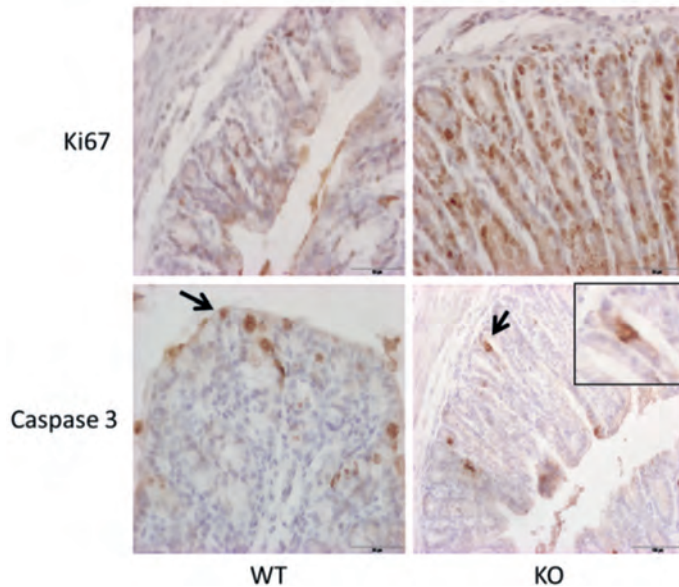
Figure 3: Ki67- and Caspase 3-staining of sections of the proximal colon of wild-type (WT) and *Muc2*-/- (KO) mice. All scale bars are 50 μm. The arrows indicate apoptotic cells, which are located primarily in the surface epithelium in WT, but predominantly near the bottom of the crypts in the *Muc2* knockout animals.
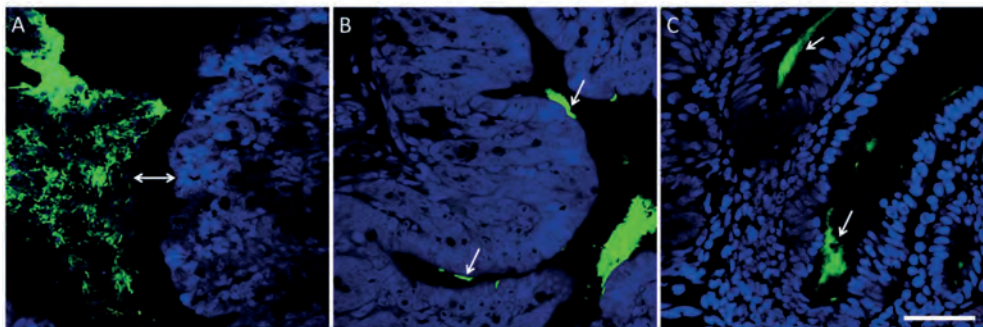

Figure 4: FISH analysis of the proximal colon of wild-type (A), *Muc2*+/- (B) and *Muc2*-/- (C) using the general bacterial probe EUB338-Alexa Fluor 488 (green) and nuclei staining DRAQ5 (blue). Scale for all panels identical, bar: 50 μm. Double arrow indicates the usually observed 'gap' between the microbiota and the epithelium in the wild-type (panel A), whereas the gap is in fact the unstained mucus-layer. The single arrows point to bacteria on epithelium (panel B) and deep within the crypt (panel C).

Weaning leads to a transient peak in the number differentially induced or repressed gene transcripts in both *Muc2*-/- and *Muc2*+/- mice

At all ages both the *Muc2*-/- and *Muc2*+/- mice showed altered gene expression in the colon, compared to WT (Fig. 5). At week 4, there were substantially larger numbers of differentially induced or repressed gene transcripts in the colon of *Muc2*-/- and *Muc2*+/- mice than at week 2 or 8 (Fig. 5).

Many differentially expressed genes in *Muc2*-/- and *Muc2*+/- mice were associated with induction of immune pathways and epithelial remodelling (see below and Fig. 6). At week 4 histopathological signs of colitis were evident in the *Muc2*-/- mice and inflammatory

pathway responses persisted to the end of the experiment (week 8). However, in *Muc2*^{+/-} mice some differentially expressed genes encoding cytokines, chemokines and cytokine receptors induced at week 4 were not altered at week 8 compared to WT mice.
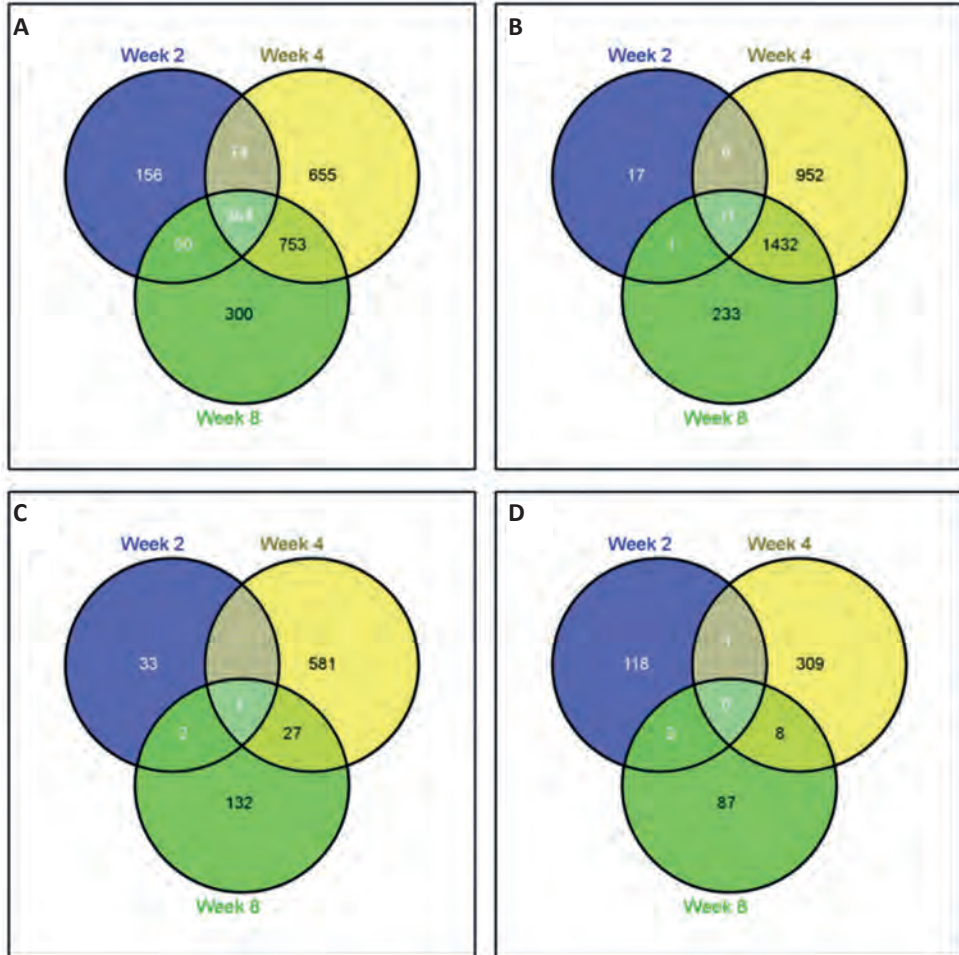
Figure 5: Venn diagram of the number of genes up-regulated (A, C) and down-regulated (B, D) in the proximal colon of *Muc2*^{-/-} (A, B) and Muc2^{+/-} (C, D) mice, compared to wild-type (WT) mice (p value < 0.05) at weeks 2, 4, and 8.

Pathways related to inflammation, cell death, ECM remodelling and cell cycle are upregulated in the colon of *Muc2*^{-/-} mice

To gain insight into the pathways affected in *Muc2*^{-/-} and *Muc2*^{+/-} mice, a Gene Set Enrichment Analysis (GSEA) [201] was performed, comparing changes in gene expression in *Muc2*^{+/-} and *Muc2*^{-/-} mice to WT at the intervals from week 2 to 4 and week 2 to 8. From week 2 to week 4, comparing *Muc2*^{-/-} with WT mice, the major cellular pathways differentially induced involve innate signalling, B and T cell activity, antigen processing,

anti-viral response, and IgA production; compatible with immune activation and inflammatory responses in the colonic mucosa. The strong induction of pathways involved in cell cycle and mitosis most likely indicates increased immune and/or epithelial cell proliferation and/or turnover (Fig. 6A and B).

GSEA week2-week4

GSEA week4-week8
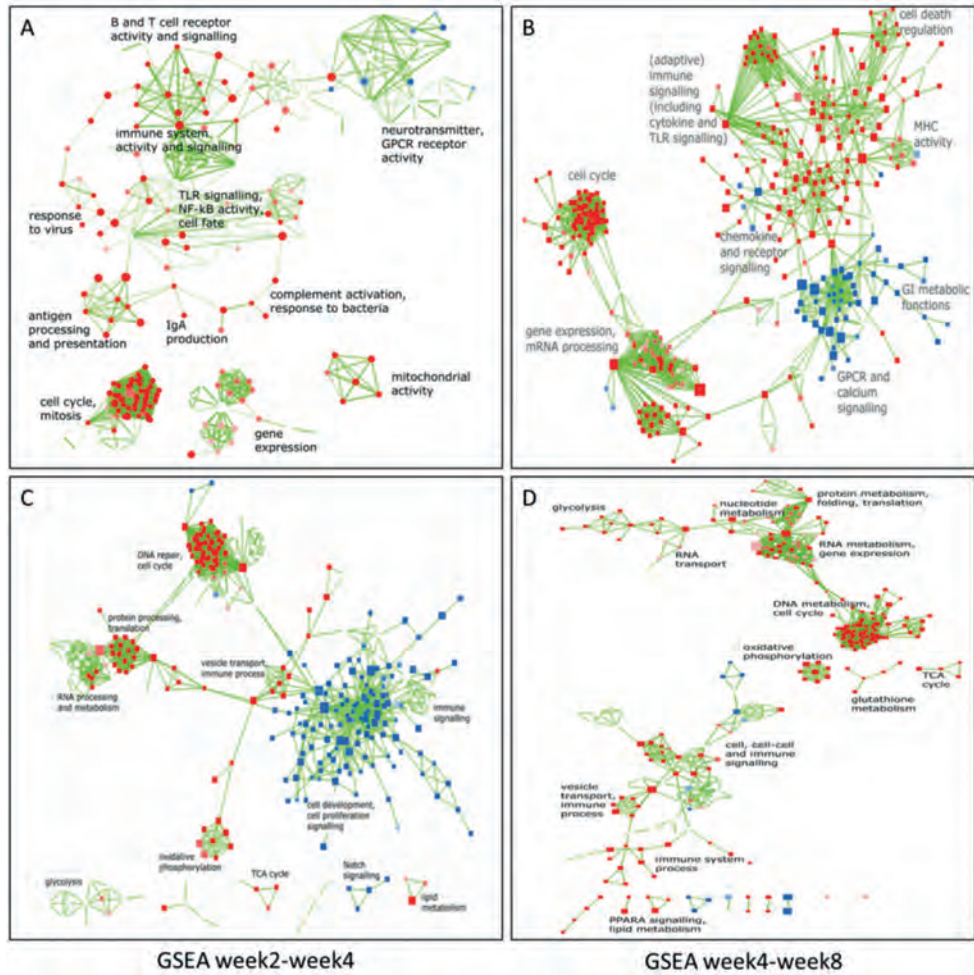
Figure 6: Network representation of gene set enrichment analysis (GSEA) profile of up-regulated (red) or down-regulated (blue) pathways in the proximal colon of *Muc2* knockout mice compared to wild-type mice at A) week 2 versus week 4 and B) week 4 versus week 8. Network representation of gene set enrichment analysis (GSEA) profile of up-regulated (red) or down-regulated (blue) pathways in the proximal colon of *Muc2*^{+/-} mice compared to wild-type mice at C) week 2 versus week 4, and D) week 4 versus week 8. The 'geography' of these representation has no implicit meaning. Nodes are coloured in more intense shades of red depending on strength of induction; or nodes are coloured in more intense shades of blue depending on strength of repression.

Several nodes in the gene networks for neurotransmitter and G protein-coupled receptor (GPCR) activity were down-regulated at week 4 in colon of *Muc2*^{-/-} mice (Fig.

6A). At week 8, similar gene sets were increased in the colon of *Muc2*^{-/-} mice as in week 4, with the addition of induced expression of genes linked to chemotaxis of granulocytes, interleukin (IL)-12 signalling and glutathione metabolism (redox homeostasis) (Fig. 6).

Seven of the 32 IBD-related genes significantly altered in expression in human IBD [224], were differentially expressed in the colon of *Muc2*^{-/-} mice at week 2 compared to WT mice (Table 1), including two matrix metalloproteinases (MMPs) that contribute to epithelial and endothelial barrier disruption and enable immune cells to infiltrate into the tissue.

Table 1: A comparison of the differentially expressed genes, involved in human IBD [224], in the colon of *Muc2*^{-/-} and heterozygote *Muc2*^{+/-} mice. Up- or down-regulated genes, compared to WT, at different time points as indicated. NS = non-significant.

Gene	Name	Genes regulated in IBD					
		Week2		Week4		Week8	
		Muc2^{+/-}	Muc2^{-/-}	Muc2^{+/-}	Muc2^{-/-}	Muc2^{+/-}	Muc2^{-/-}
Cytokine and cytokine receptor genes:							
Tnf	Tumor necrosis factor	NS	NS	NS	2.03	NS	1.84
Ifngr1	Interferon-γ receptor 1	NS	NS	NS	NS	NS	NS
Ltb	Lymphotoxin β	NS	1.38	NS	1.33	1.24	1.46
Il6ra	Interleukin 6 receptor	NS	NS	NS	NS	NS	NS
Il16	Interleukin 16	NS	NS	NS	NS	NS	NS
Il18r1	Interleukin 18 receptor 1	NS	NS	NS	NS	NS	NS
Il22ra1	Interleukin 22 receptor 1	NS	NS	NS	1.25	NS	NS
Il22ra2	Interleukin 22 receptor 2	1.26	2.19	1.30	NS	NS	-1.43
Chemokine and chemokine receptor genes:							
Ccr2	CCR2	NS	NS	NS	1.74	NS	1.38
Ccr7	CCR7	NS	NS	NS	NS	NS	NS
Ccl2	JE (hu:MCP-1)						
Ccl3	MIP-1α	NS	NS	1.37	NS	NS	1.89
Ccl5	RANTES	NS	1.28	NS	NS	NS	NS
Ccl7	MARC (hu:MCP-3)	NS	NS	1.36	NS	NS	NS
Ccl11	Eotaxin	NS	NS	NS	-1.57	NS	NS
Ccl17	TARC	NS	NS	NS	NS	NS	NS
Ccl20	MIP-3	NS	-1.42	NS	NS	NS	NS
Cxcr3	CXCR3	NS	NS	NS	NS	NS	NS
Cxcl1	Chemokine (C-X-C motif) ligand 1	NS	NS	NS	NS	NS	NS
Cxcl5	Chemokine (C-X-C motif) ligand 5						
Cxcl10	IP-10	NS	NS	NS	NS	NS	1.62

Gene involved in tissue remodeling:							
Mmp3	Stromelysin 1	NS	NS	NS	NS	1.25	1.55
Mmp7	Matrilysin	1.51	2.19	NS	1.28	1.29	1.25
Mmp9	Gelatinase B	NS	NS	NS	1.45	NS	NS
Mmp14	Membrane type1-MMP	NS	NS	NS	1.31	NS	1.20
Timp1	Tissue inhibitor of metalloproteinase 1	NS	1.13	1.34	1.32	NS	1.74
Regenerating islet-derived genes:							
Reg3g	Regenerating islet-derived 3 gamma	NS	2.41	1.72	2.25	NS	1.82
Pap	Pancreatitis associated protein	NS	NS	NS	NS	NS	NS
S-100 family genes							
S100-a8	S-100 calcium binding protein a8	NS	NS	NS	NS	NS	NS
S100-a9	S-100 calcium binding protein a9	NS	NS	NS	NS	NS	NS
Multidrug resistance gene:							
Abcb1a	ATP-binding cassette, subfamily B (MDR/TAP), member 1A	NS	NS	NS	-1.56	NS	-1.52
Gene involved in epithelial metabolism and biosynthesis:							
Ptgs2	Prostaglandin-endoperoxide Synthase 2 (COX-2)	NS	NS	NS	1.20	NS	1.49

At week 4, 13 IBD-related genes were up-regulated, and 14 were up-regulated at week 8, concomitant with major tissue damage. IBD-related genes differentially expressed in *Muc2^{-/-}* mice at weeks 4 and 8 were MMPs *Mmp3, Mmp7*, *Mmp9*, *Cxcl10*, *IL-22ra2* and *IL-22ra1*, which were all up-regulated except for the IL-22 receptor (*IL-22ra1*) at week 8. Relative expression of the IL-22 receptor (*IL-22ra1*) was increased at week 4 and week 8 compared to week 2, whereas, *IL-22ra2*, the soluble antagonist of *IL-22ra1*, was significantly down-regulated at these times. The most strongly down-regulated gene at week 4 and 8 was *Abcb1a*, a gene expressing an epithelial cell surface-located transporter that is proposed to export toxins from the mucosa into the lumen.

Interestingly, seven other of these IBD-related genes *Ltb*, *IL22ra2*, *Ccl5*, *Ccl20*, *Mmp7*, *Timp 1* and *Reg3γ* were already altered before the onset of histopathology. These genes are related to mucosal healing and defences, and chemotactic responses. A heat-map was generated for immunity genes including those that encode PRRs, cytokines, antimicrobial (poly)peptides, components of the NF-κB pathway, T cell markers (CD3e) and T-helper (CD4), Tregs (Foxp3), and Th17 (RORγδ) subsets that were differentially expressed in the proximal colon of *Muc2^{-/-}* vs. WT mice at weeks 2, 4, and 8 (Fig. 7).

In *Muc2^{-/-}* mice transcription of several TLR genes was up-regulated (*Tlr4, -7, -8, -9, -12,* and *-13*), whereas *Tlr2* and *Tlr5*, which were strongly repressed at weeks 4 and 8.

The genes encoding antimicrobial stress proteins *Reg3β* and *Reg3γ* were strongly up-regulated, but the beta-defensin (Defb)37 encoding gene was down-regulated. The up-regulated *Tnf-α*, *Cd3ε*, *Cd4*, and *Cd8* suggest an increased infiltration and/or activity of T cells. At 2 weeks, even before histological signs of colitis were apparent, many immune-related genes were upregulated in the colon. This included inflammatory cytokines, T cell markers, innate defence factors and regulators of inflammatory processes such as inhibitor of NF-κB epsilon and the soluble antagonist of IL-22 receptor signalling.
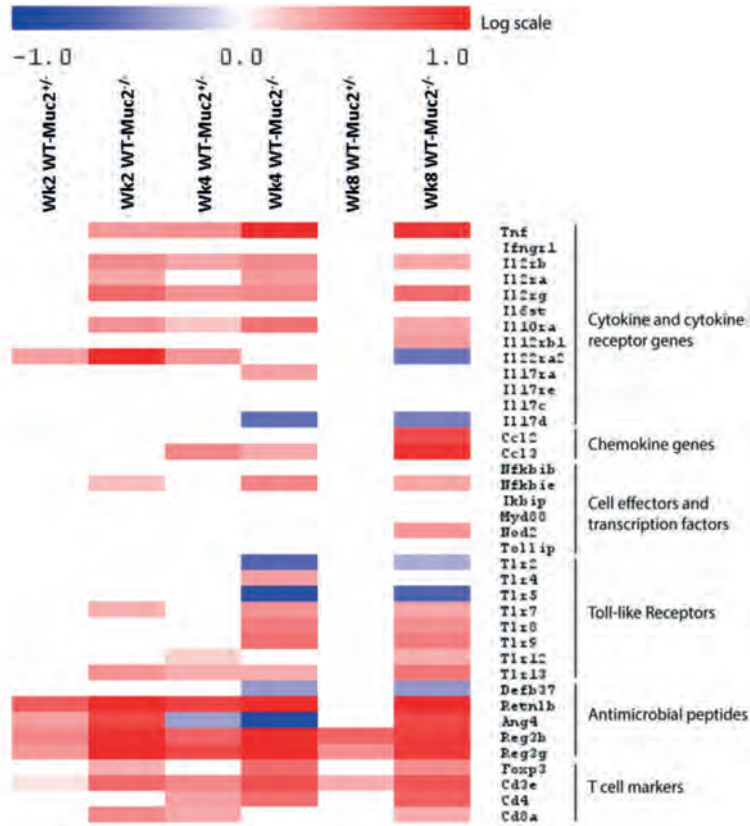
Figure 7: Heat maps of immunity-related genes differentially expressed in proximal colon, using genes differentially expressed in *Muc2*−/− versus wild-type (WT), or *Muc2*+/− versus wild-type (WT) mice with week 8 as a reference. In red genes are represented, which are up-regulated and in blue the genes that are down-regulated. The intensity of the colour is related to the level of expression.

The transcriptome of *Muc2*+/− mice reveals a homeostatic response to decreased mucus production

A large number of differentially expressed genes are identical in *Muc2*+/− and *Muc2*−/− mice when compared to WT at each age, suggesting that these changes are brought about by similar mechanisms in both genotypes. For example, of the genes differentially

regulated at week 2, 19 were up-regulated and 36 down-regulated in both *Muc2*^{+/-} and *Muc2*^{-/-} mice (data not shown). GSEA of the networks affected in the proximal colon of *Muc2*^{+/-} revealed that DNA repair, energy metabolism and cell cycle pathways were strongly up-regulated at weeks 2, 4, and 8 (Fig. 6C and D). Expression of these pathways was also altered in *Muc2*^{-/-} mice compared to WT although the magnitude of the changes was greater than in *Muc2*^{+/-} mice. Even though *Muc2*^{+/-} mice do not develop colitis, IBD-related genes *IL-22ra2* and *Mmp3* were differentially expressed in *Muc2*^{+/-} mice compared to WT at week 2; this increased to 5 genes (*IL-22ra*, *Ccl3*, *Ccl7*, *Timp1*, and *Reg3γ*) at week 4, and 3 genes (*Ltb*, *Mmp3,* and *Mmp7*) at week 8 (Table 1). Genes up-regulated in both *Muc2*^{-/-} and *Muc2*^{+/-} mice at either weeks 4 or 8 encode cytokines *(Ccl3*, *Ccl22)*, antimicrobial protein *(Reg3γ)*, tissue-remodelling enzymes *(Mmp3*, *Mmp7*, and *Timp1),* and lymphotoxin B. These genes are involved in innate defence including chemotactic functions as well as remodelling of the extracellular matrix and mucosal healing, both signs of tissue destructive processes.

Muc2 deficiency affects colon microbiota composition, diversity, and richness in early life

16S ribosomal RNA (rRNA) gene derived microbiota profiles were obtained from faeces of 2-, 4-, and 8 weeks-old WT, *Muc2*^{+/-}, and *Muc2*^{-/-} mice. At 2 weeks, the faecal content of *Muc2*^{-/-} mice displayed a significantly higher microbial diversity than WT and *Muc2*^{+/-} mice (P<0.05), due to increased richness of the profiles as measured at the probe level (Fig. 8A and B).

Furthermore, redundancy analysis (RDA) established that at weeks 2, 4, and 8 the microbiota composition could be discriminated on basis of the host's genotype (Fig. 9A - C). The differences in colonic microbiota composition of *Muc2*^{-/-} mice and the other groups of mice were largest at week 2 and decreased over time (Fig. 9C). The WT mice are characterized by higher relative abundances of members of the *Clostridium* clusters IV and XIVa compared to the *Muc2*^{-/-} mice at each time point. *Bifidobacterium*, a well-known early life microbe in humans, had also higher relative abundances in the WT relative to the *Muc2*^{-/-} mice at weeks 2 and 4, but not at 8 weeks. Remarkably, the microbiota composition of *Muc2*^{+/-} mice displays an intermediate situation between the WT and *Muc2*^{-/-} mice at all time points (Fig. 9A-C).

Taking the diversity, richness, and RDA plots into account there are indications that in WT and *Muc2*^{+/-} mice there is an initial colonization by a more constrained group of bacteria (2 weeks), which reached higher relative abundance in the WT and *Muc2*^{+/-} mice, compared to the *Muc2*^{-/-} mice that are colonized by a more diverse microbial community. During further development of the colonic ecology at 4 and 8 weeks, the microbiota composition becomes more similar among mice with different genotypes, both with respect to diversity and richness as well as in composition.
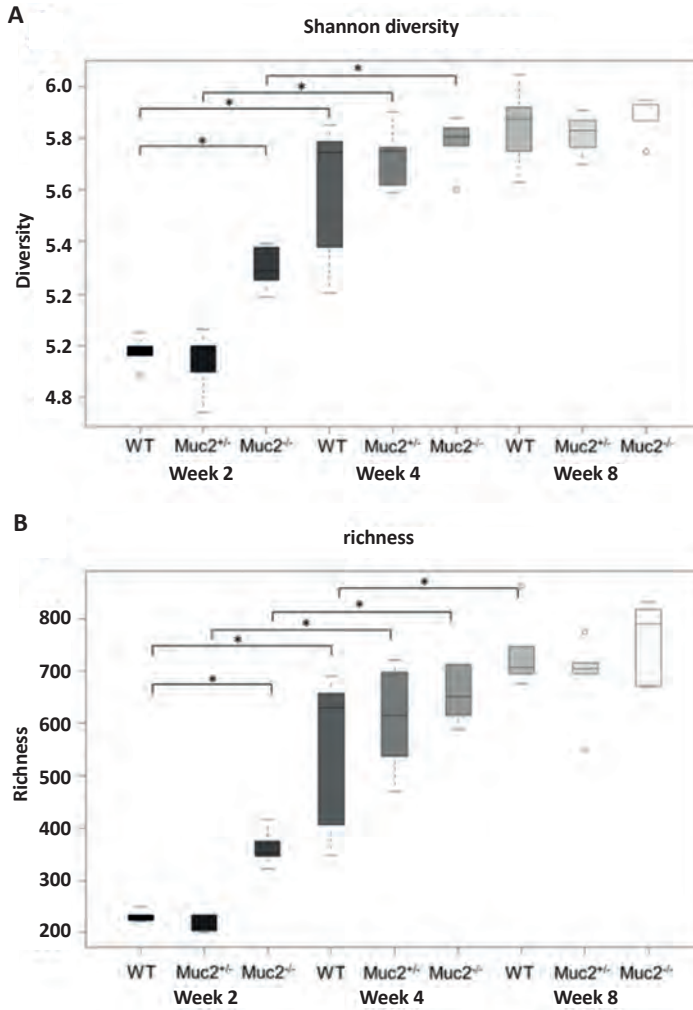
Figure 8: Box-and-whiskers-plot showing the diversity (Shannon index) of microbiota in colon of WT, *Muc2*^{+/-} and *Muc2*^{-/-} mice (A). Box-and-whiskers-plot showing the richness of microbiota in colon of WT, *Muc2*^{+/-}, and *Muc2*^{-/-} mice (B). Statistically significant differences among groups and time points were indicated (*, p<0.05).

Figure 9: Redundancy Analysis (RDA) representing microbial ecology of *Muc2⁻/⁻* (green cluster), *Muc2⁺/⁻* (red cluster), and WT (black cluster) in the proximal colon at weeks 2 (A), 4 (B), and 8 (C). Scores of all individual mice are indicated in each of panels A-C; the clusters include all mice within a given genotype.

Specific bacterial clusters correlate with altered gene expression of mucosal responses to stress and bacteria, prior to colitis development

To identify bacteria that might be correlated with early changes in colon gene expression, we focused on the data from week 2, which was prior to the onset of any histopathology in the *Muc2*$^{-/-}$ mice. Microbiota and transcriptomics data from week 2 were combined for individual mice of all genotypes to investigate direct correlations between gene expression and microbiota composition in these samples. Age and genotype were the major drivers of changes in gene expression and microbial composition (Fig. 6 and 8), and thus in this analysis, any correlations found between gene expression and microbiota will be the implicit result of variation in genotype. Four bacterial clusters strongly correlated positively (red) or negatively (blue) with six clusters of genes (about 100 genes per cluster; Fig. 10).
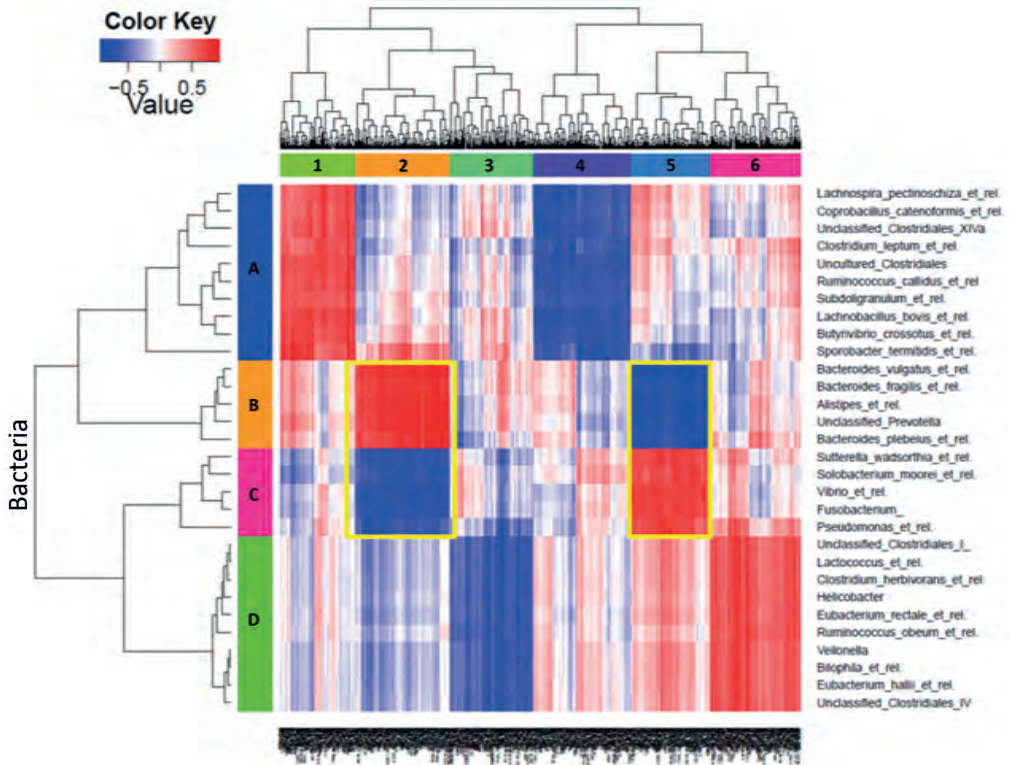
Figure 10: Heat-map of correlation analysis of MITChip (vertical) and transcriptome (horizontal) datasets at week 2. The integration of datasets was done per individual and gives direct correlation between gene expression and microbiota composition over these samples. The genotypes are the largest driver for differences in gene expression and microbiota composition, which is reflected in the high correlation clusters in the plot. In deep red, the cluster of genes that most positively correlated with one group of bacteria. In deep blue, the cluster of genes that most negatively correlated with a respective group of bacteria. Framed in yellow the clusters discussed in more detail in the text of this chapter.

Strongest correlations between microbiota members (orange in the vertical bar) and specific changes in mucosal gene expression (orange and blue in horizontal bar) were detected for *Bacteroides plebeius et rel.*, unclassified *Prevotella*, *Alistipes et rel.*, *Bacteroides fragilis et rel.*, and *Bacteroides vulgatus et rel.* (Fig 10). These bacteria had higher relative abundances (data not shown) in the *Muc2*^{-/-} mice compared to WT and displayed a positive correlation with immune response genes. A positive correlation was also found with stress response genes involved in apoptosis and cell proliferation (Table 2). Conversely, other microbial groups (pink in the vertical bar) displayed opposite correlations with the same mucosal gene sets, including *Pseudomonas et rel.*, *Fusobacterium vibrio et rel.*, *Solobacterium moorei et rel.*, and *Sutterella wadsorthia et rel.*.

Discussion

Previously, microarray analysis and qPCR of gene transcripts from colon of *Muc2*^{-/-} and WT mice at 2 and 4 weeks of age revealed distinct phases in colitis development pre- and post-weaning, which were presumed the result of changes in microbiota diversity and/or density [193]. Here we extended these comparisons to 8 weeks of age, as the first several days after weaning are characterized by a relatively chaotic pattern of microbial colonization leading towards an adult-like microbiota, and driving transient host-microbiota responses that lead to an adult-microbiota accommodating homeostatic state [237]. As predicted, the largest number of differentially expressed genes in *Muc2*^{-/-} compared to WT mice was found at weaning (1607 genes) and subsequently reduced to 533 genes in week 8. The pathways differentially expressed from week 2 to week 8 in *Muc2*^{-/-} compared to WT mice were diverse immune pathways consistent with immune activation and inflammatory responses in the colonic mucosa. There was also a strong induction of pathways involved in cell death, cell cycle, mitosis and remodelling of the extracellular matrix, as a response to the tissue destructive processes observed by histology. As in other mouse models of colitis a substantial number of the 32 genes known to be up- or down-regulated in human IBD (Table 1) [224] were differentially expressed in the colon of *Muc2*^{-/-} mice compared to WT mice [201, 224]. The most strongly up-regulated genes include genes encoding MMPs, an important family of metal-dependent enzymes that are responsible for the breakdown and reconstitution of extracellular matrix (ECM) in normal physiological processes, like tissue remodelling, during development, growth and wound repair. These ECM remodelling enzymes are also up-regulated in human IBD and rodent models of colitis and linked to loss of epithelial barrier integrity, inflammation and tissue destruction.

Table 2: Gene ontology terms from the gene cluster 2 (orange in the horizontal bar) correlated with microbiota (orange and pink vertical bars) as shown in figure 10. *; genes significantly up-regulated (Fold-change > 1.2 ; p value < 0.05).

GOID	GOTerm	Pvalue	GeneCount	GeneName
GO:0043170	macromolecule metabolicprocess	0.003191	53	
GO:0044260	cellular macromolecule metabolicprocess	0.006806	47	
GO:0019222	regulation of metabolicprocess	0.009964	39	
GO:0060255	regulation of macromolecule metabolicprocess	0.003132	35	
GO:0006950	response tostress	8.84E-05	28	S100a14*,Fos*,Hbegf*,Il1rn*,Apobec1*,Krt20*,Dsc2,Anxa3*,Casp8,Pdia5*,Proc,Anxa2,Tlr7*, Pik3cg, Txndc5, Mapk13, Cd55, Hmgcl, Foxa3, Ruvbl2, Optn, Tnfrsf14, Nudt16,Os9,Eno3, Clca3*, Ang4*,Pnliprp2
GO:0009605	response to externalstimulus	2.62E-05	22	Itln1, S100a14*, Fos*, Il1rn*, Apobec1*, Ccl9*, Dsc2, Anxa3, Lgals3, Casp8, Proc,Anxa2,Pla2g10*,Tlr7*,Pik3cg,Cd55,Hmgcl,Foxa3,Optn,Tnfrsf14,Ccl6*,Ang4*
GO:0051246	regulation of protein metabolicprocess	0.00188	17	
GO:0002376	immune systemprocess	0.005061	17	S100a14*, Fos*, Il1rn*, Apobec1*, Ccl9*, Anxa3, Lgals3, Casp8, Anxa2, Pla2g10, Tlr7,Pik3cg,Klf10, Cd55, Tnfrsf14, Ccl6*,Ang4*
GO:0043207	response to external bioticstimulus	0.000484	11	
GO:0051707	response to otherorganism	0.000484	11	Itln1,S100a14*,Fos*,Il1rn*,Apobec1*,Anxa3,Casp8,Tlr7*,Optn,Tnfrsf14*,Ang4*
GO:0009607	response to bioticstimulus	0.000754	11	
GO:0044092	negative regulation of molecularfunction	0.006828	10	
GO:0001944	vasculaturedevelopment	0.001773	9	
GO:0001525	angiogenesis	0.000516	8	
GO:0009617	response tobacterium	0.001775	8	S100a14*,Fos*,Il1rn*,Anxa3*,Casp8,Optn,Tnfrsf14*,Ang4*
GO:0048514	blood vesselmorphogenesis	0.002008	8	
GO:0001568	blood vesseldevelopment	0.004588	8	

3

Table 2: continued.

GOID	GOTerm	Pvalue	GeneCount	GeneName
GO:0051270	regulation of cellular componentmovement	0.007115	8	
GO:0098542	defense response to otherorganism	0.002368	7	S100a14*,Apobec1*, Anxa3,Tlr7*,Optn,Tnfrsf14*,Ang4*
GO:0071496	cellular response to externalstimulus	0.001336	6	Fos*, Dsc2, Casp8, Tlr7*, Foxa3,Optn
GO:0030335	positive regulation of cellmigration	0.002529	6	
GO:2000147	positive regulation of cellmotility	0.002813	6	
GO:0051272	positive regulation of cellular componentmovement	0.003172	6	
GO:0040017	positive regulation oflocomotion	0.003868	6	
GO:0042594	response tostarvation	0.000947	5	
GO:0042742	defense response tobacterium	0.003503	5	S100a14*, Anxa3*, Optn, Tnfrsf14*, Ang4*
GO:0070613	regulation of proteinprocessing	0.009256	5	
GO:0002573	myeloid leukocytedifferentiation	0.009472	4	Fos*, Casp8, Anxa2,Klf10
GO:0002763	positive regulation of myeloid leukocytedifferentiation	0.001249	3	Fos*, Casp8, Klf10
GO:0007173	epidermal growth factor receptor signalingpathway	0.003741	3	
GO:0045639	positive regulation of myeloid celldifferentiation	0.004638	3	
GO:0038127	ERBB signalingpathway	0.005234	3	
GO:0030316	osteoclastdifferentiation	0.005873	3	
GO:0002687	positive regulation of leukocytemigration	0.006558	3	S100a14*, Lgals3,Tnfrsf14*

In contrast to *Muc2*^{-/-}, the *Muc2*^{+/-} mice did not develop colitis during the 8 week period. However, the colonic mucus layer was significantly thinner in *Muc2*^{+/-} than in WT mice, which was also associated with altered mucosal gene expression. At week 2 and week 8 the affected gene networks in *Muc2*^{+/-} mice were mainly associated with mucosal healing and innate defence including chemotactic functions although there was transient increase in inflammatory genes (e.g. *Tnf* and cytokine receptors for *IFNγ*, *IL-2*) at week 4 resembling the transient inflammatory state observed in colonisation studies with germ-free mice [237]. Thus the *Muc2*^{+/-} genotype appeared to exacerbate the transient inflammatory response to the changing microbial ecology of the colon around weaning. Several of the genes differentially expressed in the *Muc2*^{+/-} mice were IBD-related, for example, the intestinal Reg3 secreted stress proteins and MMPs.

As pathobionts are known to play a role in the pathophysiology IBD we investigated the impact of the *Muc2* genotype on the temporal development of the microbiota at 2, 4, and 8 weeks. Initial colonization of microbiota in WT and *Muc2*^{+/-} mice involved a more constrained group of bacteria as compared to the *Muc2*^{-/-} mice, although during prolonged colonization the microbiota composition became more similar in all mice, but still consistently discriminated the groups of mice according to their genotype. This suggests that Muc2 shapes the microbiota colonising the colon, especially in the 2 weeks postnatal, pre-weaning period, although a role of the antimicrobial factors that were more highly expressed in *Muc2*^{-/-} mice compared to WT or *Muc2*^{+/-} mice can also play a role. In the case of the *Muc2*^{+/-} mice, which still produce a mucus layer, the altered microbiota might be due to the host mucosal responses identified by transcriptomics. The WT mice are characterized by higher relative abundances of members of the *Clostridium* clusters IV and XIVa compared to the *Muc2*^{-/-} mice. A decrease in abundance of these *Clostridium* clusters, which are members of the phylum Firmicutes have been consistently described in many studies on IBD patients [225].

To identify bacteria that might be correlated with early changes in colon gene expression we used the linear multivariate method PLS method [232] for each time point, as previously described [233]. Interestingly these analyses revealed that even at 2 weeks, therefore prior to the onset of colitis in the *Muc2*^{-/-} mice, *Bacteroides plebeius et rel.*, Unclassified *Prevotella*, *Alistipes et rel.*, *Bacteroides fragilis et rel.*, and *Bacteroides vulgatus et rel.* were positively correlated with the induction of mucosal gene expression associated with immune and stress responses (Table 2). These bacterial groups were more abundant in *Muc2*^{-/-} mice than in WT littermates. An increased relative abundance of Bacteroidetes has been observed in only some animal models of colitis [238] [239]. Nevertheless, *B. thetaiotaomicron* and *B. vulgatus* have been demonstrated to induce colitis in experimental rodent models, in which other commensal species do not induce colitis [227] [240] [241] [242]. *Nod2* mutations that disrupt bacterial recognition are one of the highest risk factors for CD. Recently expansion of *B. vulgatus*, was shown to mediate exacerbated

inflammation in *Nod2*$^{-/-}$ mice upon small-intestinal injury, providing further evidence for its colitogenic potential in IBD [243]. A subset of intestinal *B. fragilis* strains produce an exotoxin (ETBF strains) associated with diarrheal disease and a number of studies have shown associations of this species with IBD and colorectal cancer [244].

Recently, inflammation was shown to select for modifications of the Bacteroidetes lipopolysaccharide, which increased their resistance to inflammation-associated antimicrobial peptides by four orders of magnitude [245]. These findings support the idea that in *Muc2*$^{-/-}$ mice, the innate inflammatory responses driven by increased contact of commensals with the epithelium leads to increased abundance of colitogenic members of the Bacteroidetes phylum, which contribute to the onset of colitis.

Acknowledgements

Chapter 4

Intestinal barrier impairment in ageing mice predispose to "inflammageing" in the intestinal mucosa

Bruno Sovran[1,3], Floor Hugenholtz[5], Marlies Elderman[3,4], Adriaan A. Van Beek[1,3], Katrine Graversen[2], Myrte Huijskes[2], Mark V. Boekschoten[1,7], Michiel Kleerebezem[1,2,6], Huub F.J. Savelkoul[3], Paul De Vos[1,4], Jan Dekker[2] and Jerry M. Wells[1,2]

[1] Top Institute Food and Nutrition, Wageningen, the Netherlands
[2] Host-Microbe Interactomics Group, Wageningen University and Research Center, Wageningen, the Netherlands
[3] Cell Biology and Immunology Group, Wageningen University and Research Center, Wageningen, the Netherlands
[4] University Medical Center of Groningen, Groningen, the Netherlands
[5] Laboratory of Microbiology, Wageningen University and Research Center, the Netherlands
[6] NIZO food research, Ede, the Netherlands
[7] Division of Human Nutrition, Wageningen University and Research Center, Wageningen, the Netherlands

Abstract

There is a major lack of knowledge on how ageing affects intestinal physiology. Understanding age-related changes in the intestine and their impact on the microbiota and immune regulation is a goal of clear relevance to health and longevity as it provides us with insights for new strategies to prevent degeneration of intestinal barrier functions. The aims were to investigate effects of ageing on mouse intestinal physiology, morphology, mucus barrier properties, immune regulation, and bacterial compartmentalization.

C57BL/6 mice (litter mates) were sacrificed respectively at 10 weeks and 19 months of age. Carnoy's solution fixed sections of ileum and colon were used to investigate tissue morphology, mucus barrier thickness, and spatial compartmentalization of bacteria to the lumen. Faecal microbiomics and tissue transcriptomics were used to determine effects of ageing on microbiota and mucosa physiology, including immunity.

Aged mice showed marked changes in intestinal morphology compared to young adult mice. The colonic mucosa was thicker with more immune cell infiltration than in younger mice. Furthermore, the mucus layer was reduced about 6-fold relative to young mice, and was more easily penetrable by luminal bacteria. H&E stained tissue sections of the small intestinal mucosa of old and young mice were similar in appearance. However, a noticeable difference in old mice was that the mucus was more easily penetrable by luminal bacteria. Transcriptomics data indicate a significant down-regulation of innate and adaptive immunity in small and large intestine of old mice. Microbiomics data show a significant decrease in *Akkermansia muciniphilia* and *Lactobacillus gasseri* in old mice.

We conclude that ageing has marked effects on the gut barrier, including mucosal thickening and mucus depletion. In old mice there is increased contact between the epithelium and microbiota associated with chronic low-grade mucosal inflammation and a dysbalanced microbiota, implicated in the pathology of several chronic disorders.

Introduction

Ageing is an ill-defined process involving changes in various body systems, which converts a mature, fit person into an increasingly infirm one. With the passage of time, individuals show decreasing cell-protection mechanisms and detrimental physiological changes in metabolic processes and physiological functions of various tissues including the heart, brain, and skeletal muscles [138]. This leads to increased morbidity and mortality due to autoimmune diseases, cancer and infectious disease [134][135][149], as well as a decline of mental health, well-being, and cognitive abilities [136][137].

One of the most important effects of the ageing process is a significant decline of the efficacy of both the adaptive and innate immune systems, which has been described in several species [246][247]. Studies on oral and parenteral vaccination in naturally ageing mice showed that age-associated decrease in antigen-specific immune responses occurs earlier in the mucosal immune system than in systemic immune system [166]. It is considered that aged humans exhibit a loss of naive T cells and a more restricted T cell repertoire [150]. Furthermore, aging results in decreased human $CD8^+$ cytotoxic T lymphocyte responses, restricted B cell clonal diversity, failure to produce high-affinity antibodies, and an increase in memory T cells [151][152]. It has been suggested that although certain dendritic cell (DC) populations are fully functional in ageing [153][154], both foreign and self-antigens induce enhanced pro-inflammatory cytokines [155][155]. This enhancement of inflammation can be detrimental. However, very old individuals with a more balanced pro- and anti-inflammatory phenotype may be the most fortunate [156][157]. The association of inflammation in ageing has been termed 'inflammageing' [158].

Aging significantly increases the vulnerability to gastrointestinal (GI) disorders with approximately 40% of geriatric patients reporting at least one GI complaint during routine physical examination [142]. Despite the need to further understand age-associated factors that increase the susceptibility to GI dysfunction, there is a paucity of studies investigating the key factors in aging that affect the GI tract. To date these studies suggest in old baboons (1). An increase in inflammatory cytokines [167] and miR-29a a potential biomarker for colorectal neoplasia; (2). A decline in the IgA-mediated mucosal immunity [166]; (3). Increased intestinal permeability to macromolecules with age [145][146]. Specifically, advancing age was shown to correlate with an enhanced transepithelial permeability of D-mannitol, indicating that there may be an age-associated decline in barrier function [147]; and (4). Altered intestinal smooth muscle contractility [143], as well as the neural innervations of the GI tract musculature [144]. In humans, the decreased intestinal motility results in a slower intestinal transit leading to constipation [148].

The human microbiome is reported to have increased abundance of *Bacteroides* ssp. in elderly subjects (>65 years) [159][160]. However, other authors have concluded that

differences in the microbiota of humans are only seen in centenarians with increased inflammatory cytokine responses, and not in elderly subjects with an average age 70 ± 3 years [161]. In centenarians, the microbiota differs significantly from the adult-like pattern, by having a low diversity in terms of species composition. Bacteroidetes and Firmicutes still dominate the gut microbiota of extremely old people (representing over 93% of the total bacteria) but compared to younger adults, there was a decreased abundance of the Firmicutes subgroups, specifically *Clostridium* cluster XIVa, an increase in Bacilli, and a rearrangement of the *Clostridium* cluster IV composition [161]. Moreover, the gut microbiota of centenarians is enriched in Proteobacteria, a group containing ''pathobionts'', shown to cause harm in a compromised or susceptible host [162] [163].

To avoid chronic inflammatory reactions to the intestinal microbiota, mammals minimize contact between luminal microorganisms and the intestinal epithelial cell surface. This is achieved primarily through the secretion of mucus by goblet cells in the epithelium, in addition secretion of antimicrobial factors and IgA into the lumen also play a role by inhibition of bacterial growth and immune exclusion of bacteria [29] [188]. The highest densities of bacteria are found in the colon and here the mucus forms a thick stratified inner layer which is impermeable to bacteria and a loose outer layer mixed with bacteria and luminal content [66]. Both mucus layers have essentially the same composition, suggesting the outer mucus layer arises from limited proteolytic cleavage and volumetric expansion of the inner layer.

Mucus is formed from Muc2 the major secreted intestinal mucin and its absence in *Muc2⁻/⁻* mice leads to colitis, which starts in the distal colon and spreads to the proximal colon [248] [193]. Colitis is associated with increased microbiota diversity and an early colonization with pathobionts such as *Bacteroides fragilis* (Chapter 3). Moreover it has been shown that even decreased Muc2 production, as observed in *Muc2⁺/⁻* mice perturbs intestinal homeostasis and microbiota composition (Chapter 3). This highlights the importance of mucus quantity and quality in the maintenance of intestinal homeostasis. Mucosal inflammation negatively effects the mucus barrier with decreased production and increased permeability to bacteria which if unresolved leads to a vicious cycle of inflammation and barrier destruction [110] [111].

Given the age-dependent effects on the gut barrier described to date we hypothesized that the mucus barrier may be affected in old age and that this could have a major impact on mucosal physiology and the microbiota. To date knowledge of the impact of ageing on the human mucus barrier is limited to studies on gastric mucus [117] [249]. Moreover none of the studies in ageing mice have deeply investigated the effects of age on physiology of the small and large intestine. Such knowledge might provide new insights into the dynamics of the interplay between the host and microbiota in elderly and have implications for future interventions, for example by manipulation of the

microbiota. We investigated age-dependent changes in mucus barrier and the impact on mucosal physiology using histology, (immuno)-histology and Fluorescent *in situ* Hybridization (FISH) techniques to obtain temporal data on morphological changes, mucus production, and compartmentalization of bacteria in the lumen. Additionally microbiota composition was determined with Mouse Intestinal Tract Chip (MITChip) and transcriptomics data was obtained from colonic tissue.

Materials and Methods

Animals

C57BL/6 mice (Harlan Laboratories, USA) were housed in a specific pathogen-free environment with *ad libitum* access to D12450B diet (10% fat) (Research Diets Services BV, Wijk bij Duurstede, the Netherlands), and acidified tap water in a 12-hour light/dark cycle. The University Medical Center of Groningen (UMCG) Animal Ethics Committee (Groningen, the Netherlands) approved the animal experiments.

Experimental set up

Groups of 8-week-old males (n=5) were housed in individual ventilated cages, and sacrificed at 8 weeks and 19 months of age. Ileal and colonic tissues were fixed in Carnoy's fixative and embedded in paraffin as previously described [123]. Additionally, segments of ileum and colon were frozen in liquid nitrogen and stored at -80°C for RNA and protein assays. Faecal material was collected at 2, 8, 13, 15, and 19 months (sacrifice) and stored at -80°C.

Histology

Paraffin sections (5 μm) of ileum and colon were attached to poly-L-lysine-coated glass slides (Thermo scientific, Germany). After overnight incubation at 37°C, slides were de-waxed and hydrated step-wise using 100% xylene followed by several solutions of distilled water containing decreasing amounts of ethanol. Sections were stained with hematoxylin and eosin (H&E) and Periodic Acid Schiff (PAS)/Alcian blue [194]. Mucus layer thickness was measured (10 measurements per section / 2 sections per animal / 5 animals per condition) using Image J software (NIH, Maryland, USA).

Immunohistochemistry

The slides were deparaffinised and antigen retrieval was performed by heating the sections for 20 min in 0.01 M sodium citrate (pH 6.0) at 100°C. Sections were washed for 3 h with 3 changes of Tris-Buffered Saline (TBS). Non-specific binding was reduced using 10% (v/v) goat serum (Invitrogen, Life technologies Ltd, Paisley, UK) in TBS for 30 min at room temperature. T cells CD3 marker was detected by

incubating the sections with anti-CD3 antibody (Invitrogen, Life technologies Ltd, Paisley, UK) diluted 1:100 in TBS, overnight at 4°C. Leukocytes were detected by incubating the sections with anti-CD45 antibody diluted 1:100 in TBS, overnight at 4°C. Paneth cells were identified staining for the lysozyme expression, detected by incubating the sections with anti-lysozyme antibody (Invitrogen) diluted 1:100 in TBS, overnight at 4°C. Cell proliferation marker Ki67 was detected by incubating the sections with anti-Ki67 antibody (Abcam, Cambridge Science Park, Cambridge, UK) diluted 1:200 in TBS, 90 min at room temperature. Apoptotic cells were identified by staining for cleaved-Caspase 3 expression using an anti-Caspase-3 antibody (Abcam) diluted 1:200 in TBS, overnight at 4°C. Muc2 was detected by staining of the sections with anti-Muc2 antibody (kindly gifted by Dr. Gunnar Hansson) diluted 1:500 in TBS, and goat-anti-rabbit Alexa 488 conjugated antibody (1:1000) (Molecular Probes, Life Technologies Ltd, Paisley, UK) in TBS.

Detection of bacteria using fluorescent *in situ* hybridization (FISH)

The slides were deparaffinised with xylene and rehydrated in a series of ethanol solutions to 100% ethanol. The tissue sections were incubated with the universal bacterial probe EUB338 (5'-GCTGCCTCCCGTAGGAGT-3') (Isogen Bioscience BV, De Meern, the Netherlands) conjugated to Alexa Fluor488. A 'non-sense' probe (5'-CGACGGAGGGCATCCTCA-3') conjugated to Cy3, was used as a negative control. Tissue sections were incubated overnight with 0.5 µg of probe in 50 µL of hybridization solution (20 mmol/L Tris-HCl (pH 7.4), 0.9 mol/L NaCl, 0.1% (w/v) SDS) at 50°C in a humid environment using a coverslip to prevent drying of the sample. The sections were washed with (20 mmol/L Tris-HCl (pH 7.4), 0.9 mol/L NaCl) at 50°C for 20 min and then washed 2 times in PBS for 10 min in the dark and incubated with DRAQ5 (Invitrogen) (1:1000) for 1 h at 4°C to stain nuclei. Sections were washed 2 times in PBS for 10 min, mounted in fluoromount G (SouthernBiotec, Alabama, USA) and stored at 4°C.

Transcriptome analysis

Quantity and quality of colonic and ileal RNA (5 arrays of individual mice per group) was assessed using spectrophotometry (ND-1000, NanoDrop Technologies, Wilmington, NC, USA), and Bionanalyzer 2100 (Agilent, Santa Clara, CA, USA), respectively. RNA was only used to generate cDNA and perform microarray hybridisation when there was no evidence of RNA degradation (RNA Integrity Number > 8). 100 ng of total RNA was labelled using the Ambion WT Expression kit (Life Technologies Ltd, Paisley, UK) together with the Affymetrix GeneChip WT Terminal Labelling kit (Affymetrix, Santa Clara, CA, USA). Labelled samples were hybridised to Affymetrix GeneChip Mouse Gene 1.1 ST arrays. Hybridisation, washing, and scanning of the array plates were performed on an Affymetrix GeneTitan Instrument, according to the manufacturer's

recommendations.

Quality control of the datasets obtained from the scanned Affymetrix arrays was performed using Bioconductor [195] packages integrated in an on-line pipeline [196]. Probe sets were redefined according to Dai *et al.* [197] utilising current genome information. In this study, probes were reorganised based on the Entrez Gene database (remapped CDF v14.1.1). Normalised expression estimates were obtained from the raw intensity values using the Robust Multiarray Analysis (RMA) pre-processing algorithm available in the Bioconductor library affyPLM using default settings [198].

Differentially expressed probe sets were identified using linear models, applying moderated t-statistics that implemented empirical Bayes regularization of standard errors [199]. A Bayesian hierarchical model was used to define an intensity-based moderated T-statistic (IBMT), which takes into account the degree of independence of variances relative to the degree of identity and the relationship between variance and signal intensity [200]. Only probe sets with a fold-change (FC) of at least 1.2 (up/down) and p value < 0.05 were considered to be significantly different. Biological interaction networks among regulated genes activated in response to ageing were identified using Ingenuity Pathways Analysis (IPA) (Ingenuity System). IPA utilizes a large expert-curated repository of molecule interactions, regulatory events, gene-to-phenotype associations, and chemical knowledge, mainly obtained from peer-reviewed scientific publications, that provides the building blocks for network construction. IPA annotations follow the GO annotation principle, but are based on a knowledge base of > 1,000,000 protein-protein interactions. The IPA output signalling pathways with statistical assessment of the significance of their representation based on Fisher's Exact Test. Our IPA analyses compared differentially regulated genes in the ileum and colon of old males compared to young mice. The input was all differentially regulated genes (p value < 0.05, FC > 1.2 and intensity > 20) of ileum and colon.

Bacterial DNA extraction and microbiota profiling

The DNA from ileal content and faeces was extracted using the repeated bead-beating-plus column method [250]. Microbiota composition was analysed by Mouse Intestinal Tract Chip (MITChip), a diagnostic 16S rRNA array that consists of 3,580 unique probes especially designed to profile mouse intestine microbiota [203]. 16S rRNA gene amplification, *in vitro* transcription and labelling, and hybridization were carried out as described previously [204]. The data was normalized and analysed using a set of R-based scripts in combination with a custom-designed relational database, which operates under the MySQL database management system. For the microbial profiling the Robust Probabilistic Averaging (RPA) signal intensities of 2667 specific probes for the 94 genus-level bacterial groups detected on the MITChip were used

[205]. Diversity calculations were performed using a microbiome R-script package (https://github.com/microbiome). Multivariate statistics, redundancy analysis (RDA), and Principal Response Curves (PRC), were performed in Canoco 5.0, and visualized in triplots or a PRC plot [206].

Multivariate integration and correlation analysis

To get insight into the interactions between changes in gene expression and microbiota composition, the datasets per time point were combined using the linear multivariate method partial least squares (PLS) [232], as described before [233]. By this integration, the two datasets were integrated per individual mouse. Both datasets were log2 transformed before analysis and the canonical correlation framework of PLS was used [234]. The correlation matrices were visualized in clustered image maps [235]. Analyses were performed in R using the library mixOmics [236].

Results

Age-associated changes in the intestine

In H&E stained ileum tissue of 19-month old mice and young (8 weeks old) mice (Fig. 1), the villi were significantly (p<0.001) longer in 19 month-old mice compared to young mice (Fig. 1E). This phenomenon was recently linked to perturbation of intestinal homeostasis [251]. Additionally lymphoid structures resembling solitary intestinal lymphoid tissue (SILT) [252] were observed more frequently in colon of 19 month-old mice than 8 week old mice and comprised mainly of CD45-positive haematopoietic cells, B-cells (B220-positive cells) and some CD3-positive T-cells (Fig. 1F-I).

In the ileum of old mice there were fewer lysozyme-positive cells at the bottom of the crypts than in young mice, suggesting reduced Paneth cell activity and redeced production of innate antimicrobial factors (Fig. 2).
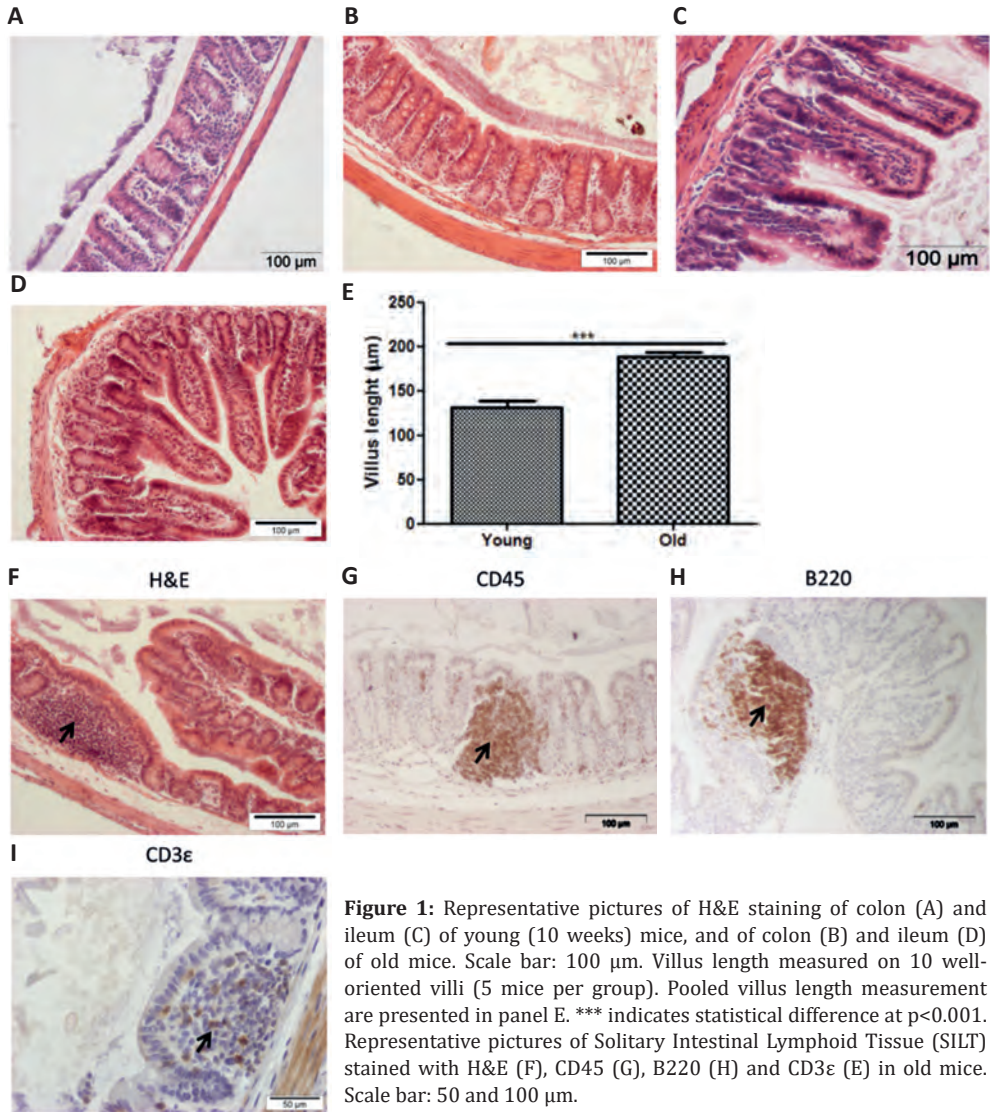
Figure 1: Representative pictures of H&E staining of colon (A) and ileum (C) of young (10 weeks) mice, and of colon (B) and ileum (D) of old mice. Scale bar: 100 μm. Villus length measured on 10 well-oriented villi (5 mice per group). Pooled villus length measurement are presented in panel E. *** indicates statistical difference at p<0.001. Representative pictures of Solitary Intestinal Lymphoid Tissue (SILT) stained with H&E (F), CD45 (G), B220 (H) and CD3ε (E) in old mice. Scale bar: 50 and 100 μm.
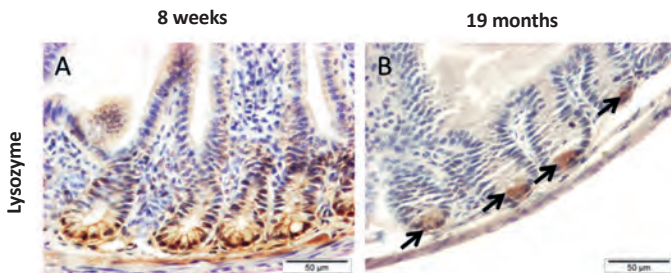
Figure 2: Representative immune histochemistry of lysozyme in ileal tissues from 8 week-old (A) and 19 month-old (B) mice. Scale bar: 50 μm. Arrows point to a SILT.

The inner mucus layer is thinner in old mice than young mice and permeable to bacteria

Alcian blue-staining was used to identify acidic carbohydrates like Muc2, and PAS for neutral carbohydrates, both of which occur on the Muc2 glycoprotein. In wild-type mice we observed a firm layer of mucus (around 25 µm thick) covering the colon epithelium. The mucus appeared to be organised into stacked layers with a stratified appearance as previously described [66]. Mice 19 months of age showed a much thinner (1-5 µm) than 8 week-old mice, or even an absent mucus layer (Fig. 3B-D). The mucus layer was even thinner or absent on top of the SILT, due to the absence of mucus-secreted goblet cells in this area (Fig. 3H).
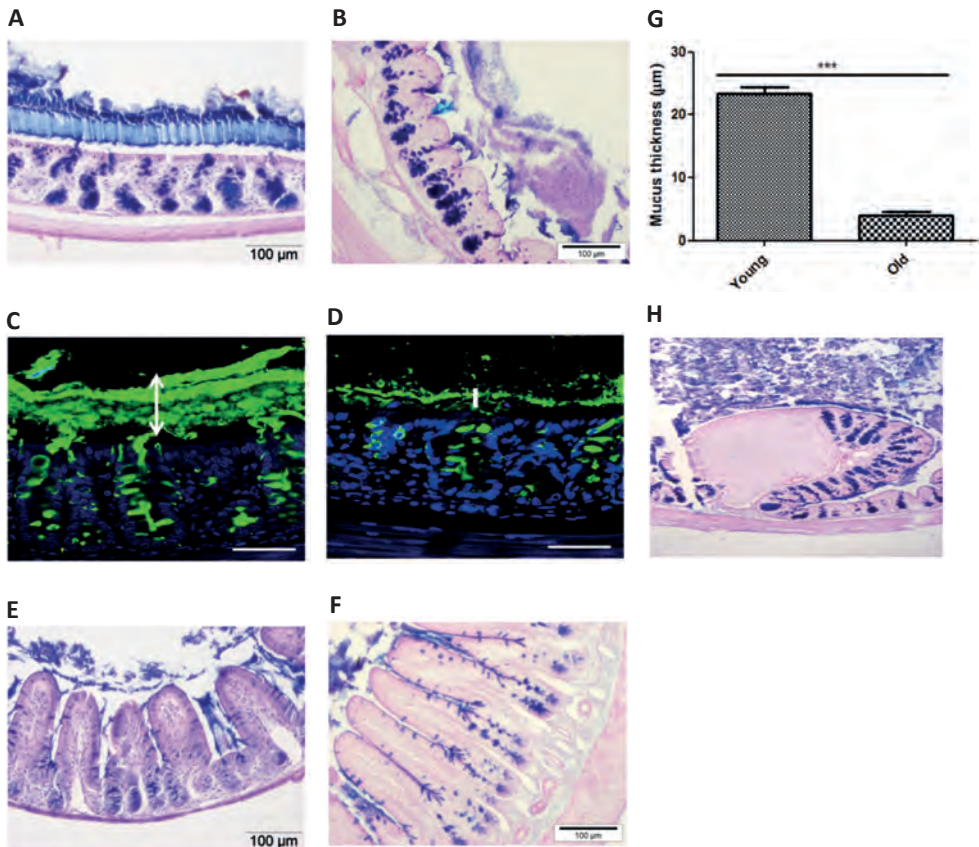

Figure 3: Representative pictures of PAS/Alcian Blue staining of colon (A) and ileum (E) of 10 week-old mice, and of colon (B) and ileum (F) of 19 months-old mice. Scale bars: 100 µm. Muc2 staining (in green; cell nuclei in blue) of colon of young mice (C) and old mice (D). Double arrow represents the mucus layer (C). Vertical bar represents the mucus layer thickness (D). Horizontal white bars represents the scale of 50 um. Scale bars: 50 µm. Mucus thickness measured (10 measurements per section, 2 sections per animal) in 5 colonic tissues of young and old mice, respectively. Pooled mucus measurements are presented in panel G. *** indicates statistical difference at p<0.001. Representative pictures of PAS/Alcian Blue staining of colonic SILT (H).

The effect of ageing on the spatial compartmentalisation of bacteria in both small intestine and colon was investigated by FISH. The thinner mucus layer in old mice was associated with increased contact of the epithelium with intestinal microbiota. For example, in small intestine and colon of young mice we observed in a clear "gap" of about 50 μm in between the microbiota and the epithelium (Figs. 3 and 4). This "gap" corresponded to the thick mucus layer in between the surface of the epithelium and the luminal content (Fig. 4).
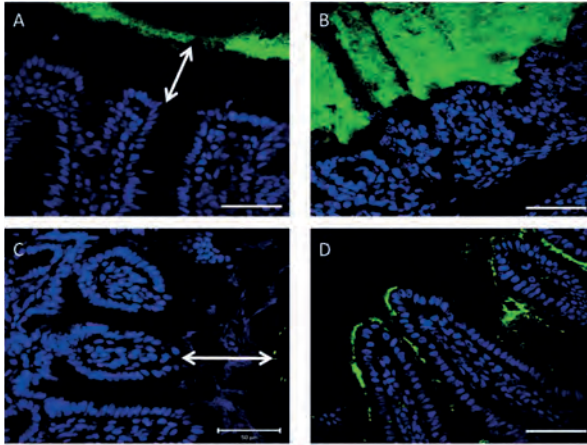
Figure 4: FISH analysis of sections of the colon (A) and ileum (C) of 8 week-old mice using the general bacterial probe EUB338-Alexa Fluor 488 (green), and nuclear staining DRAQ5 (blue), and similar analysis of sections of the colon (B) and ileum (D) of 19 month-old mice. Arrows indicate the distance between bacteria and epithelium. Scale bars: 50 μm.

At many locations in the small intestine and colon of 19 month-old mice the microbiota was frequently observed in direct contact with epithelial surfaces, due to a dysfunctional mucus barrier, which was never observed in the young mouse (Fig. 4).
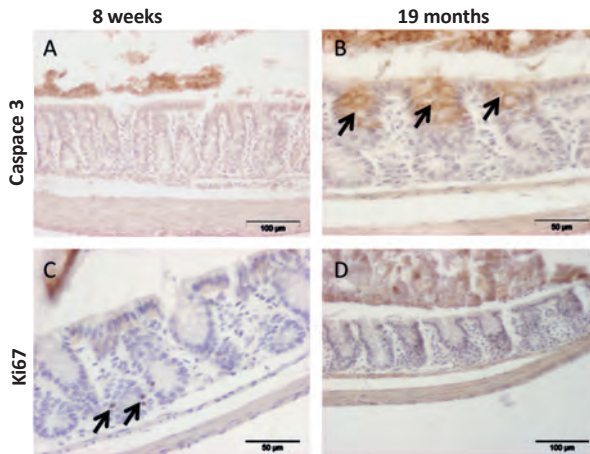
Figure 5: Caspase 3 (A-B) and Ki67 (C-D) staining of colon in young control (8 weeks) and old (19 months) mice. Arrows show apoptotic goblet cells in old colon (B) and proliferative cells in crypts of young control (C). Scale bars: 50 and 100 μm.

Apoptotic cell staining in colon tissue (cleaved Caspase 3) showed a significant proportion of goblet cells in the upper part of the crypts were apoptotic (Fig. 5A and B). No compensatory epithelial proliferation (Ki67 staining) was observed in aged

mice to counter balance goblet cell apoptosis. As a consequence, aged mice have less mucus-producing cells than their younger counterparts, explaining the reduced mucus thickness (Fig 5D), without a decrease in *Muc2* transcription (data not shown).

Genes functioning in innate and adaptive immunity pathways are down-regulated in the colon and ileum of ageing mice

In the large intestine, a transcriptomics approach was used to gain more insight into the potential pathways and mechanisms that might be modulated by the processes of ageing. Applying the following criteria, FC > 1.2, p-value < 0.05 and signal intensity > 20 in at least one of the arrays, we found 1503 differentially expressed genes (759 up-regulated and 744 down-regulated) in old mice versus young mice (data not shown).

A heat-map was generated for immunity-related genes, including those that encode pattern recognition receptors (PRRs), cytokines, chemokines, immunoglogulins, antimicrobial (poly)peptides, T cell markers (CD3ε), and T-helper (CD4 or CD8) and Tregs (Foxp3) subsets that were differentially expressed in the proximal colon of 19 month-old mice (Fig. 6A). The down-regulated *Cd3ε*, *Cd4*, and *Cd8* suggest a decreased abundance of T cells. The strong down-regulation of chemokine genes and immunoglobulin expression suggest a decrease in immune responsiveness and B cell activity.

In the ileum 930 genes were found expressed (428 up-regulated and 502 down-regulated) in old versus young mice (data not shown). The Gene Ontology Biological Processes annotations of the differentially expressed genes showed that processes predominantly related to adaptive immunity were strongly down-regulated in the small intestine of old mice.

The most down-regulated pathways were CTLA4 Signalling in Cytotoxic T Lymphocytes, T Cell Receptor Signalling, Natural Killer Cell Signalling, Role of NFAT in Regulation of the Immune Response, CD28 Signalling in T Helper Cells (Supplementary data, Fig. S1).

An expression heat-map was generated for immunity-related genes including those that encode pattern recognition receptors (TLRs etc.), cytokines, chemokines, immunoglogulins, antimicrobial (poly)peptides, T cell markers (CD3ε) and T-helper (CD4 or CD8) and Tregs (Foxp3) subsets that were differentially expressed in the ileum of 19 month-old males (Fig. 6B). As found in the colon, genes related to innate and adaptive immunity were strongly down-regulated in old mice compared to young mice.

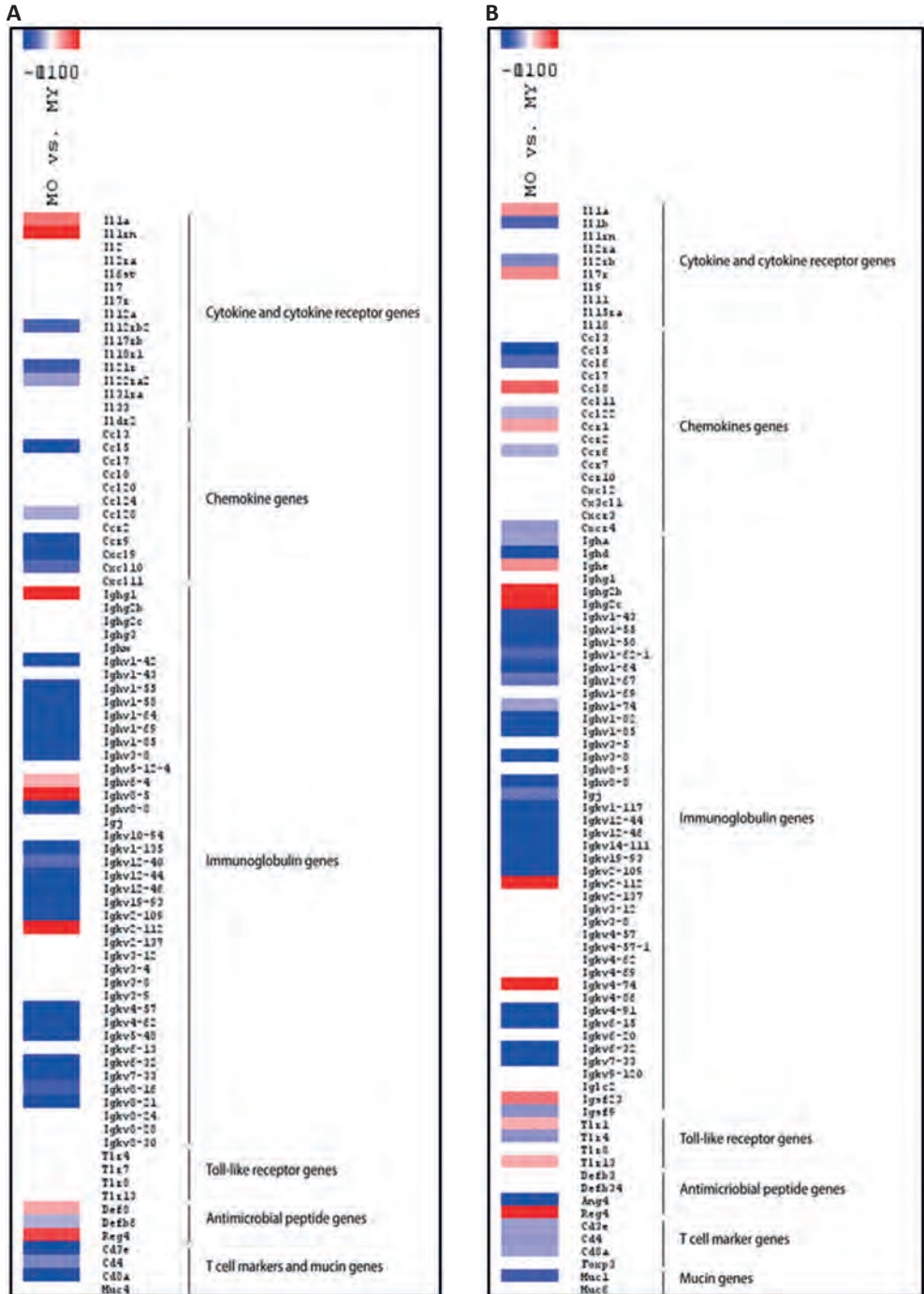**Figure 6:** Heat maps of immunity-related genes differentially expressed in proximal colon (A) and ileum (B), using genes differentially expressed in old (O) versus young (Y) mice. In red, genes are represented, which are up-regulated and in blue the genes that are down-regulated. Scale: Log2 (FC) = -1 (blue) < 0 (white) < 1 (red). The intensity of the colour is proportional to change in expression.

Ageing is associated with altered intestinal microbiota

To investigate the impact of ageing on the colonization pattern of the colon, 16S DNA microbiota profiles of faeces from 2.5, 8, 13, 15, and 19 month-old C57BL/6 mice were determined using the MITChip microarray [203]. The faecal content of 15 - and 19 months-old mice displayed a significantly higher microbial diversity than young mice ($P < 0.05$), due to increased richness in bacterial taxonomic units (Fig. 8). The intermediate ages (7 and 12 months) displayed similar diversity and richness as the young mice (Fig. 7).
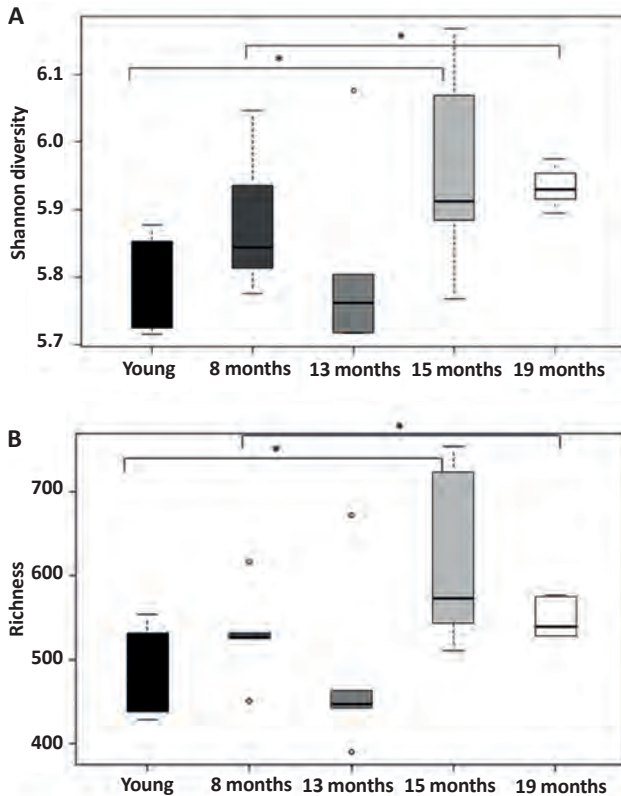
Figure 7: Box-and-whiskers-plot showing the diversity (Shannon index) of microbiota in colon of young (2.5 months), 8 months, 13 months, 15 months, and 19 months of age (A). Box-and-whiskers-plot showing the richness of microbiota in colon of young, 8 months, 13 months, 15 months, and 19 months of age (B). Statistically significant differences among groups and time points were indicated (*, p<0.05).

Nevertheless, redundancy analysis (RDA) clearly established that at 8, 13, 15, and 19 months of age the microbiota composition was clearly distinct compared to 8 week-old mice (Fig. 8).

Akkermansia muciniphila, *Porphyromonas asaccharolytica et rel.*, *Collinsella*, *Corynebacterium et rel.*, and *Lactobacillus gasseri et rel.*, were significantly less present in old mice compared to young mice (Fig. 9), whereas *Lachnospira pectinoschiza et rel.*, and *Butyrivibrio crossotus et rel.*, were significantly more present in old mice (Fig. 9).
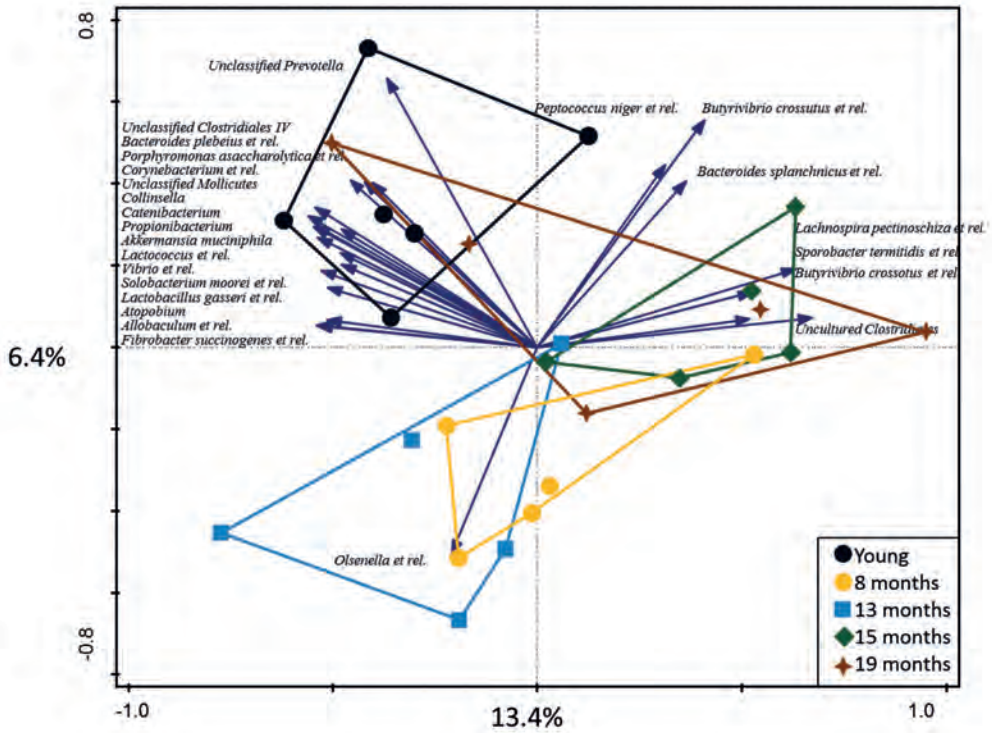
Figure 8: Redundancy Analysis (RDA) representing microbial ecology of young (2.5 months) mice (black cluster), 8 months (yellow cluster), 13 months (blue cluster), 15 months (green cluster) and 19 months (brown cluster) in the faeces.
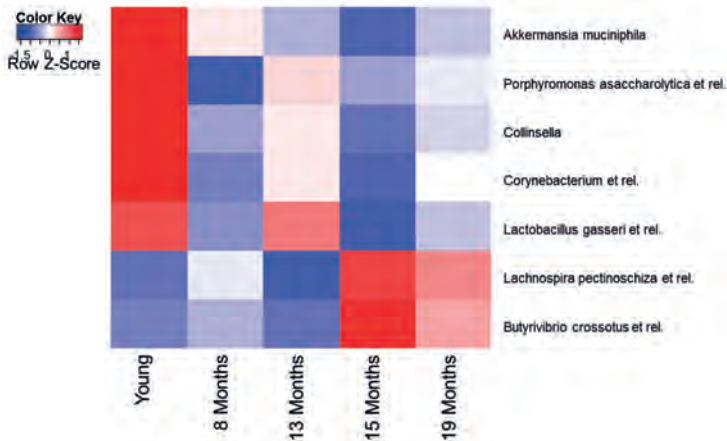
Figure 9: Heat map of bacteria significantly changed within age. In red, bacteria which are significantly more present in faeces and in blue the bacteria that are significantly less present in young (2.5 months, 8 months, 13 months, 15 months and 19 months of age. Scale: Log2 (FC) = -1 (blue) < 0 (white) < 1 (red). The intensity of the colour is proportional to change in bacterial presence.

Specific bacterial clusters correlate with altered gene expression of mucosal responses to bacteria in ageing mice

To identify bacteria that are correlated with observed effects of ageing in colon gene expression, we performed a multivariate integration and correlation analysis on the data from 19 months-old mice. Microbiota and transcriptomics data were pooled for individual mice to investigate direct correlation between gene expression and microbiota composition over these samples. Four bacterial clusters (A-D) strongly correlated either positively (red) or negatively (blue) with 6 clusters of genes (1-6; about 100 genes per cluster) (Fig. 10). The individual genes in the gene cluster 5 are listed in Supplementary material, Table S1.
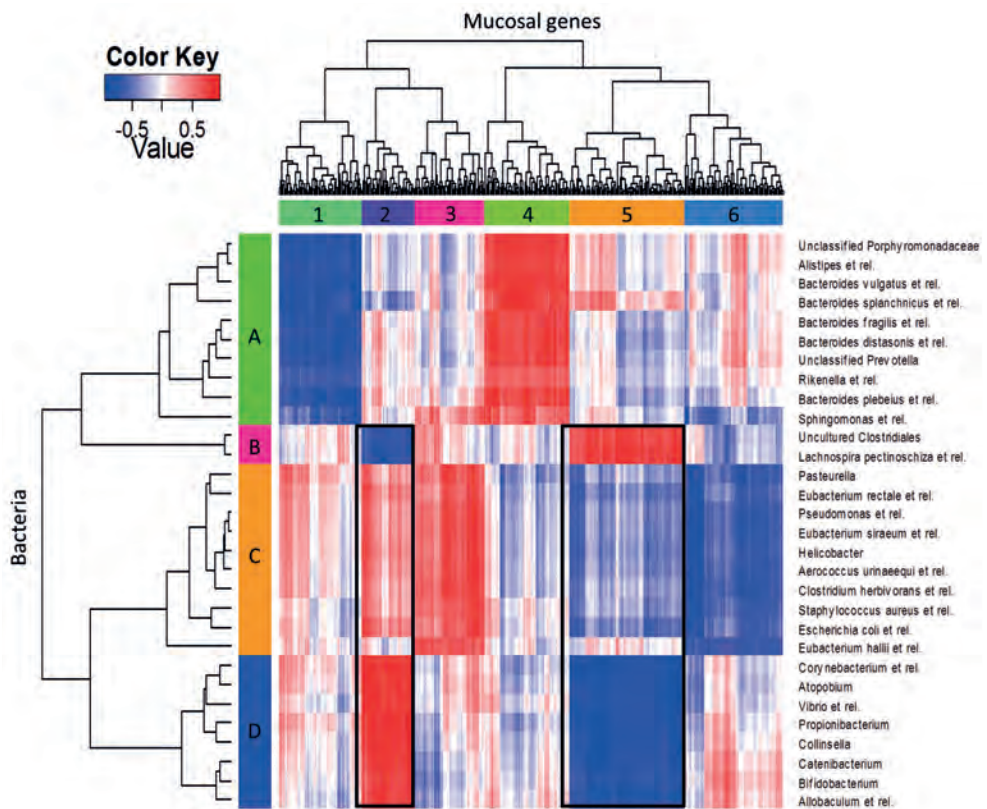
Figure 10: Heat-map of correlation analysis of MITChip (vertical) and transcriptome (horizontal) datasets of mice at 19 months of age. The integration of datasets was done per individual mice (5 mice per group) and gives direct correlation between gene expression and microbiota composition over these samples. In deep red, the cluster of genes that most positively correlated with one group of bacteria. In deep blue, the cluster of genes that most negatively correlated with a respective group of bacteria. The intensity of the colour is proportional to change in expression. Framed in black; the gene clusters 2 and 5 discussed in more detail in the chapter. Six main gene clusters (1-6) and 4 main bacterial clusters (A-D) were identified. The individual genes in the respective gene clusters are listed in Supplementary table S1.

Strongest correlations between microbiota members (cluster B, Fig. 10) and specific changes in mucosal gene expression (clusters 2 and 5) were detected for uncultured Clostridiales and *Lachnospira pectinoschiza et rel.* (Fig. 10). These bacteria had higher relative abundances (Fig. 9) in the mice of 15 and 19 months of age compared to young mice and displayed a positive correlation with immune response genes (gene cluster 5) (Supplementary data, Table S1). A positive correlation was also found with stress response genes involved in apoptosis and cell proliferation, as well as immune genes. Conversely, other microbial groups (indicated blue in the colour key), which are more present in young mice (Figs 9 and 10), displayed opposite correlations with the same mucosal gene sets, including several bacterial groups of Actinobacteria (*Corynebacterium et rel., Atopobium, Bifidobacterium, Collinsella and Propionibacterium*) and the bacterial groups *Vibrio et rel.*, *Allobaculum et rel.*, and *Catenibacterium*.

Discussion

Old age is associated with increased intestinal permeability, reduced sIgA production and susceptibility to gastrointestinal disorders in elderly subjects [164] [166] [147]. However, none of the previous studies in mice or humans investigated the effect of ageing on mucosal tissue transcriptomes or the mucus barrier thickness and permeability. In 19 month old mice the colon mucus was significantly thinner than in young mice. Similar observation were recently reported in colon of rat [249]. In the small and large intestine of 19 month old mice a higher proportion of apoptotic goblet cells were present in the upper part of the crypts, together with less PAS/Alcian blue positive goblet cells than in young mice, supporting the notion that the reduced mucus thickness is due to presence of fewer Muc2 secreting goblet cells. Only the goblet cell lineage appeared to be affected by increased apoptosis and increased epithelial cell proliferation (Ki67 staining) appeared to be unchanged. Another factor potentially contributing to the shrinkage of mucus could be the reduced expression of *Muc1*. In *Muc1*^{-/-} mice shrinkage of the secreted mucus is also observed, independent of any change in *Muc2* gene expression [253]. The reasons for this are not clear but could be related to loss of Muc1 signalling, increased endothelium reticulum stress or loss of interactions between membrane tethered Muc1 and secreted mucin. A consequence of the reduced mucus thickness in old mice was increased contact of luminal bacteria with the colon and ileum epithelium. Surprisingly, this chronic contact of bacteria with epithelium was not associated with the development of colitis, contrary to which was observed in *Muc2*^{-/-} mice (Chapter 3). The absence of colitis could be due to the down-regulation of immunity genes in the mucosa of old mice.

In the colon where bacteria are most abundant, we observed an increased number of lymphoid structures known as SILT. SILT develops early after birth under the

continuous exposure to commensals and potential pathogens [254], and appeared to be mainly composed by B-cells as previously reported [252]. The MyD88 dependence of SILT development is consistent with their higher frequency in old mice and increased epithelial contact with bacteria and bacterial MAMPs.

In old mice transcription of genes related to innate and adaptive immunity such as immunoglobulins (in particular IgA) were strongly down-regulated compared to young mice. The reduced activity of these barrier functions in old mice is likely to contribute to the perturbation of intestinal homeostasis and result in the increased contact of the epithelium with potentially harmful antigens and microbes [29] [188].

The human microbiome of in elderly subjects (around 65 years) has overall a reduced diversity but increased abundance of *Bacteroides ssp.* [159] [160]. This is however, inconsistent with other studies showing that differences in the microbiota of humans are only seen in centenarians with increased inflammatory cytokine responses, and not in elderly subjects with an average age 70 ± 3 years [161]. However, this finding was not observed in old mice. To identify bacteria that might be correlated with changes in colon gene expression we used the linear multivariate method partial least squares (PLS) method [232] for each time point, as previously described [233]. We found that uncultured *Clostridiales* and *Lachnospira pectinoschiza et rel.* had higher relative abundances in the old mice of 15 and 19 months of age compared to young mice and displayed a positive correlation with immune response genes. A positive correlation was also found with stress response genes involved in apoptosis and cell proliferation, as well as immune genes. *Akkermancia municiphilia* was also strongly decreased with ageing. *Akkermansia muciniphila* is a Gram-negative bacterium, which in mice is the only species belonging to the phylum Verrucomicrobia [255]. It interacts via its mucin-degrading capabilities with enteroendocrine cells to modulate gut barrier function, and it is capable of producing certain short chain fatty acids (SCFAs) with a direct action on the G-protein receptor 43 (GPR43) [221]. It has been shown that induction of IBD in mice with dextran sodium sulfate (DSS) reduces the number of extracellular vesicles derived from *A. muciniphila*, and feeding DSS-induced mice such vesicles reduces the severity of IBD [256], which fits well with observations in humans [257]. *Lactobacillus gasseri* was also strongly decreased with ageing. It has been previously shown that *L. gasseri* has anti-inflammatory properties and reduces effects of colitis in *IL-10*^{-/-} mice model [258]. These results highlight a low-grade effect of ageing on the intestinal microbiota, reducing the presence of bacteria such as *A. municiphila* and *L. gasseri*, which have been previously associated with beneficial effects on health.

In summary these findings show for the first time a deleterious effects of ageing on the barrier function of intestinal mucus, resulting in increased contact of the epithelium with the resident microbiota. This was linked to increased apoptosis of goblet cells

and decreased lysozyme production in the small intestinal crypts. Moreover, mucus barrier dysfunction was associated with reduced innate immunity, mucosal T cell functions and immunoglobulin production. These processes are linked to changes in the microbiota composition and reduced diversity in old mice, as reported in human microbiota studies in elderly subjects. Although more challenging it will be important to determine whether the mucus barrier deteriorates with increasing age in humans and has negative affects in other organs and the systemic immune system. Strategies to maintain the gut barrier function may slow down the effects of ageing in the gut, which could have a major impact on health and the systemic effect of ageing.

Acknowledgements

4

Supplementary data

Supplementary Figure S1: Top 15 pathways significantly (-log(pvalue)>5) regulated in ileum of 19 month-old mice compared to young mice (8 weeks). In red the percentage of genes up-regulated, and in green the percentage of genes downregulated in a pathways.

Supplementary Table S1: Top 20 Gene ontology terms from the gene cluster 5 (Figure 10) positively correlated with microbiota. In bold are depicted the genes (and associated GO terms) related to immunity.

GO ID	GO Term	P-value	Z-score	Genes
GO:0006809	nitric oxide biosynthetic process	0.000111	-2.96922	CYP1B1;RORA;DDAH2
GO:0030198	extracellular matrix organization	4.15E-05	-2.3808	KLK7;CYP1B1;EFEMP1;CMA1;ITGB2; FGF2;DDR2;ADAMTS5;MMP12;KDR
GO:0043062	extracellular structure organization	4.25E-05	-2.3805	KLK7;CYP1B1;EFEMP1;CMA1;ITGB2; FGF2;DDR2;ADAMTS5;MMP12;KDR
GO:0006956	**complement activation**	**0.018531**	**-3.78328**	**C1QB;C4A;CFH;VSIG4**
GO:0002253	**activation of immune response**	**0.006734**	**-3.37902**	**C1QB;C5AR1;C4A;MNDA;CFH;ITGB 2;TXK;VSIG4**
GO:0002042	cell migration involved in sprouting angiogenesis	0.004054	-3.01007	FGF2;KDR
GO:0072376	protein activation cascade	0.026542	-3.51392	C1QB;C4A;CFH;VSIG4
GO:0046209	nitric oxide metabolic process	0.000837	-2.69417	CYP1B1;RORA;DDAH2
GO:0021702	cerebellar Purkinje cell differentiation	0.003153	-2.64119	ATXN2;RORA
GO:0002003	angiotensin maturation	0.002742	-2.63503	CPA3;CMA1
GO:0035338	long-chain fatty-acyl-CoA biosynthetic process	0.00506	-2.67396	ACSL1;ELOVL4
GO:0006959	**humoral immune response**	**0.064291**	**-3.09382**	**C1QB;C4A;CFH;VSIG4**
GO:0031017	exocrine pancreas development	0.001676	-2.45392	IGF1;PDX1
GO:1903053	regulation of extracellular matrix organization	0.005601	-2.71018	CYP1B1;DDR2
GO:0001945	lymph vessel development	0.001676	-2.3934	HEG1;KDR
GO:0046949	fatty-acyl-CoA biosynthetic process	0.006169	-2.6396	ACSL1;ELOVL4
GO:0050679	positive regulation of epithelial cell proliferation	0.001537	-2.37395	5AR1;IGF1;FGF2;MMP12;KDR
GO:0043534	blood vessel endothelial cell migration	0.008685	-2.64136	FGF2;KDR
GO:1903034	regulation of response to wounding	0.003822	-2.45453	ADAMTS18;C4A;CFH;CMA1;RORA;S CARA5;FGF2
GO:0010762	regulation of fibroblast migration	0.006169	-2.60514	FGF2;DDR2
GO:0006957	**complement activation, alternative pathway**	**0.003153**	**-2.44503**	**CFH;VSIG4**

4

Chapter 5

Sexually dimorphic characteristics of the small and large intestine of ageing mice

Bruno Sovran[1,2], Marlies Elderman[2,3] Floor Hugenholtz[4], Katrine Graversen[1], Myrte M. Huijskes[1], Mark V. Boekschoten[2,5], Paul De Vos[2,3], Jan Dekker[1], Jerry M. Wells[1,2] and Marijke M. Faas[2,3]

[1] Host-Microbe Interactomics Group, Wageningen University and Research Center, Wageningen, the Netherlands
[2] Top Institute Food and Nutrition, Wageningen, the Netherlands
[3] University Medical Center of Groningen, Groningen, the Netherlands
[4] Laboratory of Microbiology, Wageningen University and Research Center, the Netherlands
[5] Division of Human Nutrition, Wageningen University and Research Center, Wageningen, the Netherlands

Abstract

Background: The involvement of intestinal barrier function and the microbiota in Gastrointestinal (GI)-related disorders is well documented but more knowledge is needed on how sexual dimorphism affects intestinal physiology. This aim is of clear relevance to health and longevity, as it should be considered in future clinical trials and might provide insights for development of gender-specific approaches to prevent degeneration of intestinal barrier functions.

Methods: Tissue morphology (H&E), mucus barrier function (Periodic Acid Schiff (PAS)/Alcian blue), and bacterial compartmentalization (fluorescent *in-situ* hybridization staining of bacteria) were investigated by staining segments of ileum and colon fixed in Carnoy's fixative from male, female, and ovariectomized female C57BL/6 mice at 2.5 and 19 months of age. Ingenuity pathway analysis (IPA) of transcriptome data from ileum and colon tissue was used to identify significant pathways responsible for gender differences in the mucosal barrier and to identify mucosal genes showing sexually dimorphic expression. IPA was used to correlate sexually dimorphic genes with biological function and disease networks. Faecal microbiota were compared to determine the effects of age and gender and correlated to differences in transcriptomic data from the intestine.

Results: Mucus thickness in the colon was significantly reduced in 19 month-old mice. Sexually dimorphic effects were observed on colon mucus thickness but only in aged mice. Old and ovariectomized females showed a significantly thicker inner layer of mucus than old males, despite having similar amounts of *Muc2* transcripts. Gender differences were also observed in the staining intensity of the Paneth cell marker lysozyme suggesting increased production of antimicrobial factors in females. In the ileum, the main pathways significantly down-regulated in males were related to immunity but in females and ovariectomized females these same pathways were strongly up-regulated. Microbiomic data show a significant decrease in *F. prauznitzii* in ovariectomized female mice, whereas the same bacteria are increased in male and female mice.

Conclusion: The deterioration of the colon mucus thickness in aged mice is more pronounced in males than females and ovariectomized females. Nevertheless, all aged mice failed to compartmentalise the microbiota to the lumen, and bacteria were seen in contact with epithelium. Genes displaying sexually dimorphic gene expression in both the small and large intestine are correlated with disease development and cellular processes associated with epithelial turnover.

Introduction

Increasing evidence from studies in humans suggests increased incidence of IBD and worse severity of disease in women than men, although not all studies were consistent [259]. Some studies fail to demonstrate a relationship between gender and disease severity, but note that age is reciprocally related to disease severity [260][261]. Others have identified female IBD patients as having a lower rate of remission and less immunosuppressive medications than males [262]. However, recently, large epidemiological studies have suggested that oestrogens promote the development of ulcerative colitis (UC) [263][264].

Several studies using mouse knockout models have shown that defects in the pathways maintaining epithelial integrity and the mucus barrier lead to loss of homeostasis in the colon, barrier destruction and colitis triggered by bacterial antigens and microbe-associated molecular patterns [265][266][267][268][121]. Increased mucosal permeability and loss of epithelial integrity is recognized to play a role in the pathophysiology of a variety of gastrointestinal related disorders including mucosal infections, celiac disease, post-infectious irritable bowel syndrome (IBS), metabolic syndrome, food allergy and inflammatory bowel disease (IBD) [269]. Life stress and gastrointestinal infections represent the greatest risk factors for the development of IBS [270][271], and women are more likely to initiate IBS-like symptoms following an episode of infectious gastroenteritis [272][273]. Differences in immune cell infiltration of the colonic mucosa such as mast cells have been shown to correlate with symptomatic differences between the sexes in IBS.

In mice the gut barrier has been shown to deteriorate with age (**Chapter 4**). The thickness and stability as well as the viscoelastic properties of intestinal mucus are crucial for maintaining homeostasis [1][274], as evidenced by the fact that *Muc2$^{-/-}$* mice lacking the major secreted mucus develop colitis by around 5 weeks of age (**Chapter 3**) [121]. Decreased mucus production and increased permeability as well as reduced production of antimicrobials including Paneth cell factors play a role in perpetuating IBD and have been well described in human IBD patients and in experimental models of colitis [275][276][277]. Oestrogen has been shown to increase mucus content of cervical mucus and increase viscosity-related barrier protection [274]. Sheth *et al.* demonstrated that there was preservation of the intestinal mucus layer in females and postulated that this may have a protective effect against shock-induced gut injury and subsequent remote organ injury [278][173][174].

Studies in female rats indicated that ovariectomy is associated with a shortened life span [183], and that the pathological deficiency or loss of ovarian function is associated with the derangement of energy metabolism and immune function (rodents and humans) [184]. In addition, menopause is associated with metabolic dysfunction [184] and pathologies involving inflammation (e.g., osteoporosis and metabolic disorders, including diabetes, atherosclerosis, joint diseases, and neurodegeneration) [186][187].

Increased knowledge on these mechanisms might contribute significantly to disease prevention and treatment, for instance by optimizing dietary recommendations and pharmacological protocols in a gender-specific way. The results of these studies raise the possibility that gender differences in mucus barrier might influence disease susceptibility. Thus the main goal of this study was to investigate gender differences in intestinal physiology by examining mucus thickness and distribution as well as Paneth cell production of antimicrobial factors in young mice (2.5 month-old) and old (19 month) mice. Additionally, a group of mice ovariectomised at 15 months were included in the study to mimic the effects of menopause in humans. Microbiota were compared across groups to determine whether there was an effect of age and gender and correlated to differences in transcriptomic data from the intestine to identify the principal pathways responsible for gender differences in the gut barrier.

Materials and Methods

Animals

C57BL/6 mice (Harlan Laboratories, the Netherlands) were housed in a specific pathogen-free (SPF) environment in individual ventilated cages with *ad libitum* access to D12450B diet (10% fat) (Research Diet Services B.V., Wijk bij Duurstede, the Netherlands), and acidified tap water in a 12-hour light/dark cycle. The University Medical Center of Groningen (UMCG) Animal Ethics Committee (Groningen, the Netherlands) approved the animal experiments.

Experimental set up

Groups of 8 weeks-old male and female littermates were housed in groups of 5 mice according to gender in individual ventilated cages, and sacrificed at 8 weeks and 19 months of age. Half of the female mice were ovariectomized at 15 months to mimic menopause. During the ovariectomy procedure, the mice were anesthetized with isoflurane and oxygen and two small incisions were made on both ventral sides. Both ovaries were localized, ligated and removed. After surgery the mice received palliative medicine (Temgesic). At 8 weeks and 19 months of age ileal and colonic tissues were fixed in Carnoy's fixative and embedded in paraffin. Additionally, segments of ileum and colon were frozen in liquid nitrogen and stored at -80°C for RNA and protein assays. Faeces were collected at 2.5, 8, 13, 15 and 19 months (sacrifice) and stored at -80°C.

Histology

Paraffin sections (5 μm) of ileum and colon were made with a microtome Microm HM350, (Thermo scientific) and attached to poly-L-lysine-coated glass slides (Thermo scientific). After overnight incubation at 37°C, slides were deparaffinised and hydrated

step-wise using 100% xylene followed by several solutions of distilled water containing decreasing amounts of ethanol. Sections were stained with hematoxylin and eosin (H&E) and Period Acid Schiff (PAS)/Alcian blue [194]. Mucus layer thickness was measured (10 measurements per section / 2 sections per animal / 5 animals per condition) using Image J software (NIH, Maryland, USA).

Immunohistochemistry

Paraffin sections (5 μm) were deparaffinised and rehydrated, and antigen retrieval was performed by heating the sections for 20 min in 0.01 M sodium citrate (pH 6.0) at 100°C. Sections were washed for 3 h with 3 changes of Tris-Buffered Saline (TBS). Non-specific binding was reduced using 10% (v/v) goat serum (Invitrogen, Life technologies Ltd, Paisley, UK) in TBS for 30 min at room temperature. CD3+ T cells were detected by incubating the sections with anti-CD3 antibody (Invitrogen) diluted 1:100 in Tris-Buffered Saline (TBS), overnight at 4°C. Leukocytes were detected by incubating the sections with anti-CD45 antibody diluted 1:100 in TBS, overnight at 4°C. Paneth cells were identified by staining for the lysozyme expression, detected by incubating the sections with anti-lysozyme antibody (Invitrogen) diluted 1:100 in TBS, overnight at 4°C, and goat-anti-rabbit secondary antibody (1:1000). Muc2 was detected by staining the sections with anti-Muc2 antibody (kindly gifted by Dr. Gunnar Hansson, Gothenburg University, Sweden) diluted 1:500 in TBS, and goat-anti-rabbit Alexa 488 conjugated antibody (1:1000) (Molecular Probes, Life Technologies Ltd, Paisley, UK) in TBS.

Detection of bacteria using fluorescence *in situ* hybridization (FISH)

Paraffin sections (5 μm) were deparaffinised with xylene and rehydrated in a series of ethanol solutions to 100% ethanol. The tissue sections were incubated with the universal bacterial probe EUB338 (5'-GCTGCCTCCCGTAGGAGT-3') (Isogen Bioscience BV, De Meern, the Netherlands) conjugated to Alexa Fluor488. A 'non-sense' probe (5'-CGACGGAGGGCATCCTCA-3') conjugated to Cy3, was used as a negative control. Tissue sections were incubated overnight with 0.5 μg of probe in 50 μL of hybridization solution (20 mmol/L Tris-HCl (pH 7.4), 0.9 mol/L NaCl, 0.1% (w/v) SDS) at 50°C in a humid environment using a coverslip to prevent drying of the sample. The sections were washed with (20 mmol/L Tris-HCl (pH 7.4), 0.9 mol/L NaCl) at 50°C for 20 min and then washed 2 times in PBS for 10 min in the dark and incubated with DRAQ5 (Invitrogen) (1:1000) for 1 h at 4°C to stain nuclei. Sections were washed 2 times in PBS for 10 min, mounted in Fluoromount G (SouthernBiotec, Alabama, USA) and stored at 4°C.

Transcriptome analysis

Total RNA was isolated using the RNeasy® kit (Qiagen) with a DNase digestion step according to the manufacturer's protocol. Quantity and quality of colonic and ileal RNA

5

(5 arrays of individual mice per group) was assessed using spectrophotometry (ND-1000, NanoDrop Technologies, Wilmington, NC, USA), and Bionanalyzer 2100 (Agilent, Santa Clara, CA, USA), respectively. RNA was only used to generate cDNA and perform microarray hybridisation when there was no evidence of RNA degradation (RNA Integrity Number > 8). 100 ng of total RNA was labelled using the Ambion WT Expression kit (Life Technologies Ltd, Paisley, UK) together with the Affymetrix GeneChip WT Terminal Labelling kit (Affymetrix, Santa Clara, CA, USA). Labelled samples were hybridised to Affymetrix GeneChip Mouse Gene 1.1 ST arrays. Hybridisation, washing, and scanning of the array plates were performed on an Affymetrix GeneTitan Instrument, according to the manufacturer's recommendations.

Quality control of the datasets obtained from the scanned Affymetrix arrays was performed using Bioconductor [195] packages integrated in an on-line pipeline [196]. Probe sets were redefined according to Dai *et al.* [197] utilising current genome information. In this study, probes were reorganised based on the Entrez Gene database (remapped CDF v14.1.1). Normalised expression estimates were obtained from the raw intensity values using the Robust Multiarray Analysis (RMA) pre-processing algorithm available in the Bioconductor library affyPLM using default settings [198].

Differentially expressed probe sets were identified using linear models, applying moderated t-statistics that implemented empirical Bayes regularization of standard errors [199]. A Bayesian hierarchical model was used to define an intensity-based moderated T-statistic (IBMT), which takes into account the degree of independence of variances relative to the degree of identity and the relationship between variance and signal intensity [200]. Only probe sets with a fold-change of at least 1.2 (up/down) and p value < 0.05 were considered to be significantly different. Biological interaction networks among regulated genes activated in response to ageing were identified using Ingenuity Pathways Analysis (IPA) (Ingenuity System). IPA utilizes a large expert-curated repository of molecule interactions, regulatory events, gene-to-phenotype associations, and chemical knowledge, mainly obtained from peer-reviewed scientific publications, that provides the building blocks for network construction. IPA annotations follow the GO annotation principle, but are based on a knowledge base of > 1,000,000 protein-protein interactions. The IPA output signalling pathways with statistical assessment of the significance of their representation based on Fisher's Exact Test. Our IPA analyses included comparison of differentially regulated genes in the ileum and colon of old males, old females, and old ovariectomized females compared to young mice. The input was all differentially regulated genes (p value < 0.05, fold-change > 1.2 and intensity > 20) of ileum and colon.

Bacterial DNA extraction and microbiota profiling

The DNA from the ileal content and faeces was extracted using PowerSoil® DNA extraction kit (MO BIO Laboratories, Carlsbad, CA, USA). Microbiota composition was analysed by Mouse Intestinal Tract Chip (MITChip), a diagnostic 16S rRNA array that consists of 3,580 unique probes especially designed to profile mouse intestine microbiota [203]. 16S rRNA gene amplification, *in vitro* transcription and labelling, and hybridization were carried out as described previously [204]. The data were normalized and analysed using a set of R-based scripts in combination with a custom-designed relational database, which operates under the MySQL database management system. For the microbial profiling the Robust Probabilistic Averaging (RPA) signal intensities of 2,667 specific probes for the 94 genus-level bacterial groups detected on the MITChip were used [205]. Diversity calculations were performed using a microbiome R-script package (https://github.com/microbiome). Multivariate statistics, redundancy analysis (RDA) and Principal Response Curves (PRC), were performed in Canoco 5.0, and visualized in triplots or a PRC plot [206].

Results

Gender differences influence intestinal morphology

Young males and females showed no differences in intestinal morphology (not shown). Therefore, the genders were considered as one group, and all comparisons between old mice were compared to the pooled group of young mice. Lymphoid structures, identified as solitary intestinal lymphoid tissue (SILT) [252] containing mainly B220 positive B-cells were evident in the colon of 19 month-old male, female and ovariecomized female mice but not young mice (Fig. 1).

The ileum of old male, female and ovariectomized mice showed no signs of mucosal changes, other than that the villi were significantly (p<0.001) longer compared to young mice (Fig. 2A-B). The villi of ovariectomized females were significantly shorter than in 19 months-old male and females (p<0.05), but still longer than in young mice (non-significant) (Fig. 2C).

Fewer Paneth cells were present in ileum of old females and ovariectomized females than younger counterparts and histochemical staining for lysozyme was less intense than in young controls and old males (Fig. 3). Old male mice showed less lysozyme positive cells and these were confined to the bottom of the crypts, as compared with young males (Fig. 3).
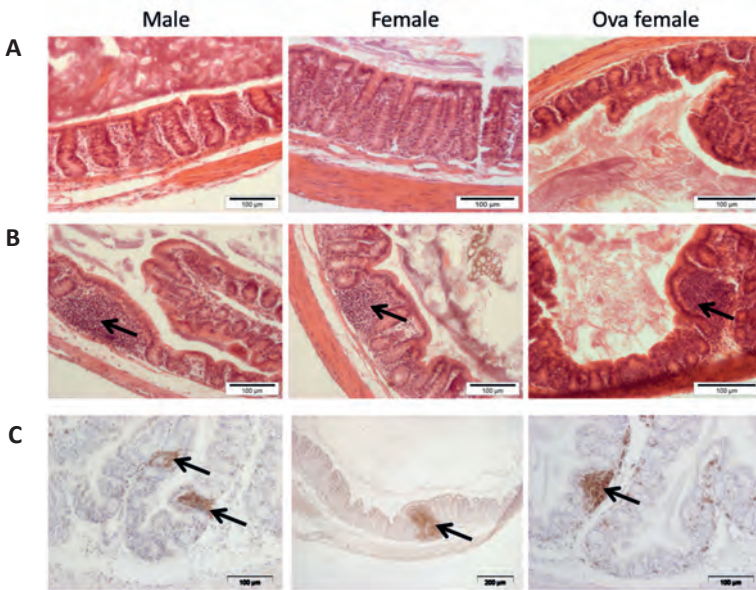
Figure 1: Representative pictures of H&E staining of colon of old (19 month-old) male, old female and ovariectomized (ova) female mice (A). Representative pictures of Solitary Intestinal Lymphoid Tissue (SILT) stained with H&E (B) and anti-CD45 antibodies (C) in old male, old female and ovariectomized mice (SILT, indicated by arrows). Scale bars: 100 and 200 μm.

Figure 2: Representative pictures of H&E staining of ileum of young (8 week-old) and old (19 month-old) male mice (A), young, old female and ovariectomized (ova) female (B). Villus length measured on 10 well-oriented villi (5 mice per group). Pooled villus length measurements are presented in panel C. Scale bars: 100 μm.
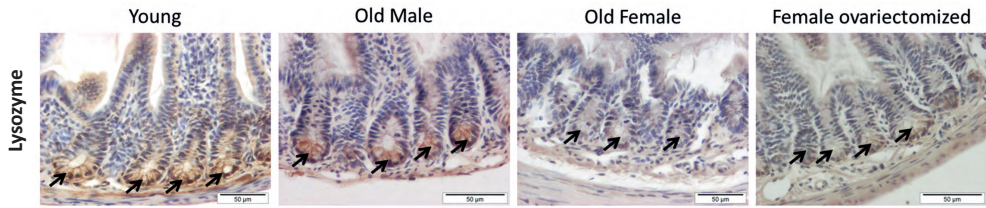
Figure 3: Representative immune histochemistry of lysozyme in ileal tissues from young mice (2.5 months), old male, female and ovariectomized female mice (19 months). Paneth cells are indicated with arrows. Scale bars: 50 µm.

Sexually dimorphic effects on mucus thickness in aged mice

Alcian blue staining was used to identify acidic carbohydrates such as Muc2, and PAS for neutral carbohydrates, both of which occur on the Muc2 glycoprotein. Young male and female mice showed similar mucus layer morphology; therefore only one representative image is shown for young mice (Fig. 4A).

Old male mice showed a thinner (approx. 5 µm) secreted firm mucus layer than young mice (20-25 µm), and in some tissue sections it was even absent (Fig. 4A and B). A thicker mucus layer was present in the colon of old ovariectomized female mice compared to old male mice, but it was still thinner compared to young female mice (Fig. 4). FISH detection of bacteria revealed that the colonic mucus layer of old male mice failed to prevent contact of the epithelium with intestinal microbiota (Fig. 4B). Despite having a thicker mucus layer than the males, old females and ovariectomized females also failed to effectively compartmentalise the microbiota to the lumen (Fig. 4C).

Gender differences in intestinal tissue transcriptomes are evident in young mice and increase with age

A transcriptomics approach was used to gain more insight into the potential pathways or mechanisms that might be modulated by gender differences. A cut-off for fold-changes in relative expression value > 1.2, p-value < 0.05 and a signal intensity > 20 were applied in all comparisons. A total of 859 genes in the ileum and 455 in the colon were differentially expressed in young males compared to young females.

Numerous genes (about 300 up- and down-regulated in both ileum and colon) were differentially expressed in old male, female and ovariectomized female compared to their young counterparts. IPA comparisons of the significantly affected pathways in the ileum, revealed that in males differentially expressed genes participating in pathways related to immunity and were significantly down-regulated compared to their counterparts (Fig. 5A). In contrast, immunity pathways were significantly upregulated in the ileum of old female and old ovariectomized females compared to young females. In the colon, the majority of the significantly regulated pathways were down-regulated in both old male, female and ovariectomized females compared to young mice. These
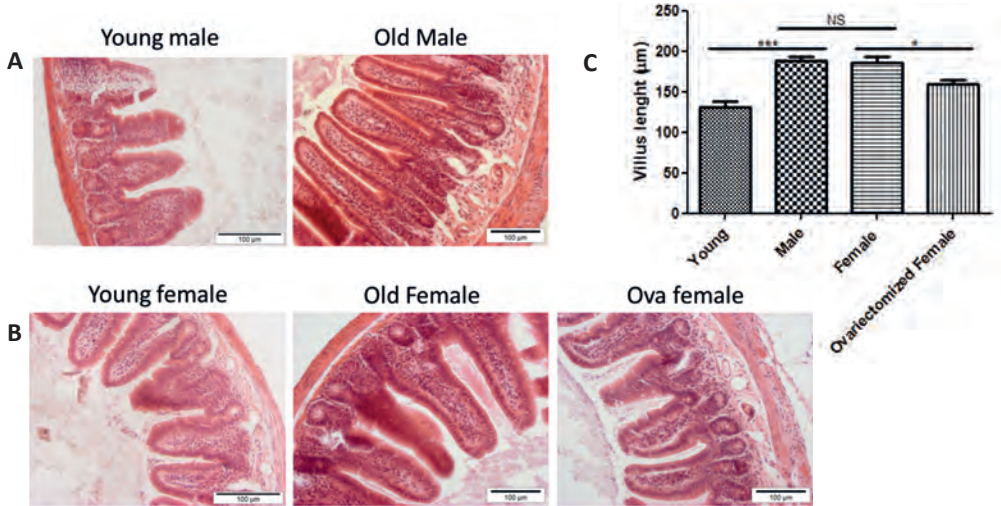
Figure 4: Representative pictures of PAS/Alcian Blue staining of colon of young (8 week-old) mice, old (19 month-old) male, old female and ovariectomized female (A). Scale bars: 100 µm. Muc2 staining (green) of colon of young mice, old male, female and ovariectomized female mice (B). Scale bars: 50µm. FISH analysis of the colon of young mice, old male, old female and ovariectomized female mice, using the general bacterial probe EUB338-Alexa Fluor 488 (green), and nuclear staining DRAQ5 (blue). The apical membranes of the epithelial cells are indicated by a dashed white line (C). Arrow represents the gap between bacteria and epithelium in young healthy colon. Scale bars: 50 µm. Mucus thickness measured in PAS/Alcian Blue stained sections (10 measurements per section, 2 sections per animal) in 5 colonic tissues of young and old mice, respectively. Pooled mucus measurements are presented in panel D. *** indicates statistical difference at p<0.001.

pathways were related to lipid metabolism (PPARγ signalling, inhibition of RXR function), immunity (signalling of T helper cells, CD40 signalling) and were mainly down regulated. Pathways related to oxidative stress were mainly up-regulated in old male and female mice but not in ovariectomized female mice compared to young mice (Fig. 5B).

Genes displaying sexually dimorphic gene expression in the small and large intestine are correlated with cellular functions linked to cell cycle, cell development and turnover and disease development.

Ingenuity pathway analysis (IPA) was applied to identify the top biological functionality and disease as well as the functional networks of the sexually dimorphic genes. By analysing the physiological ('Bio') functions in detail, IPA revealed that genes displaying sexually dimorphic expression in small intestine and colon represented various general cellular function including cellular development, and cell death (Tables 1 and 2).

Table 1: Top 'Bio' functions and 'diseases and disorder' linked to the sexually dimorphic genes in the small intestine, according to IPA. Comparisons where made between old male (MO) and old female (FO) and ovariectomized female (FO(ova)) mice.

Sex dimorphism	Diseases and disorder	P value	Molecules
MO vs. FO	Dermatological Diseases and Conditions	2.06E-02 –4.04E-06	21
	Developmental Disorder	2.06E-02 –4.04E-06	50
	Hereditary Disorder	2.06E-02 –4.75E-06	30
	Metabolic Disease	1.87E-02 –4.75E-06	15
	Inflammatory Response	2.06E-02 –5.13E-05	67
MO vs. FO(ova)	Connective Tissue Disorders	9.65E-03 –5.08E-07	44
	Inflammatory Disease	9.65E-03 –5.08E-07	45
	Skeletal and Muscular Disorders	9.65E-03 –5.08E-07	47
	Immunological Disease	9.65E-03 –2.57E-06	47
	Cancer	9.65E-03 –2.64E-07	54
FO vs. FO(ova)	Neurological Disease	1.64E-02 –3.30E-06	36
	Metabolic Disease	1.64E-02 –1.07E-05	25
	Cardiovascular Disease	1.43E-02 –1.18E-05	26
	Inflammatory Disease	1.64E-02 –1.18E-05	30
	Organismal Injury and Abnormalities	1.64E-02 –1.18E-05	56

5

Sex dimorphism	Bio Functions	P value	Molecules
MO vs. FO	Cellular Development	2.31E-02 −1.28E-05	121
	Cell-to-Cell Signalling and Interaction	2.31E-02 −1.18E-04	61
	Cellular Assembly and Organization	2.31E-02 −2.05E-04	22
	DNA Replication, Recombination and Repair	2.31E-02 −2.05E-05	14
	Cell Death and Survival	2.31E-02 −2.05E-05	132
MO vs. FO(ova)	Cellular Development	9.65E-03 −9.27E-05	61
	Cellular Growth and Proliferation	9.65E-03 −9.27E-05	65
	Cell Morphology	9.65E-03 −1.28E-04	20
	Cell-To-Cell Signalling and Interaction	9.65E-03 −1.86E-04	35
	Cellular Movement	9.65E-03 −2.07E-04	40
FO vs. FO(ova)	Cell-To-Cell Signalling and Interaction	1.64E-02 −1.58E-09	77
	Lipid Metabolism	1.64E-02 −2.35E-05	32
	Small Molecule Biochemistry	1.64E-02 −2.35E-05	38
	Molecular Transport	1.64E-02 −5.71E-05	37
	Cell Death and Survival	1.60E-02 −6.70E-05	55

Regarding disease development, IPA revealed that in the small intestine and colon, genes displaying sexually dimorphic expression were mainly involved in metabolic diseases, inflammation and cancer (Tables 1 and 2).

Table 2: Top 'Bio' functions and 'diseases and disorder' linked to the sexually dimorphic genes in the colon, according to IPA. Comparisons where made between old male (MO) and old female (FO) and ovariectomized female (FO(ova)) mice.

Sex dimorphism	Diseases and disorder	P value	Molecules
MO vs. FO	Cancer	2.06E-02 − 4.04E-06	35
	Tumor Morphology	2.06E-02 − 4.04E-06	11
	Organismal Injury and Abnormalities	2.06E-02 − 4.75E-06	39
	Renal Urological Disease	1.87E-02 − 4.75E-06	10
	Metabolic Disease	2.06E-02 − 5.13E-05	5
MO vs. FO(ova)	Neurological Disease	1.44E-02 − 7.68E-07	44
	Organismal Injury and Abnormalities	1.45E-02 − 1.76E-05	122

	Reproductive System Disease	1.38E-02 – 1.76E-05	102
	Cancer	1.51E-02 – 3.33E-05	161
	Tumor Morphology	1.23E-02 – 3.77E-05	11
FO vs. FO(ova)	Cancer	4.75E-02 – 3.04E-03	12
	Connective Tissue Disorder	4.75E-02 – 3.04E-03	4
	Dermatological Diseases and Conditions	4.69E-02 – 3.04E-03	10
	Developmental Disorders	4.75E-02 – 3.04E-03	10
	Endocrine System Disorder	3.88E-02 – 3.04E-03	5

Sex dimorphism	Bio Functions	P value	Molecules
MO vs. FO	Cell Death and Survival	2.06E-02 –4.04E-06	51
	Cellular Assembly and Organization	1.38E-02 –4.75E-05	10
	Cellular Compromise	1.38E-02 –4.75E-05	11
	Molecular Transport	1.60E-02 -4.75E-05	18
	Small Molecule Biochemistry	1.60E-02 -4.75E-05	20
MO vs. FO(ova)	Cellular Development	1.29E-02 –1.81E-06	78
	Cellular Growth and Proliferation	1.29E-02 –3.54E-05	77
	Cell Death and Survival	1.47E-02 –4.99E-06	69
	Gene Expression	1.05E-02 –2.12E-06	53
	Cellular Movement	1.42E-02 –3.03E-06	52
FO vs. FO(ova)	Cell-to-Cell Signalling and Interaction	4.97E-02 –1.85E-05	27
	Cell Morphology	4.19E-02 –2.76E-03	9
	Carbohydrate Metabolism	3.44E-02 –3.04E-03	4
	Cell Cycle	4.75E-02 –1.04E-03	5
	Cellular Assembly and Organization	4.97E-02 –3.04E-03	11

5
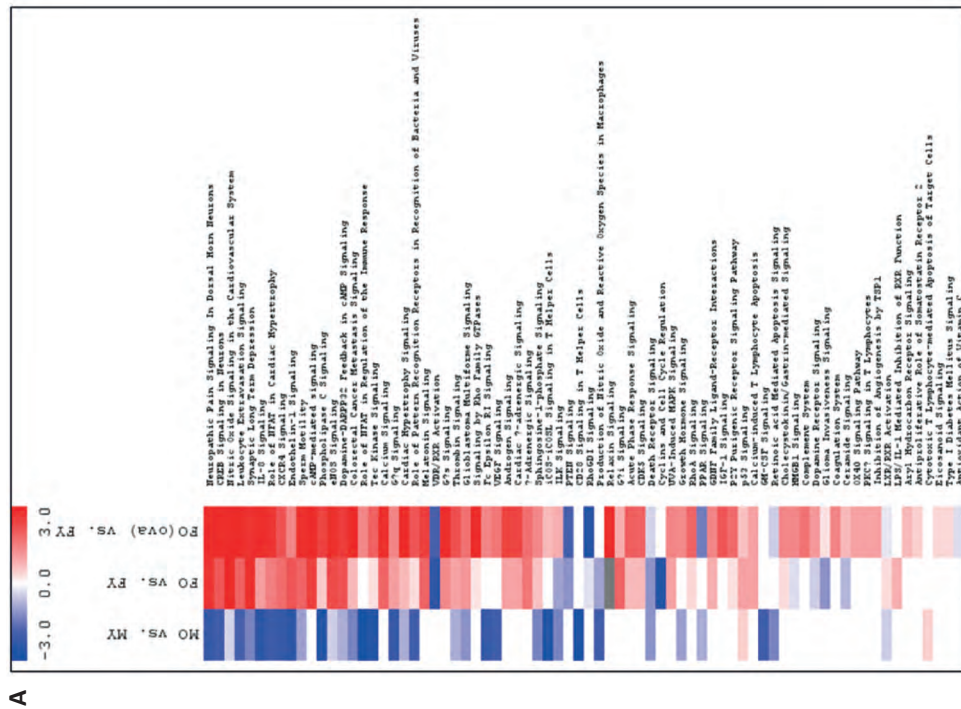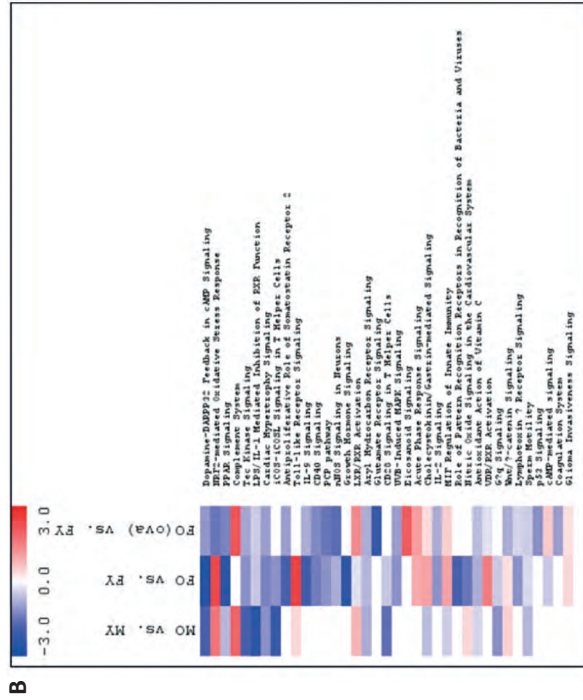
Figure 5: Heat maps of differentially expressed pathways in proximal colon (A) and ileum (B), using genes differentially expressed in male old (MO) versus male young (MY) mice, female old (FO) versus female young (FY) and ovariectomized female (FO(ova)) versus female young (FY). In red, genes are represented, which are up-regulated and in blue the genes that are down-regulated. The intensity of the colour is proportional to change in expression.

Gender differences affect microbiota composition, diversity, and richness in the gut

16S ribosomal RNA (rRNA) gene derived microbiota profiles were obtained from faeces of 2.5, 8, 13, 15, and 19 months-old male and female mice. In male mice, the microbial diversity and richness of microbiota significantly increased with age reaching a plateau at 15 months. The same trend was seen in faecal microbiota of female mice although diversity and richness scores were significantly lower at 19 months than 15 months (Fig. 6).
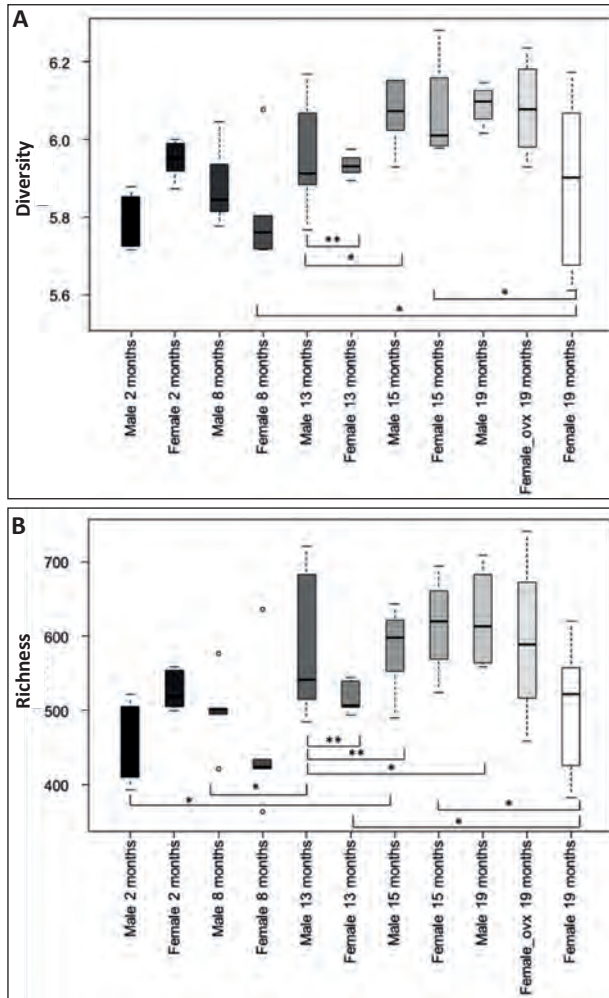
Figure 6: Box-and-whiskers-plot showing the diversity (Shannon index) of microbiota in faeces of 2 months, 8 months, 13 months, 15 months, and 19 months of age in male, female and ovariectomized female (A). Box-and-whiskers-plot showing the richness of microbiota in colon of 2 months, 8 months, 13 months, 15 months, and 19 months of age in male, female and ovariectomized female (B). Statistically significant differences among groups and time points were indicated (*, $p<0.05$; **, $p<0.01$).

Furthermore, redundancy analysis (RDA) established that in male, female, and ovariectomized females, the microbiota composition could be discriminated on the basis of age. At 19 months RDA analysis showed that the microbiota composition of male, female and ovariectomized was clearly distinct compared to 2 months-old mice (Fig. 7).

Figure 7: Redundancy Analysis (RDA) representing microbial ecology of old male, old female and old ovariectomized female of 2.5, 8, 13, 15 and 19 months in the faeces.
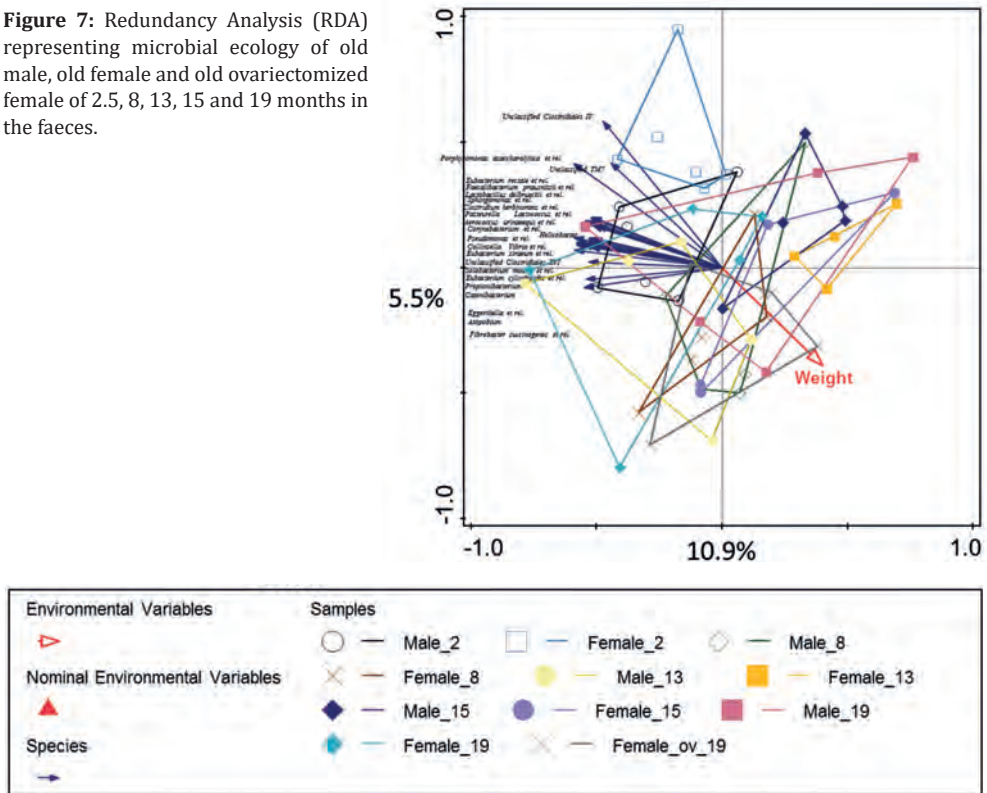
The differences in colonic microbiota composition of males and ovariectomized females were largest compared to females (Fig. 8).

In females, the microbiota composition was significantly different to males, especially at 2, 13, and 19 months of age. The variability of 19 month-old female microbiota could be explained by the increased abundance of bacterial taxons compared to males or ovariectomized females (Fig. 8).
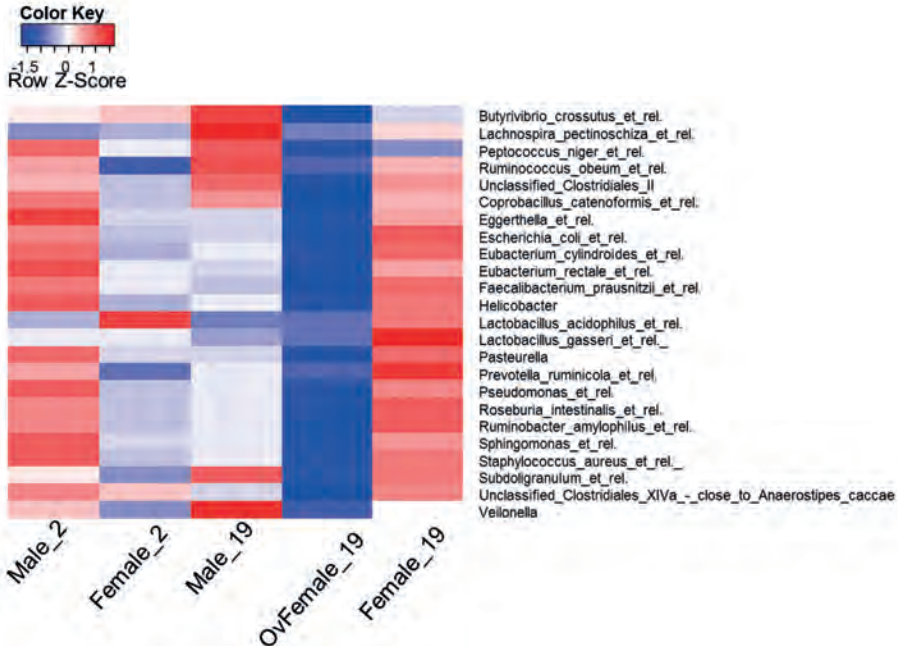
Figure 8: Heat maps of bacteria significantly present in male, female, and ovariectomized female mice, at 2 and 19 months of age. In red, bacteria are represented, which are significantly more present, and in blue the bacteria that are significantly less present in faeces of the respective mice at the given age. The intensity of the colour is proportional to change.

Specific bacterial clusters correlate with gender-specific expression of genes participating in immune pathways

To identify bacteria that might be correlated with gender differences in colon gene expression, microbiota, and transcriptomics data from male, female, and ovariectomized females at age of 19 months were combined for individual mice to investigate direct correlations between gene expression and microbiota composition in these samples. Three bacterial clusters strongly correlated positively (red) or negatively (blue) with six clusters of genes (about 100 genes per cluster; Fig. 9).

Strongest correlations between microbiota members (cluster B (orange) in the vertical bar) and specific changes in mucosal gene expression (gene clusters 1 and 4 in horizontal bar) were detected for the bacteria in cluster B (Fig. 9). These bacteria had higher relative abundances in the female mice compared to male and ovariectomized female and displayed a positive correlation with immune response (Supplementary data; Tables S1 and S2). Gene cluster 4 displayed positive correlations with bacterial cluster B. Genes belonging to Gene Ontology (GO) terms such as "positive regulation of defence response", "defence response to other organisms", "activation of innate immune responses" were strongly altered in gene cluster 4 (Supplementary data; Tables S1 and S2).
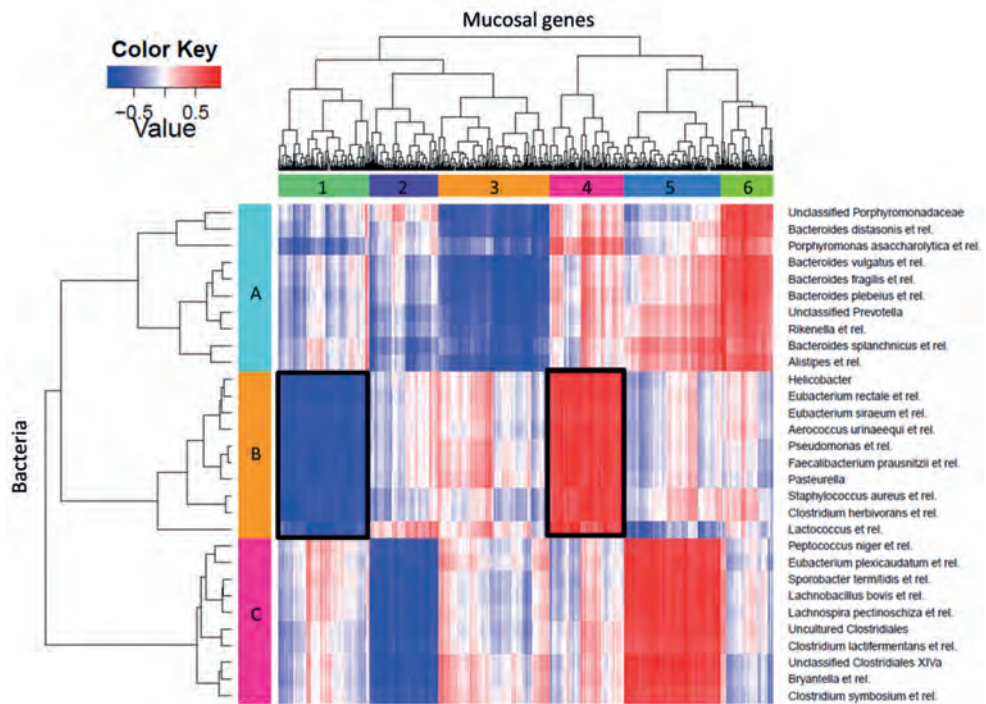
Figure 9: Heat-map of correlation analysis of MITChip (vertical) and transcriptome (horizontal) datasets of male, female, and ovariectomized female mice at 19 months of age. The integration of datasets was done per individual mouse (5 mice per group) and gives the direct correlations between gene expression and microbiota composition over these samples. In deep red, the cluster of genes that most positively correlated with a respective group of bacteria. In deep blue, the cluster of genes that most negatively correlated with a respective group of bacteria. Framed in black; the clusters discussed in more detail in the text. Six main gene clusters (1-6) and 3 main bacterial clusters (A-C) were identified.

Discussion

Several gut-related disorders are associated with an increased intestinal permeability [269] and in IBD reduced production of mucus and antimicrobial production potentiate inflammatory responses to the resident microbiota. Here we showed sexual dimorphic effects on the thickness of the firm mucus layer in the colon but only in old (19 month) mice. Male mice showed a significant shrinkage of the colonic mucus layer, associated with bacterial penetration and direct contact with the epithelium. Female and ovariectomized female mice had a significant thicker mucus layer than males, but the barrier was nevertheless ineffective at preventing contact of bacteria with the epithelium.

Publications describing the effects of gender or oestrogens in the mouse DSS model of acute inflammatory colitis are inconsistent with each other. For example, one study

showed that males were more susceptible to colitis with increased colon shortening, worse stool score, more profound histological injury, and higher levels of TNF-α in colon homogenates [279] than females. Moreover, in the same study, administration of 17-β-estradiol in ovarectomized mice attenuated histological injury and stool score, partly explaining why female mice are protected from DSS colitis [279]. This is in disagreement with evidence that human IBD is of worse severity in females. However, other studies in the mouse DSS model reported a deleterious influence of oestrogen in the treatment of colitis [280] and a exacerbation of some disease clinical parameters by oestrogens [281].

Studies in the mouse 2,4,6 Trinitrobenzenesulfonic acid model of Th1-mediated colitis are not consistent with the opinion that human IBD is of higher severity in females. In this mouse model, oestrogen was protective, reducing inflammation and production of proinflammatory cytokines such as macrophage migration inhibitory factor (MIF) and IL-1β in mucosal tissue [282]. In the same publication, oestrogen was shown to lower disease activity and down-regulate MIF protein content in the DSS colitis rat model. Moreover, the lower susceptibility of females to colitis was confirmed in acid acetic and dinitrobenzene sulfonic acid (DNBS)-induced inflammation [283] [280], and the HLA-B27 transgenic rat model [284].

Oestrogen has previously been shown to increase mucus content of cervical mucus and increase viscosity-related barrier protection [274] suggesting that a similar mechanism may explain the increased mucus thickness in colon in female mice. However this does not explain why mice ovariectomised at 15 months have a thicker mucus layer than the males, unless the effects of reduced oestrogen are indirect and take several months to have an effect on mucus thickness. Previously, intestinal HT29-MTX cells exposed to oestrogen for 3 days were shown to produce increased amounts of the membrane-bound mucin 1 (MUC1) and to be protected against oxidant injury [285]. In our study, *Muc1* gene was strongly down-regulated in old male and old ovariectomized females compared to their corresponding young gender. However, in female mice *Muc1* expression was not changed over time supporting the evidence for regulation of MUC1 by oestrogen. The relevance of this finding to the secreted MUC2 mucus layer is however unclear, especially as MUC2 was not among the genes showing sexually dimorphic expression in our study. This may be due to the fact that mucus is highly glycosylated in the Golgi apparatus and its secretion and proper assembly in the lumen may be influenced by several factors including epithelial stress and the cytokine milieu. In the small intestine changes in mucus production were not apparent but we observed increased length of the villi in old mice. This has been previously reported in *Muc2*^{-/-} mice and is associated with upregulation of the IL-22 dependent network of genes involved in epithelial proliferation and barrier defence (Chapter 2) [251].

In the intestine, Paneth cells are the main source of antimicrobial peptides [286] [287] [288]. Paneth cells are located primarily in the small intestine, where they secrete mediators of host defence that protect against enteric bacterial pathogens [289] [290]. When functioning optimally, Paneth cells contribute to homeostasis. However, Paneth cell dysfunction may predispose to intestinal inflammation. Humans with Crohn's disease of the ileum have a reduced production of Paneth cell antimicrobial peptides that is independent of the degree of intestinal inflammation [291]. In ageing mice, Paneth cells activity was significantly decreased compared to young mice. The decrease was more decreased in females and ovariectomized females compared to males.

To shed light on the pathways that might be linked to these sexually dimorphic changes in intestinal barrier functions we compared transcriptomes of the ileum and colon mucosal tissue of male, female and ovariectomized female of 10 week and 19 month-old mice. Relatively few genes were differentially expressed in young mice (2.5 month old), which is compatible with a previous study of mucosal gene expression in prepubescent 2 weeks-old mouse pups [292]. Sexually dimorphic gene expression in the ileum of old mice was linked to pathways involved in immune activation and was increased in female and ovarectomized female mice compared to male mice. This is consistent with mucosal gene expression studies performed on human small intestinal biopsies and several studies on the effects of gender on immune cell function [174] [292]. This higher baseline level of immune activation in the intestine of females compared to their male counterparts may predispose them to inflammation-associated diseases. Despite the role of NF-κB activation in triggering inflammatory responses TLR activation by commensal bacteria was previously shown to play a crucial role in the recovery from epithelial damage induced by DSS [293]. Similarly mice with a knockout of NEMO (ikappa kinase gamma), an activator of NF-kB, develop spontaneous colitis due to the role of NF-kB in inducing epithelial repair and innate effector mechanisms in the intestine [294] [295] [296]. Furthermore, TLR signalling, and in particular TLR-2 signalling and PKCα and PKCδ activation has also been implicated in tight junction function modulation, and epithelial permeability [297]. Thus the reduced expression of immune gene pathways in old male mice compared to old female mice may be linked to their increased susceptibility to colitis.

In the colon of 19 month-old mice, pathways significantly down-regulated in old mice compared to young mice were associated with decreased peroxisome proliferator–activated receptor γ (PPARγ) signalling and inhibition of retinoid X receptor (RXR) function. Ligand activation of PPARγ and its heterodimeric partner, RXR has been reported to protect against colitis [298]. Moreover knockouts of these receptors leads to increased susceptibility to colitis [298]. Thus the decreased activity of these pathways might be linked to intestinal disease susceptibility in old mice.

Further analysis of transcriptome linked genes displaying sexually dimorphic gene expression in the small and large intestine showed that these were correlated with biological functions linked to cell cycle, cell death and cell development. These transcript differences could be reflective of increased proliferative/regenerative gut microenvironment in females presumably due to higher epithelial turnover. Additionally, the genes displaying sexually dimorphic expression were involved in metabolic diseases, inflammation and cancer in both females and males (Tables 1 and 2).

Many studies have shown an impact of the microbiota composition on host physiology and disease but there are few studies on gender differences in microbiota [292]. Here we identified microbiota differences between mouse gender, which increased with age. In our study, microbial diversity and richness increased over time, reaching a plateau around 12 months. At 19 months, only female mice showed a decrease in diversity and richness, which was also observed in human centenarians. The core microbiota of elderly subjects was also shown to be distinct from that of young adults, with reduced diversity, a greater proportion of *Bacteroides spp*. And distinct abundance patterns of Clostridium group [159] [160]. However, others have reported that changes in the microbiota are seen only in centenarians with increased inflammatory cytokine responses, but not in the general elderly population (average age 70 ± 3 years) [161].

To identify bacteria that might be correlated with changes in colon gene expression we used the linear multivariate method partial least squares (PLS) method [232] for each time point, as previously described [233]. We found that uncultured *Clostridiales* and *Lachnospira pectinoschiza et rel.* had higher relative abundances in old male mice of 15 and 19 months of age compared to young mice and displayed a positive correlation with immune response genes. A positive correlation was also found with stress response genes involved in apoptosis and cell proliferation, as well as immune genes. *Akkermancia municiphilia* was also strongly decreased with ageing. *Akkermansia muciniphila* is a Gram-negative bacterium, which in mice is the only species belonging to the phylum Verrucomicrobia [255]. It interacts via its mucin-degrading capabilities with enteroendocrine cells to modulate gut barrier function, and it is capable of producing certain short chain fatty acids (SCFAs) with a direct action on the G-protein receptor 43 (GPR43) [221]. It has been shown that induction of IBD in mice with DSS reduces the number of extracellular vesicles derived from *A. muciniphila*, and feeding DSS-treated mice such vesicles reduces the severity of colitis [256], which correlates well with observations in humans [257]. As a consequence, the presence of less Akkermansia in old mice is a sign of homeostatic impairment of the intestine.

The bacteria significantly increased in males and females were strongly reduced in ovariectomized females. It has been described that specific bacterial groups as Bifidobacterium, Lactobacillus or Faecalibacterium, could modulate the inflammatory

response at the level of the gut epithelium [299] [38] [300]. *Faecalibacterium prausnitzii* strains have been shown to have anti-inflammatory activities in mice, capable of attenuating colitis and their increased abundance in females might be related to the gender differences observed in this study [300] [38].

Conclusions

In old mice, females have a thicker firm mucus layer in the colon than males, suggesting males may be more susceptible to colitis than females. Although, the differences in mucus were not seen in young mice (10 weeks) this finding is consistent with most of the studies on the effects of gender on colitis in mouse models. However, the colonic mucus layer in old females and males (19 months), as well as ovariectomised mice was equally permeable to bacteria, suggesting that an enhanced barrier effect is not linked to the reduced severity of experimental colitis in female mice. The increased immune activity in females might positively affect mucus production and therefore explain the gender differences observed in mucus thickness. Changes in microbiota composition and diversity are comparable with other studies performed in humans.

In summary, we showed that sexual dimorphism in relation to ageing of intestine induces barrier impairment, particularly mucus layer shrinkage associated with reduction of innate and adaptive immune system effectors that are secreted into the intestinal lumen, associated with increased oxidative stress. Knowledge of sexually dimorphic effects in intestinal function are important for future strategies aimed at designing disease prevention and treatment strategies for men and women.

Acknowledgements

Supplementary data

Table S1: Gene ontology terms from the gene cluster 4 correlated with microbiota cluster B as shown in figure 9. Immune pathways are in bold.

GO Terms	P-value	Z-score	Genes
positive regulation of organic acid transport (GO:0032892)	0.005024	-2.78571	GRIK1;TNFRSF11A
regulation of glutamate receptor signalling pathway (GO:1900449)	0.008149	-2.76244	NETO2;CACNG2
membrane hyperpolarization (GO:0060081)	0.005846	-2.75932	GRIK1;CACNG2
positive regulation of ERBB signalling pathway (GO:1901186)	0.00426	-2.67984	EPGN;NUP62
negative regulation of epidermal growth factor receptor signalling pathway (GO:0045742)	0.0039	-2.67324	EPGN;NUP62
mitotic nuclear envelope disassembly (GO:0007077)	0.011945	-2.46638	NUP214;NUP62
nuclear envelope disassembly (GO:0051081)	0.013147	-2.46484	NUP214;NUP62
membrane disassembly (GO:0030397)	0.013147	-2.45901	NUP214;NUP62
response to other organism (GO:0051707)	0.014351	-2.37508	IFITM3;FAM111A;CLEC7A;COTL1;IKBKG;HIST2H2BE
positive regulation of defense response (GO:0031349)	**0.029868**	**-2.35056**	**CLEC7A;RFTN1;TNFRSF11A;IKBKG**
defense response to other organism (GO:0098542)	**0.013543**	**-2.33801**	**IFITM3;FAM111A;CLEC7A;COTL1;HIST2H2BE**
positive regulation of secretion (GO:0051047)	0.030211	-2.33145	TWIST1;STXBP5;GRIK1;TNFRSF11A
positive regulation of epithelial cell proliferation (GO:0050679)	0.024713	-2.32053	EPGN;KDR;TWIST1
carbohydrate derivative transport (GO:1901264)	0.015701	-2.30879	GLTPD2;SLC29A1
negative regulation of viral genome replication (GO:0045071)	0.013767	-2.30868	IFITM3;FAM111A
regulation of MAP kinase activity (GO:0043405)	0.030211	-2.30683	EPGN;NUP62;TNFRSF11A;IKBKG
regulation of trans membrane transporter activity (GO:0022898)	0.023428	-2.2699	TWIST1;NETO2;CACNG2
regulation of organic acid transport (GO:0032890)	0.015701	-2.26756	GRIK1;TNFRSF11A
regulation of transporter activity (GO:0032409)	0.028791	-2.26404	TWIST1;NETO2;CACNG2
ameboidal-type cell migration (GO:0001667)	0.01651	-2.26295	KDR;FAT2;TWIST1
nucleobase-containing compound transport (GO:0015931)	0.007779	-2.26016	NUP214;NUP62;RFTN1;SLC29A1
regulation of receptor activity (GO:0010469)	0.006636	-2.24506	EPGN;NETO2;CACNG2
cellular response to carbohydrate stimulus (GO:0071322)	0.020634	-2.24061	CLEC7A;SLC29A1
membrane depolarization (GO:0051899)	0.011203	-2.23649	GRIK1;CACNG2;SLC29A1

5

ossification (GO:0001503)	0.014181	-2.22879	SIK3;TWIST1;TNFRSF11A
pattern recognition receptor signalling pathway (GO:0002221)	**0.023852**	**-2.22812**	**CLEC7A;RFTN1;IKBKG**
mitotic cell cycle(GO:0000278)	0.029841	-2.22408	NUP214;RFC4;PSMD4;NUP62;MCPH1
innate immune response-activating signal transduction (GO:0002758)	**0.024713**	**-2.21732**	**CLEC7A;RFTN1;IKBKG**
RNA transport(GO:0050658)	0.028791	-2.20544	NUP214;NUP62;RFTN1
nucleic acid transport (GO:0050657)	0.028791	-2.20286	NUP214;NUP62;RFTN1
positive regulation of angiogenesis (GO:0045766)	0.009864	-2.20102	ADM2;KDR;TWIST1
establishment of RNA localization (GO:0051236)	0.028791	-2.19779	NUP214;NUP62;RFTN1
activation of innate immune response (GO:0002218)	**0.027855**	**-2.19528**	**CLEC7A;RFTN1;IKBKG**
activation of immune response (GO:0002253)	**0.156213**	**-2.37209**	**CLEC7A;RFTN1;IKBKG;VSIG4**
regulation of viral genome replication (GO:0045069)	0.026125	-2.15743	IFITM3;FAM111A
epithelial cell migration (GO:0010631)	0.033039	-2.14141	KDR;FAT2
positive regulation of innate immune response (GO:0045089)	**0.049052**	**-2.13089**	**CLEC7A;RFTN1;IKBKG**
regulation of angiogenesis (GO:0045765)	0.04245	-2.12229	ADM2;KDR;TWIST1
regulation of phosphatidylinositol 3-kinase signaling (GO:0014066)	0.033948	-2.10747	KDR;TWIST1

Table S2: Gene ontology terms from the gene cluster 1 correlated with microbiota cluster B as shown in figure 9.

GO Terms	P-value	Z-score	Genes
prepulse inhibition (GO:0060134)	0.001234	-2.77426	GRID2;SLC6A3
positive regulation of cell fate commitment (GO:0010455)	0.001421	-2.69766	PAX6;SPDEF
regulation of transcription involved in cell fate commitment (GO:0060850)	0.003073	-2.87914	PAX6;ETV2
peptidyl-proline hydroxylation (GO:0019511)	0.001421	-2.47785	PDIA2;EGLN3
cell fate determination (GO:0001709)	0.000731	-2.41641	HOXA2;PAX6;ATOH1
transcription from RNA polymerase II promoter (GO:0006366)	0.000392	-2.40003	PAX6;YBX2;NELFB;ETV2;ETV4;ATOH1;ETS2;SPDEF
gland development (GO:0048732)	0.00155	-2.32952	CDKN1C;HOXA3;PAX6;JARID2;KLF1
protein hydroxylation (GO:0018126)	0.002055	-2.55821	PDIA2;EGLN3
glandular epithelial cell differentiation (GO:0002067)	0.003073	-2.61207	PAX6;SPDEF
positive regulation of epithelial cell differentiation (GO:0030858)	0.001158	-2.26286	PAX6;ETV2;ATOH1
motor neuron axon guidance (GO:0008045)	0.004613	-2.74889	HOXA2;ETV4
peptidyl-proline modification (GO:0018208)	0.001351	-2.20772	PDIA2;EGLN3;FKBP5

columnar/cuboidal epithelial cell development (GO:0002066)	0.004613	-2.70177	PAX6;SPDEF
reproductive structure development (GO:0048608)	0.00342	-2.35073	FZD1;CDKN1C;ETV2;TLR5;HS6ST1
anterior/posterior pattern specification (GO:0009952)	0.002681	-2.29488	HOXA3;HOXA2;PAX6;HOXB7
myeloid cell differentiation (GO:0030099)	0.002941	-2.26559	CDKN1C;ETV2;HOXB7;KLF1
embryonic morphogenesis (GO:0048598)	0.004249	-2.39884	CDKN1C;HOXA3;HOXA2;PAX6;HOXB7;ATOH1
regulation of sodium ion transmembrane transporter activity (GO:2000649)	0.006441	-2.65823	STOM;ATP1B1
regulation of cell fate commitment (GO:0010453)	0.006441	-2.45574	PAX6;SPDEF
photoreceptor cell maintenance (GO:0045494)	0.006441	-2.44691	BBS1;LCA5
regulation of sodium ion transmembrane transport (GO:1902305)	0.009936	-2.57256	STOM;ATP1B1
lung alveolus development (GO:0048286)	0.009936	-2.35011	FZD1;HS6ST1
neuron projection guidance(GO:0097485)	0.012856	-2.33942	CNTN2;HOXA2;PAX6;ETV4;ATOH1
axon guidance (GO:0007411)	0.012856	-2.3368	CNTN2;HOXA2;PAX6;ETV4;ATOH1
regionalization (GO:0003002)	0.014697	-2.32869	HOXA3;HOXA2;PAX6;HOXB7
regulation of epithelial cell differentiation (GO:0030856)	0.008652	-2.25846	PAX6;ETV2;ATOH1
regulation of neuron differentiation (GO:0045664)	0.018832	-2.29712	GRID2;CNTN2;HOXA2;PAX6;ATOH1
negative regulation of epithelial cell proliferation (GO:0050680)	0.008865	-2.22922	CDKN1C;PAX6;ETV4
thymus development (GO:0048538)	0.01142	-2.20626	HOXA3;JARID2
cellular response to external stimulus (GO:0071496)	0.033894	-2.20395	NR1H4;TLR5;FOXA3
cilium organization (GO:0044782)	0.012424	-2.19605	BBS1;TTLL3;TTC17
cellular component assembly involved in morphogenesis (GO:0010927)	0.034351	-2.18572	BBS1;TTLL3;MYLK3
neuron migration (GO:0001764)	0.010204	-2.16916	CNTN2;PAX6;ATOH1
negative regulation of neuron differentiation (GO:0045665)	0.018937	-2.18467	CNTN2;HOXA2;PAX6
regulation of organ morphogenesis (GO:2000027)	0.019947	-2.18065	FZD1;HOXB7;ETV4
erythrocyte differentiation (GO:0030218)	0.015235	-2.15956	ETV2;KLF1
hematopoietic or lymphoid organ development (GO:0048534)	0.029502	-2.15619	HOXA3;JARID2;KLF1
sodium ion transport (GO:0006814)	0.017006	-2.15531	SLC9A3;WNK4;ATP1B1
central nervous system development (GO:0007417)	0.008443	-2.10067	PAX6;JARID2;ATOH1

5

Chapter 6

**Supplementation with *L. plantarum* WCFS1
reverts age-related decline of mucus barrier
in fast ageing *Ercc1*$^{-/\Delta 7}$ mice**

Adriaan A. van Beek[1,2], Bruno Sovran[2,3], Floor Hugenholtz[2,4], Ben Meijer[1], Joanne Hoogerland[1], Mark Boekschoten[2,5], Jan J.H. Hoeijmakers[6], Paul de Vos[2,7], Jerry M. Wells[3], Pieter J.M. Leenen[8], Rudi W. Hendriks[9], Huub F.J. Savelkoul[1]

[1] Cell Biology and Immunology Group, Wageningen University, Wageningen, the Netherlands
[2] Top Institute Food and Nutrition, Wageningen, the Netherlands
[3] Host Microbe Interactomics, Wageningen University, Wageningen, the Netherlands
[4] Laboratory of Microbiology, Wageningen University, Wageningen, the Netherlands
[5] Human Nutrition, Wageningen University, Wageningen, the Netherlands
[6] Department of Genetics, Erasmus University Medical Center, Rotterdam, the Netherlands
[7] University of Groningen, Groningen, the Netherlands
[8] Department of Immunology, Erasmus University Medical Center, Rotterdam, the Netherlands
[9] Department of Pulmonary Medicine, Erasmus University Medical Center, Rotterdam, the Netherlands

Abstract

Probiotics are known to be able to improve immunity, intestinal barrier and gut microbiota composition, also in the context of ageing. In this study we investigated the effect on immunity and intestinal barrier in wild-type ($Ercc1^{+/+}$) mice and fast ageing $Ercc1^{-/\Delta7}$ mice (median lifespan 20 weeks) after 10-week supplementation of three candidate probiotic strains, *L. plantarum* WCFS1, *L. casei* BL23, and *B. breve* DSM20213. Observed effects in immunity and intestinal barrier were linked to gene regulation in ileum and colon, and fecal microbiota composition.

Effects of the bacterial supplementations on intestinal barrier and immunity were most apparent in aged $Ercc1^{-/\Delta7}$ mice compared with $Ercc1^{+/+}$ mice, showing that ageing profoundly influences the response to the different interventions. Moreover, the different bacterial strains elicited distinct responses in immunity and intestinal barrier. Supplementation of *L. casei* induced systemic inflammation, marked by increased frequencies of Ly6C^{hi} monocytes, neutrophils, and Th17 cells in spleen. Exacerbation of age-related decline of gut tissue and mucus integrity was observed after supplementation with *B. breve*. Supplementation of *L. plantarum* ameliorated the age-related decline in intestinal barrier of $Ercc1^{-/\Delta7}$ mice. Fecal microbiota composition only slightly shifted upon bacterial supplementation, whereas analysis of gene expression corroborated histological findings.

We conclude that the $Ercc1^{-/\Delta7}$ model can be used to study the effect of long-term probiotic interventions on ageing. Our data provide an example of how bacterial supplementation can restore age-related decline in intestinal barrier, and highlights the caution needed in the selection of candidate probiotic strains for supplementation to ageing individuals.

Introduction

Multiple types of DNA damage lead to a decline in the regenerative potential of tissues due to stem cell exhaustion, one of the hallmarks of ageing [301]. With age, hematopoietic stem cells (HSC) acquire defects [302] [303]. HSC do not efficiently generate lymphoid cells, whereas relatively more myeloid cells are generated [304] [305], also known as the myeloid bias. Furthermore, thymus and bone marrow involute, and long-lived B cells accumulate, leading to decreased T and B cell production [306] [307] [308]. Immunity and gut microbiota composition are intimately linked with each other [161], and these change with age, leading to immunosenescence and low-grade inflammation ("inflammageing") [161] [309].

A crucial component of the intestinal barrier is secreted mucus comprising of a highly glycosylated MUC2 which polymerizes through the *N*- and *C*-termini into large net-like polymers, which, after secretion from goblet cells, form a transparent gel-like structure [61]. In healthy conventional mice, the secreted mucus forms a firmly adherent layer (about 50 μm in tissue explants) over the colon epithelium that serves to spatially compartmentalize bacteria to the lumen [61]. *Muc2*^{-/-} spontaneously develop colitis after weaning, demonstrating the important barrier function of mucus [121]. In the ileum, however, increased expression of the IL-22-mediated network genes involved in epithelial repair and barrier defense, including *Fut2*, *Reg3β*, *Reg3γ*, *Relmb*, appear to be sufficient to maintain homeostasis and prevent epithelial damage due to inflammatory responses to bacteria (Chapter 2) [251]. Recently, the thickness of the firm mucus barrier in the colon was shown to be thinner and more permeable to bacteria in 18- to 19-month-old mice than in young 10- week-old mice (Chapter 4). Secreted mucus is an important substrate for specific gut microbiota, such as *Akkermansia muciniphila* [7], and the MUC2 glycoprotein regulates immunity by inducing tolerogenic signals in mucosal dendritic cells [92]. Changes in mucus quantity and integrity, therefore, influence gut microbiota and immunity (Chapter 2)[251] [92].

It has been shown that specific food-ingredients such as probiotic supplementation to elderly subjects lead to changes in fecal microbiota composition and defecation frequency [310] [309] [311] [312] [313] [314] [315] [316]. Probiotics are live bacteria that confer health benefits to the host, for example by competing with pathogens, regulating immunity and enhancing intestinal barrier function [297] [317] [269] and might therefore prevent some of the undesired immune and barrier effects related to ageing. Supplementation of elderly subjects with *Bifidobacterium lactis* HN019 increased the proportions of total CD4^{+} T cells, CD25^{+} activated T cells, and CD56^{+} NK cells. Additionally this strain elevated the *ex vivo* phagocytic capacity of mononuclear and polymorphonuclear phagocytes and the tumoricidal activity of NK cells after supplementation to elderly subjects [318] [319]. In mice, probiotic supplementation with *Bifidobacterium animalis* LKM512 decreased colon permeability, extended lifespan and improved quality of life [320]. Supplementation

of aged mice with *Lactobacillus paracasei* NCC2461 resulted in increased IgG2a titers after antigenic challenge [321]. Besides these studies, little is known about how prolonged exposure to probiotics impact on the effects of ageing on the intestinal barrier and systemic immune system.

Several fast ageing mouse models exist, but we have recently described the suitability of the *Ercc1*[-/Δ7] mouse model for ageing and its effects on immunity and intestinal barrier (van Beek *et al.*, unpublished). The fast ageing phenotype of *Ercc1*[-/Δ7] mice (median lifespan 20 weeks) is caused by impaired capacity of the ERCC1 protein, which is involved in nucleotide excision repair and recombination repair [322] [323]. We previously also showed that the immune system of *Ercc1*[-/Δ7] mice is positively sensitive to e.g. tryptophan restriction diet (van Beek *et al.*, unpublished), indicating the possibility to modulate the fast ageing phenotype in *Ercc1*[-/Δ7] mice by diet.

The aim of this study was to investigate the potential of long-term supplementation with candidate probiotic strains for amelioration of the effects of ageing on intestinal barrier function in *Ercc1*[-/Δ7] mice. We analyzed distribution and activation of immune cells in various mucosal and peripheral lymphoid organs. To determine effects on intestinal barrier, we analyzed tissue integrity, mucus barrier, gene regulation, and microbiota composition in the gut.

Materials and Methods

Mice

The generation and characterization of *Ercc1*[+/Δ7] and *Ercc1*^{-/+} mice has been previously described [324]. *Ercc1*[-/Δ7] mice were obtained by crossing *Ercc1*[+/Δ7] with *Ercc1*^{-/+} mice of pure C57Bl6/J and FVB backgrounds to yield *Ercc1*[-/Δ7] with an F1 C57Bl6J/FVB hybrid background. Wild-type littermates were used as controls. Typical unfavorable characteristics, such as blindness in an FVB background or deafness in a C57Bl6/J background, do not occur in this hybrid background.

Mice were clinically diagnosed daily, and weighed, visually inspected, and scored for gross morphological and motor abnormalities weekly. Since *Ercc1*[-/Δ7] mice were smaller, food was administered within the cages and water bottles with long nozzles were used from around two weeks of age. Animals were maintained in a controlled environment (20-22°C, 12h light - 12h dark cycle) and were housed in individual ventilated cages under SPF conditions. Experiments were performed in accordance with the Principles of Laboratory Animal Care and with the guidelines approved by the Dutch Ethical Committee in full accordance with European legislation. All animals were bred and maintained in the animal facility of Erasmus University Medical Center (Rotterdam, NL) on AIN93G synthetic pellets (Research Diet Services B.V., Wijk bij Duurstede, the

Netherlands; gross energy content 4.9 kcal/g dry mass). At the age of 5 weeks, mice were transferred to the animal facility of Wageningen University (Wageningen, NL). Mice had free access to AIN93 D12450B diet (Research Diet Services, Wijk bij Duurstede, NL; gross energy content 3.9 kcal/g dry mass).

Genotyping

Genotyping was performed on DNA isolated from toe. *Ercc1* alleles were genotyped by PCR using the following primers: Exon-7 sense: 5'-AGCCGACCTCCTTATGGAAA; Intron-7 antisense: ACAGATGCTGAGGGCAGACT; Neo[R] sense: 5'-TCGCCTTCTTGACGAGTTCT; and 3'-UTR antisense: 5'-CTAGGTGGCAGCAGGTCATC. A 0.5kb fragment was generated from the delta allele using primers Neo and UTR, a 0.4kb from the knockout allele using Neo and Intron primers, whereas a 0.25kb fragment was amplified from the wild type or delta allele using the Exon/Intron primerset. Cycling conditions were 95°C for 15sec, 62°C for 15sec, 72°C for 30sec (35 cycles), followed by an extension at 72°C for 5min. The amplified fragments were size separated on a 2% agarose gel.

Bacterial cultures and supplementation

Lactobacillus plantarum WCFS1, *Lactobacillus casei* BL23, and *Bifidobacterium breve* DSM20213 were grown on MRS medium (Merck, Darmstadt, Germany) until stationary phase, frozen in glycerol, and stored in -80°C until use. Viability was assessed through plating on MRS agar and expressed as colony forming units (CFU)/mL. Upon use, bacteria were thawed and 10x diluted in $NaHCO_3$/PBS buffer. Around $2 * 10^8$ CFU in 200 µL were administered to mice by gavage, three times per week. Treatment of mice started at 6 weeks of age until sacrifice at 16 weeks or (moribund) kill.

In vivo immunization and antibody detection

Primary and secondary T-cell dependent (TD) immune responses were measured 7 days after primary i.p. immunization (0.1 mg TNP-KLH in 0.8 mg alum) and 7 days after i.p. booster immunization (0.1 mg TNP-KLH in PBS). The primary immunization was performed at 8 weeks of age, booster doses were injected at 12 weeks of age. Total and TNP-specific Ig subclasses were determined by sandwich ELISA as previously described [325].

General flow cytometry procedures

Single-cell suspensions of bone marrow (BM) were obtained by crushing femurs, tibias, iliac crests, and sternum with mortar and pestle. BM cells were then filtered on a 40 µm cell strainer. A proportion of the BM cells were frozen for later use *in vitro*. Spleen, mesenteric lymph nodes (MLN), Peyer's patch (PP), thymus and peritoneal cavity single cell suspensions were obtained by gently pushing cells through a 40 µm cell strainer

with a syringe. All cells were stained for extracellular markers and dead cells were identified with fixable live/dead stain (Ebioscience, San Diego, CA, USA), after which intracellular staining was enabled by fixing and permeabilizing cells with Fix/Perm buffer (Ebioscience) according to manufacturer's instructions. Antibodies used for flow cytometric measurements are listed in Supplementary Table S1. All flow cytometric measurements were performed on a Canto II flow cytometer (BD Biosciences, Erembodegem, Belgium). FlowJo vX.07 software (Tree Star) was used for data analysis.

B cell purification and cultures of naive B2 cells

Splenic cells were depleted for activated B cells, B1 cells, (pre)plasma cells and non-B cells using biotinylated anti-CD5, CD11b, CD43, CD95, CD138, Gr-1 and TER-119 and streptavidin-conjugated magnetic beads (BD Biosciences). After depletion of labeled cells with Imagnet (BD Biosciences), purity of naive B2 cells typically exceeded 95% as verified by flow cytometric measurements. Purified naive B2 cells were cultured at 1.2 x 10^6 cells/mL for 3 or 7 days in the presence of 10 μg/mL F(ab'2) goat anti-mouse-IgM (Jackson Immunoresearch), 5 μg/mL LPS (*S. minnesota*, Sigma), 5 μg/mL LPS + 0.1 μg/mL IL-4 (BioLegend), 1 μM CpG (ODN1668, Invitrogen) or 20 μg/mL anti-CD40 (3/23, BD Biosciences).

Spleen cultures

Splenic cells were cultured at 1 x 10^6 cells/mL for four days in the absence or presence of concanavalin A (ConA). Proliferation was measured by Ki-67 (Ebioscience). Supernatants were stored at -20°C for maximally 3 months. After thawing, IL-2, IL-4, IL-6, IL-10, IL-17A, IFN-γ, and TNF were measured with the Cytometric Bead Array (CBA) Th1/Th2/Th17 Kit (BD Biosciences), according to manufacturer's instructions. Samples were acquired on a Canto II flow cytometer.

Histology

Paraffin sections (5 μm) of ileum colon were attached to poly-L-lysine-coated glass slides (Thermo scientific, Germany). After overnight incubation at 37°C, slides were de-waxed and hydrated step-wise using 100% xylene followed by several solutions of distilled water containing decreasing amounts of ethanol. Sections were stained with hematoxylin and eosin (H&E) and PAS/Alcian blue [194]. Mucus layer thickness and crypt length were measured (10 measurements per section / 2 sections per animal / 5 animals per condition) using ImageJ software (NIH, Maryland, USA).

Detection of bacteria using fluorescent *in situ* hybridization (FISH)

The slides were deparaffinized with xylene and rehydrated in a series of ethanol solutions to 100% ethanol. The tissue sections were incubated with the universal bacterial probe EUB338 (5'-GCTGCCTCCCGTAGGAGT-3') (Isogen Bioscience BV, De Meern, the Netherlands) conjugated to Alexa Fluor488. A 'non-sense' probe (5'-CGACGGAGGGCATCCTCA-3') conjugated to Cy3, was used as a negative control. Tissue sections were incubated overnight with 0.5 µg of probe in 50 µL of hybridization solution (20 mmol/L Tris-HCl (pH 7.4), 0.9 mol/L NaCl, 0.1% (w/v) SDS) at 50°C in a humid environment using a coverslip to prevent drying of the sample. The sections were washed with (20 mmol/L Tris-HCl (pH 7.4), 0.9 mol/L NaCl) at 50°C for 20 min and then washed 2 times in PBS for 10 min in the dark and incubated with DRAQ5 (Invitrogen) (1:1000) for 1 h at 4°C to stain nuclei. Sections were washed 2 times in PBS for 10 min, mounted in fluoromount G (SouthernBiotec, Alabama, USA) and stored at 4°C.

RNA isolation and transcriptome analysis

Total RNA was isolated using the RNeasy kit (Qiagen) with a DNase digestion step according to the manufacturer's protocol. One microgram of RNA was reverse transcribed using a qScript cDNA synthesis kit (Quanta Biosciences, Gaithersburg, MD) according to the manufacturer's protocol. Quantity and quality of ileal and colonic RNA (3-6 arrays of individual mice per group) was assessed using spectrophotometry (ND-1000; NanoDrop Technologies, Wilmington, NC) and Bionanalyzer 2100 (Agilent, Santa Clara, CA), respectively. RNA was only used to generate cDNA and perform microarray hybridization when there was no evidence of RNA degradation (RNA Integrity Number > 8). One hundred nanogram of total RNA was labeled using the Ambion WT Expression kit (Life Technologies Ltd, Paisley, United Kingdom) together with the Affymetrix GeneChip WT Terminal Labeling kit (Affymetrix, Santa Clara, CA). Labelled samples were hybridized to Affymetrix GeneChip Mouse Gene 1.1 ST arrays. Hybridization, washing, and scanning of the array plates were performed on an Affymetrix GeneTitan Instrument, according to the manufacturer's recommendations. Quality control of the data sets obtained from the scanned Affymetrix arrays was performed using Bioconductor [195] packages integrated in an online pipeline [196]. Probe sets were redefined according to Dai *et al.* [197] using current genome information. In this study, probes were reorganized based on the Entrez Gene database (remapped CDF v18.0.1). Normalized expression estimates were obtained from the raw intensity values using the Robust Multiarray Analysis preprocessing algorithm available in the Bioconductor library affyPLM using default settings [198]. Differentially expressed probe sets were identified using linear models, applying moderated T-statistics that implemented empirical Bayes regularization of SEs [199]. A Bayesian hierarchical model was used to define an intensity-based moderated T-statistic, which takes into account the degree of independence of

variances relative to the degree of identity and the relationship between variance and signal intensity [200]. Only probe sets with a fold change of at least 1.2 (up or down) and p<0.05 were considered to be significantly different. Pathway analysis was performed by Gene Set Enrichment Analysis (GSEA) [202] [201]. Potential upstream regulators were identified through the use of QIAGEN's Ingenuity Pathway Analysis (IPA®, QIAGEN Redwood City, www.qiagen.com/ingenuity).

Bacterial DNA extraction and microbiota profiling

Microbiota composition in feces was analyzed by Mouse Intestinal Tract Chip (MITChip), a diagnostic 16S rRNA gene array that consists of 3580 unique probes especially designed to profile mouse intestine microbiota [203]. 16S rRNA gene amplification, in vitro transcription and labeling, and hybridization were carried out as described previously [204]. The data were normalized and analyzed using a set of R-based scripts in combination with a custom-designed relational database, which operates under the MySQL database management system. For the microbial profiling, the Robust Probabilistic Averaging signal intensities of 2667 specific probes for the 94 genus-level bacterial groups detected on the MITChip were used [205]. Diversity calculations were performed using a microbiome R-script package (https://github.com/microbiome). Multivariate statistics, redundancy analysis, and principal response curves were performed in Canoco 5.0 and visualized in triplots or a principal response curves plot [206].

Statistical analysis

To test differences between treatment groups, unpaired t tests were performed in GraphPad Prism software version 5.0.3 (San Diego, CA, USA). Significant differences were indicated by asterisks: *= p<0.05; **= p<0.01; ***= p<0.001.

Results

To investigate effects of long-term bacterial supplementation on ageing immunity and intestinal barrier, we supplemented 6-week-old *Ercc1*-/Δ7 and *Ercc1*+/+ mice one of three candidate probiotic strains: *Lactobacillus plantarum* WCFS1, *Lactobacillus casei* BL23, or *Bifidobacterium breve* DSM20213 (or ATCC15700). Previously, probiotic activity has been shown for *L. plantarum* WCFS1 [326] [327] [328] [329] [330] [331] [332] and *L. casei* BL23 [333] [334] [335]. Relatives of *B. breve* DSM20213 have also shown probiotic activity [336].

L. casei supplementation induces systemic inflammation

First, we evaluated changes in distribution of immune cells in mucosal and peripheral immune organs. B cell frequencies were reduced in PP and MLN after *L. casei* supplementation in *Ercc1*-/Δ7 mice (Suppl. Fig. S1). In contrast, frequencies of T cells were increased. In spleen, B cell frequencies were decreased (p=0.057) after *L. casei* supplementation, but no changes in T cell frequencies were observed (data not shown). Ly6C^{hi} monocyte (CD11b$^+$Ly6G$^-$CD68$^+$, Fig. 1A) and neutrophil (CD11b$^+$CD68^{int}Ly6C^{int}Ly6G$^+$) frequencies were increased after *L. casei* supplementation (Fig. 1B, C). In addition, RORγt$^+$ Th17 cells were increased after *L. casei* supplementation (Fig. 1D). A four-day culture of splenocytes stimulated with concanavalin A, showed increased IL-17A production (Fig. 1E) and decreased T cell proliferation in splenocytes derived from *L. casei*-treated mice (Suppl. Fig. S2A). Purified naive B2 cells were stimulated with several ligands, for three or seven days. Decreased CD86 expression in B cells derived from mice supplemented with *L. casei* was observed after three-day stimulation with LPS and IL-4 (Suppl. Fig. S2B).

As the observed changes in cell distribution can be explained by decreased migration or production of lymphocytes, or increased migration or production of myeloid cells, we investigated the distribution of B cells and myeloid cells in BM and T cells in thymus. In BM, we observed significantly higher CD11b$^+$Ly6G$^+$ neutrophil frequencies after *L. casei* supplementation (35% vs. 29% in control, data not shown). Total CD19$^+$CD45R$^+$ B cell frequencies were significantly decreased after *L. plantarum* and *L. casei* supplementation, but not after *B. breve* supplementation (Suppl. Fig. S3A). *L. casei* supplementation reduced sIgκ/λ$^+$cIgM$^+$IgD^{hi} recirculating mature, sIgκ/λ$^+$cIgM$^+$IgD^{lo} immature, and cIgM$^+$CD2$^+$ small resting pre-B cells, but to a lesser extent cIgM$^+$CD2$^-$ large cycling pre-B and cIgM$^-$CD2$^-$ pro-B cells (Suppl. Fig. S3B-F), indicating that *L. casei* supplementation arrests B cell development in BM. In thymus, only *L. casei* supplementation caused changes in cell distribution, in particular increasing CD3$^-$CD4$^-$CD8$^-$ double negative (DN) stages at the expense of CD3$^-$CD4$^+$CD8$^+$ double positive (DP) frequencies (Suppl. Fig. S4).

6

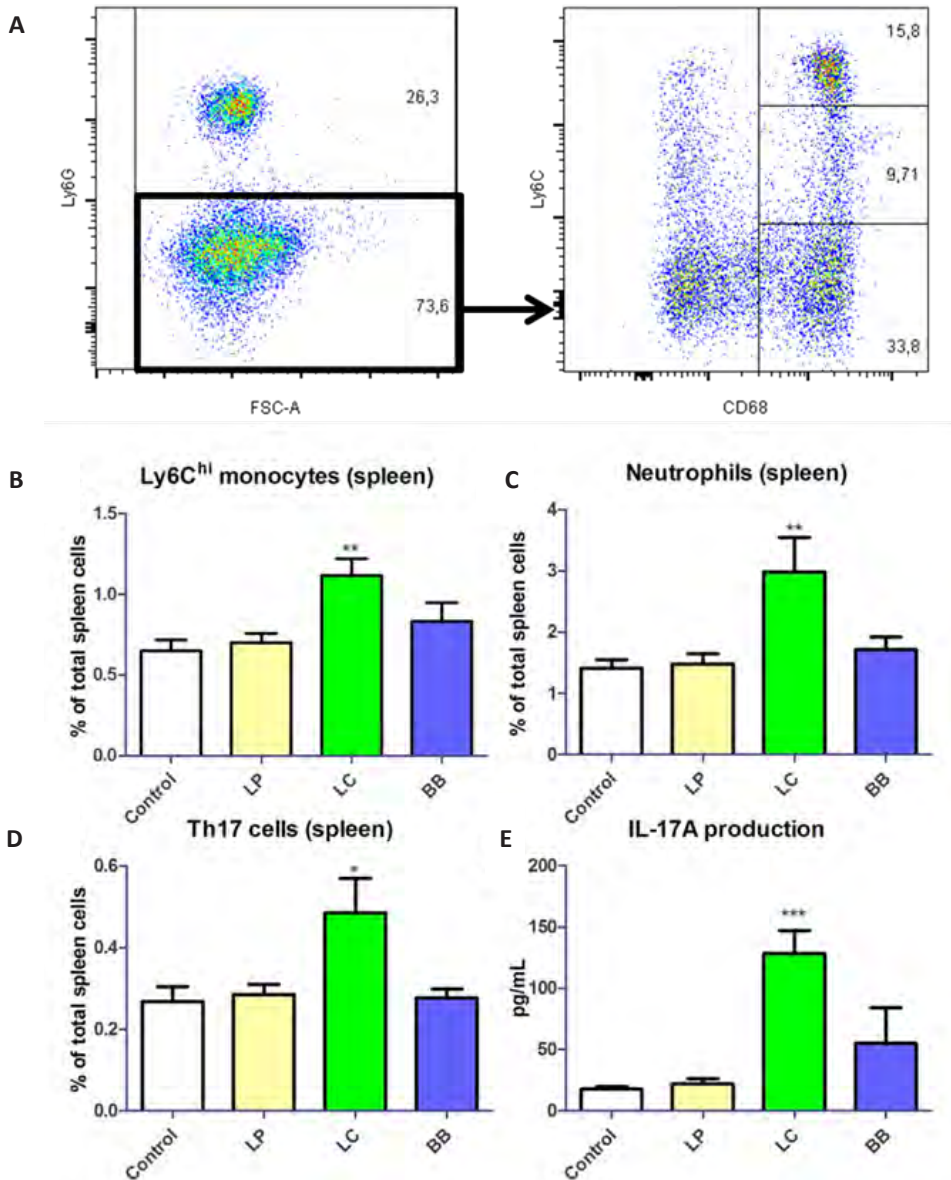Collectively, these data show that long-term *L. casei* supplementation induced systemic inflammation in aged *Ercc1*$^{-/\Delta7}$ mice.

Figure 1: *L. casei* supplementation of *Ercc1*$^{-/\Delta7}$ mice caused increased Ly6C^{hi} monocyte, neutrophil and Th17 frequencies in spleen, accompanied by increased IL-17A production in splenocytes. A) Flow cytometric analysis of neutrophils and monocytes. Splenic CD11b$^+$ cells were gated for Ly6G$^+$ neutrophils and Ly6G$^-$ CD68$^+$ monocytes. Monocytes were further divided in Ly6C^{hi}, Ly6C^{int}, and Ly6C^{lo} monocytes. B-E) Mean frequencies, concentrations, and relative fluorescence intensities were determined by flow cytometry, and using a Cytometric Bead Array. Th17 cells were defined as CD3e$^+$CD4$^+$CD8a$^-$RORγt$^+$. IL-17A production was determined in supernatants of splenocytes stimulated with ConA for four days. Data represent the mean + S.E.M. from 4-6 animals per group.

Bacterial supplementation alters mucosal integrity and mucus barrier in ageing ileum

As bacteria were supplemented by oral gavage, the effects of bacterial supplementation on tissue integrity in the ileum were investigated by histological methods. The histology of the ileum of aged *Ercc1*$^{-/\Delta7}$ mice was comparable to that of aged *Ercc1*$^{+/+}$ mice (Fig. 2). However, bacteria were found closer to epithelium in aged *Ercc1*$^{-/\Delta7}$ mice than in *Ercc1*$^{+/+}$ mice, despite there being no discernable differences in the overall location of the secreted mucus (Fig. 2). Supplementation with *L. plantarum* and *L. casei* did not change tissue and mucus integrity, or mucus location (data not shown). In contrast, supplementation with *B. breve* caused extensive villus atrophy (Fig. 2).

Different bacterial supplements regulate distinct growth factors and cytokines

To examine the observed differences in integrity of ileum tissue of aged *Ercc1*$^{-/\Delta7}$ mice at molecular level, we performed gene expression microarrays. All the bacterial supplements significantly altered expression of hundreds of genes compared with control mice: 465 genes by *L. plantarum*, 350 genes by *L. casei*, and 879 genes by *B. breve* (Fig. 3). The genes differentially regulated by the different bacterial supplementations were distinct from each other (Fig. 3). Gene set enrichment analysis (GSEA) showed that supplementation with *L. plantarum* significantly enhanced general processes such as cell growth and proliferation, DNA repair, immunity, barrier function, and metabolism (Suppl. Table S2), whereas this was not the case after supplementation with *L. casei* or *B. breve.* In fact some gene sets associated with these processes were significantly decreased in *L. casei-* and *B. breve-* treated mice compared with control mice. The significantly enriched gene sets identified in transcriptomes of mice administered *B. breve* were correlated with deterioration of tissue and mucus barrier integrity. Increased expression of E-cadherin, integrins, tight junction proteins and Wnt signaling after *L. plantarum* supplementation might point to maintenance of barrier function.
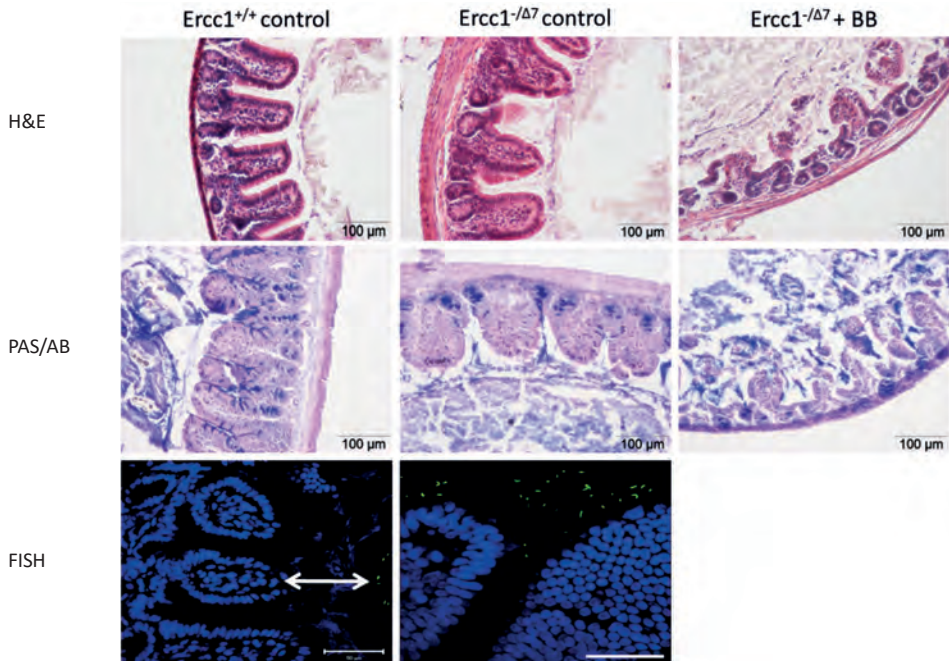
6

Figure 2: Representative pictures of H&E, PAS/Alcian Blue staining of ileum of *Ercc1*$^{+/+}$, aged *Ercc1*$^{-/\Delta7}$ and aged *Ercc1*$^{-/\Delta7}$ supplemented with *B. breve* (BB). Scale bars: 100 μm for H&E and PAS/AB staining. FISH staining (in green; cell nuclei in blue) of ileum of *Ercc1*$^{+/+}$, aged *Ercc1*$^{-/\Delta7}$ and aged *Ercc1*$^{-/\Delta7}$ supplemented with *B. breve* (aged *Ercc1*$^{-/\Delta7}$ + BB). Scale bars: 50 μm.

Next, we determined potential upstream regulators that can explain the observed gene expression changes, using Ingenuity Upstream Regulator Analysis. We focused on cytokines, growth factors and unclassified factors (including immunoglobulins). Upstream regulators predicted to be involved in the gene expression changes in ileum of aged *Ercc1*$^{-/\Delta7}$ mice after supplementation with *L. plantarum* and *B. breve* are listed in Table 1. In this analysis, no differences between control and *L. casei* supplementation were observed, fully in line with histology results.

Some upstream regulators were shared among the differentially expressed gene networks of *L. plantarum*- and *B. breve*-treated mice compared with control mice. For example, TNF was inhibited in both groups, whereas epidermal growth factor (EGF), insulin 1, insulin-like growth factor (IGF)-1, IL-1α and TGF-β1 were predicted to be activated in both groups (p<0.05). Growth hormone was predicted to be activated and insulin induced gene 1 (INSIG1) was predicted to be inhibited only after *L. plantarum* supplementation. IFN-γ, IFN-β, and heat shock protein 90 (Hsp90) were predicted to be inhibited, and glial cell line-derived neurotrophic factor (GDNF) was predicted to be activated only in the *B. breve*-treated mice.
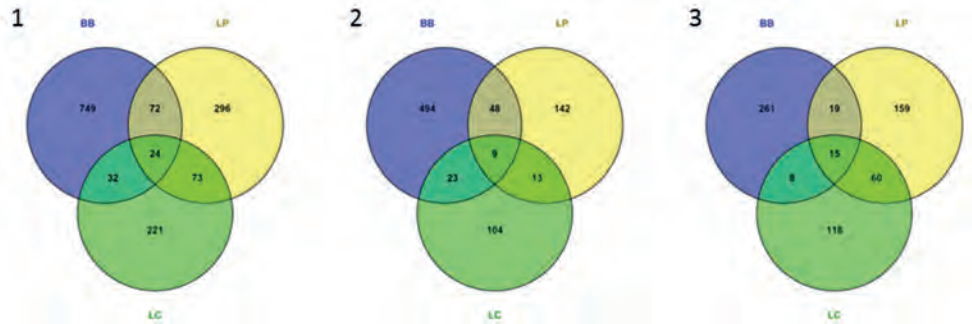
Figure 3: Venn diagrams of differentially regulated genes in ileum of aged *Ercc1*^{-/Δ7} after bacterial supplementation. Venn diagram of the total number of genes altered in the ileum of aged *Ercc1*^{-/Δ7} mice treated with *L. plantarum* (LP), *B. breve* (BB), or *L. casei* (LC), compared with control-treated *Ercc1*^{-/Δ7} mice (1). Venn diagram of the number of genes up-regulated (2) and down-regulated (3) in the ileum of aged *Ercc1*^{-/Δ7} mice treated with LP, BB, or LC (p<0.05 and >1.2-fold difference).

Table 1. Common and specific potential upstream regulators in ileum of aged *Ercc1*^{-/Δ7} mice after bacterial supplementations *L. plantarum* (LP), *L. casei* (LC), or *B. breve* (BB) as determined by Ingenuity Pathway Analysis. Analysis of potential upstream regulators was restricted to "cytokines", "growth factors" and "others". Cut-off values for activation z-score ≥ 1.5 or ≤ -1.5 and p<0.05. Up regulated in green, down regulated in red.

Upstream regulators	LP	LC	BB
Ins1	3.4		1.4
IL-1α	2.2		2.4
IGF-1	2.2		1.9
EGF	1.9		2.1
TGF-β1	1.6		2.1
TNF	-2.1		-1.2
IFN-α2			-3.1
ADIPOQ			2.6
IFN-γ			-2.5
GDNF			2.4
GH	2.4		
Hsp90			-2.2
INSIG1	-2.2		
VEGF			2.0
PDGFBB	1.9		-0.1
FGF8			2.0
SCAP	2.0		
RETN	1.9		
FSH			1.9
CaM			1.6
FGF21	0.1		1.5
IFN-β1			-1.5

Legend: ADIPOQ = adiponectin; CaM = calmodulin; EGF = epidermal growth factor; FGF = fibroblast growth factor; FSH = follicle stimulating hormone; GDNF = glial cell line-derived neurotrophic factor; GH = growth hormone; Hsp = heat shock protein; IFN = interferon; IGF = insulin-like growth factor; Ins = insulin; INSIG = insulin induced gene; PDGF = platelet-derived growth factor; SCAP = SREBP cleavage-activating protein; RETN = resistin; TGF = transforming growth factor; TNF = tumor necrosis factor; VEGF = vascular endothelial growth factor.

6

Mucus barrier function restored in aged *Ercc1*^{-/Δ7} mice supplemented with *L. plantarum*

Because bacterial supplementation altered mucosal and systemic immunity, or ileum barrier integrity compared with control mice, we investigated the tissue integrity and mucus barrier in colon. As previously reported for wild-type mice and *Ercc1*$^{-/\Delta 7}$ mice (chapter 4 and van Beek *et al.*, unpublished), colon of aged *Ercc1*$^{-/\Delta 7}$ mice compared with colon of *Ercc1*$^{+/+}$ mice showed age-dependent decline of tissue and mucus integrity (Fig. 4, 5). Aged *Ercc1*$^{-/\Delta 7}$ mice supplemented with *L. plantarum* showed a thicker colonic inner mucus layer compared with control mice (Fig. 4, 5). The effect of this treatment on the spatial compartmentalization of bacteria in the colon was visualized using FISH. We observed a restored inner mucus layer with a clear 'gap' of about 20 μm between the microbiota and the epithelium, as observed in *Ercc1*$^{+/+}$ mice (Fig. 4, 5). In association with this finding, less inflammation was observed in the colon of mice treated with *L. plantarum* compared with control, as evidenced by less immune cell infiltration and a thinner mucosa than the aged *Ercc1*$^{-/\Delta 7}$ mice and aged *Ercc1*$^{-/\Delta 7}$ mice supplemented with *L. casei* or *B. breve* (Fig. 4). In contrast, supplementation of aged *Ercc1*$^{-/\Delta 7}$ mice with *B. breve* led to a thinner mucus barrier and evidence of increased epithelial damage compared with aged *Ercc1*$^{-/\Delta 7}$ control mice.
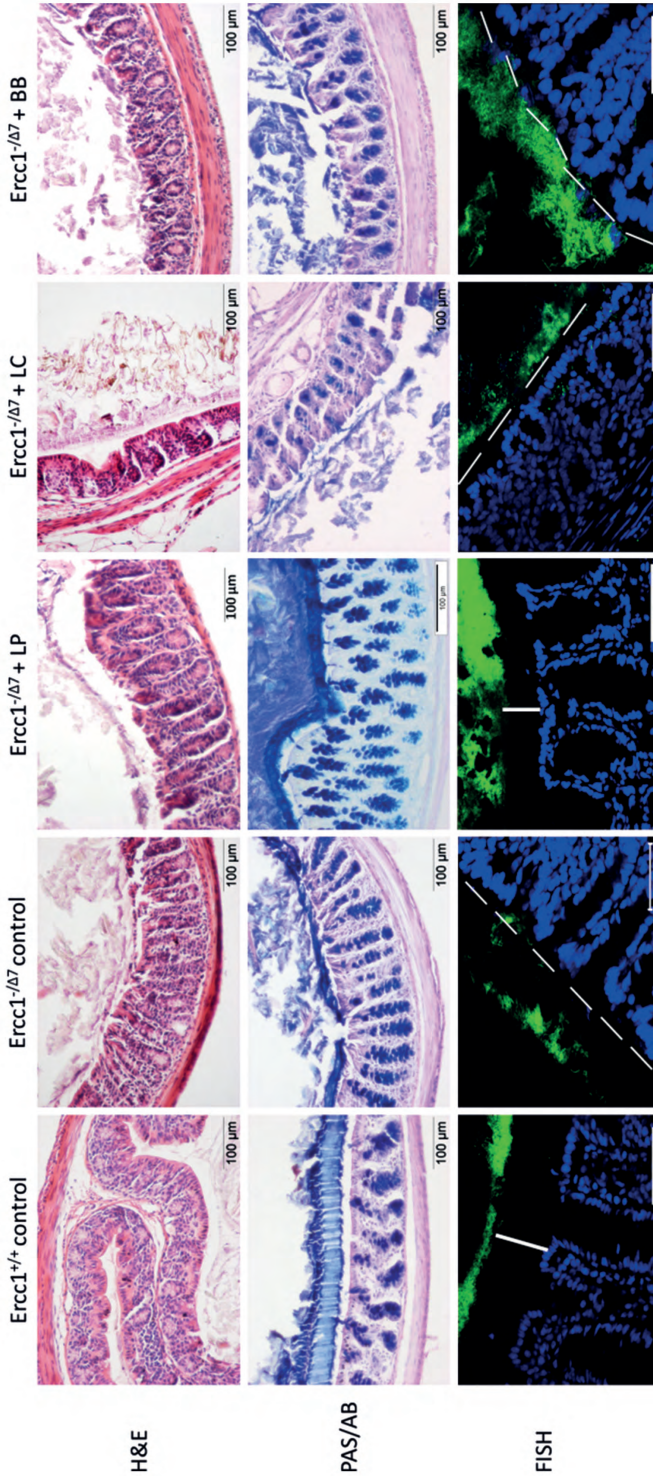
Figure 4: Treatment with *L. plantarum* improves the colonic mucus barrier function and the intestinal tissue integrity of aged *Ercc1*^−/Δ7 mice. *Representative pictures of colon of 4-6 mice per group stained with H&E, PAS/Alcian Blue, and FISH, of *Ercc1*^+/+, aged *Ercc1*^−/Δ7 and aged *Ercc1*^−/Δ7 mice supplemented with *L. plantarum* (LP), *L. casei* (LC), or *B. breve* (BB). Scale bars histological pictures: 100 μm; Scale bars FISH: 50 μm. Dashed lines represent the top of the epithelium. Vertical bar represents the mucus layer*
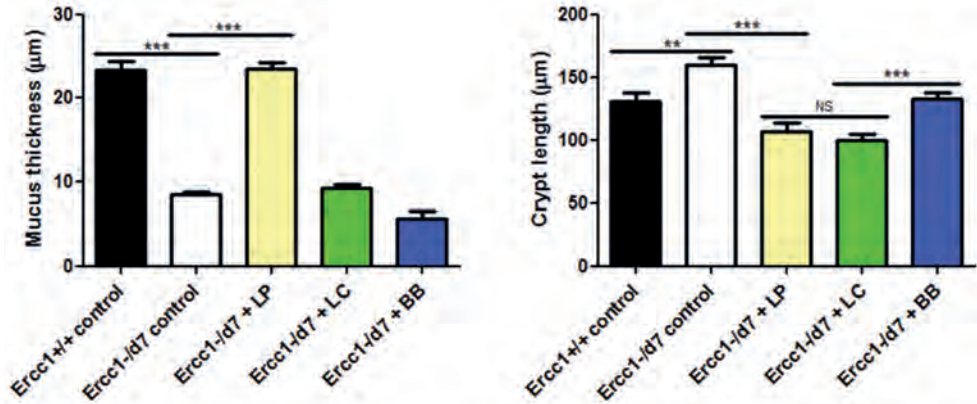
6

Figure 5: *L. plantarum* supplementation completely restored age-related decline in mucus thickness in *Ercc1*^{-/Δ7} mice. Mucus thickness and crypt length measurement as determined by ImageJ. Measurements based on PAS/Alcian Blue staining of colon of *Ercc1*^{+/+}, aged *Ercc1*^{-/Δ7} and aged *Ercc1*^{-/Δ7} mice supplemented with *L. plantarum* (LP), *L. casei* (LC), or *B. breve* (BB). Data represent the mean + S.E.M. from 4-6 animals per group. ***p<0.001; **p<0.01.

Regulation of pro-inflammatory cytokines in colon after *L. plantarum* supplementation

Next, we performed transcriptome analysis on tissue from the proximal colon. Gene expression microarrays performed on colon revealed lower numbers of regulated genes (compared with ileum): 84 by *L. plantarum*, 238 by *L. casei*, and 384 by *B. breve* (Fig. 6).
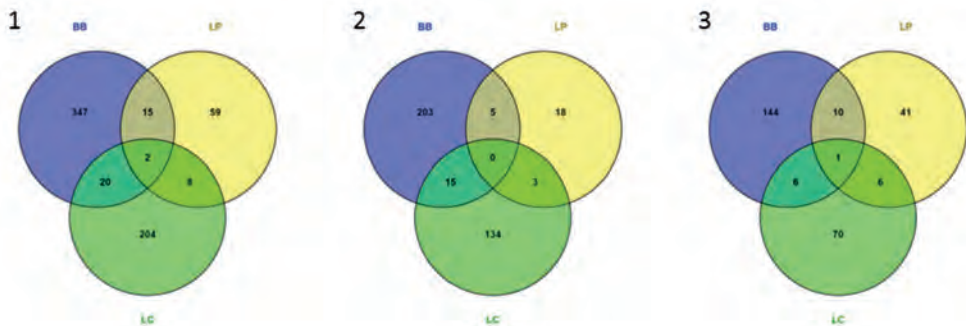

Figure 6: Venn diagrams of differentially regulated genes in colon of *Ercc1*^{-/Δ7} mice after bacterial supplementation. Total number of genes altered in the proximal colon of aged *Ercc1*^{-/Δ7} mice treated with *L. plantarum* (LP), *B. breve* (BB), or *L. casei* (LC), compared with control-treated *Ercc1*^{-/Δ7} mice (1). Venn diagram of the number of genes up-regulated (2) and down-regulated (3) in the proximal colon of aged *Ercc1*^{-/Δ7} mice treated with LP, BB, or LC (p<0.05 and >1.2-fold difference).

As in ileum, a distinct set of genes was differentially expressed in the different bacterial supplemented mice compared with control mice (Fig. 6). Apolipoprotein (*APO*) *A-1*, and *APOA-4* were upregulated more than 2-fold after *L. plantarum* supplementation. In addition, suppressor of cytokine signaling (*SOCS*) *3* and Toll-like receptor (*TLR*) *4* were more than 1.2-fold upregulated in *L. plantarum* treated mice. Several immunoglobulin-related genes

were upregulated after administration of *L. casei*, whereas defensin 40β was 1.3-fold downregulated. Defensin 24α was upregulated more than 6-fold after administration of *B. breve*, while *TLR6*, *TLR7*, and *CCL3* (*MIP-1α*) were more than 1.2-fold downregulated.

GSEA showed that *L. plantarum* supplementation enhanced growth and cell cycle, DNA repair, immunity, barrier function, and metabolism (Suppl. Table 3). Supplementation with *L. casei* enhanced growth and cell proliferation, and unfolded protein response (UPR), while supplementation with *B. breve* enhanced metabolism and Wnt signaling.

Upstream regulators that can explain the observed gene expression changes were identified using Ingenuity Upstream Regulator Analysis and focusing on cytokines, growth factors and unclassified factors (including immunoglobulins). Upstream regulators predicted to be involved in the gene expression changes in colon of aged *Ercc1*$^{-/\Delta7}$ mice upon supplementation with the different candidate probiotics are listed in Table 2. Inflammatory cytokines (GM-CSF, IFN-γ, IL-1β, and IL-4) and CD40L (CD154) were predicted to be more activated in colon of mice supplemented with *L. plantarum*, compared with colon of mice supplemented with control. In contrast, IFN-γ and IgG were predicted to be inhibited in colon of mice supplemented with *B. breve*. EGF, insulin, and platelet-derived growth factor (PDGF) BB were predicted to be activated by both *L. plantarum* and *B. breve* supplementation. No specific upstream regulators, other than resistin-like β, were identified in colon from *L. casei*-treated mice.

Ageing and bacterial supplementation associated with altered microbiota composition

To investigate the impact of genotype and bacterial supplementation in *Ercc1*$^{-/\Delta7}$ mice on the microbial community, 16S rRNA gene microbiota profiles of feces from 6- and 16-week-old *Ercc1*$^{+/+}$ and aged *Ercc1*$^{-/\Delta7}$ mice receiving control or a candidate probiotic were analyzed. The microbial diversity and richness in *Ercc1*$^{-/\Delta7}$ at 6 weeks was significantly less than in *Ercc1*$^{+/+}$ (Suppl. Fig. S5A, B). The bacterial supplementations did not alter diversity or richness.

Redundancy analysis (RDA) showed different microbial communities in aged control *Ercc1*$^{-/\Delta7}$ and bacterial supplemented *Ercc1*$^{-/\Delta7}$ groups at 16 weeks of age, though not significant and the bacterial supplemented groups were overlapping (Fig. 7). RDA indicated 10.1% of the variance within the microbiota could be explained by bacterial supplementation. The x-axis explains 4.9% of the variance and separates mainly *Ercc1*$^{-/\Delta7}$ mice supplemented with bacterial strains from the control *Ercc1*$^{-/\Delta7}$ mice. The y-axis contributes 3.6% to the microbiota variance but does not result in a clear separation between groups.

6

Table 2. Common and specific potential upstream regulators in colon of aged *Ercc1*$^{-/\Delta7}$ mice after bacterial supplementations *L. plantarum* (LP), *L. casei* (LC), or *B. breve* (BB) as determined by Ingenuity.
Analysis of potential upstream regulators was restricted to "cytokines", "growth factors" and "others". Cut-off values for activation z-score ≥ 1.5 or ≤ -1.5 and p<0.05. Up-regulated in green and down-regulated in red.

Upstream regulators	LP	LC	BB
EGF	2.4		3.3
IFN-γ	2.0		-1.5
Insulin	1.4		2.0
PDGFBB	2.0		1.2
CSF2 (GM-CSF)	2.0		-0.7
IgG			-2.4
IL-1β	1.7		0.7
EDN1			2.2
LEP	2.2		
IL-4	2.2		
WNT3A			2.2
RETNLB		2.0	
CD40L (CD154)	2.0		
VIP			2.0
Klra4 (includes others)			-1.9
IGF-1	1.8		
FGF2		1.7	
APP	1.5		

Legend: APP = amyloid β precursor protein; CSF = colony-stimulating factor; EDN = endothelin; EGF = epidermal growth factor; FGF = fibroblast growth factor; GDNF = glial cell line-derived neurotrophic factor; GM-CSF = granulocyte-macrophage stimulating factor; IFN = interferon; IGF = insulin-like growth factor; Klra = killer cell lectin-like receptor, subfamily A; LEP = leptin; PDGF = platelet-derived growth factor; RETNLB = resistin-like β; VIP = vasoactive intestinal peptide.

To assess whether significant changes in the microbial genus-like bacterial groups existed between the genotypes and bacterial supplementations, the Wilcoxon test was performed. It resulted in only one taxon that was significantly altered between control mice and mice supplemented with bacterial strains. *Subdoligranulum* was higher (p<0.05) in the aged *Ercc1*$^{-/\Delta7}$ mice supplemented with *L. casei* and it was higher (p=0.052) in *Ercc1*$^{-/\Delta7}$ mice supplemented with *B. breve* compared with *Ercc1*$^{-/\Delta7}$ control mice. *Akkermansia muciniphila* were less present (p=0.055) in *Ercc1*$^{-/\Delta7}$ mice supplemented with *L. plantarum* compared with control-treated mice. *Eubacterium plexicaudatum* and a close relative to *Anaerostipes caccae* were higher (p=0.063) in *Ercc1*$^{-/\Delta7}$ mice supplemented with *L. casei*.

Overall, the microbial differences between control mice and bacterial supplemented mice were small. Larger differences were observed between *Ercc1*$^{+/+}$ and aged *Ercc1*$^{-/\Delta7}$ mice.
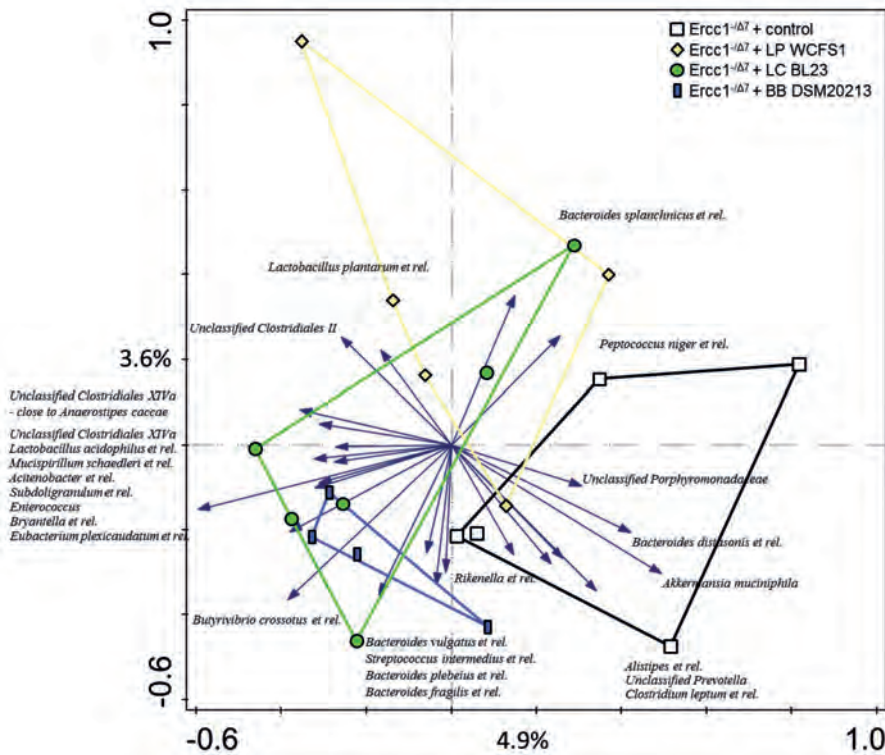
Figure 7: Bacterial supplementations shift colonic microbiota composition in *Ercc1*[-/Δ7] mice. Redundancy analysis of the microbial composition after bacterial supplementations, on genus-like level of the MITChip analysis. The explanatory variables used, were the four aged *Ercc1*[-/Δ7] mouse groups, which in total explained 10.1% of the variation.

Integrative analysis of gene regulation and microbiota composition in colon reveals correlation between microbial species and senescence pathways

To gain insight into mechanisms explaining differential host responses to bacterial supplementations, we determined the association between regulation of gene expression and microbiota composition in colon. The correlation pattern between gene expression and microbiota was visualized in a heat map. The clustered heatmap revealed seven gene expression clusters (1-7) and four microbiota clusters (A-D) (Fig. 8). The strongest correlations were observed for bacterial cluster D, and gene clusters 1 and 6. Bacterial cluster D, however, includes many background species, with the exception of *Subdoligranulum*, which showed the least correlation in this cluster. Most of these species did not show up in RDA plot (Fig. 7) and showed hardly any overlapping response towards each of the bacterial supplementations. In contrast, species in bacterial cluster A, B, and C showed up in the RDA (Fig. 7). Bacterial clusters B and C consist of many of the *Bacteroidetes* species, which positively correlated with the aged *Ercc1*[-/Δ7] control mice

in the RDA (Fig. 7). These two bacterial clusters positively correlated with gene clusters 2 and 7. Genes in cluster 2 were related to the Wnt pathway, and to pathways involved in tissue polarity. Genes in cluster 7 included genes regulating cell communication, senescence, EGFR1 signaling, autophagy (Atg16L1), and TLR signaling pathways.
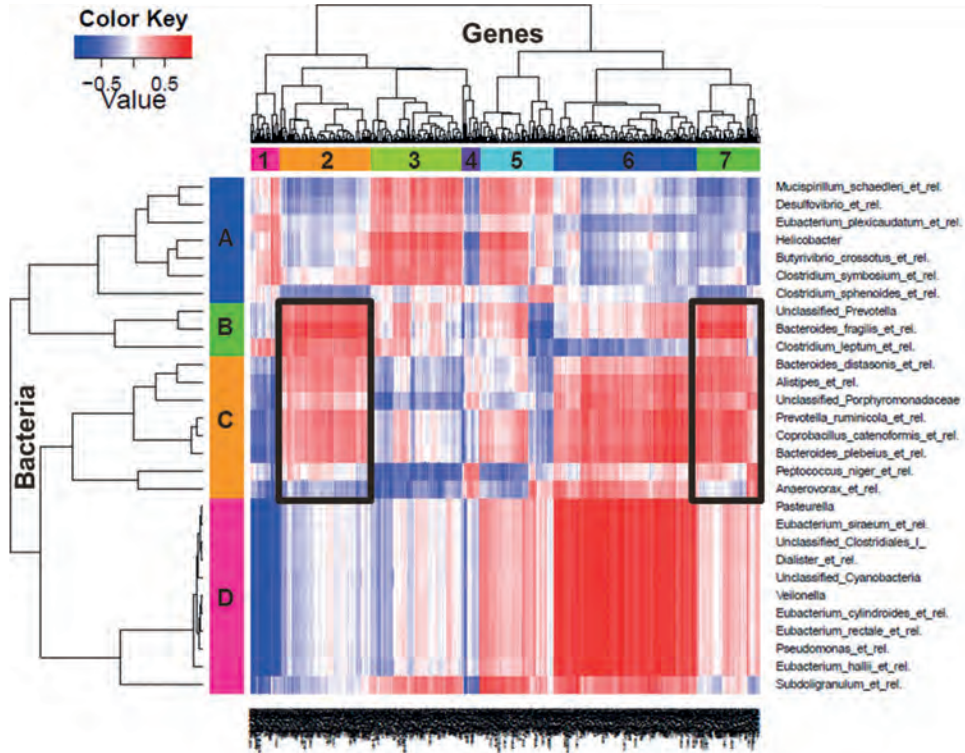

Figure 8: Integration of gene expression in colon with fecal microbiota composition. Heat map shows the correlation between gene expression in colon and relative abundance of bacteria. Positive correlations are depicted in red, negative correlations are depicted in blue. Greater intensity of color indicates stronger correlation. Indicated clusters show strongest positive correlation between bacteria cluster D and gene clusters 1 and 6. Bacterial cluster D, however, was excluded as it contains many background species. Two other bacteria clusters (B and C) and two gene clusters (2 and 7) were also strongly positively correlated.

Discussion

Here, we present a comprehensive analysis of the effect of supplementation with candidate probiotics on cellular parameters of ageing immunity and intestinal barrier. We linked observed effects in immune cell composition and intestinal barrier to gene regulation and gut microbiota composition.

We found that the effects of the candidate probiotic strains were most apparent on intestinal barrier and mucosal and systemic immunity in aged *Ercc1*[-/Δ7] mice compared with *Ercc1*^{+/+} mice. Since *Ercc1*[-/Δ7] mice represent aged mice at the tested time point (16-week-old), this implies that ageing profoundly influences the response to the supplementation of bacterial strains. Moreover, we found that the different strains elicited distinct responses in immunity and intestinal barrier, indicating the importance to include such analysis in the search for truly beneficial strains in the context of ageing. In fact, supplementation of *L. plantarum* WCFS1 restored age-related decline in intestinal barrier of *Ercc1*[-/Δ7] mice, whereas supplementation of *L. casei* BL23 had no effects. Supplementation of *B. breve* DSM20213 exacerbated the age-related decline in intestinal barrier. It has been shown in previous studies that strains such as *L. casei* and *B. breve* have beneficial effects [333] [334] [335] [336]. The observation, that these strains are virtually having no effect in young *Ercc1*^{+/+} mice but severe deteriorating effects on systemic immunity or barrier function in aged *Ercc1*[-/Δ7] mice, suggests that caution should be taken in administering probiotics into different age classes without confirming their benefit to elderly subjects.

Table 3. Summary of effects on intestinal barrier and immunity of *Ercc1*^{+/+} mice, aged *Ercc1*[-/Δ7] mice, and *Ercc1*[-/Δ7] mice after bacterial supplementations *L. plantarum* (LP), *L. casei* (LC), or *B. breve* (BB).

	Intestinal barrier[1]	Immunity[2]
Ercc1[-/Δ7] control	-	-
Ercc1[-/Δ7] + LP	+	=
Ercc1[-/Δ7] + LC	=	-
Ercc1[-/Δ7] + BB	-	=

[1]Ileum and colon taken together; [2]Mucosal and systemic immunity taken together. + indicates improved situation compared with control; = indicates no difference compared with control; - indicates deteriorated situation compared with control. *Ercc1*[-/Δ7] control mice were compared with *Ercc1*^{+/+} mice.

We observed that detrimental effects on intestinal barrier are not necessarily translated into changes in immune cell frequencies, or vice versa (Table 3). Supplementation with *B. breve* exacerbated the age-related decline of tissue integrity in ileum and colon, but did not show any changes in mucosal or systemic immunity. The opposite was observed after *L. casei* supplementation, causing no visible differences in intestinal barrier, but

causing several signs of systemic inflammation, such as neutrophil and Ly6C^{hi} monocyte influx, and increased Th17 cell frequencies in spleen. These might be linked to the observed general decrease in B cell frequencies following *L. casei* supplementation. There is evidence that neutrophils in bone marrow are primed by peptidoglycan (PGN) derived from gut microbiota [337]. A role for microbiota in basophil hematopoiesis has also been described [338]. The effects of microbiota-derived signals on priming e.g. B or T cells, or changing their development during hematopoiesis have not been previously described. Our study suggests a link between microbiota, intestinal barrier, and bone marrow B cells. Specific precursor stages (i.e. small resting pre-B cells) were decreased after *L. casei* supplementation, and to a lesser extent after *L. plantarum* supplementation. In the case of *L. plantarum* supplementation, we suggest that improved intestinal barrier function might alter circulating microbiota-derived products such as PGN and LPS. Indeed, even in HSC, chronic exposure to LPS caused age-related damage [339]. Decreased B cell lymphopoiesis raises the question whether *Ercc1*$^{-/\Delta 7}$ treated with bacterial supplementations are capable of mounting a proper primary or secondary immune response. Preliminary data of experiments testing the capacity to mount an antigen-specific immune response, show that antibody titers against TNP-KLH are not affected (data not shown).

The *Ercc1*$^{-/\Delta 7}$ model presents a feasible model to perform lifespan studies, assessing effects of dietary (or other) interventions on lifespan. A previous study in wild-type mice showed extended lifespan after *B. animalis* supplementation [320].

In our study, we observed that *L. plantarum* improved colonic morphology and mucus barrier. *L. plantarum* is known for its moderately pro-inflammatory profile, and relatively high IL-10 induction, when tested in human PBMC cultures [332] [340], human monocyte-derived DC cultures [341], and a peanut allergy mouse model [331]. Indeed, several upstream regulators predicted to be activated after *L. plantarum* supplementation included the inflammatory cytokines GM-CSF, IFN-γ, IL-1β, and IL-4. Combined with the improved overall makeup of the colon after *L. plantarum* supplementation, we therefore conclude that it might be beneficial to increase action of inflammatory cytokines in the ageing colon. In further support of this conclusion, we did not observe these transcriptional changes after *L. casei* or *B. breve* supplementation. A 'tonic' level of constitutive TLR activation by commensal bacteria was previously shown to be crucial in the recovery from DSS induced epithelial damage due to the role of NF-κB in epithelial repair processes [342]. This notion that "physiological inflammation" is required for intestinal homeostasis is also supported by studies using epithelium-specific iκB kinase-γ (or NEMO) ablation in mice. These mice develop spontaneous colitis due to the failure of NF-κB to induce epithelial repair and steady-state production of innate effector mechanisms in the intestine [343]. TLR2 signaling has been implicated in tight junction regulation *in vivo* and *in vitro* [297]. Thus is it possible that aged mice have sub-optimal level of TLR stimulation in the

intestine to promote innate barrier defenses and that this is enhanced by *L. plantarum.*

It has been reported that cytokine profiles of TLR stimulated of whole-blood from elderly individuals is altered compared with young adults, favoring IL-6, TNF, and IL-10 production, at the expense of e.g. IL-12, and IL-1β [344]. Our findings in the *Ercc1*[-/Δ7] model challenge the use of IL-10/IL-12 (or IL-10/TNF) ratios in elderly subjects to screen for candidate probiotics with anti-inflammatory capacities [340]. It might even be that strains scoring high IL-10/IL-12 ratios are not beneficial in the ageing context, because IL-12 induction is impaired in ageing while IL-10 production is generally elevated [344] (van Beek *et al.*, unpublished).

We report only minor shifts in gut microbiota composition after each of the bacterial supplementations. Correlation of microbiota composition with gene expression in colon revealed an association between higher abundance of *Bacteroidetes* and gene pathways involved in tissue polarity and senescence in aged *Ercc1*[-/Δ7] control mice. Higher abundances of *Bacteroidetes* in frail or elderly subjects was previously reported [345], indicating a negative association with ageing.

We also observe mild changes in gene regulation, but GSEA and Ingenuity Upstream Regulator Analysis show clear effects of *L. plantarum* and *B. breve*, which corroborate histological findings. Endoplasmic reticulum (ER) stress responses or unfolded protein responses (UPR), were predicted to be activated in the colon of *L. casei*-treated mice. Misfolded proteins trigger UPR that is in turn coupled to inflammation [346]. With ageing, ER stress is increased, and UPR are changed [347]. Single mutations in mouse *Muc2* can cause accumulation of MUC2 in ER which triggers UPR and increased levels of inflammatory cytokines [348] [117]. Higher quantitative demands for MUC2 synthesis, such as an increased bacterial load in contact with the epithelium, which is observed in ageing mice, will further challenge the endoplasmic reticulum folding system and trigger UPR and inflammation. A consequence of ER stress is the aggregation of improperly folded MUC2 protein, defects in polymerization and reduced secretion, explaining the previously reported reduction of mucus thickness and barrier function in naturally aged mice (Chapter 4).

To explain why *L. plantarum* supplementation prevents age-related decline in intestinal barrier, it might be worthwhile to create or use existing mutant *L. plantarum* strains. Testing the wild-type and mutant *L. plantarum* strains could give insight in the molecules involved in the interaction with gut microbiota and epithelium. Furthermore, mono-colonization with *L. plantarum* in germ-free *Ercc1*[-/Δ7] mice would give insight into the effect of only *L. plantarum*, without interactions with the existing gut microbiota. In addition, investigation of the capacity to produce polyamines by *L. plantarum* would be of interest, as polyamines improved health status and may promote longevity in mice [320] [349].

6

We conclude that the *Ercc1*$^{-/\Delta7}$ model can be used to study the effect of long-term probiotic interventions on ageing. Our data provide an example of how bacterial supplementation can restore age-related decline in intestinal barrier, and highlights the caution needed in the selection of candidate probiotic strains for supplementation to ageing individuals.

Acknowledgements

Supplementary data

Supplementary Table S1: Used antibodies in flow cytometry.

Target	Format	Clone	Company
CD2	PE	RM2-5	BD
CD3e	APC-Efluor780 PerCP-Cy5.5	17A2 145-2C11	Ebioscience BD
CD4	APC-H7	GK1.5	BD
CD8a	PE	53-6.7	BD
CD11b	APC-Cy7 PE-Cy7	M1/70	BD Ebioscience
CD16/32	Purified	2.4G2	BD
CD19	PerCP-Cy5.5 APC-Efluor780	1D3	Ebioscience
CD25	APC	3C7	BD
CD45R/B220	BV421	RA3-6B2	BD
CD68	FITC	FA-11	BioLegend
IgD	PE PerCP-Efluor710	11.26.2ca 11-26c	BD Ebioscience
Igκ	FITC	187.1	BD
Igλ	FITC	R26-46	BD
IgM	APC Efluor450	II/41	Ebioscience
Ki-67	PE-Cy7	SolA15	Ebioscience
Ly6C	PerCP-Cy5.5	HK1.4	Ebioscience
Ly6G	BV421	1A8	BD
RORγt	AF647	Q31-378	BD

Supplementary Table S2: Biological processes regulated by bacterial supplementations in ileum of aged *Ercc1*[-/Δ7] mice treated with *L. plantarum* (LP), *L. casei* (LC), or *B. breve* (BB).
Gene sets significantly regulated (p<0.05, FDR<0.2) by bacterial supplementations compared with control were determined by gene set enrichment analysis. To highlight prevalent biological functions, gene sets were manually clustered.

|	LP	LC	BB
Growth/cell cycle	+	-	+/- (decreased apoptosis)
DNA repair	+	-	
Immunity	+ - IgA production, antigen presentation, adaptive immune signaling		-
Barrier function	+*		
Metabolism	+	-	+/-
Nutrient sensing	-	-	-

*a.o. tight junction, integrin 1, E-cadherin

6

Supplementary Table S3: Biological processes regulated by bacterial supplementations in colon of aged *Ercc1*^{-/Δ7} mice treated with *L. plantarum* (LP), *L. casei* (LC), or *B. breve* (BB).

Gene sets significantly regulated (p<0.05, FDR<0.2) by bacterial supplementations compared with control were determined by gene set enrichment analysis. To highlight prevalent biological functions, gene sets were manually clustered.

	LP	LC	BB
Growth/cell cycle	+	+	
DNA repair	+		-
Immunity	+		-
Barrier function	+		
Metabolism	+		+
Nutrient sensing	-		-
		UPR + NOD-like receptor signaling +	Wnt signaling +

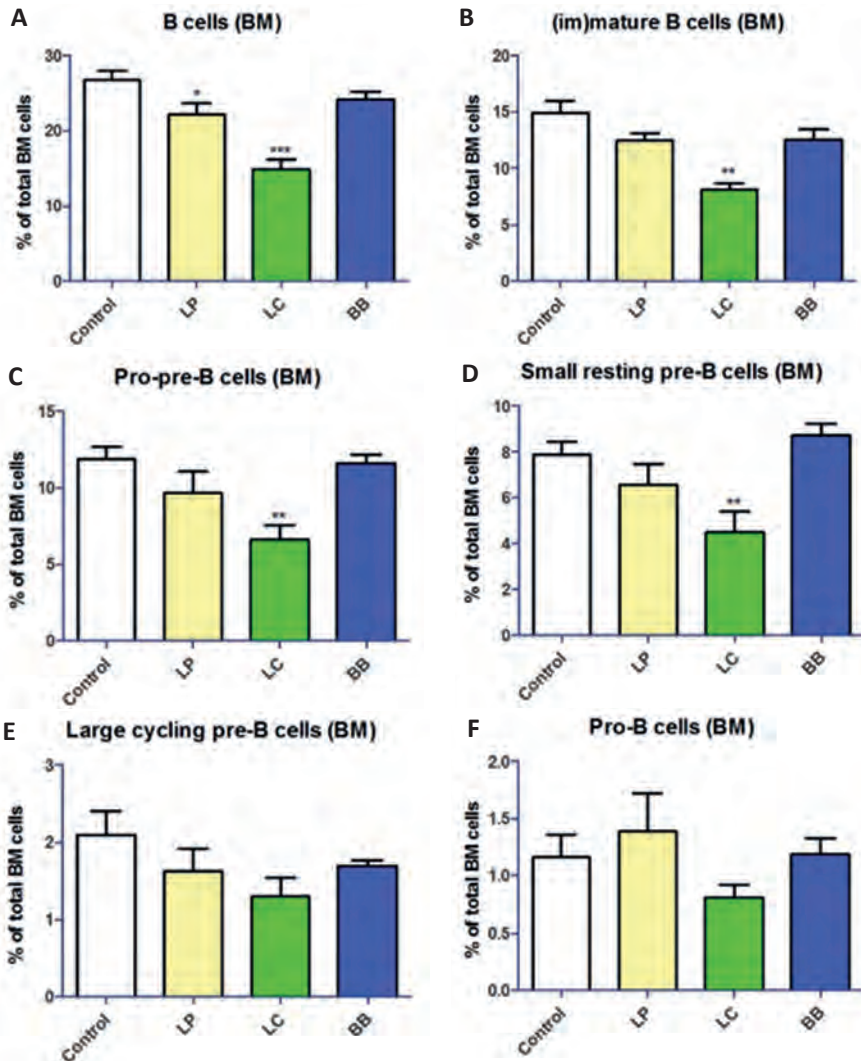UPR = unfolded protein responses
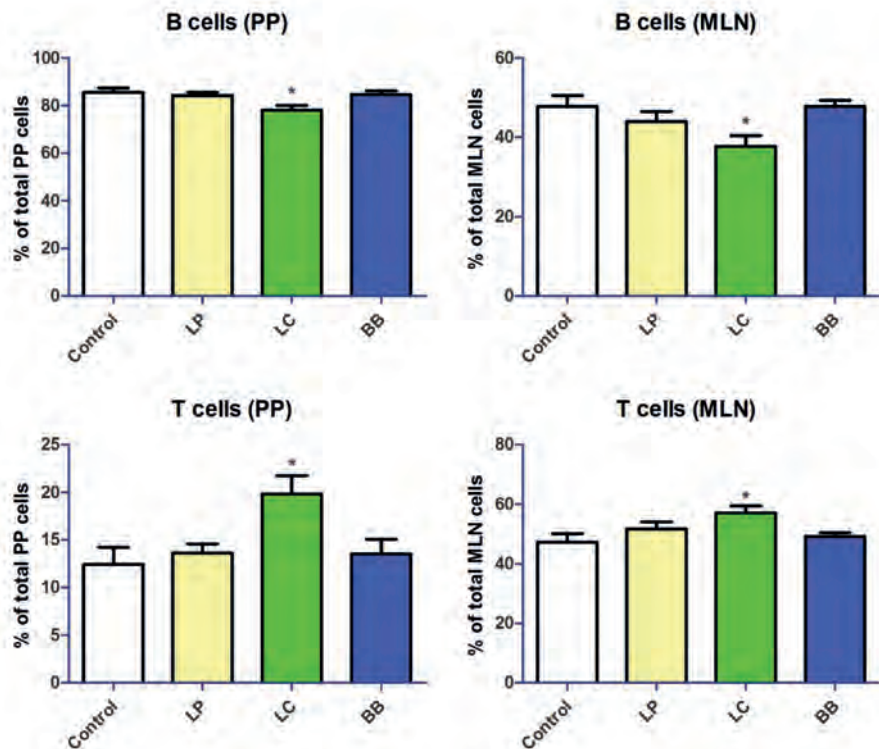
Supplementary Figure S1: Distribution of B cells and T cells in Peyer's patches and mesenteric lymph nodes affected in *Ercc1*^{-/Δ7} mice after *L. casei* treatment. Mean frequencies were determined by flow cytometry. B cells were defined as CD19+CD3e-, T cells were defined as CD3e+CD19-. Data represent the mean + S.E.M. from 4-6 animals per group.
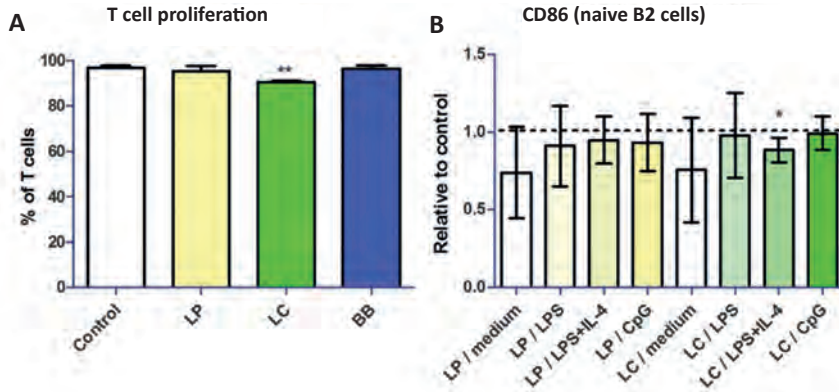
Supplementary Figure S2: *L. casei* **supplementation to** *Ercc1*[-/Δ7] **mice caused decreased T cell proliferation and altered B cell responses** *in vitro.* A) T cell proliferation was determined by Ki-67 measurements in splenocytes stimulated with ConA for four days. Data represent the mean + S.E.M. from 4-6 animals per group. B) Purified naive B2 cells were cultured for three days in the presence of medium only, LPS, LPS and IL-4 together, or CpG, after which median fluorescence intensity (MFI) of CD86 was determined. MFI was expressed relative to three-day cultures of naïve B2 cells derived from control mice. Data represent the mean + 95% confidence interval from 4-6 animals per group.

6

A B cells (BM)

B (im)mature B cells (BM)

C Pro-pre-B cells (BM)

D Small resting pre-B cells (BM)

E Large cycling pre-B cells (BM)

F Pro-B cells (BM)

Supplementary Figure S3: Bacterial supplementations affected frequencies of total B cells, (im)mature B cells, and subsets of pro-pre-B cells in bone marrow of aged *Ercc1*$^{-/\Delta7}$ mice. Mean frequencies were determined by flow cytometry. B cells were defined as CD19$^+$CD45R$^+$. Mature and immature B cells were defined as sIgκ/λ$^+$, pro-pre-B cells as sIgκ/λ$^-$. Small resting pre-B cells were defined by cIgM$^+$CD2$^+$, large cycling pre-B cells by cIgM$^+$CD2$^-$, and pro-B cells by cIgM$^-$CD2$^-$. Data represent the mean + S.E.M. from 4-6 animals per group.
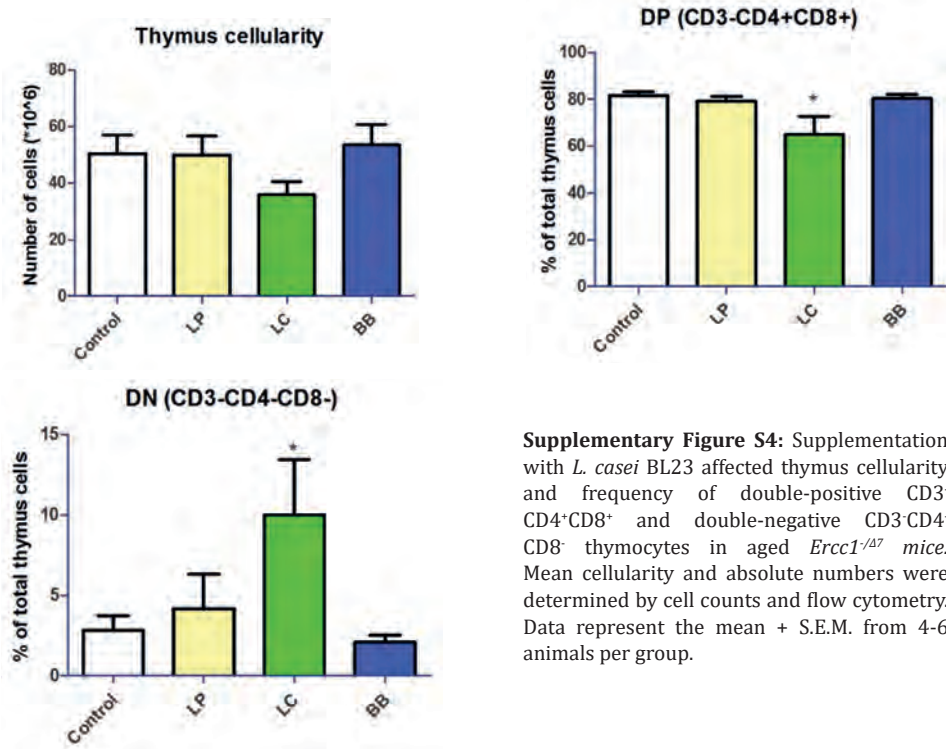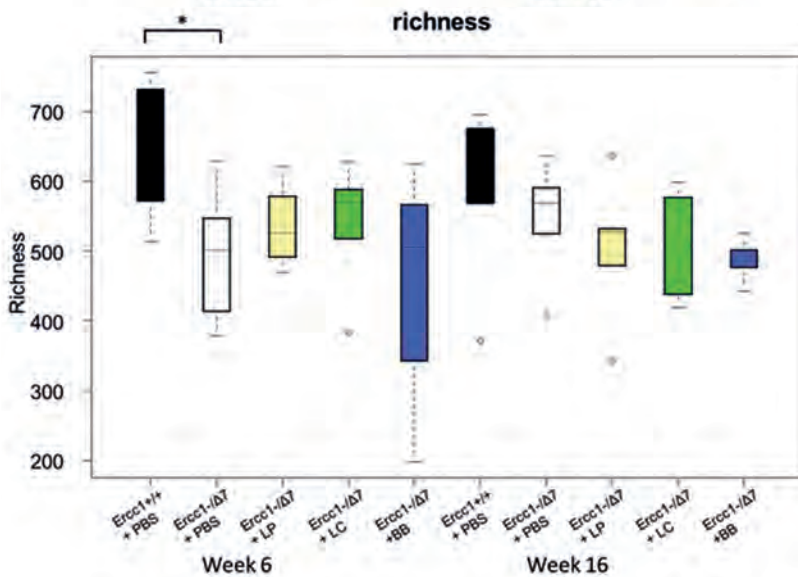
Supplementary Figure S4: Supplementation with *L. casei* BL23 affected thymus cellularity and frequency of double-positive CD3-CD4+CD8+ and double-negative CD3-CD4-CD8- thymocytes in aged *Ercc1*$^{-/\Delta7}$ *mice.* Mean cellularity and absolute numbers were determined by cell counts and flow cytometry. Data represent the mean + S.E.M. from 4-6 animals per group.

6

A
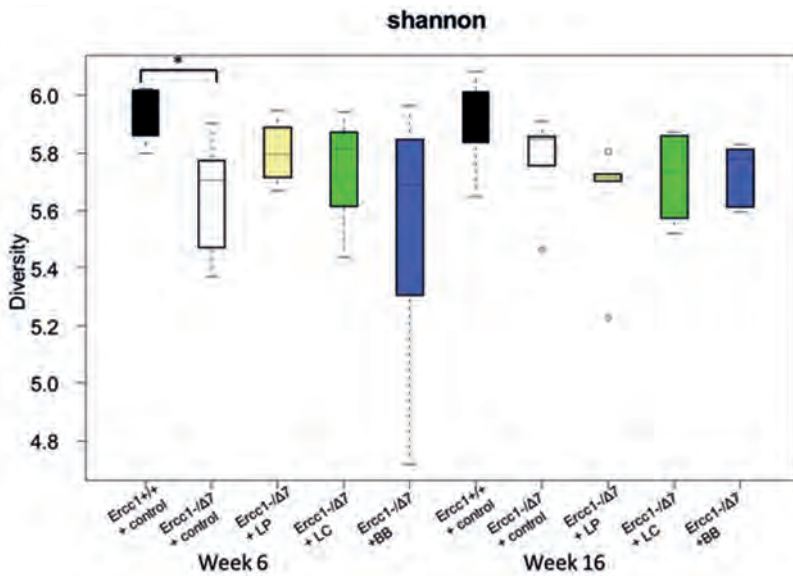
B

Supplementary Figure S5: Bacterial supplementations do not alter diversity or richness of gut microbiota. A) Shannon diversity of the five mouse groups at week 6 and 16: *Ercc1*^{+/+} control, aged *Ercc1*[-/Δ7] control, aged *Ercc1*[-/Δ7] supplemented with *L. plantarum* (LP), *L. casei* (LC), or *B. breve* (BB). B) Microbial Richness of the above-indicated five groups at week 6 and 16. *p<0.05

Chapter 7

Structure and permeability of mucus in the mouse intestine and its influence on bacterial localization and immune sampling

Bruno Sovran[1,2], Oriana Rossi[2], Wayne Young[4], Anja Taverne-Thiele[2], Jasper Kamphuis[2], Raymon van Dijk[2], Paul de Vos[1,3], Nicole Roy[4], Jan Dekker[1] and Jerry M. Wells[1,2]

Submitted for publication

[1] Top Institute Food and Nutrition, Wageningen, the Netherlands
[2] Host-Microbe Interactomics Group, Animal Sciences Department, Wageningen University and Research Center, Wageningen, the Netherlands
[3] University Medical Center of Groningen, Groningen, the Netherlands
[4] Food Nutrition and Health, AgResearch Grasslands, Palmerston North, New Zealand

Abstract

The objectives of this study were to obtain a better understanding of the mucosal interactions and immune sampling of bacteria in gnotobiotic and conventional mice. This study focused on uptake of the bacteria in the small intestinal lymphoid tissue including Peyer's patches (PPs) and mesenteric lymph nodes (MLNs). *Lactobacillus plantarum* was chosen as a model organism and was administered to germ-free (GF) mice. Lymphoid and mucosal tissues were collected after 20 hours or after 21 days of colonization. Sections of the ileal and colonic tissue were fixed or cryopreserved for histochemical and immunofluorescent microscopy. Different fixation methods were used to visualize the mucus and determine its thickness in the colon. A new technique was developed to assess mucus permeability in the small and intestine and colon. The intracellular viable lactobacilli were enumerated in immune cells isolated from resected PPs and MLNs of gnotobiotic mice.

Bacteria were not seen below the mucus layers in the colon using different staining methods, demonstrating that in both the small intestine and colon the secreted mucus presents a formidable physical barrier to the direct interaction of bacteria with the epithelial surface. The exception was segmented filamentous bacteria, which were found underneath the mucus layer and attached to villus epithelial cells. Lactobacilli were taken up in the organized lymphoid structures of the small intestine and transported within immune cells to the mesenteric lymph nodes (MLNs). Sampling of bacteria by PPs is facilitated by the relatively low abundance of goblet cells and lack of secreted mucus in the dome of the PP. The recovery of live lactobacilli from immune cells in the PP and MLN indicates that they are being continuously sampled in the PP and transported through the lymphatic system to the MLNs.

Introduction

The gastrointestinal tract (GIT) is a harsh environment and the epithelium is subjected to continuous physical and chemical assaults from ingested food as well as digestive secretions including proteases, enzymes, hydrochloric acid and bile acids [350] [351]. Furthermore, the intestinal microbiota has potential to cause inflammatory reactions in the mucosa if they reach the epithelial surface in sufficient quantities [352]. For protection, the gastrointestinal epithelium is covered by mucus, the main constituent being the secreted gel forming mucin MUC5AC in the stomach and MUC2 in the large and small bowel [64]. Mucins are large glycoproteins where the glycans make up more than 80% of the molecular mass. Mucin *O*-gycosylation occurs at the so-called PTS-sequences, which are rich in proline, threonine and serine, which are highly *O*-glycosylated and constitute the mucin domains. The gel-forming mucin MUC2 oligomerizes into large net-like polymers when the *C*- and *N*-termini form disulfide-bond stabilized di- and trimers [353]. Gel-forming secreted mucins are produced, stored, and released by specialized cells called goblet cells in the intestine, characterized by their distended theca containing mucin granules [64]. In humans, the goblet-to-enterocyte-ratio increases from the proximal to distal intestine, with an estimated 4%, 6%, 12%, and 16% of goblet cells in the epithelium of the duodenum, jejunum, ileum, and distal colon, respectively [354].

There are relatively few bacteria residing in the stomach and the proximal small intestine, but the number increases to approximately 10^8 bacteria per ml of luminal content in the distal ileum and around 10^{11}/g in the colon [1]. In the colon bacteria are separated from the epithelium by an inner mucus layer that is physically impenetrable to bacteria [66]. Above the inner mucus layer bacteria are intermingled with lose mucus and the contents of the lumen [64]. Colonic microbiota benefit the host through the fermentation of otherwise indigestible complex carbohydrates into short-chain fatty acids, including butyrate, which is used by intestinal epithelial cells as an energy source [352] [4]. In the small intestine aggregates of lymphoid follicles known as Peyer´s patches (PP) are mainly responsible for the induction of adaptive mucosal immune responses, leading to secretory immunoglobulin A secreting plasma cells in the lamina propria (LP). The luminal antigens are sampled and transported across the epithelium to the lymphoid tissue by specialized M cells present in the follicle-associated epithelium (FAE) overlaying the PP [355] [356]. Recently it has also been suggested that goblet cells can act as sampling sites for dendritic cells [357]. The presence of goblet cells in the follicular epithelium and presence of mucus layer over the PP has been differently reported in the literature suggesting it may vary according to intestinal location or between animal species [74] [87]. No consensus has been reached concerning the number of goblet cells on the domes and whether the PP is covered by a mucus layer [86] [88]. Recently Ermund *et al.,* showed that when mouse ileal biopsies containing PPs were mounted in a horizontal

Ussing-type Chamber in the presence of secretagogues to stimulate mucus production, a continuous mucus layer of easily removable mucus covered the dome of the PPs [89]. The flow of mucus over the PP from goblet cells in the villi may be one explanation for the observations of mucus seen over the PP, although goblet cells were identified in the follicular epithelium by immunoflourescent staining.

The gastrointestinal mucus system has been relatively poorly explored and understood as it is essentially invisible and collapses upon the commonly used formaldehyde fixation. A large step forward was taken by Atuma *et al.,* who could visualize the luminal surface of the mucus by adding charcoal particles to intestinal explants and measure the mucus thickness [1]. This data was generated on rat intestinal tissue rather than mice, which are more commonly used for studies of gastrointestinal physiology and pathophysiology. Mucus permeability has also been assessed using *ex vivo* tissue mounted in a horizontal perfusion chamber with the apical surface facing upward [132]. Movement of different sized fluorescent beads through the mucus is then assessed using confocal microscopy. However, these techniques, require specialized microscopy equipment and can only be performed for up to 2 hours after mounting, making them too labour intensive to perform on multiple experimental animals in intervention or challenge studies.

Assessing the mucus thickness by histological methods is complicated by the fact that it collapses in formaldehyde fixed-histological sections. However, the Carnoy fixation and paraffin embedding technique prevents complete shrinkage of the mucus and has been used to assess mucus thickness by immunofluorescent antibody or PAS/Alcian blue staining in mice. There are no comparative studies on mucus thickness in mice using different histological approaches. Thus first aim of this study was to compare measurements of mucus thickness throughout the mouse intestinal tract including the Peyer's Patches (PP) using different histological methods and determine the location and immune sampling of bacteria in conventional and GF mice monocolonised with a model commensal organism *Lactobacillus plantarum*. Lymphoid and mucosal tissues were collected after 20 h or after 21 days of colonization with *L. plantarum* when the mucosal immune system had reached maturity. Sections of the ileal and colonic tissue were fixed or cryopreserved for histochemical and immunofluorescent histochemistry. Immune cells were isolated from the resected PPs and MLNs for enumeration of intracellular lactobacilli. For comparison, tissue and organ samples were also collected from conventional mice of the same genetic background as the GF mice. Additionally an *ex vivo* technique was developed to investigate mucus permeability, using fluorescent beads of 1, 2 and 10 µm diameter. Distance between beads and epithelium was measured and compared with distance between bacteria and tissue in natural conditions.

Materials and Methods

Animals

The *in vivo* studies were conducted under the oversight of the Crown Research Institute Animal Ethics Committee (Palmerston North, New Zealand) according to the New Zealand Animal Welfare Act 1999, Animal Ethics application number 12501. For the *in vivo* studies, conventional Balb/c mice (CLEA Japan, INC. Tokyo, Japan) were housed under specific pathogen-free conditions. All mice were fed AIN-93M diet (Research Diets, New Jersey, US) and were housed with 12 hour light/dark cycles and at an environmental temperature of 21-22°C. Germ-free (GF) Balb/c mice from the same supplier were housed in individual cages within gnotobiotic isolators and given the same diet sterilised by gamma-irradiation (25 kGy), and autoclaved sterile water. All bedding material was sterilized by gamma-irradiation (25 kGy). Access to food and water was provided *ad libitum*, and food intake was measured weekly.

For the *ex vivo* studies, male C57BL/6 mice were housed in a specific pathogen-free environment with *ad libitum* access to 10% fat diet (Research Diets Services BV, Wijk bij Duurstede, the Netherlands), and acidified tap water in a 12-hour light/dark cycle. The Animal Ethics Committee of the University of Wageningen (Wageningen, the Netherlands) approved these animal experiments.

Histology

Whole tissue from duodenum, jejunum, ileum (including PPs), proximal colon, and distal colon with faecal content was fixed in methanol-Carnoy's fixative. Five micron-thick paraffin sections of tissue were attached to poly-L-lysine-coated glass slides (Thermo scientific, Germany). After overnight incubation at 37°C, slides were deparaffinised using a series going from xylene to distilled water with decreasing ethanol steps. Sections were stained in 3% (w/v) Alcian Blue (8GX Acros Organics, New Jersey, USA) for 35 min, rinsed in running tap water for 2 min and then rinsed in distilled water. The sections were submerged in periodic acid 0.5% (w/v) for 10 min and rinsed for 1 min in distilled water. After this washing step the sections were incubated in Schiff's reagents (Merck, Germany) for 45 min and washed in freshly prepared SO_2 water (10 ml of 10% $K_2S_2O_5$ (Merck, Germany), 10 ml of HCl (1 mol/L) and 180 ml of distilled water) for 3 times 2 min, followed by a washing step in tap water for 5 min. After this step the sections were submerged 2 times for 3 min in 100% ethanol followed by submersion in xylene for 3 times 5 min, and then finally mounted in DPX mounting reagent (BDH Gurr Certistain, England) and air-dried overnight at 37°C.

Sections were also stained with Crossmon Trichrome. Muscles were stained in red and collagen in green with orange G. Acid fuchsin was used to stain bacteria. After washing in distilled water, light green 1% solution was used as a counterstaining for mucus.

After this step the sections were submerged 2 times for 3 min in 100% ethanol followed by submersion in xylene for 3 times 5 min, and then finally mounted in DPX mounting reagent (BDH Gurr Certistain, England) and air-dried overnight at 37°C.

Immunohistochemistry

Paraffin sections of both ileum and colon were cut at 5 μm and attached to poly-L-lysine-coated slides (Thermo scientific). After overnight incubation at 37°C, slides were deparaffinised as above. An antigen retrieval step was performed by heating the sections for 20 min in 0.01 M sodium citrate (pH 6.0) at 100°C. Sections were washed for 3 h with 3 changes of PBS. A blocking step to reduce non-specific binding was included using 5% (v/v) goat serum (Invitrogen, Life technologies Ltd, Paisley, UK) in PBS for 30 min at room temperature. MUC2 was detected by incubating the sections with a custom designed anti-MUC2 antibody [66] diluted 1:500 in PBS containing 1% (v/v) goat serum and incubated overnight at 4°C. After primary incubation, sections were washed 3 times in PBS for 10 min, and the staining was visualized using a secondary antibody (goat-anti-rabbit Alexa 488 or Cy3; Invitrogen, Carlsbad, CA, USA). DNA was stained using 0.1% DRAQ5 (Invitrogen Invitrogen, Carlsbad, CA, USA). Images were acquired using a laser-scanning microscope.

Fluorescent *in-situ* Hybridization (FISH)

The slides were deparaffinised with xylene and rehydrated in a series of ethanol solutions to 100% ethanol. The tissue sections were incubated with the universal bacterial probe EUB338 (5'-GCTGCCTCCCGTAGGAGT-3') (Isogen Bioscience BV, De Meern, the Netherlands) conjugated to Alexa Fluor488. A 'non-sense' probe (5'-CGACGGAGGGCATCCTCA-3') conjugated to Cy3, was used as a negative control. Tissue sections were incubated with 0.5 μg of probe in 50 μL of hybridization solution (20 mmol/L Tris-HCl (pH 7.4), 0.9 mol/L NaCl, 0.1% (w/v) SDS) at 50°C overnight in a humid environment using a coverslip to prevent drying of the sample. The sections were washed (20 mmol/L Tris-HCl (pH 7.4), 0.9 mol/L NaCl) at 50°C for 20 min. Sections were washed 2 times in PBS for 10 min in the dark and incubated with DRAQ5 (Invitrogen) (1:1000) for 1 h at 4°C to stain nuclei. Sections were washed 2 times in PBS for 10 min, mounted in fluoromount G (SouthernBiotec, Alabama, USA) and stored at 4°C.

An *ex vivo* method for assessing mucus permeability

Segments of small intestine and colon of about 3 cm long were cut. One side of the tissue was shut with surgical suture, and a suspension of 1 μm, 2 μm and 10 μm fluorescently labelled Melamine Resin Particles (Sigma) mixed in PBS, or a solution of 5% (w/v) corn-starch, were gently introduced into the lumen using a catheter and the segment sealed with another suture. After incubation in RPMI in a shaking incubator

(300 rpm) at 37°C, the tissue was snap frozen and stored at -80°C. The tissue was then cryosectioned, and post-fixation performed with absolute ethanol for 15 minutes, followed by hydration in a series of solutions containing a decreasing percentage of ethanol in demineralized water. PAS/AB staining was performed as above and confocal laser scanning microscopy was performed on sections incubated in 0.1% DRAQ5 in PBS and mounted with Fluoromount-G (see above). Bead distribution in the tissue was visualized by 3D projection through z-stacks (Fig. 1).
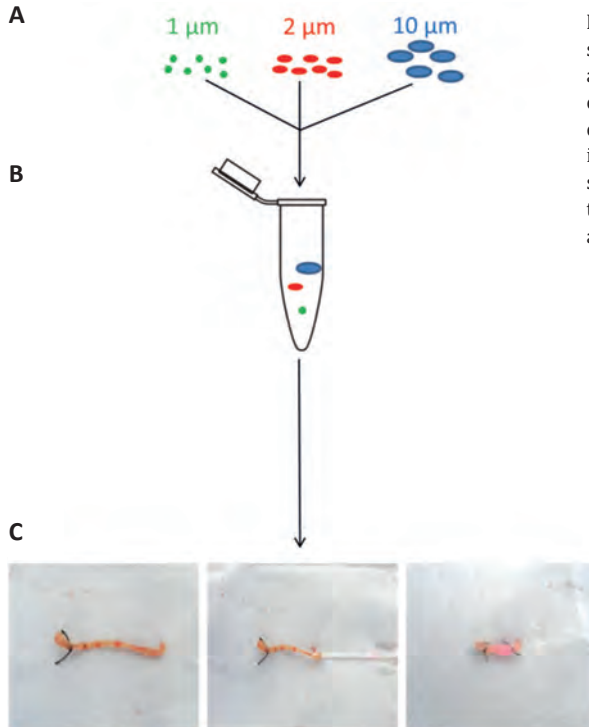

Figure 1: Outline of the *ex vivo* protocol to study mucus permeability. A suture is made at one end of a section of the small intestine or colon (A). Using a catheter suspension of beads in 5% corn starch were gently introduced to the lumen and the tissue segment tied with another suture (B). The tissue is then ready for emersion in RPMI and incubation at 37°C (C).

Mucus thickness measurement

Segments of small intestine and colon containing faecal pellets were cut, cryosectioned, fixed with ethanol, and stained with PAS/AB (see above). The thickness of the firm mucus layer was measured every 100 µm in transversal sections of the colon, where the mucus layer was homogenous and the tissue undamaged. The average mucus thickness was calculated for each slide and a total of 5 slides per tissue sample were processed. Pictures of the slides were processed *in silico* using ImageJ, measuring thickness by conversion of pixels to distance using the scale provided by microscope.

Bacteria

L. plantarum strain WCSF1, was cultured at 37°C in deMan, Rogosa Sharpe (MRS) medium containing 5 µg/ml erythromycin overnight and stored in aliquots in MRS plus 10% (v/v) glycerol at -80°C. On the day of administration, one aliquot was thawed and grown in MRS plus 5 mg/ml erythromycin to an OD at 600nm of 1-1.5, then harvested by centrifugation, washed in PBS and resuspended in sterile PBS prior to inoculation.

***In vivo* experiment and collection of tissue samples**

GF and conventional mice were divided in 2 groups, each of which received different treatments and 2 control groups.
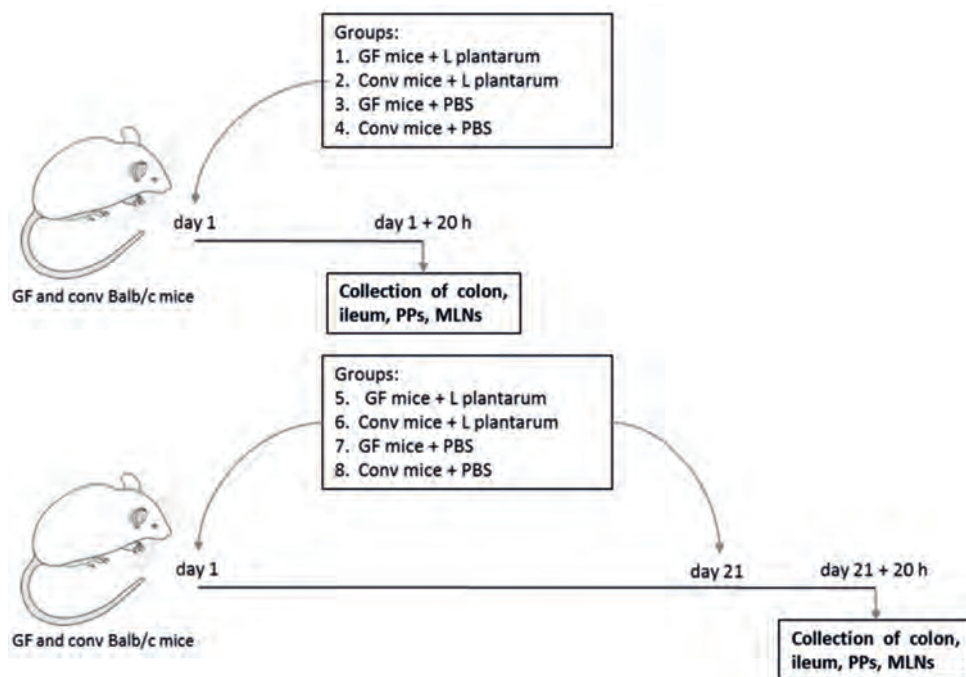

Figure 2: Outline of the *in vivo* experiments performed on germ free (GF) and conventional (conv) Balb/c mice; Lp, *L. plantarum*.

GF mice from group 1 (n=6) and conventional mice from group 2 (n=6) received 10^8 CFU/100 µl of *L. plantarum* by oral gavage on day 1 and were euthanized 20 h later (n=6); GF mice from group 3 (n=4) and conventional mice from group 4 (n=4) received 100 µl of PBS by oral gavage on day 1 and were euthanized 20 h later; GF mice from group 5 (n=6) and conventional mice from group 6 (n=6) received 10^8 CFU/100 µl of *L. plantarum* by oral gavage on day 1 and day 21 and were euthanized 20 h after day 21 and GF mice from group 7 (n=4) and conventional mice from group 8 (n=4) received 100 µl of PBS by oral gavage on day 1 and day 21 and were euthanized 20 h after day 21.

For splenocyte isolation, spleens were gently pushed through 100 µm gauge cell strainers. The cell suspension was made up to 10 ml with PBS (4°C), and then centrifuged at 300 g (4°C) for 5 minutes following which the supernatant was discarded. Red blood cells were lysed by adding 2 ml of ACK lysis buffer (150 mM NH_4Cl, 1mM $KHCO_3$, 0.1 mM Na2EDTA pH 7.3). Cells were then incubated for 5 minutes at room temperature. Lysis was stopped by adding 10 ml of PBS (4°C) to each tube, which were then mixed by inversion, followed by centrifugation at 300 g (4°C) for 5 minutes. The supernatant was discarded and the cell pellet resuspended in 1 ml of PBS (4°C).

Mesenteric lymph nodes (MLNs) were removed *in situ* from mesenteric tissue, the fat removed from the lymph nodes before the MLN were dispersed by pushing through 100 µm gauge cell strainers. The cell suspension was washed by adding 10 ml of PBS (4°C), followed by centrifugation at 300 g (4°C) for 5 minutes. The supernatant was discarded and the cells re-suspended in 1 ml of PBS (4°C).

PP were dissected from the ileum, pierced with a syringe needle, and then incubated in 3 ml of Rosewell Park Memorial Institute (RPMI) medium with collagenase type IV (Sigma C5138, 100 U/ml) in a shaking incubator at 15 min at 37°C. The collagenase was then neutralised by adding 9 ml of RMPI + 10% (v/v)FCS. The cell suspension was filtered by passing through a 100 µm gauge cell strainer. The cells were then centrifuged at 300 g (4°C) for 5 minutes. The cells were washed once more by adding 10 ml PBS (4°C), followed by centrifugation at 300 g (4°C) for 5 minutes. The supernatant was discarded and the cell pellet was resuspended in 1 ml of PBS (4°C).

To enumerate live bacteria, serial dilutions of PBS suspension with single cells isolated from spleens, MLNs and PPs of mice were plated on de Man, Rogosa, Sharpe medium (MRS).

Results

Mucus structure and thickness in the small and large intestine of GF, monocolonized and conventional mice

Carnoy's fixation and paraffin embedding followed PAS/Alcian blue staining of mucins revealed a thin mucus layer around the villi in the duodenum and jejunum, while in the ileum it was observed as a thicker layer on top of the villi spatially separating the luminal contents including bacteria from contact with the epithelium (Fig. 3). Fewer goblet cells were present in the epithelium of the small intestine than in the colon. The same results were found in monocolonized mice and conventional mice (Supplementary Figure S1). In GF mice, the firm mucus layer in the colon was thinner suggesting less mucus production (Supplementary Figure S1b), but after 21 days of colonization the thickness was similar to that of conventional mice (Supplementary Figure S1c). The mucus layer

7

was also thinner in GF mice colonised with *L. plantarum* for 20 h, than in mice, colonized with *L. plantarum* for 21 days (not shown). FISH staining of bacteria showed that most of the bacteria were above the mucus on top of the villi, although a few bacteria were occasionally observed in the mucus being expelled from goblet cells near the top of the villi (Fig. 3B). Additionally we evaluated Crossmon staining as a method to visualize bacteria and mucus in ileum and colon (Fig. 3 C, D and E). The mucus itself is not as darkly stained by this method, although a spatial separation of bacteria from the epithelial was just as apparent as with immunofluorescent microscopy. In the ileum of conventional mice and *L. plantarum* colonized mice (21 days), the location of the bacteria was the same as that observed using FISH, the exception being conventional mice supplied by CLEA Japan, INC. (Tokyo, Japan) where segmented filamentous bacteria (SFB), were observed underneath the mucus layer and attached to the villous epithelium (Fig. 3C and D) [358]. Only a few bacteria were seen in the lumen of *L. plantarum* colonized mice (1 day) (not shown). As expected no bacteria were observed in GF mice (Fig. 3C).
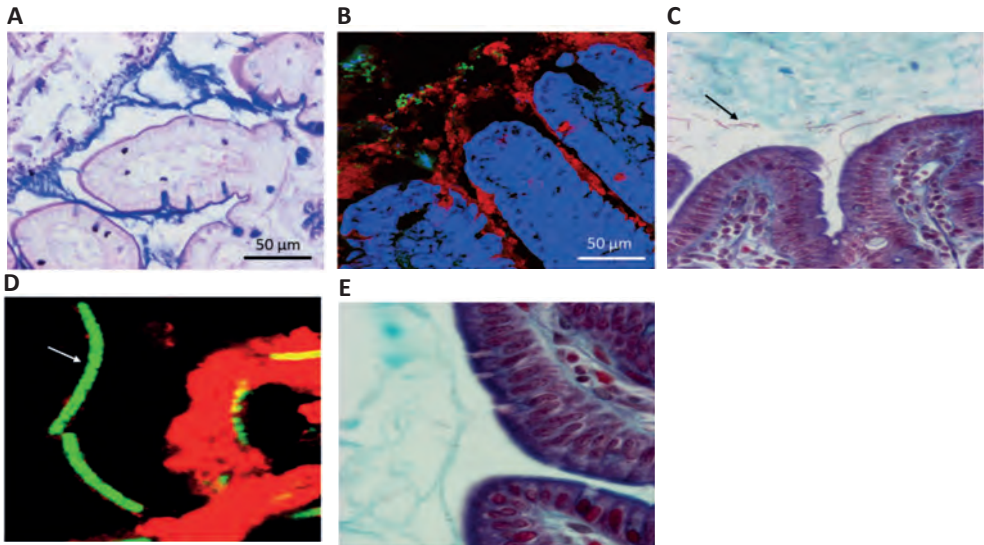

Figure 3: Mucus morphology in the small intestine fixed in Carnoy. PAS/Alcian Blue staining of the ileum (A). Mucus (red) and bacteria (green) co-stained with anti-MUC2 antibody and EUB338-Alexa488 FISH probe, respectively, on a DRAQ5-stained tissue (blue). Scale bars: 50 µm (B). Sections of Carnoy's-fixed ileum from a conventional mouse stained with Crossmon (C) and FISH (SFB in green, mucus in red) (D). A germ-free mouse stained with Crossmon (E) Arrows in C indicate segmented filamentous bacteria.

In PAS/Alcian blue stained sections of Carnoy-fixed tissue the thickness and location of the colonic mucus is dramatically different to the small intestine. The mucus forms two layers with different physical properties as previously described [77]. A firm mucus layer was located between the epithelium and the luminal content (Fig. 4A). This layer was relatively devoid of bacteria, as evidenced immunofluorescent detection of MUC2

and FISH detection of bacteria (Fig. 4B). The bacteria were present in the layer of 'loose' mucus above the firm layer, which is also mixed with the faecal material (Fig. 4B). When the mucus layer was seen to be homogeneous, measurements of mucus thickness (10 per picture) were performed using ImageJ software and the average mucus thickness calculated to be 23 μm (± 6 μm) in healthy mice (not shown). The spatial separation of bacteria from the epithelium was also observed in Crossmon stained colon sections from gnotobiotic mice and conventional mice.
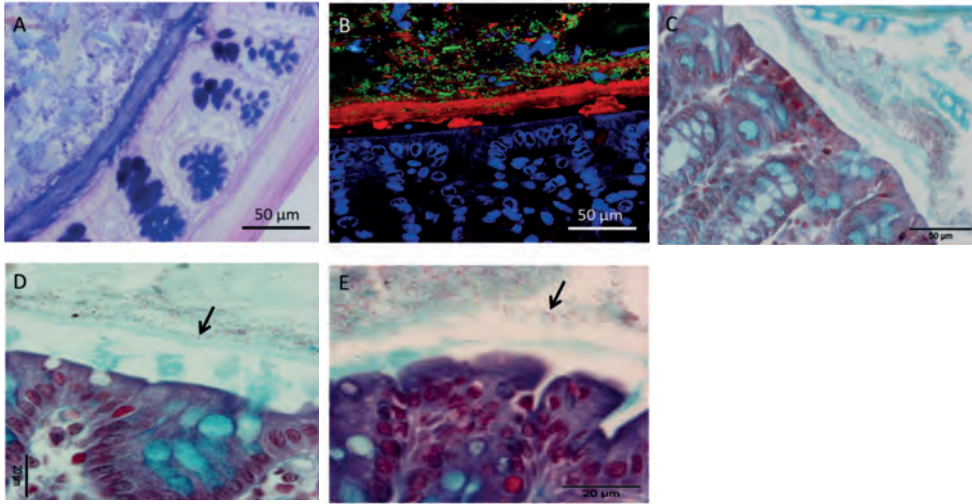

Figure 4: Mucus morphology in the colon fixed with Carnoy. PAS/Alcian Blue staining of the colon (A). Mucus (red) and bacteria (green) co-stained with anti-Muc2 antibody and EUB338-Alexa488 FISH probe, respectively, on a DRAQ5-stained tissue (blue). Scale bars: 20 μm (B). Sections of Carnoy's-fixed colon from conventional mouse stained with Crossman (C). Sections of Carnoy's-fixed colon from a L. plantarum colonized mouse after 1 day stained with Crossman (D). Sections of Carnoy's-fixed colon from a L. plantarum colonized mouse after 21 days stained with Crossman (E). Arrows in C indicate L. plantarum present in the loose mucus.

In the colon of conventional mice, the microbiota could be visualized on top of the firm mucus layer covering the epithelium and within the loose mucus and faecal material (Fig. 4B) [66]. A few bacteria were observed in the loose colon mucus in *L. plantarum* monocolonized GF mice, but they do not resemble the bacteria observed in conventional mice (Fig. 4C). As expected, no bacteria were seen in the ileum or colon of GF mice even at higher magnification (Supplementary Figure S2).

As mucus structure and thickness might be altered by the method used to fix or stain the tissue similar measurements were made using cryopreserved tissue and a different technique. Fresh tissue samples were first frozen in liquid nitrogen with luminal faeces to keep the mucus in place. Thicker sections were prepared (18 μm) than with Carnoy's-fixed tissue (5 μm) to maintain faeces in the lumen and visualize the mucus layers (Fig. 5). After cryosectioning different post-fixation protocols were used to optimize the

7

preservation of the mucus layer. Preservation of the mucus structure was obtained by post-fixation in absolute ethanol and measurements of mucus thickness resulted in an average thickness of 25 μm (± 4 μm), which was in good agreement with that obtained using Carnoy's-fixative. Thus this technique could be a valuable alternative to Carnoy's fixation, allowing immunohistochemical staining with many antibodies that do not work after water-free fixation such as Carnoy.
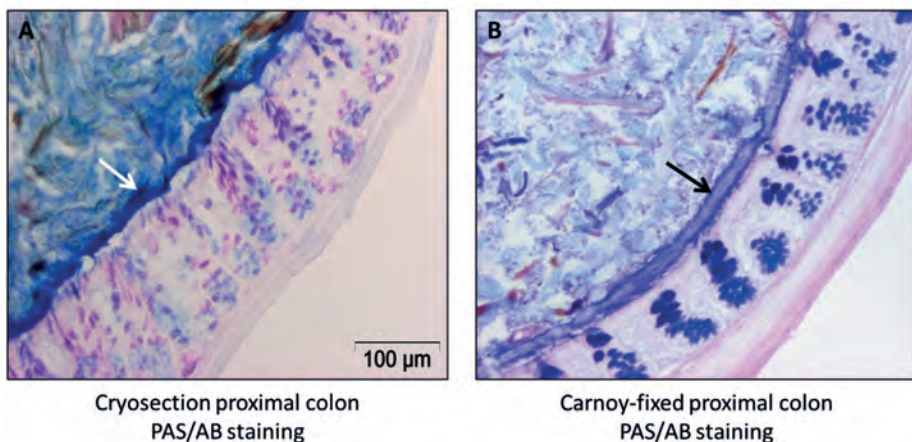

Figure 5: PAS/Alcian Blue staining of the large intestine after cryopreservation and cryosectioning (A) or Carnoy fixation (B). Arrows point the inner mucus layer. Scale bar: 100 μm.

Assessment of mucus permeability using a novel *ex vivo* method

Mucus secreted by healthy explants of colon tissue mounted in Ussing chambers has been shown to be impermeable to bacteria but there are no studies on the small intestine. To measure permeability of the small intestinal mucus we developed a novel *ex vivo* technique to preserve the mucus and assess its permeability to beads of different sizes (1, 2 and 10 μm). The beads were perfused in the lumen of an ileum segment and incubated with shaking in RPMI culture medium for 30 minutes at 37°C. After incubation, tissue was snap frozen in liquid nitrogen, prepared for cryosectioning and the location of fluorescent beads was subsequently visualized by laser scanning confocal microscopy. In the small intestine the smallest fluorescent beads (1 and 2 μm) were found within the small intestinal mucus and occasionally in contact with villus epithelial cells (Fig. 8 C-D). A 3D projection revealed that some of the beads associated with the tissue were not on the surface of the cut section (Supplementary Figure S3). Thus we concluded that some beads were actually inside the tissue and not moved over the tissue surface during sectioning. In contrast, the mucus in the colon was impenetrable to beads 1-2 um and larger (Fig. 6 A-B). These results showed that mucus in the small intestine is more easily penetrable by 1-2 μm particles than the mucus in the colon.
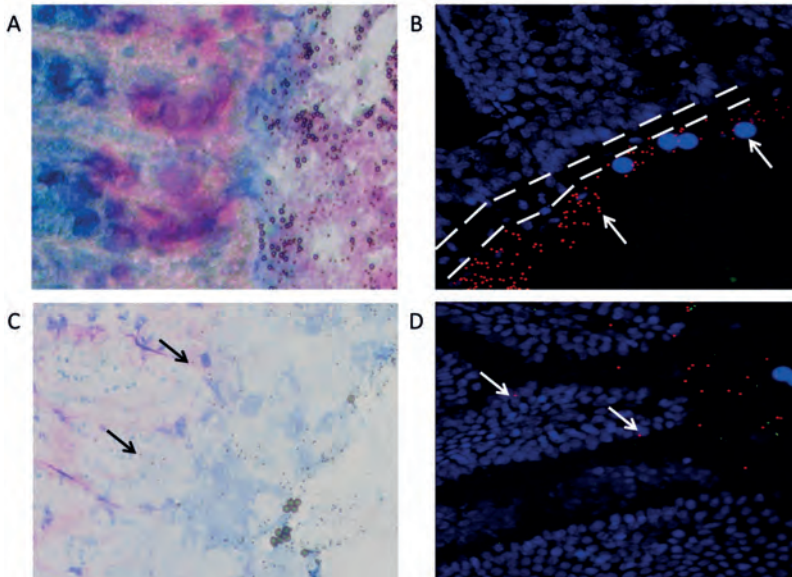
Figure 6: PAS/Alcian blue staining of proximal colon (A) and ileum (C) sample perfused with mix (1,2 and 10 µm) of melamine beads solution. Tissue is stained in pink, mucus in blue. Black arrows point to beads in tissue. Localization of fluorescent beads of 1 µm (green), 2 µm (red) and 10 µm (bright blue) in proximal colon (B) and ileum (D). Cell nuclei are visible as irregularly shaped blue elements. Bead localization is pointed by white arrows. White dotted lines indicate the position of the inner mucus layer in the colon.

The domes of PPs are not covered by mucus and contain few goblet cells

The presence of mucus overlaying the PP and goblet cell numbers were investigated by staining Carnoy's-fixed tissue PAS/Alcian Blue. The PP from (5 individual mice) lacked a mucus layer over the dome and goblet cells in this region of the follicular epithelium (Fig. 7A). A few MUC2-stained goblet cells were identified at the periphery of the Peyer's patch dome, close to the villi. The secreted mucus forms a layer around the villi but does not cover the dome of the PP (Fig. 7B). Therefore, the luminal content will be in contact with the follicular epithelium allowing immune sampling by M cells in the follicular epithelium (Fig. 7C).
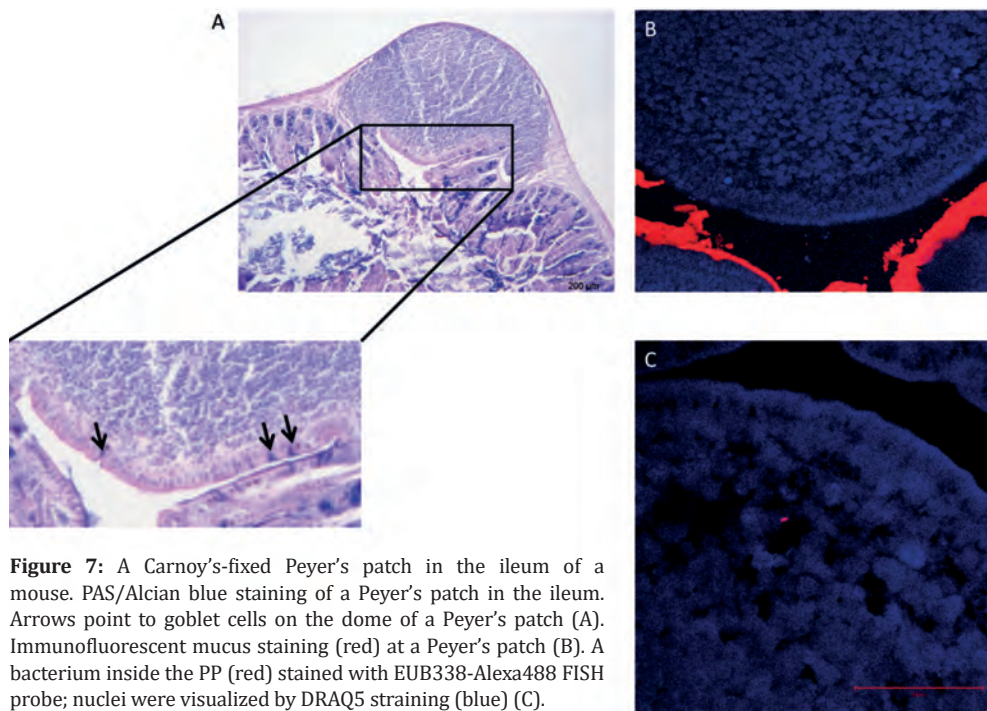
7

Figure 7: A Carnoy's-fixed Peyer's patch in the ileum of a mouse. PAS/Alcian blue staining of a Peyer's patch in the ileum. Arrows point to goblet cells on the dome of a Peyer's patch (A). Immunofluorescent mucus staining (red) at a Peyer's patch (B). A bacterium inside the PP (red) stained with EUB338-Alexa488 FISH probe; nuclei were visualized by DRAQ5 straining (blue) (C).

Viable *L. plantarum* can be recovered from immune cells within the PP and MLNs

To investigate immune sampling of bacteria in PP and the migration of bacteria within immune cells in the lymphoid system, resected PPs and MLNs from both groups of mice were used to generate immune cell suspensions that were counted and then gently lysed and plated on agar plates to enumerate bacterial colony forming units. As expected, no bacteria were recovered from the PPs of GF mice but live bacteria were recovered from PPs of all the mice colonized by *L. plantarum* (Table 1). The CFU of bacteria recovered per host immune cell was highly variable between mice and in the range of 10 to 100 CFU per million immune cells at 20 h and 21 days, although the CFU/cell tended to be higher in the group of mice colonized with *L. plantarum* for 21 days (Table 1). These counts most likely underestimate the total number of *L. plantarum* in PPs and MLNs cells, because we previously showed that *L. plantarum* is killed by mouse macrophages and DCs in 1-2 hours [359].

In mice colonized by *L. plantarum*, bacteria were recovered from MLN cells presumably due to phagocytosis by dendritic cells in the PP or lamina propria that can migrate to the draining lymph nodes and induce T cell responses. There was a large variation in CFU count and for some mice no bacteria were detected, although only some of the MLNs were used for this experiment. *L. plantarum* was recovered in low numbers from the splenic cells of only one mouse although this was probably not due to bacteraemia

as the mouse appeared normal. It is possible that antigen-presenting cells from the gut-associated lymphoid tissue carrying *L. plantarum* entered the circulation and were detected in the spleen.

Table 1: CFU of *L. plantarum* recovered from isolated lymphoid cells from individual GF mice inoculated with *L. plantarum* for the indicated amount of time.

Inoculation	CFU/10⁶cell PP 20 h	CFU/10⁶cell MLN 20 h	CFU/10⁶cell PP day 21	CFU/10⁶cell MLN day 21	CFU/10⁶cell Spleen day 21
L. plantarum	97.1	62.2	1330	21.7	zero
L. plantarum	No PP	zero	144	186	20.8
L. plantarum	27.2	37.6	4230	1.26	zero
L. plantarum	814	zero	163	Zero	zero
L. plantarum	1080	25	12.2	Zero	zero
L. plantarum	10.5	0.909	1050	6.69	zero
L. plantarum	97.1	62.2	1330	21.7	zero
PBS	zero	zero	zero	Zero	zero
PBS	zero	zero	zero	Zero	zero
PBS	zero	zero	zero	Zero	zero

Discussion

Recent studies in mice have shown that in the colon, the secreted mucus forms a firmly adherent layer on top of the surface of the epithelium that is devoid of bacteria and an outer 'loose' mucus layer that is contact with bacteria and faecal material [360]. This observation was made in tissue sections fixed in a water-free fixative such as Carnoy, to maintain the lumen material and preserve the structure of the mucus layer [123]. In the colon the firm mucus layer on top of the epithelium appears to be stratified and more intensely stained than the loose mucus using Alcian blue/PAS staining suggesting this layer contains a higher concentration of mucin glycoprotein or constitutes a more condensed form. Carnoy fixative is known to be aggressive and change protein conformation [361] [362] [363] therefore, we investigated the use of other techniques which naturally fix the tissue and keep the structure and properties of the intestinal mucus. The cryosections needed to be around 18 µm thick to keep faecal content in the section and preserve mucus morphology and structure. For both methods the thickness of the inner mucus layer in the colon was 23 to 25 µm and the overall structure was comparable (Fig 5). Paraffin sections do not show a gap between tissue and faeces, suggesting the section might shrink in its entirety. This shrinking might also occur during fixation in Carnoy's fixative

prior to paraffin embedding, although it was reported to be minimal [364]. One advantage of the cryosection method is that loss of antigenic epitopes is less problematic than in Carnoy's fixative, providing more options for immunohistochemistry.

Although the thickness varied between tissue sections, the firm mucus in the colon was notably thinner in GF mice, but after colonization with *L. plantarum* for 21 days, it was similar to the conventional group. This is consistent with published observations of reduced mucus production in GF animals and with the concept that metabolites and other components of the microbiota are key regulators of colonic mucus secretion [365] [366]. The appearance of both firm and loose mucus in GF mice suggests that the conversion of firm mucus layers into loose mucus does not depend on the presence of bacteria. Using FISH and the Crossmon staining method combined with Carnoy's fixation we were able to visualize the compartmentalization of the microbiota to the loose outer mucus layer in the colon, as previously described using immunofluorescent microscopy [66]. Although microscopy techniques cannot exclude the presence of small numbers of bacteria in the firm mucus, it is evident that these events are rare. Previously Johansson *et al.*, showed using semi-quantitative qPCR of the bacterial 16S gene that there was bacterial DNA present in the firm mucus, but it was much less than in the loose mucus [66].

The mucus layer in the small intestine appears to be thinner, as previously demonstrated using different techniques [1], and has the appearance of densely stained strands residing between the villi and in-between the tops of the villi and the ileal content. Bacteria rarely penetrated the mucus layer in the small intestine, and when observed only single bacteria were seen in contact with the epithelium. However, the small intestinal mucus appeared to be permeable to the smallest fluorescent beads (1-2 μm green beads), some of which were seen in direct contact with epithelium and inside the tissue. The exclusion of bacteria may therefore be due to sIgA and secreted antimicrobial proteins (e.g. Reg3β and Reg3γ) in the mucus, which have been shown to contribute to the spatial compartmentalization of bacteria [78] [22] [70]. In conventional mice bacteria are rarely seen in contact with the epithelium although microbial metabolites and other components might be able to diffuse through the firm mucus layer to trigger epithelial signalling and crosstalk to the immune cells in the lamina propria. The exception is SFB which are known to be present in small intestine of mice from some suppliers. The most intriguing feature of SFB is their apparent intimate association with epithelial cells in the terminal ileum and their capacity to stimulate Th17 effector cell differentiation which contributes to protection against infection [358].

In all mouse PPs examined, the domes of the PP were not covered in mucus and goblet cells tended to be at the edges of the PP close to adjacent villi. This is consistent with the recovery of live *L. plantarum* from immune cells isolated from the PPs and MLNs of monocolonized mice. The counts of viable *L. plantarum* were highly variable between

mice, which may have been influenced by the location of the PPs or MLNs but overall, higher numbers of bacteria per cell (up to 1 in 236 total cells) were recovered from mouse PPs after 21 days colonization than after 20 h colonisation. This is likely to be an underestimate of the number of *L. plantarum* sampled by DC as they are killed in the phagosome with a few hours [341]. DCs are estimated to be around 2% of the total PP cell population depending on the gender of the mice [367], suggesting that a high proportion of PP DCs might be associated with bacteria. MLNs were also found to contain viable *L. plantarum,* but the numbers were lower than in PPs. As *L. plantarum* were not seen in contact with the epithelium in the ileum, it seems most likely that DCs in the PPs migrated through the lymphatics to the draining lymph nodes. The lower CFU recovered from the MLNs may be due to the variability of counts in the resected MLNs and or extended time of *L. plantarum* in APCs increasing the likelihood of phagosomal killing.
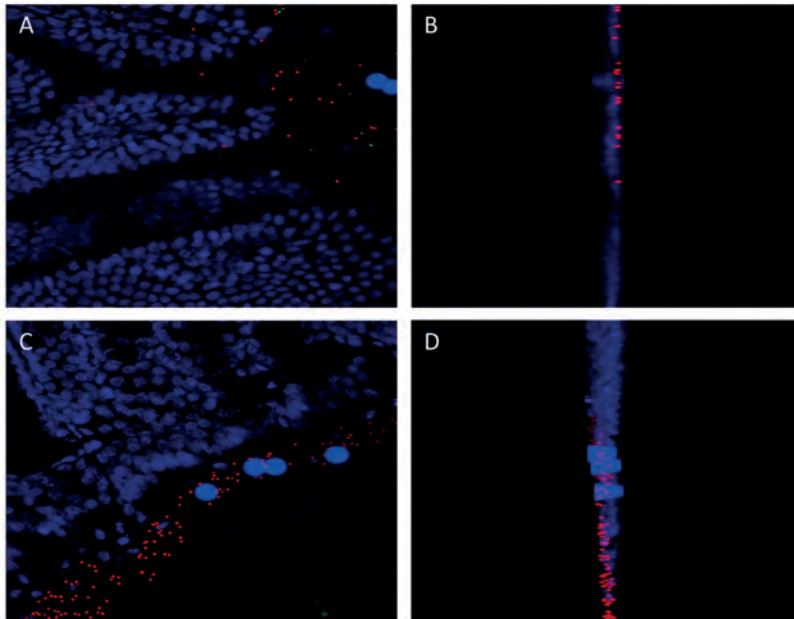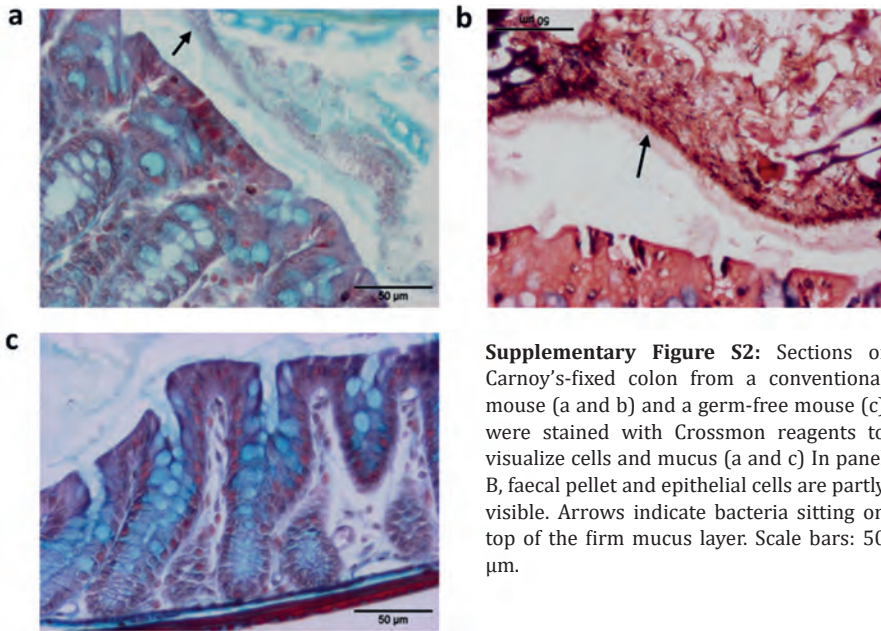
The preliminary study described in this chapter focused on PPs and antigen sampling. However, the colon also contains an additional type of lymphoid tissue, the solitary intestinal lymphoid tissues (SILT), which can develop in mature isolated lymphoid follicles (ILFs) [368-370]. Like the PPs, ILFs can also function as inductive sites for mucosal immune responses [369].

In summary, we show that the mucus structure and thickness are maintained in thick cryosections of intestinal tissue and comparable to that observed using Carnoy fixative, thereby providing more options for immunohistochemistry. The mucus structure and thickness was similar in conventional and monocolonized mice and equally effective at compartmentalising the bacteria to the lumen. In the small intestine the mucus is thinner and more permeable to small 1-2 μm beads than the colon. Nevertheless, bacteria were rarely seen in contact with the villi, the exception being SFB. In *L. plantarum* monocolonized mice viable bacteria were recovered from isolated immune cells in the PP and MLN cells (most likely within DCs). *L. plantarum* is rapidly killed by DCs and macrophages, implying that immune sampling occurred at much higher rates than that estimated by recovery of intracellular viable bacteria. As contact of intact bacteria with the small intestinal epithelium was rarely observed, uptake in the PPs or ILFs seems to be the predominant mechanism for immune sampling of commensal bacteria. This appears to be facilitated by anatomical features of the PPs, which lacked mucus on top of the PP dome *in vivo* and relatively few goblet cells in the follicle-associated epithelium (FAE).

7

Supplementary data
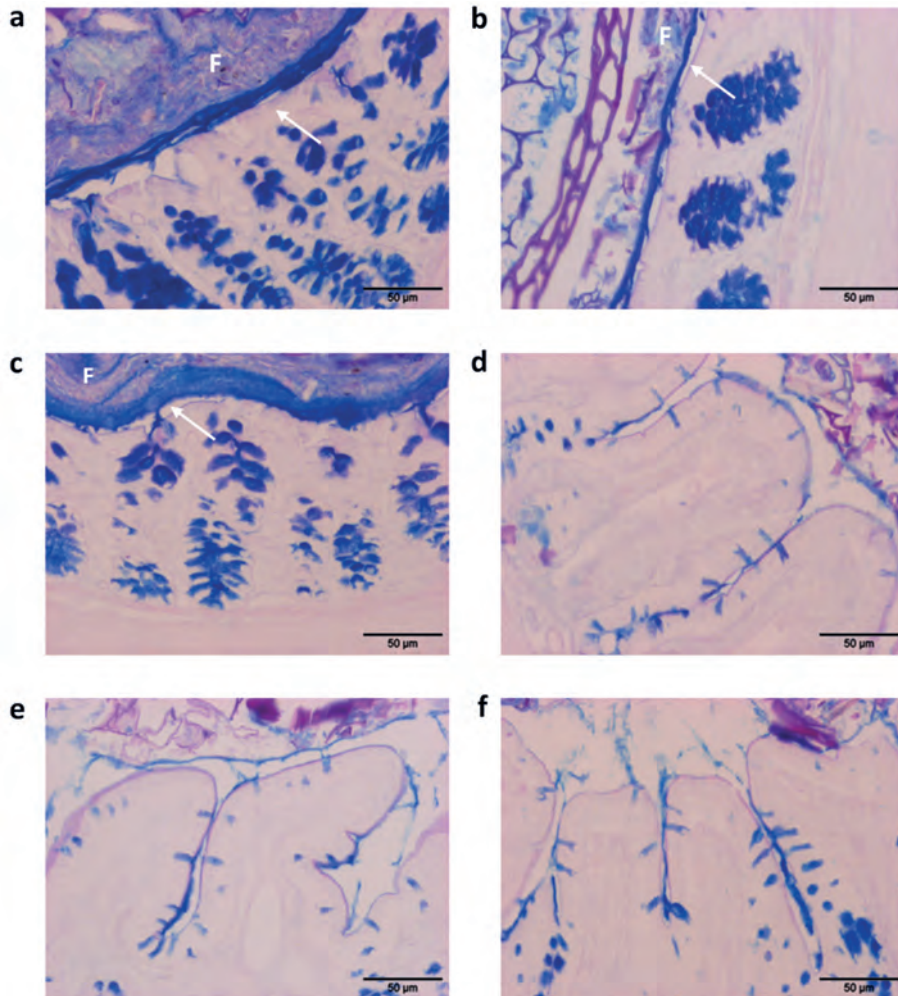
Supplementary Figure S1: Sections of Carnoy's-fixed colon (a, b and c) and ileum (d, e and f) from a conventional mouse (a, d), germ free mice (b, e) and a germ free mouse administered *L. plantarum* (c, f) on day 1 and 21. Sections were stained with Alcian blue/PAS. White arrows in a, b and c indicate the firm mucus layer. Blue stained goblet cells are seen in the colon crypts (a, b, c) and villus epithelium (d, e, f). F, fecal material in colon.

Supplementary Figure S2: Sections of Carnoy's-fixed colon from a conventional mouse (a and b) and a germ-free mouse (c) were stained with Crossmon reagents to visualize cells and mucus (a and c) In panel B, faecal pellet and epithelial cells are partly visible. Arrows indicate bacteria sitting on top of the firm mucus layer. Scale bars: 50 μm.

Supplementary Figure S3: Localization of fluorescent beads of 1 μm (green), 2 μm (red) and 10 μm (bright blue) in the small intestine (A) and large intestine (C). Cell nuclei are visible as irregularly shaped blue elements. 3D projections at 90° of small intestine (B) and large intestine (D). The tissue and the beads are in the same view, proving that the beads seen inside the ileal tissue are not there because of a technical issue.

Chapter 8

General discussion and future perspectives

Bruno Sovran

The first direct evidence for the role of epithelial integrity in preventing intestinal inflammation came from a chimeric mouse model in which cells of the crypt villus axis small bowel expressed a dominant negative mutant of N-cadherin, thereby disrupting the cell-to-cell interactions that help to maintain junctional integrity and epithelial regeneration [265]. The regions of the intestine expressing N-cadherin were more leaky than the areas expressing E-cadherin and developed focal lesions due to inflammation. Since then, knockout mice with defects in in the pathways maintaining epithelial integrity, epithelial stress responses or the regulation of mucosal immune responses have been shown to lead to barrier disruption and colitis triggered by bacterial antigens and microbe-associated molecular patterns (MAMPs) [371] [266] [267] [268] [343]. Despite these observations it has become evident that homeostasis is not maintained by "passive mechanisms" involving a lack of responsiveness to microbes. Indeed Toll-like receptor (TLR) activation by commensal bacteria was shown to be crucial in the recovery from epithelial damage induced by Dextran Sodium Sulfate (DSS) [342]. Similarly, mice with a knockout of NEMO (i-kappa kinase gamma), an activator of NF-κB, develop spontaneous colitis due to the role of NF-κB in inducing epithelial repair and innate effector mechanisms in the intestine [343]. Additionally, TLR signalling, and in particular TLR-2 signalling and PKCα and PKCδ activation has also been implicated in tight junction (TJ) regulation through effects on TJ protein phosphorylation and composition in the intestine [297].

The importance of having secreted mucus in the intestine is evident from research on mucus-deficient mice which develop spontaneous colitis after weaning [118] [121] [193]. In other murine models of intestinal inflammation a decline (or even absence) of the mucus layer has been shown to contribute to the pathophysiology [110] [111]. Thus the epithelial barrier is dynamic and the biological mechanisms controlling its maintenance and renewal are crucial for homeostasis and intestinal health. Despite the recent advances in our understanding of the complex mechanisms maintaining epithelial barrier functions there is still much to be learned about the role of mucus, the effects of ageing on the gut barrier and the consequences of a dysfunctional mucus barrier on host responses. With these aims in mind the specific objectives were to study the effects of mucus deficiency, which is a feature of inflammatory bowel disease (IBD), and the effects of ageing and gender differences on mucus production and other aspects of intestinal homeostasis and microbiota. Different mice models and multidisciplinary approach including transcriptomic, microbiota profiling and histology were used to explore the role of mucus in the intestine of healthy and diseased mice as well as ageing mice. The new knowledge and insights gained from these studies and remaining gaps in our understanding are discussed in the following sections.

8

The structure, organization and functions of intestinal mucus

The necessity of the mucus barrier to prevent colitis was first demonstrated in the *Muc2⁻/⁻* mice which spontaneously develop colitis after about 4 weeks [118] [119] [120]. The weaning period was associated with the onset of colitis, evidenced by increased thickness of the mucosa associated with hyper-proliferation, apoptosis in crypts, ulceration accompanied by faecal blood, and weight-loss [121] [193]. In these initial studies no pathology was described in the ileum and possible effects of mucus deficiency on small intestinal physiology and long-term health were not investigated.

In healthy conventional mice, the colonic secreted mucus forms a firmly adherent layer (about 25 μm thick) on top of the surface of the colon epithelium that is devoid of bacteria [1] (**Chapter 7**). An outer 'loose' mucus layer is also visible that is contact with bacteria and faecal material [360] (Fig. 1). The firm mucus layer is notably thinner in germ-free (GF) mice, but increases to the thickness of conventional mice after colonization (**Chapter 7**).
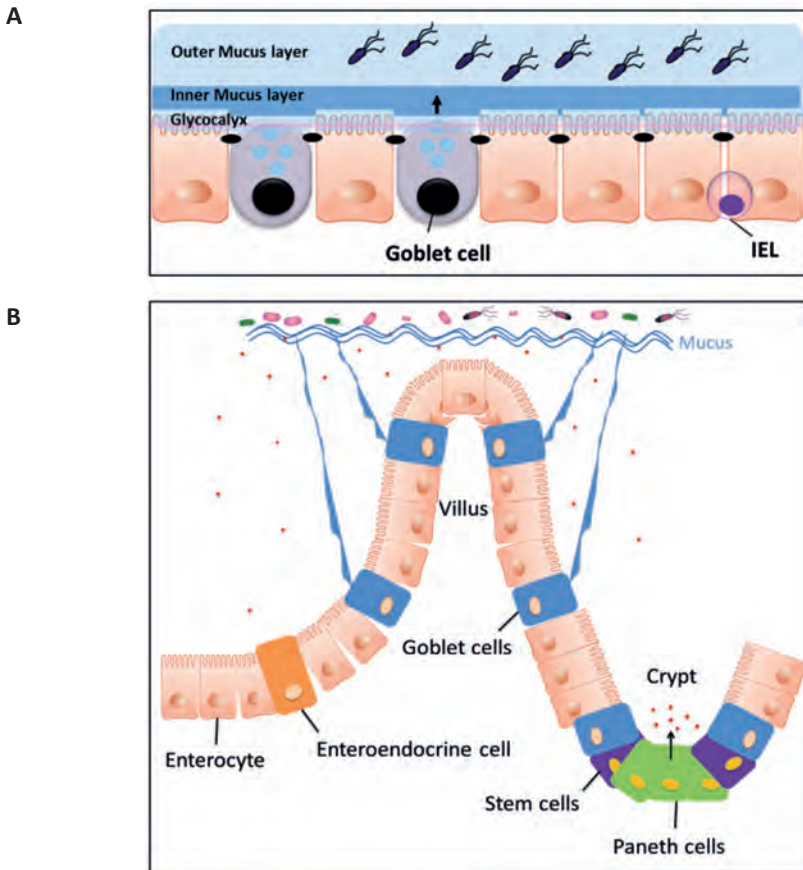
A

B

Figure 1: Structure and organization of the secreted intestinal mucus barrier in the mouse intestine (A: large intestine ; B: small intestine).
Legend: IEL: Intra-epithelial Lymphocytes

This is consistent with published observations of reduced mucus production in GF animals and with the concept that bacterial short-chain fatty acid metabolites and other components of the microflora are key regulators of colonic mucus secretion [365] [366] [372]. The appearance of both firm and loose mucus in GF mice suggests that the conversion of firm mucus layers into loose mucus does not depend on the presence of bacteria. The visualization of a firm mucus layer is possible only by using specific histological techniques, that preserve the structure of the mucus layer such as Carnoy fixative. The presence of a faecal pellet in the lumen is essential to get a firm homogenous mucus layer between the faeces and the epithelium. Thus our knowledge of the structure of mucus layers *in vivo* and in humans is largely based on the results of histology in rodent models.

In the mouse small intestine, the epithelial surface from the crypt bottoms to the villi tip is completely covered by mucus that seems not to be attached very rigidly [1] [77] (**Chapter 7**). This loose structure may facilitate nutritional uptake, but also bacterial sampling. Glycosylated MUC2 was recently shown to confer tolerogenic properties to epithelial-associated dendritic cells (DCs) through interaction with a galectin 3-dectin 1-FcγRIIB receptor complex [92]. Lamina propria (LP) DCs of *Muc2*^{-/-} mice produce increased amounts of pro-inflammatory cytokines and decreased amounts of anti-inflammatory cytokines than conventional mice. This was consistent with fewer regulatory T cells in the small intestinal mucosa of *Muc2*^{-/-} mice. Additionally, glycosylated MUC2 was shown to promote tolerance to ovalbumin (OVA) in an OVA-induced delayed type hypersensitivity (DTH) response to mice immunized systemically with OVA. In *Muc2*^{-/-} mice tolerance was not induced but restored when OVA was administered by gavage in combination with MUC2. MUC2 also enhanced epithelial expression of B cell cytokines and trypsin-like serine protease, promoting development of tolerogenic DCs and anti-inflammatory mechanisms contributing to gut homeostasis, possibly through the same receptor-complex [92]. Despite the absence of these tolerogenic mechanisms *Muc2*^{-/-} mice do not develop ileitis in our hands (**Chapter 2**). The only noticeable morphological difference between wild type (WT) and *Muc2*^{-/-} mice was an increased length of the villi due to hyper-proliferation of the intestinal epithelium.

To explore the mechanisms maintaining homeostasis in *Muc2*^{-/-} and *Muc2*^{+/-} mice we obtained transcriptomics data from the ileum at 2, 4, and 8 weeks old mice. Gene set enrichment analysis (GSEA) of genes significantly expressed in increased quantities in *Muc2*^{-/-} ileum was consistent with up-regulation of epithelial cell proliferation and increased villus length (**Chapter 2**). *Reg3* genes were also significantly up-regulated in the ileum of *Muc2*^{-/-} and *Muc2*^{+/-} mice after weaning. Expression of REG3 proteins is induced during infection or inflammation (24), and was shown to be dependent on IL-22 signalling (25), a finding consistent with enhanced IL-22 signalling in the *Muc2*^{-/-} transcriptome (**Chapter 2**). IL-22 also regulates cellular stress response, apoptosis, and

8

wound healing pathways in intestinal epithelial cells (IECs) via the signal transducer and activator of transcription 3 (STAT3) pathway (26). LP ILC3 were recently shown to produce IL-22 through sensing of bacteria via an unknown mechanism [27] leading to increased expression of REG3 proteins and FUT2. The *Fut2* gene, encoding an α-1,2-fucosyltransferase responsible for enzymatic linkage of α1,2-linked fucose to cell membrane attached and secretory mucins of the intestinal mucosa [28], was significantly up-regulated in the ileum of adult *Muc2*^{-/-} mice (**Chapter 2**). It has been shown that at weaning when the transition toward adult-type colonization by microbiota occurs, *Fut2* mRNA is increased leading to expression of fucosylated epitopes in the colonic epithelium and fucose decoration of mucins [29] [30] [31] [32]. This may be a mechanism to promote colonization by preferred groups of symbionts that produce beneficial short-chain fatty acids and provide colonization resistance against pathogens. Weaning was associated with major changes in the transcriptome of all mice, and the highest number of differentially expressed genes compared to adults, reflecting temporal changes in microbiota. This is consistent with our observation of increased bacterial contact with the epithelium in *Muc2*^{-/-} mice (Fig. 2) and the IL-22 mediated effects on epithelial expression and proliferation reported here. Based on these findings we proposed a key role for the IL-22/STAT3 pathway in maintaining homeostasis in the ileum when the mucus barrier is absent (Fig. 2) (**Chapter 2**). The same mechanism is also predicted to play a role in mucosal homeostasis when there is more 'bacterial sensing' due to barrier dysfunction or mucosal infection, as depicted in Figure 2.

However, the essential role of IL-22 in maintaining homeostasis in the small intestine when there is reduced mucus production needs to be confirmed, for example by administration of IL-22 blocking antibodies to *Muc2*^{+/-} mice. In the future the IL-22 network of gene regulation elaborated on in this thesis could be verified in an organoid model of the small intestinal epithelium. For example by adding IL-22 with and without NF-kappaB pathway agonists to organoid cultures and assessing expression of the IL-22 gene network by transcriptomics or qPCR. It is now possible to generate monolayers of untransformed epithelial cells from organoid cultures of WT and *Muc2*^{-/-} ileum that contain all the epithelial cell types present *in vivo*. Additionally, antagonists of the STAT3 pathway could then be used to further dissect the regulatory responses to IL-22 in different cell types (e.g. expression of *Reg3*, *Fut2* and proliferative factors). This might provide more insights into the mechanisms behind the IL-22/STAT3 pathway and its role in maintaining small intestinal homeostasis and have implications for future therapeutic strategies.

Although the colon produces IL-22 it was clearly not enough to prevent colitis as in the ileum. This could be due to the fact that there are many more bacteria in the colon with potential to colonize the epithelium and induce inflammatory responses. Additionally the ileum possesses different innate mechanisms to control microbiota, such as Reg3β

and Reg3γ, which are highly expressed in small intestinal Paneth cells and produced in much lower amounts in the colon than in the ileum [373].
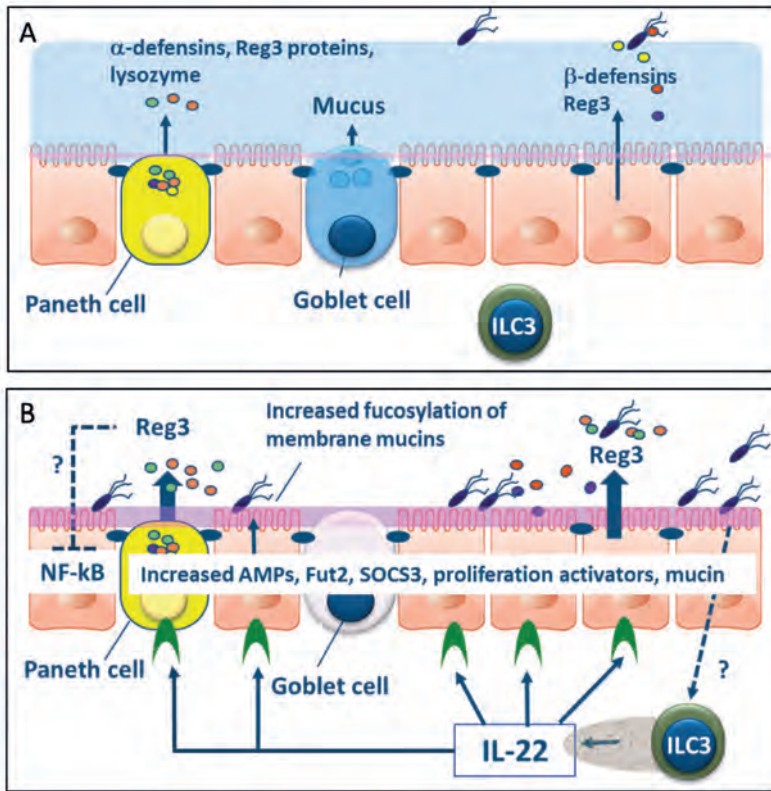

Figure 2: The IL-22-STAT3 pathway plays a key role in the maintenance of ileal homeostasis in MUC2-deficient mice. Schematic representation of the small intestine of a wild-type mice (A). Schematic representation of the small intestine of *Muc2-/-* mice showing known functions of IL-22 (B). The anti-inflammatory mechanism of PAP (Reg3β) on NF-κB driven inflammatory pathways is shown as a dotted line as it has only been described for human colonic tissue and the precise mechanisms are not known. We speculate that IL-22 might also regulate *Fut2* (shown as a dotted line). Mucus is indicated in blue, fucosylation is indicated in pink.
Legend: IEL: Intra-epithelial Lymphocytes; DC: Dendritic Cell; AMPs: Antimicrobial Peptides; SOCS3: Suppressor of cytokine signalling 3.

In conclusion the results of **Chapters 2** and **7** provide further evidence for the important barrier function of mucus in limiting contact of the epithelium with luminal bacteria, particularly in the colon. In the small intestine the general absence of goblet cells on the dome of PPs results in the absence of a mucus layer over the follicular-associated epithelium (**Chapter 7**). This allows bacterial sampling by M cells and the induction of mucosal immune responses in the lymphoid tissue, resulting in sIgA production to support mucosal barrier function (**Chapter 7**).

8

A temporal study of colitis development and associated changes in the microbiota in *Muc2*^{-/-} mice

Previously, gene transcript analysis from colon of *Muc2*^{-/-} mice revealed distinct phases in colitis development pre- and 1 week after-weaning, which were presumed the result of changes in microbiota diversity and/or density [193]. As the weaning period is known to be a rapidly changing period of intestinal development [374] we repeated the transcriptomics study, including samples from 8 week-old adult mice and also investigated the effects on microbiota. Heterozygote *Muc2*^{+/-} mice were also included in this study as they were predicted to produce less secreted mucus and we wanted to assess their usefulness as a model of a compromised mucus barrier.

As pathobionts are known to play a role in the pathophysiology IBD we investigated the impact of the MUC2 genotype on the temporal development of the microbiota. Initial colonization of microbiota in WT and *Muc2*^{+/-} mice involved a more constrained group of bacteria as compared to the *Muc2*^{-/-} mice, although during prolonged colonization the microbiota composition became more similar in all mice, but still consistently discriminated the groups of mice according to their genotype (**Chapter 3**). This suggests that MUC2 shapes the microbiota colonising the colon, especially in the 2 weeks postnatal, pre-weaning period, although a role of the antimicrobial factors that were more highly expressed in *Muc2*^{-/-} mice compared to WT or *Muc2*^{+/-} mice can also play a role. In the case of the *Muc2*^{+/-} genotype mice, which still produce a mucus layer, the altered microbiota might be due to the mucosal responses identified by transcriptomics (e.g. increased relative amounts of REG3 proteins and defensins).

To identify bacteria that might be correlated with early changes in colon gene expression we used the linear multivariate method partial least squares (PLS) method [232] for each time point, as previously described [233]. The ileum, of patients with Crohn's disease is colonized by adherent-invasive E. coli (AIEC), a pathogenic group of *E. coli* able to adhere to and invade intestinal epithelial cells. Several independent studies have reported the abnormal presence of AIEC associated with ileal mucosa of CD patients and proposed a role in the pathophysiology of IBD [375 376 377 378 379 380]. However, increased abundance of *E. coli* during colitis development was not observed in the *Muc2*^{-/-} mice model.

Despite the absence of changes in *E. coli* abundance, we showed that even prior to the onset of colitis in the *Muc2*^{-/-} mice, *Bacteroides plebeius et rel., Unclassified Prevotella, Alistipes et rel., Bacteroides fragilis et rel., and Bacteroides vulgatus et rel.* were positively correlated with the increased expression of gene clusters associated immune and stress responses (**Chapter 3**). These bacterial groups were more abundant in *Muc2*^{-/-} mice than in WT littermates. An increased relative abundance of *Bacteroides* has been observed in only some animal models of colitis [238 239]. In humans several, but not all studies on IBD patients are consistent with major changes in abundance of *Bacteroides* in active disease.

Thus the possible involvement of pathobiont species in the pathophysiology might also depend on host genetics, resident microbiota and/or other lifestyle factors such as the diet. Nevertheless, *B. thetaiotaomicron* and *B. vulgatus* have been demonstrated to induce colitis in experimental rodent models, in which other commensal species do not induce colitis [227] [240] [241] [242]. *Nod2* mutations that disrupt bacterial recognition are one of the highest risk factors for Crohn's disease (CD). Recently expansion of *B. vulgatus*, was shown to mediate exacerbated inflammation in *Nod2*^{-/-} mice upon small-intestinal injury, providing further evidence for its colitogenic potential in IBD [243]. A subset of intestinal *B. fragilis* strains produce an exotoxin (ETBF strains) associated with diarrheal disease and a number of studies have shown associations of this species with IBD and colorectal cancer [244]. Overall the findings support the idea that in *Muc2*^{-/-} mice, the innate inflammatory responses driven by increased contact of commensals with the epithelium leads to increased abundance of colitogenic members of the Bacteroidetes phylum, which contribute to the onset of colitis **(Chapter 3).**

Application of *Muc2*^{+/-} mice to study colitis development and markers of a compromised colonic mucus barrier

In contrast to *Muc2*^{-/-}, the *Muc2*^{+/-} mice did not develop colitis during the 8 week period. However, the colonic mucus layer was significantly thinner in *Muc2*^{+/-} than in WT mice, which was also associated with altered mucosal gene expression (**Chapter 3**). At week 2 and week 8 the affected gene networks in *Muc2*^{+/-} mice were mainly associated with mucosal healing and innate defence including chemotactic functions although there was transient increase in inflammatory genes (e.g. *Tnf* and cytokine receptors for *IFNγ*, *IL-2*) at week 4 resembling the transient inflammatory state observed in colonisation studies with GF mice [237]. Thus the *Muc2*^{+/-} genotype appeared to exacerbate the transient inflammatory response to the changing microbial ecology of the colon around weaning. This indicated that changes in mucus barrier function have large effects on intestinal homeostasis (**Chapter 3**).

The majority of the published studies did not extensively characterize the role of mucus in shaping intestinal microbiota composition, and its role in the development of colitis [118] [121] [122]. Therefore, microbiota profiling on *Muc2*^{-/-} mice faeces was the first step to get insight on the role of mucus on shaping the microbiome. To get more insight in the role of the microbiota in the development of the colitis, faecal transplantation from the *Muc2*^{-/-} mice could be performed in GF mice to see if they develop inflammatory mucosal responses. However, establishing and running GF facilities is expensive and requires special expertise and infra-structure. Compared with animals living in a conventional microbiological environment, GF animals display an immature and underdeveloped lymphoid system [381]. A generally accessible alternative to using GF animals for studying host-microbe interaction *in vivo* is to deplete animals of their intestinal microbiota

8

by administrating a combination of broad-spectrum antibiotics. However, several published papers that report to have applied this intestinal microbiota depletion protocol describe incomplete depletion of the cultivable bacteria [382] [383]. Another option is to use reversible colonization of GF mice with an *E. coli* strain harbouring multiple auxotrophic mutations [384].

On the basis of the results obtained to date the heterozygote *Muc2*^{+/-} mice appear to be a promising model of gut barrier dysfunction (**Chapter 3**). More research is warranted to assess whether the epithelial stress markers identified in this model are observed in early stages of colitis development and in human diseases associated with deterioration of gut barrier function and loss of epithelial integrity. To be routinely used as disease biomarkers they ideally would have a causal relationship with the physiological changes been evaluated, correlate with disease status and be readily measurable in faeces, urine or blood.

Intestinal ageing induces a low-grade mucus barrier dysfunction partly depending on gender dimorphism

In **Chapter 4** we characterized the effects of ageing on the gut barrier function in mice. Previously, it was shown that the intestinal barrier function is compromised by ageing, and that susceptibility to infection increases in elderly individuals [164]. However, no extensive studies have been performed on the age related decline in gut barrier function and specifically the effects on mucus.

In **Chapter 5** we showed that in old mice (19 month) there is a decrease in the mucus thickness in the colon, and this was influenced by gender as the females showed a thicker mucus layer than males. However, in both old male and female mice the mucus layer thickness was ineffective in compartmentalising the microbiota to the lumen (**Chapter 5**). This phenomenon was also observed in fast-ageing mice model (*Ercc1*[-/Δ7]) which have an impaired DNA repair capacity, causing more rapid accumulation of DNA damage, the hallmark of natural ageing (**Chapter 6**). Despite the reduced thickness of the colonic mucus in naturally (**Chapter 5**) and fast (**Chapter 6**) ageing mice, the expression of the *Muc2* transcript was not altered. Thus processes that compromise the assembly or secretion of MUC2 might affect the mucus thickness. Stress induced by physiological perturbations in the intestine can lead to accumulation of unfolded proteins at the endoplasmic reticulum (ER). Improperly folded or glycosylated MUC2 may aggregate and not assemble into a network structure with the correct gel forming properties [346] [117]. ER stress is a classic feature of secretory cells leading to activation of the unfolded protein response (UPR). The UPR response is induced by intestinal inflammation and in future studies this should be measured to see if it correlates the observed changes in mucus properties in aging mice.

Mucins carry a vast array of oligosaccharide structures, with the glycosyltransferase profile expressed by the host determining the type of linkages and glycan structures present on the secreted mucins [385]. Alterations in mucin glycosylation have been associated with a number of diseases such as colitis, colonic cancer and inflammatory bowel diseases in humans [386] [387] [388] [389] [390] and mouse models [107] [108] [114]. Therefore, an alteration of mucin glycosylation might also be the cause of mucus barrier impairment in ageing mice. Impairment of the mucus barrier in old mice was associated with reduction of decreased expression of many genes associated with innate immunity, T cell-specific gene transcripts and T cell signalling pathways involved in the activity of cytotoxic T cells, T helper cells and natural killer cells.

Changes in the gut microbiota in terms of composition and functionality has previously been compared in young adults and elderly human subjects [161] [159] [160]. It has been postulated that the microbiota of elderly subjects (65-70 years) might contribute to the development of immunosenescence and inflammageing [309] [391]. However, significant differences in microbiota composition and diversity were only observed in centenarians compared to younger adults [161]. In old mice, decreased microbiota composition and diversity were also observed.

However, these studies on ageing have not extensively characterized the role of microbiota in the development of intestinal inflammageing. To get more insight in the role of the microbiota in intestinal ageing, faecal transplantation from ageing mice could be performed in GF young mice. However, for the same reasons as mentioned above, GF mice and antibiotic treatments might not be the best approaches to study the effect of the microbiota in ageing.

Live span studies comparing GF fast-ageing ERCC1 mice with GF WT mice or reversibly colonised GF mice could be used gain insights into the role of the microbiota in ageing. If GF mice have a reduced life span, this would be that the microbiota play a key role in regulating host physiology throughout lifespan. In the opposite case, the microbiota might be identified as having an instrumental role in the process of ageing in intestine and increase inflammageing.

Mucus barrier function can be restored with probiotic intervention in ageing mice

Ageing affects the intestinal barrier function and therefore to some extent intestinal homeostasis. Therefore, interventions have been performed to slow down the development of intestinal disorders or reduce the effects of ageing. Changes in diet are one of the most efficient and direct ways to induce changes in intestinal physiology. Probiotics, live bacteria that confer health benefits to host, exert beneficial effects by competing with pathogens, regulating immunity and enhancing intestinal barrier function [297] [317]. It has been shown that probiotic supplementation to elderly subjects

8

was beneficial and accompanied by changes in gut microbiota composition and immunity [392] [309] [311] [312] [313] [314] [315]. However, none of the studies previously performed investigated the effects of probiotic strains on slowing down the effects of ageing on the gut barrier integrity. Therefore, we performed a comprehensive analysis of the effect of bacterial supplementations on ageing immunity and intestinal barrier (**Chapter 6**). We linked effects in immunity and intestinal barrier to gene regulation and gut microbiota composition. Such a study would be laborious and costly in time and resources to setup with naturally aged mice but the fast-ageing mice model (*Ercc1$^{-/\Delta7}$*) might be an alternative model as we showed that the effects of natural ageing on the mucus barrier, immunity and microbiota are also observed in fast-ageing mice (**Chapter 6**).

Probiotic interventions with *Lactobacillus plantarum* WCFS1, *Lactobacillus casei* BL23 and *Bifidobacterium breve* DSM20213 showed different effects on ageing mice (**Chapter 6**). *L. plantrarum* WCFS1 is known for its pro-inflammatory profile *in vitro* and Th2 skewing properties in models of allergic sensitization [341] [331], especially in Th2 polarized conditions. In *Ercc1$^{-/\Delta7}$* mice, supplementation of *L. plantarum* WCFS1 restored age-related decline in intestinal barrier by improving mucus barrier function and restoring bacterial compartmentalization to the lumen (Fig. 3). In contrast supplementation of *L. casei* BL23 and *B. breve* DSM20213 did not change or further increased the decline age-related decline in intestinal barrier.

The mechanism behind the protective effect of *L. plantarum* in aged mice remains unknown but might be due to polyamine production, which has been shown to increases life span in model organisms. Polyamines have also been involved in stress resistance and might help prevent deterioration of the gut barrier due to ER stress. This notion should be checked by administration of polyamines (including those extracted from *L. plantarum*) to fast-ageing mice. Furthermore polyamines should be measured in all three probiotics and in the mice faeces to see if *L. plantarum* produces high amounts compared to the other strains. Furthermore, mono-colonization with *L. plantarum* in germfree (GF) *Ercc1$^{-/\Delta7}$* mice would give insights in the effect of only *L. plantarum*, without interactions with the existing gut microbiota. The *Ercc1$^{-/\Delta7}$* were supplemented with *L. plantarum* for 10 weeks (3 times a week, 10^9 CFU), which might also affect the outcome of this experiment. A test with a reduced time of supplementation (2-3 weeks) might also give insights in the optimal time of *L. plantarum* supplementation for getting mucus barrier restoration in *Ercc1$^{-/\Delta7}$* mice.

Our data provide an example of how bacterial supplementation can restore age-related decline in intestinal barrier, and also underscores the need to exercise caution when considering long-term supplementation of candidate probiotics to elderly subjects (**Chapter 6**).
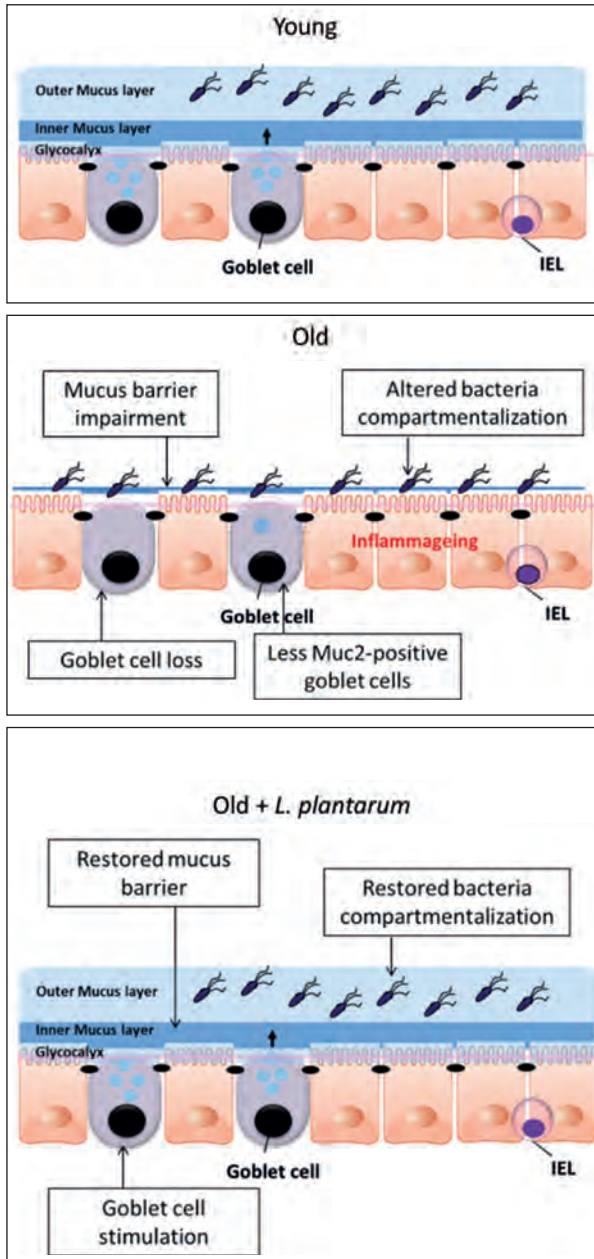
Figure 3: The secreted mucus plays a key role in the maintenance of colonic homeostasis in mice. Ageing causes goblet cell loss associated with mucus depletion, impairment of the mucus barrier function and altered bacteria compartmentalization. Supplementation of *L. plantarum* WCFS1 induced hypersecretion of mucus (increased mucus thickness) and restores mucus barrier function and compartmentalization of bacteria to the lumen. IEL: intraepitelial lymphocytes

8

Factors influencing mucus in health and disease

The mucus barrier is essential for maintaining intestinal homeostasis. The absence of MUC2 in the colon leads to colitis and its absence in the ileum leads to long term perturbations of gene networks involved in maintaining homeostasis, which may increase the risk of developing diseases (e.g. cancer).

As shown in *Muc2*^{+/-} mice, changes (even minor) in mucus thickness can lead to development of inflammation (**Chapter 3**). Thus environmental factors influencing mucus hyper- and hypo-secretion and mucus permeability are important to consider in a health perspective. Several factors may influence the secretion of mucus and therefore contribute to reinforce or impair the barrier (Fig. 4).
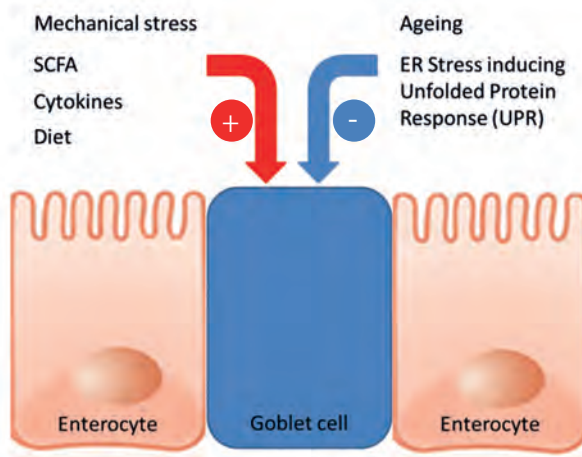
Figure 4: Schematic representation of the different factors which influence mucus secretion.

- *Mechanical stress to tissue*

  The mucus acts as a gel, covering the epithelium and facilitating the passage of the luminal content from the duodenum to the distal colon. Therefore, when the faecal content is pushed down the intestine, the mechanical stress on tissue releases fresh mucus from the goblet cells. This way a distance is always kept between the faeces and the intestine, avoiding direct contact of the epithelium with antigens and bacteria [393] [394].

- *Colonization*

  In conventional mice, the colonic mucus layer is known to be hardly penetrable by bacteria and form a barrier of about 25 μm thick between the epithelium and the luminal content. The firm mucus is notably thinner in GF mice, but increases after colonization, to be similar to the conventional mice. This is consistent with

published observations of reduced mucus production in GF animals and with the concept that metabolites and other components of the microflora are key regulators of colonic mucus secretion [365] [366]. The appearance of both firm and loose mucus in GF mice suggests that the conversion of firm mucus layers into loose mucus does not depend on the presence of bacteria.

- *Immune regulation*

  The intestinal goblet cells are under direct regulation by the immune system. During parasitic helminth infections, goblet cell hyperplasia occurs leading to mucus hypersecretion [395] [396]. These infections elicit a T helper type 2 (Th2) response with increased levels of cytokines such as interleukin IL-4, IL-5, IL-9, and IL-13, where IL-13 is considered the major effector cytokine. Intestinal epithelial cells have been shown to express the IL-4Ra and IL13Ra1 subunits, making it likely that IL-13 acts directly on the epithelium to induce goblet cell hyperplasia via STAT6 (signal transducer and activator of transcription-6) signalling [397]. In addition to the importance of Th2 cytokines in regulation of goblet cell function, recent findings also implicate the Th17-associated cytokine IL-22 in regulation of goblet cell differentiation and mucin expression as IL-22-deficient mice fail to increase *Muc2* expression and have reduced levels of goblet cell hyperplasia in response to *Nippostrongylus brasiliensis* and *Trichuris muris* infections compared with wild-type animals [398]. These effects were observed in the presence of increased levels of IL-4 and IL-13, suggesting overlapping pathways for induction of mucin expression and goblet cell differentiation. Less is understood on the role of Th1 cytokines such as interferon-γ and tumour necrosis factor-α, and Th17 cytokines such as IL-23 and IL-17 in regulation of goblet cell function.

- *SCFA*

  There is now an abundance of evidence to show that short-chain fatty acids (SCFAs) play an important role in the maintenance of health and the development of disease. SCFAs are a subset of fatty acids that are produced by the gut microbiota during the fermentation of partially and non-digestible polysaccharides. In particular butyrate, acetate and propionate, are the most abundant products of carbohydrate fermentation by the microbiota. Butyrate is metabolised as an energy source by epithelial cells and is particularly relevant in diseases such as IBD in which there is a reduction in intestinal Firmicutes, a phylum that includes many anaerobic butyrate producers. In the inflamed gut dysbiosis may therefore indirectly contribute to mucus barrier dysfunction, via the reduction in butyrate production.

  Studies have shown that SCFA can stimulate mucus production in colon. Butyrate, but not lactate or succinate, was shown to stimulate mucus release in the rat colon [399].

8

Furthermore, SCFA can stimulate epithelial MUC2 expression through prostaglandin production by intestinal myofibroblasts [400].

Deficiencies in mucins exacerbate various intestinal diseases such as mucositis but can be remediated via oral supplementation of butyrate, which decreases gut permeability [401]. Consistent with this, supplementation of either butyrate or propionate could induce both *Muc2* mRNA expression and MUC2 secretion in human goblet-like cell line LS174T [372] suggesting that SCFAs might be critical bacterial products promoting gut integrity.

- *Ageing*

  Ageing has marked effects on the intestinal barrier, including mucosal thickening, mucus depletion, increased mucus permeability to commensals. This leads to an altered colonic microbiota and chronic low-grade mucosal inflammation, which has been implicated in the pathology of several chronic disorders (**Chapter 4**). Inflammation induces epithelial stress and the accumulation of unfolded proteins in the ER in secretory cells. ER stress is observed in many diseases, including cancer, diabetes, autoimmune conditions, liver disorders, obesity and neurodegenerative disorders. Protein folding is important to cellular function. Secreted, membrane-bound and organelle-targeted proteins are typically processed and folded in the ER in eukaryotes [402] [347] [403]. Intracellular perturbations caused by various stressors may disturb the specialized environment of the ER leading to the accumulation of unfolded proteins [404] [405]. Cellular adaptation to ER stress is achieved by the activation of the UPR, which is an integrated signal transduction pathway that modulates many aspects of ER physiology. However, when these mechanisms of adaptation are insufficient to handle the unfolded protein load, cells undergo apoptosis. The decline of the mucus barrier in old mice might be due to UPR, which is in turn coupled to inflammation [346]. Single mutations in mouse *Muc2* can cause accumulation in the ER, triggering a UPR response and increased levels of inflammatory cytokines [117] [348]. Higher quantitative demands for MUC2 synthesis, such as an increased bacterial load in contact with the epithelium, which is observed in ageing mice, will further challenge the ER folding system and trigger UPR responses and inflammation.

Future perspectives

The different mice models and the multidisciplinary approach implemented in this thesis research have brought new insight in the dynamics of mucus in health and the effects of natural processes such as ageing on the intestinal barrier. Ideas for future experiments to confirm hypotheses rising directly from the research described in thesis were mentioned above. Below I discuss some of the issues and possible approaches to carry out translational research on the regulation and function of mucus in humans that would build on current knowledge and understanding in the field.

Can mucus properties be assessed in human samples?

The techniques currently used to study mucus or goblet cells are not optimal to perform mechanistic work. The classical techniques of tissue sampling such as tissue resection from euthanized animals are not applicable to human studies for obvious practical and ethical considerations. Moreover it was shown that the faecal content has to be kept in the mouse colon tissue samples during fixation and sectioning otherwise the firm mucus layer is lost during the straining procedure. This is not possible with human tissue as small biopsies are normally collected with endoscopic forceps causing most of the mucus layer to be lost in subsequent procedures (Fig. 5).
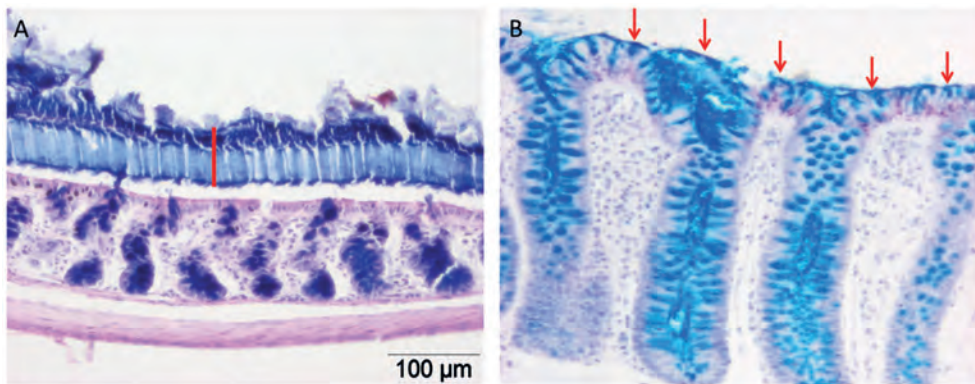
Figure 5: PAS/Alcian blue staining of mice colon (A) and human colonic biopsy (B) fixed in Carnoy. The mucus is stained in blue and tissue in purple. Red arrows show the thin mucus covering the epithelium. The red bar shows the mucus thickness in mice colon (unpublished Sovran *et al.*). Human biopsies kindly gifted by Dr. Johansson (Gothenburg University, Sweden).

A combination of *in-vitro* and *ex-vivo* work might help to get insights in mucus dynamics and goblet cells functions. The organoid culture system, which contain all the functional cells of the gut (stem cells, Paneth cells, enterocytes, and goblet cells) may be the best model for such experiments [129]. Organoids generated from isolated crypts or stem cells replicate and differentiate into a "mini human gut" containing all the cell types present

8

in the epithelium *in vivo*. It is also possible to preferentially differentiate the organoids into a specific cell type including goblet cells using differentiation factors added to the culture medium. Furthermore, it is now possible to dissociate organoids and generate confluent monolayers of polarised untransformed epithelial cells [130]. The latter models could be used to study the effects of different ER stress inducers on mucus secretion as well as its properties and permeability. The impact of host mutations associated with IBD could also be investigated in these models by generating organoids from individual patients with these respective mutations. Potential therapeutic strategies could also be tested in such models to provide insights in their mechanistic effects on the human intestine and goblet cells.

The human organoid tissue system as a model for future mechanistic work on goblet cells

The organoid culture system might help verifying the effects of different substances (e.g. cytokines, SCFAs etc.) or processes (oxidative stress) influencing the goblet cells and their mucus. For example, treatment of the organoids with SCFAs could help to verify the influence of butyrate on the goblet cells, and understand by which mechanisms they stimulate secretion of mucus. In this thesis, we highlighted a role for IL-22-STAT3 pathway in maintaining ileal homeostasis when the mucus barrier is compromised. Treatment of organoid cultures with IL-22 (or an agonist/antagonist of IL-22) might give insights in the effects of this cytokine on the goblet cell function, and therefore verify the role of IL-22 in the intestinal homeostasis.

Mechanisms of membrane-bound mucins in intracellular signalling

The epithelial glycocalyx comprises several non-secreted transmembrane mucins including MUC1, MUC3, MUC4, MUC13, and MUC17. The membrane-associated mucins are normally shed and replaced, but this process can be accelerated upon bacterial adhesion, helping to protect the epithelium from microbial invasion. Apart from their barrier function against potential pathogens, specific membrane-tethered mucins have also been shown to modulate responses to inflammatory cytokines [74]. However, the mechanisms of signalling are still unknown.

The organoid culture system might help understanding the mechanisms of membrane-bound mucins signalling. Mouse organoids made from mucin-deficient mice e.g. $Muc1^{-/-}$ and $Muc2^{-/-}$ mice models, could be used to understand better the signalling of membrane-bound mucin in the context of a deficiency in MUC2, or understand the role of MUC1 in the signalling. Other models could be created with other mucin-deficient mouse lines.

Concluding remarks

The use of a multi-disciplinary approach including the use of different mouse models, trancriptomics, microbiota profiling and histology gave insights in the important role played by the mucus in the maintenance of the intestinal barrier in health. This approach appears to have been very successful in delivering an important resource that complements previous studies on mucus barrier function in health and disease. The positive correlations identified in this thesis between the multi-variate datasets, including the linkages identified between microbial groups and specific host function in all mice models, support the prominent role of the microbiota in the modulation of the host's physiology, in the context of a compromised mucus barrier. This effect seems to be enhanced in the large intestine, where a thick mucus layer is necessary to maintain intestinal homeostasis. In the small intestine, other factors can help maintaining the homeostasis even in models of colitis development, via IL-22 and the regulation of secreted antimicrobial factors.

In conclusion, the work described in this thesis demonstrates the role of the mucus in both small and large intestine in maintaining gut homeostasis. The research on probiotic interventions to restore mucus secretion in ageing mice opens up new possibilities to enhance barrier function and unravel the underlying mechanisms. Ultimately this might lead to new strategies to maintain intestinal health.

8

References

1. Atuma C, Strugala V, Allen A, Holm L. The adherent gastrointestinal mucus gel layer: thickness and physical state in vivo. American journal of physiology Gastrointestinal and liver physiology 2001; 280(5): G922-929.
2. Artis D. Epithelial-cell recognition of commensal bacteria and maintenance of immune homeostasis in the gut. Nature reviews Immunology 2008; 8(6): 411-420.
3. Eckburg PB, Bik EM, Bernstein CN, Purdom E, Dethlefsen L, Sargent M *et al.* Diversity of the human intestinal microbial flora. Science 2005; 308(5728): 1635-1638.
4. Backhed F, Ley RE, Sonnenburg JL, Peterson DA, Gordon JI. Host-bacterial mutualism in the human intestine. Science 2005; 307(5717): 1915-1920.
5. Tap J, Mondot S, Levenez F, Pelletier E, Caron C, Furet JP *et al.* Towards the human intestinal microbiota phylogenetic core. Environmental microbiology 2009; 11(10): 2574-2584.
6. Qin JJ, Li RQ, Raes J, Arumugam M, Burgdorf KS, Manichanh C *et al.* A human gut microbial gene catalogue established by metagenomic sequencing. Nature 2010; 464(7285): 59-U70.
7. Derrien M, Vaughan EE, Plugge CM, de Vos WM. Akkermansia muciniphila gen. nov., sp nov., a human intestinal mucin-degrading bacterium. International Journal of Systematic and Evolutionary Microbiology 2004; 54: 1469-1476.
8. Belkaid Y, Hand TW. Role of the microbiota in immunity and inflammation. Cell 2014; 157(1): 121-141.
9. Wu HJ, Wu E. The role of gut microbiota in immune homeostasis and autoimmunity. Gut microbes 2012; 3(1): 4-14.
10. Hooper LV, Macpherson AJ. Immune adaptations that maintain homeostasis with the intestinal microbiota. Nature reviews Immunology 2010; 10(3): 159-169.
11. Ayabe T, Satchell DP, Wilson CL, Parks WC, Selsted ME, Ouellette AJ. Secretion of microbicidal [alpha]-defensins by intestinal Paneth cells in response to bacteria. Nature immunology 2000; 1(2): 113-118.
12. Dann SM, Eckmann L. Innate immune defenses in the intestinal tract. Current opinion in gastroenterology 2007; 23(2): 115-120.
13. Ouellette AJ, Bevins CL. Paneth cell defensins and innate immunity of the small bowel. Inflammatory bowel diseases 2001; 7(1): 43-50.
14. Ganz T. Defensins: antimicrobial peptides of innate immunity. Nature reviews Immunology 2003; 3(9): 710-720.
15. Salzman NH, Underwood MA, Bevins CL. Paneth cells, defensins, and the commensal microbiota: A hypothesis on intimate interplay at the intestinal mucosa. Seminars in immunology 2007; 19(2): 70-83.
16. Selsted ME, Ouellette AJ. Mammalian defensins in the antimicrobial immune response. Nature immunology 2005; 6(6): 551-557.
17. Harder J, Bartels J, Christophers E, Schroder JM. Isolation and characterization of human beta-defensin-3, a novel human inducible peptide antibiotic. The Journal of biological chemistry 2001; 276(8): 5707-5713.
18. Liu AY, Destoumieux D, Wong AV, Park CH, Valore EV, Liu L *et al.* Human beta-defensin-2 production in keratinocytes is regulated by interleukin-1, bacteria, and the state of differentiation. J Invest Dermatol 2002; 118(2): 275-281.
19. Jia HP, Schutte BC, Schudy A, Linzmeier R, Guthmiller JM, Johnson GK *et al.* Discovery of new human beta-defensins using a genomics-based approach. Gene 2001; 263(1-2): 211-218.
20. Garcia JR, Krause A, Schulz S, Rodriguez-Jimenez FJ, Kluver E, Adermann K *et al.* Human beta-defensin 4: a novel inducible peptide with a specific salt-sensitive spectrum of antimicrobial activity. FASEB journal : official publication of the Federation of American Societies for Experimental Biology 2001; 15(10): 1819-1821.
21. Sorensen OE, Thapa DR, Rosenthal A, Liu L, Roberts AA, Ganz T. Differential regulation of beta-defensin expression in human skin by microbial stimuli. Journal of immunology 2005; 174(8): 4870-4879.
22. Vaishnava S, Yamamoto M, Severson KM, Ruhn KA, Yu X, Koren O *et al.* The antibacterial lectin RegIIIgamma promotes the spatial segregation of microbiota and host in the intestine. Science 2011; 334(6053): 255-258.
23. Vora P, Youdim A, Thomas LS, Fukata M, Tesfay SY, Lukasek K *et al.* Beta-defensin-2 expression is regulated by TLR signaling in intestinal epithelial cells. Journal of immunology 2004; 173(9): 5398-5405.

24. Lasserre C, Christa L, Simon MT, Vernier P, Brechot C. A Novel Gene (Hip) Activated in Human Primary Liver-Cancer. Cancer research 1992; 52(18): 5089-5095.

25. Lasserre C, Simon MT, Ishikawa H, Diriong S, Nguyen VC, Christa L *et al.* Structural Organization and Chromosomal Localization of a Human Gene (Hip/Pap) Encoding a C-Type Lectin Overexpressed in Primary Liver-Cancer. European Journal of Biochemistry 1994; 224(1): 29-38.

26. Cash HL, Whitham CV, Behrendt CL, Hooper LV. Symbiotic Bacteria Direct Expression of an Intestinal Bactericidal Lectin. Science 2006; 313(5790): 1126-1130.

27. Cash HL, Whitham CV, Hooper LV. Refolding, purification, and characterization of human and murine RegIII proteins expressed in Escherichia coli. Protein Expression and Purification 2006; 48(1): 151-159.

28. Mestecky J, Russell MW. Specific antibody activity, glycan heterogeneity and polyreactivity contribute to the protective activity of S-IgA at mucosal surfaces. Immunology Letters 2009; 124(2): 57-62.

29. Macpherson AJ, Gatto D, Sainsbury E, Harriman GR, Hengartner H, Zinkernagel RM. A primitive T cell-independent mechanism of intestinal mucosal IgA responses to commensal bacteria. Science 2000; 288(5474): 2222-+.

30. Mazanec MB, Kaetzel CS, Lamm ME, Fletcher D, Nedrud JG. Intracellular Neutralization of Virus by Immunoglobulin-a Antibodies. Proceedings of the National Academy of Sciences of the United States of America 1992; 89(15): 6901-6905.

31. Mowat AM. Anatomical basis of tolerance and immunity to intestinal antigens. Nature reviews Immunology 2003; 3(4): 331-341.

32. Rescigno M, Rotta G, Valzasina B, Ricciardi-Castagnoli P. Dendritic cells shuttle microbes across gut epithelial monolayers. Immunobiology 2001; 204(5): 572-581.

33. Wells JM, Rossi O, Meijerink M, van Baarlen P. Epithelial crosstalk at the microbiota-mucosal interface. Proceedings of the National Academy of Sciences of the United States of America 2011; 108: 4607-4614.

34. Frank DN, Amand ALS, Feldman RA, Boedeker EC, Harpaz N, Pace NR. Molecular-phylogenetic characterization of microbial community imbalances in human inflammatory bowel diseases. Proceedings of the National Academy of Sciences of the United States of America 2007; 104(34): 13780-13785.

35. Ott SJ, Musfeldt M, Wenderoth DF, Hampe J, Brant O, Folsch UR *et al.* Reduction in diversity of the colonic mucosa associated bacterial microflora in patients with active inflammatory bowel disease. Gut 2004; 53(5): 685-693.

36. Rooks MG, Veiga P, Wardwell-Scott LH, Tickle T, Segata N, Michaud M *et al.* Gut microbiome composition and function in experimental colitis during active disease and treatment-induced remission. The ISME journal 2014; 8(7): 1403-1417.

37. Joossens M, Huys G, Cnockaert M, De Preter V, Verbeke K, Rutgeerts P *et al.* Dysbiosis of the faecal microbiota in patients with Crohn's disease and their unaffected relatives. Gut 2011; 60(5): 631-637.

38. Sokol H, Pigneur B, Watterlot L, Lakhdari O, Bermúdez-Humarán LG, Gratadoux J-J *et al.* Faecalibacterium prausnitzii is an anti-inflammatory commensal bacterium identified by gut microbiota analysis of Crohn disease patients. Proceedings of the National Academy of Sciences 2008; 105(43): 16731-16736.

39. Sokol H, Seksik P, Furet JP, Firmesse O, Nion-Larmurier I, Beaugerie L *et al.* Low counts of Faecalibacterium prausnitzii in colitis microbiota. Inflammatory bowel diseases 2009; 15(8): 1183-1189.

40. Fleckenstein JM, Hardwidge PR, Munson GP, Rasko DA, Sommerfelt H, Steinsland H. Molecular mechanisms of enterotoxigenic Escherichia coli infection. Microbes and infection / Institut Pasteur 2010; 12(2): 89-98.

41. Buffie CG, Pamer EG. Microbiota-mediated colonization resistance against intestinal pathogens. Nature reviews Immunology 2013; 13(11): 790-801.

42. Winter SE, Winter MG, Xavier MN, Thiennimitr P, Poon V, Keestra AM *et al.* Host-derived nitrate boosts growth of E. coli in the inflamed gut. Science 2013; 339(6120): 708-711.

43. Chassaing B, Darfeuille-Michaud A. The Commensal Microbiota and Enteropathogens in the Pathogenesis of Inflammatory Bowel Diseases. Gastroenterology 2011; 140(6): 1720-U1740.

44. Scaldaferri F, Pizzoferrato M, Gerardi V, Lopetuso L, Gasbarrini A. The gut barrier: new acquisitions and therapeutic approaches. Journal of clinical gastroenterology 2012; 46 Suppl: S12-17.

45. Camilleri M, Nadeau A, Lamsam J, Nord SL, Ryks M, Burton D *et al.* Understanding measurements of intestinal permeability in healthy humans with urine lactulose and mannitol excretion. Neurogastroenterology and motility : the official journal of the European Gastrointestinal Motility Society 2010; 22(1): e15-26.

46. Camilleri M, Madsen K, Spiller R, Greenwood-Van Meerveld B, Verne GN. Intestinal barrier function in health and gastrointestinal disease. Neurogastroenterology and motility : the official journal of the European Gastrointestinal Motility Society 2012; 24(6): 503-512.

47. Zuckerman MJ, Watts MT, Bhatt BD, Ho H. Intestinal permeability to [51Cr]EDTA in infectious diarrhea. Digestive diseases and sciences 1993; 38(9): 1651-1657.

48. Spiller RC, Jenkins D, Thornley JP, Hebden JM, Wright T, Skinner M *et al.* Increased rectal mucosal enteroendocrine cells, T lymphocytes, and increased gut permeability following acute Campylobacter enteritis and in post-dysenteric irritable bowel syndrome. Gut 2000; 47(6): 804-811.

49. Marshall JK, Thabane M, Garg AX, Clark W, Meddings J, Collins SM *et al.* Intestinal permeability in patients with irritable bowel syndrome after a waterborne outbreak of acute gastroenteritis in Walkerton, Ontario. Alimentary pharmacology & therapeutics 2004; 20(11-12): 1317-1322.

50. Piche T, Barbara G, Aubert P, Bruley des Varannes S, Dainese R, Nano JL *et al.* Impaired intestinal barrier integrity in the colon of patients with irritable bowel syndrome: involvement of soluble mediators. Gut 2009; 58(2): 196-201.

51. Bertiaux-Vandaele N, Youmba SB, Belmonte L, Lecleire S, Antonietti M, Gourcerol G *et al.* The expression and the cellular distribution of the tight junction proteins are altered in irritable bowel syndrome patients with differences according to the disease subtype. The American journal of gastroenterology 2011; 106(12): 2165-2173.

52. Wilcz-Villega E, McClean S, O'Sullivan M. Reduced E-cadherin expression is associated with abdominal pain and symptom duration in a study of alternating and diarrhea predominant IBS. Neurogastroenterology and motility : the official journal of the European Gastrointestinal Motility Society 2014; 26(3): 316-325.

53. Madara JL, Trier JS. Structural abnormalities of jejunal epithelial cell membranes in celiac sprue. Laboratory investigation; a journal of technical methods and pathology 1980; 43(3): 254-261.

54. Schulzke JD, Bentzel CJ, Schulzke I, Riecken EO, Fromm M. Epithelial tight junction structure in the jejunum of children with acute and treated celiac sprue. Pediatric research 1998; 43(4 Pt 1): 435-441.

55. Clemente MG, De Virgiliis S, Kang JS, Macatagney R, Musu MP, Di Pierro MR *et al.* Early effects of gliadin on enterocyte intracellular signalling involved in intestinal barrier function. Gut 2003; 52(2): 218-223.

56. Nikulina M, Habich C, Flohe SB, Scott FW, Kolb H. Wheat gluten causes dendritic cell maturation and chemokine secretion. Journal of immunology 2004; 173(3): 1925-1933.

57. Tytgat KM, Buller HA, Opdam FJ, Kim YS, Einerhand AW, Dekker J. Biosynthesis of human colonic mucin: Muc2 is the prominent secretory mucin. Gastroenterology 1994; 107(5): 1352-1363.

58. van Klinken BJ, Einerhand AW, Buller HA, Dekker J. The oligomerization of a family of four genetically clustered human gastrointestinal mucins. Glycobiology 1998; 8(1): 67-75.

59. Jensen PH, Kolarich D, Packer NH. Mucin-type O-glycosylation – putting the pieces together. FEBS Journal 2010; 277(1): 81-94.

60. Larsson JMH, Karlsson H, Sjovall H, Hansson GC. A complex, but uniform O-glycosylation of the human MUC2 mucin from colonic biopsies analyzed by nanoLC/MSn. Glycobiology 2009; 19(7): 756-766.

61. Johansson MEV, Ambort D, Pelaseyed T, Schutte A, Gustafsson JK, Ermund A *et al.* Composition and functional role of the mucus layers in the intestine. Cellular and Molecular Life Sciences 2011; 68(22): 3635-3641.

62. Bennett EP, Mandel U, Clausen H, Gerken TA, Fritz TA, Tabak LA. Control of mucin-type O-glycosylation: A classification of the polypeptide GalNAc-transferase gene family. Glycobiology 2012; 22(6): 736-756.

63. Dekker J, Rossen JWA, Büller HA, Einerhand AWC. The MUC family: an obituary. Trends in biochemical sciences 2002; 27(3): 126-131.

64. Johansson ME, Larsson JM, Hansson GC. The two mucus layers of colon are organized by the MUC2 mucin, whereas the outer layer is a legislator of host-microbial interactions. Proceedings of the National Academy of Sciences of the United States of America 2011; 108 Suppl 1: 4659-4665.

65. Strugala V, Allen A, Dettmar PW, Pearson JP. Colonic mucin: methods of measuring mucus thickness. The Proceedings of the Nutrition Society 2003; 62(1): 237-243.

66. Johansson ME, Phillipson M, Petersson J, Velcich A, Holm L, Hansson GC. The inner of the two Muc2 mucin-dependent mucus layers in colon is devoid of bacteria. Proceedings of the National Academy of Sciences of the United States of America 2008; 105(39): 15064-15069.

67. Johansson MEV, Sjovall H, Hansson GC. The gastrointestinal mucus system in health and disease. Nat Rev Gastroenterol Hepatol 2013; advance online publication.

68. Duerkop BA, Vaishnava S, Hooper LV. Immune Responses to the Microbiota at the Intestinal Mucosal Surface. Immunity 2009; 31(3): 368-376.

69. Flo TH, Smith KD, Sato S, Rodriguez DJ, Holmes MA, Strong RK *et al.* Lipocalin 2 mediates an innate immune response to bacterial infection by sequestrating iron. Nature 2004; 432(7019): 917-921.

70. Loonen LM, Stolte EH, Jaklofsky MT, Meijerink M, Dekker J, van Baarlen P *et al.* REG3[gamma]-deficient mice have altered mucus distribution and increased mucosal inflammatory responses to the microbiota and enteric pathogens in the ileum. 2014; 7(4): 939-947.

71. van Ampting MT, Loonen LM, Schonewille AJ, Konings I, Vink C, Iovanna J *et al.* Intestinally secreted C-type lectin Reg3b attenuates salmonellosis but not listeriosis in mice. Infection and immunity 2012; 80(3): 1115-1120.

72. Dessein R, Gironella M, Vignal C, Peyrin-Biroulet L, Sokol H, Secher T *et al.* Toll-like receptor 2 is critical for induction of Reg3 beta expression and intestinal clearance of Yersinia pseudotuberculosis. Gut 2009; 58(6): 771-776.

73. Hattrup CL, Gendler SJ. Structure and function of the cell surface (tethered) mucins. Annual review of physiology 2008; 70: 431-457.

74. McGuckin MA, Linden SK, Sutton P, Florin TH. Mucin dynamics and enteric pathogens. Nature reviews Microbiology 2011; 9(4): 265-278.

75. Linden SK, Sutton P, Karlsson NG, Korolik V, McGuckin MA. Mucins in the mucosal barrier to infection. Mucosal Immunol 2008; 1(3): 183-197.

76. Van Klinken BJ, Dekker J, Buller HA, Einerhand AW. Mucin gene structure and expression: protection vs. adhesion. The American journal of physiology 1995; 269(5 Pt 1): G613-627.

77. Ermund A, Schutte A, Johansson ME, Gustafsson JK, Hansson GC. Studies of mucus in mouse stomach, small intestine, and colon. I. Gastrointestinal mucus layers have different properties depending on location as well as over the Peyer's patches. American journal of physiology Gastrointestinal and liver physiology 2013; 305(5): G341-347.

78. Johansson ME. Mucus layers in inflammatory bowel disease. Inflammatory bowel diseases 2014; 20(11): 2124-2131.

79. Neutra MR, Mantis NJ, Kraehenbuhl JP. Collaboration of epithelial cells with organized mucosal lymphoid tissues. Nature immunology 2001; 2(11): 1004-1009.

80. Kelsall BL, Strober W. Distinct populations of dendritic cells are present in the subepithelial dome and T cell regions of the murine Peyer's patch. The Journal of experimental medicine 1996; 183(1): 237-247.

81. Neutra MR, Pringault E, Kraehenbuhl JP. Antigen sampling across epithelial barriers and induction of mucosal immune responses. Annual review of immunology 1996; 14: 275-300.

82. Owen RL. Uptake and transport of intestinal macromolecules and microorganisms by M cells in Peyer's patches--a personal and historical perspective. Seminars in immunology 1999; 11(3): 157-163.

83. Tyrer PC, Ruth Foxwell A, Kyd JM, Otczyk DC, Cripps AW. Receptor mediated targeting of M-cells. Vaccine 2007; 25(16): 3204-3209.

84. Gebert A. The role of M cells in the protection of mucosal membranes. Histochemistry and cell biology 1997; 108(6): 455-470.

85. Keita AV, Gullberg E, Ericson AC, Salim SY, Wallon C, Kald A *et al.* Characterization of antigen and bacterial transport in the follicle-associated epithelium of human ileum. Laboratory investigation; a journal of technical methods and pathology 2006; 86(5): 504-516.

86. Khan J, Iiboshi Y, Cui L, Wasa M, Okada A. Role of intestinal mucus on the uptake of latex beads by Peyer's patches and on their transport to mesenteric lymph nodes in rats. JPEN Journal of parenteral and enteral nutrition 1999; 23(1): 19-23.

87. Onori P, Franchitto A, Sferra R, Vetuschi A, Gaudio E. Peyer's patches epithelium in the rat: a morphological, immunohistochemical, and morphometrical study. Digestive diseases and sciences 2001; 46(5): 1095-1104.

88. Sansonetti PJ, Phalipon A. M cells as ports of entry for enteroinvasive pathogens: mechanisms of interaction, consequences for the disease process. Seminars in immunology 1999; 11(3): 193-203.

89. Ermund A, Gustafsson JK, Hansson GC, Keita AV. Mucus properties and goblet cell quantification in mouse, rat and human ileal Peyer's patches. PloS one 2013; 8(12): e83688.

90. Swidsinski A, Sydora BC, Doerffel Y, Loening-Baucke V, Vaneechoutte M, Lupicki M et al. Viscosity gradient within the mucus layer determines the mucosal barrier function and the spatial organization of the intestinal microbiota. Inflammatory bowel diseases 2007; 13(8): 963-970.

91. van der Waaij LA, Harmsen HJ, Madjipour M, Kroese FG, Zwiers M, van Dullemen HM et al. Bacterial population analysis of human colon and terminal ileum biopsies with 16S rRNA-based fluorescent probes: commensal bacteria live in suspension and have no direct contact with epithelial cells. Inflammatory bowel diseases 2005; 11(10): 865-871.

92. Shan M, Gentile M, Yeiser JR, Walland AC, Bornstein VU, Chen K et al. Mucus enhances gut homeostasis and oral tolerance by delivering immunoregulatory signals. Science 2013; 342(6157): 447-453.

93. Hilkens J, Ligtenberg MJ, Vos HL, Litvinov SV. Cell membrane-associated mucins and their adhesion-modulating property. Trends in biochemical sciences 1992; 17(9): 359-363.

94. Pandey P, Kharbanda S, Kufe D. Association of the DF3/MUC1 breast cancer antigen with Grb2 and the Sos/Ras exchange protein. Cancer research 1995; 55(18): 4000-4003.

95. Li Q, Ren J, Kufe D. Interaction of human MUC1 and beta-catenin is regulated by Lck and ZAP-70 in activated Jurkat T cells. Biochemical and biophysical research communications 2004; 315(2): 471-476.

96. Regimbald LH, Pilarski LM, Longenecker BM, Reddish MA, Zimmermann G, Hugh JC. The breast mucin MUCI as a novel adhesion ligand for endothelial intercellular adhesion molecule 1 in breast cancer. Cancer research 1996; 56(18): 4244-4249.

97. Komatsu M, Carraway CA, Fregien NL, Carraway KL. Reversible disruption of cell-matrix and cell-cell interactions by overexpression of sialomucin complex. The Journal of biological chemistry 1997; 272(52): 33245-33254.

98. Lillehoj EP, Kim H, Chun EY, Kim KC. Pseudomonas aeruginosa stimulates phosphorylation of the airway epithelial membrane glycoprotein Muc1 and activates MAP kinase. American journal of physiology Lung cellular and molecular physiology 2004; 287(4): L809-815.

99. Baumgart DC, Carding SR. Inflammatory bowel disease: cause and immunobiology. Lancet 2007; 369(9573): 1627-1640.

100. Dvorak AM, Osage JE, Monahan RA, Dickersin GR. Crohn's disease: transmission electron microscopic studies. III. Target tissues. Proliferation of and injury to smooth muscle and the autonomic nervous system. Human pathology 1980; 11(6): 620-634.

101. Trabucchi E, Mukenge S, Baratti C, Colombo R, Fregoni F, Montorsi W. Differential diagnosis of Crohn's disease of the colon from ulcerative colitis: ultrastructure study with the scanning electron microscope. International journal of tissue reactions 1986; 8(1): 79-84.

102. Tytgat KMAJ, vanderWal JWG, Einerhand AWC, Buller HA, Dekker J. Quantitative analysis of MUC2 synthesis in ulcerative colitis. Biochemical and biophysical research communications 1996; 224(2): 397-405.

103. Van Klinken BJ, Van der Wal JW, Einerhand AW, Buller HA, Dekker J. Sulphation and secretion of the predominant secretory human colonic mucin MUC2 in ulcerative colitis. Gut 1999; 44(3): 387-393.

104. Hanski C, Born M, Foss HD, Marowski B, Mansmann U, Arasteh K et al. Defective post-transcriptional processing of MUC2 mucin in ulcerative colitis and in Crohn's disease increases detectability of the MUC2 protein core. The Journal of pathology 1999; 188(3): 304-311.

105. Jass JR, Walsh MD. Altered mucin expression in the gastrointestinal tract: a review. Journal of cellular and molecular medicine 2001; 5(3): 327-351.

106. Dawson PA, Huxley S, Gardiner B, Tran T, McAuley JL, Grimmond S et al. Reduced mucin sulfonation and impaired intestinal barrier function in the hyposulfataemic NaS1 null mouse. Gut 2009; 58(7): 910-919.

107. An G, Wei B, Xia B, McDaniel JM, Ju T, Cummings RD *et al.* Increased susceptibility to colitis and colorectal tumors in mice lacking core 3-derived O-glycans. The Journal of experimental medicine 2007; 204(6): 1417-1429.

108. Stone EL, Ismail MN, Lee SH, Luu Y, Ramirez K, Haslam SM *et al.* Glycosyltransferase function in core 2-type protein O glycosylation. Molecular and cellular biology 2009; 29(13): 3770-3782.

109. Swidsinski A, Loening-Baucke V, Theissig F, Engelhardt H, Bengmark S, Koch S *et al.* Comparative study of the intestinal mucus barrier in normal and inflamed colon. Gut 2007; 56(3): 343-350.

110. Johansson MEV, Hansson GC. The goblet cell: a key player in ischaemia-reperfusion injury. Gut 2013; 62(2): 188-189.

111. Bergström JH, Berg KA, Rodríguez-Piñeiro AM, Stecher B, Johansson MEV, Hansson GC. AGR2, an Endoplasmic Reticulum Protein, Is Secreted into the Gastrointestinal Mucus. PloS one 2014; 9(8): e104186.

112. Abraham C, Cho JH. MECHANISMS OF DISEASE Inflammatory Bowel Disease. New England Journal of Medicine 2009; 361(21): 2066-2078.

113. Boltin D, Perets TT, Vilkin A, Niv Y. Mucin Function in Inflammatory Bowel Disease An Update. Journal of clinical gastroenterology 2013; 47(2): 106-111.

114. Fu J, Wei B, Wen T, Johansson ME, Liu X, Bradford E *et al.* Loss of intestinal core 1-derived O-glycans causes spontaneous colitis in mice. J Clin Invest 2011; 121(4): 1657-1666.

115. Bergstrom KS, Xia L. Mucin-type O-glycans and their roles in intestinal homeostasis. Glycobiology 2013; 23(9): 1026-1037.

116. Sommer F, Adam N, Johansson ME, Xia L, Hansson GC, Backhed F. Altered mucus glycosylation in core 1 O-glycan-deficient mice affects microbiota composition and intestinal architecture. PloS one 2014; 9(1): e85254.

117. Heazlewood CK, Cook MC, Eri R, Price GR, Tauro SB, Taupin D *et al.* Aberrant mucin assembly in mice causes endoplasmic reticulum stress and spontaneous inflammation resembling ulcerative colitis. PLoS medicine 2008; 5(3): e54.

118. Velcich A, Yang W, Heyer J, Fragale A, Nicholas C, Viani S *et al.* Colorectal Cancer in Mice Genetically Deficient in the Mucin Muc2. Science 2002; 295(5560): 1726-1729.

119. van Klinken BJ, Einerhand AW, Duits LA, Makkink MK, Tytgat KM, Renes IB *et al.* Gastrointestinal expression and partial cDNA cloning of murine Muc2. The American journal of physiology 1999; 276(1 Pt 1): G115-124.

120. Kim YS, Gum JR, Jr. Diversity of mucin genes, structure, function, and expression. Gastroenterology 1995; 109(3): 999-1001.

121. Van der Sluis M, De Koning BA, De Bruijn AC, Velcich A, Meijerink JP, Van Goudoever JB *et al.* Muc2-deficient mice spontaneously develop colitis, indicating that MUC2 is critical for colonic protection. Gastroenterology 2006; 131(1): 117-129.

122. Lu P, Burger-van Paassen N, van der Sluis M, Witte-Bouma J, Kerckaert JP, van Goudoever JB *et al.* Colonic Gene Expression Patterns of Mucin Muc2 Knockout Mice Reveal Various Phases in Colitis Development. Inflammatory bowel diseases 2011; 17(10): 2047-2057.

123. Johansson ME, Hansson GC. Preservation of mucus in histological sections, immunostaining of mucins in fixed tissue, and localization of bacteria with FISH. Methods in molecular biology 2012; 842: 229-235.

124. Navabi N, McGuckin MA, Linden SK. Gastrointestinal cell lines form polarized epithelia with an adherent mucus layer when cultured in semi-wet interfaces with mechanical stimulation. PloS one 2013; 8(7): e68761.

125. Van den Brink GR, Tytgat KM, Van der Hulst RW, Van der Loos CM, Einerhand AW, Buller HA *et al.* H pylori colocalises with MUC5AC in the human stomach. Gut 2000; 46(5): 601-607.

126. Evans GS, Flint N, Somers AS, Eyden B, Potten CS. The development of a method for the preparation of rat intestinal epithelial cell primary cultures. Journal of cell science 1992; 101 (Pt 1): 219-231.

127. Whitehead RH, Demmler K, Rockman SP, Watson NK. Clonogenic growth of epithelial cells from normal colonic mucosa from both mice and humans. Gastroenterology 1999; 117(4): 858-865.

128. Ootani A, Li X, Sangiorgi E, Ho QT, Ueno H, Toda S *et al.* Sustained in vitro intestinal epithelial culture within a Wnt-dependent stem cell niche. Nat Med 2009; 15(6): 701-706.

129. Sato T, Vries RG, Snippert HJ, van de Wetering M, Barker N, Stange DE *et al.* Single Lgr5 stem cells build crypt-villus structures in vitro without a mesenchymal niche. Nature 2009; 459(7244): 262-265.

130. Moon C, VanDussen KL, Miyoshi H, Stappenbeck TS. Development of a primary mouse intestinal epithelial cell monolayer culture system to evaluate factors that modulate IgA transcytosis. Mucosal Immunol 2014; 7(4): 818-828.

131. Holm L, Phillipson M. Assessment of mucus thickness and production in situ. Methods in molecular biology 2012; 842: 217-227.

132. Gustafsson JK, Ermund A, Johansson ME, Schutte A, Hansson GC, Sjovall H. An ex vivo method for studying mucus formation, properties, and thickness in human colonic biopsies and mouse small and large intestinal explants. American journal of physiology Gastrointestinal and liver physiology 2012; 302(4): G430-438.

133. Imahori K. How I understand aging. Nutrition Review 1992; 50(12): 351-352.

134. Ershler WB. Biological interactions of aging and anemia: a focus on cytokines. Journal of the American Geriatrics Society 2003; 51(3 Suppl): S18-21.

135. Gardner ID. The effect of aging on susceptibility to infection. Reviews of infectious diseases 1980; 2(5): 801-810.

136. Hoogendam YY, Hofman A, van der Geest JN, van der Lugt A, Ikram MA. Patterns of cognitive function in aging: the Rotterdam Study. European journal of epidemiology 2014; 29(2): 133-140.

137. Samaras K, Lutgers HL, Kochan NA, Crawford JD, Campbell LV, Wen W *et al.* The impact of glucose disorders on cognition and brain volumes in the elderly: the Sydney Memory and Ageing Study. Age 2014; 36(2): 977-993.

138. Pollack M, Phaneuf S, Dirks A, Leeuwenburgh C. The role of apoptosis in the normal aging brain, skeletal muscle, and heart. Annals of the New York Academy of Sciences 2002; 959: 93-107.

139. Hayflick L, Moorhead PS. The serial cultivation of human diploid cell strains. Experimental cell research 1961; 25: 585-621.

140. Campisi J. Cancer and ageing: rival demons? Nature reviews Cancer 2003; 3(5): 339-349.

141. Campisi J, d'Adda di Fagagna F. Cellular senescence: when bad things happen to good cells. Nat Rev Mol Cell Biol 2007; 8(9): 729-740.

142. Hall KE, Proctor DD, Fisher L, Rose S. American gastroenterological association future trends committee report: effects of aging of the population on gastroenterology practice, education, and research. Gastroenterology 2005; 129(4): 1305-1338.

143. O'Mahony D, O'Leary P, Quigley EM. Aging and intestinal motility: a review of factors that affect intestinal motility in the aged. Drugs & aging 2002; 19(7): 515-527.

144. Phillips RJ, Powley TL. Innervation of the gastrointestinal tract: patterns of aging. Autonomic neuroscience : basic & clinical 2007; 136(1-2): 1-19.

145. Hollander D, Tarnawski H. Aging-associated increase in intestinal absorption of macromolecules. Gerontology 1985; 31(3): 133-137.

146. Annaert P, Brouwers J, Bijnens A, Lammert F, Tack J, Augustijns P. Ex vivo permeability experiments in excised rat intestinal tissue and in vitro solubility measurements in aspirated human intestinal fluids support age-dependent oral drug absorption. European journal of pharmaceutical sciences : official journal of the European Federation for Pharmaceutical Sciences 2010; 39(1-3): 15-22.

147. Mullin JM, Valenzano MC, Verrecchio JJ, Kothari R. Age- and diet-related increase in transepithelial colon permeability of Fischer 344 rats. Digestive diseases and sciences 2002; 47(10): 2262-2270.

148. Kleessen B, Sykura B, Zunft HJ, Blaut M. Effects of inulin and lactose on fecal microflora, microbial activity, and bowel habit in elderly constipated persons. The American journal of clinical nutrition 1997; 65(5): 1397-1402.

149. Fujihashi K, Kiyono H. Mucosal immunosenescence: new developments and vaccines to control infectious diseases. Trends in immunology 2009; 30(7): 334-343.

150. Appay V, Sauce D. Naive T cells: the crux of cellular immune aging? Experimental gerontology 2014; 54: 90-93.

151. McElhaney JE, Meneilly GS, Beattie BL, Helgason CD, Lee SF, Devine RD *et al.* The effect of influenza vaccination on IL2 production in healthy elderly: implications for current vaccination practices. Journal of gerontology 1992; 47(1): M3-8.

152. Saltzman RL, Peterson PK. Immunodeficiency of the elderly. Reviews of infectious diseases 1987; 9(6): 1127-1139.

153. Asanuma H, Zamri NB, Sekine S, Fukuyama Y, Tokuhara D, Gilbert RS *et al.* A novel combined adjuvant for nasal delivery elicits mucosal immunity to influenza in aging. Vaccine 2012; 30(4): 803-812.

154. Tesar BM, Walker WE, Unternaehrer J, Joshi NS, Chandele A, Haynes L *et al.* Murine [corrected] myeloid dendritic cell-dependent toll-like receptor immunity is preserved with aging. Aging cell 2006; 5(6): 473-486.

155. Agrawal A, Agrawal S, Cao JN, Su H, Osann K, Gupta S. Altered innate immune functioning of dendritic cells in elderly humans: a role of phosphoinositide 3-kinase-signaling pathway. Journal of immunology 2007; 178(11): 6912-6922.

156. Franceschi C, Capri M, Monti D, Giunta S, Olivieri F, Sevini F *et al.* Inflammaging and anti-inflammaging: a systemic perspective on aging and longevity emerged from studies in humans. Mechanisms of ageing and development 2007; 128(1): 92-105.

157. Van Bodegom D, May L, Meij HJ, Westendorp RG. Regulation of human life histories: the role of the inflammatory host response. Annals of the New York Academy of Sciences 2007; 1100: 84-97.

158. Franceschi C, Bonafe M, Valensin S, Olivieri F, De Luca M, Ottaviani E *et al.* Inflamm-aging. An evolutionary perspective on immunosenescence. Annals of the New York Academy of Sciences 2000; 908: 244-254.

159. Claesson MJ, Cusack S, O'Sullivan O, Greene-Diniz R, de Weerd H, Flannery E *et al.* Composition, variability, and temporal stability of the intestinal microbiota of the elderly. Proceedings of the National Academy of Sciences of the United States of America 2011; 108 Suppl 1: 4586-4591.

160. Woodmansey EJ. Intestinal bacteria and ageing. Journal of applied microbiology 2007; 102(5): 1178-1186.

161. Biagi E, Nylund L, Candela M, Ostan R, Bucci L, Pini E *et al.* Through ageing, and beyond: gut microbiota and inflammatory status in seniors and centenarians. PLoS one 2010; 5(5): e10667.

162. Sansonetti PJ, Di Santo JP. Debugging how bacteria manipulate the immune response. Immunity 2007; 26(2): 149-161.

163. Round JL, Mazmanian SK. The gut microbiota shapes intestinal immune responses during health and disease. Nature reviews Immunology 2009; 9(5): 313-323.

164. Man AL, Gicheva N, Nicoletti C. The impact of ageing on the intestinal epithelial barrier and immune system. Cellular immunology 2014; 289(1-2): 112-118.

165. Valenkevich IN, Zhukova NM. [The structure of the mucous membrane of the human duodenum with aging]. Arkhiv patologii 1976; 38(3): 58-61.

166. Koga T, McGhee JR, Kato H, Kato R, Kiyono H, Fujihashi K. Evidence for early aging in the mucosal immune system. Journal of immunology 2000; 165(9): 5352-5359.

167. Al-Sadi RM, Ma TY. IL-1beta causes an increase in intestinal epithelial tight junction permeability. Journal of immunology 2007; 178(7): 4641-4649.

168. Newton JL, Jordan N, Pearson J, Williams GV, Allen A, James OF. The adherent gastric antral and duodenal mucus gel layer thins with advancing age in subjects infected with Helicobacter pylori. Gerontology 2000; 46(3): 153-157.

169. Dolle ME, Kuiper RV, Roodbergen M, Robinson J, de Vlugt S, Wijnhoven SW *et al.* Broad segmental progeroid changes in short-lived Ercc1(-/Delta7) mice. Pathobiology of aging & age related diseases 2011; 1.

170. Bermejo-Alvarez P, Lonergan P, Rath D, Gutierrez-Adan A, Rizos D. Developmental kinetics and gene expression in male and female bovine embryos produced in vitro with sex-sorted spermatozoa. Reproduction, fertility, and development 2010; 22(2): 426-436.

171. Penaloza C, Estevez B, Orlanski S, Sikorska M, Walker R, Smith C *et al.* Sex of the cell dictates its response: differential gene expression and sensitivity to cell death inducing stress in male and female cells. FASEB journal : official publication of the Federation of American Societies for Experimental Biology 2009; 23(6): 1869-1879.

172. Koopman P, Gubbay J, Vivian N, Goodfellow P, Lovell-Badge R. Male development of chromosomally female mice transgenic for Sry. Nature 1991; 351(6322): 117-121.

173. Chaloner A, Greenwood-Van Meerveld B. Sexually dimorphic effects of unpredictable early life adversity on visceral pain behavior in a rodent model. The journal of pain : official journal of the American Pain Society 2013; 14(3): 270-280.

174. Sankaran-Walters S, Macal M, Grishina I, Nagy L, Goulart L, Coolidge K *et al.* Sex differences matter in the gut: effect on mucosal immune activation and inflammation. Biology of sex differences 2013; 4(1): 10.

175. Sugiyama MG, Hobson L, Agellon AB, Agellon LB. Visualization of sex-dimorphic changes in the intestinal transcriptome of Fabp2 gene-ablated mice. Journal of nutrigenetics and nutrigenomics 2012; 5(1): 45-55.

176. Egger M, Beer AG, Theurl M, Schgoer W, Hotter B, Tatarczyk T *et al.* Monocyte migration: a novel effect and signaling pathways of catestatin. European journal of pharmacology 2008; 598(1-3): 104-111.

177. Burger D, Dayer JM. Cytokines, acute-phase proteins, and hormones: IL-1 and TNF-alpha production in contact-mediated activation of monocytes by T lymphocytes. Annals of the New York Academy of Sciences 2002; 966: 464-473.

178. Bernstein CN, Blanchard JF, Rawsthorne P, Wajda A. Epidemiology of Crohn's disease and ulcerative colitis in a central Canadian province: a population-based study. American journal of epidemiology 1999; 149(10): 916-924.

179. Lampe JW, Fredstrom SB, Slavin JL, Potter JD. Sex differences in colonic function: a randomised trial. Gut 1993; 34(4): 531-536.

180. Cremon C, Gargano L, Morselli-Labate AM, Santini D, Cogliandro RF, De Giorgio R *et al.* Mucosal immune activation in irritable bowel syndrome: gender-dependence and association with digestive symptoms. The American journal of gastroenterology 2009; 104(2): 392-400.

181. Nelson JF, Felicio LS, Randall PK, Sims C, Finch CE. A longitudinal study of estrous cyclicity in aging C57BL/6J mice: I. Cycle frequency, length and vaginal cytology. Biology of reproduction 1982; 27(2): 327-339.

182. Felicio LS, Nelson JF, Finch CE. Longitudinal studies of estrous cyclicity in aging C57BL/6J mice: II. Cessation of cyclicity and the duration of persistent vaginal cornification. Biology of reproduction 1984; 31(3): 446-453.

183. Asdell SA, Doornenbal H, Joshi SR, Sperling GA. The effects of sex steroid hormones upon longevity in rats. Journal of reproduction and fertility 1967; 14(1): 113-120.

184. Della Torre S, Benedusi V, Fontana R, Maggi A. Energy metabolism and fertility: a balance preserved for female health. Nature reviews Endocrinology 2014; 10(1): 13-23.

185. Parker WH, Broder MS, Chang E, Feskanich D, Farquhar C, Liu Z *et al.* Ovarian conservation at the time of hysterectomy and long-term health outcomes in the nurses' health study. Obstetrics and gynecology 2009; 113(5): 1027-1037.

186. Hotamisligil GS. Inflammation and metabolic disorders. Nature 2006; 444(7121): 860-867.

187. Komm BS. A new approach to menopausal therapy: the tissue selective estrogen complex. Reproductive sciences 2008; 15(10): 984-992.

188. Macpherson AJ, Harris NL. Interactions between commensal intestinal bacteria and the immune system. Nature Reviews Immunology 2004; 4(6): 478-485.

189. Hansson GC. Role of mucus layers in gut infection and inflammation. Current opinion in microbiology 2012; 15(1): 57-62.

190. Pullan RD, Thomas GA, Rhodes M, Newcombe RG, Williams GT, Allen A *et al.* Thickness of adherent mucus gel on colonic mucosa in humans and its relevance to colitis. Gut 1994; 35(3): 353-359.

191. Johansson ME, Gustafsson JK, Sjoberg KE, Petersson J, Holm L, Sjovall H *et al.* Bacteria penetrate the inner mucus layer before inflammation in the dextran sulfate colitis model. PloS one 2010; 5(8): e12238.

192. Chow J, Tang H, Mazmanian SK. Pathobionts of the gastrointestinal microbiota and inflammatory disease. Current opinion in immunology 2011; 23(4): 473-480.

193. Burger-van Paassen N, van der Sluis M, Bouma J, Korteland-van Male AM, Lu P, Van Seuningen I *et al.* Colitis development during the suckling-weaning transition in mucin Muc2-deficient mice. American Journal of Physiology-Gastrointestinal and Liver Physiology 2011; 301(4): G667-G678.

194. Yamabayashi S. Periodic acid-Schiff-alcian blue: a method for the differential staining of glycoproteins. The Histochemical journal 1987; 19(10-11): 565-571.

195. Gentleman RC, Carey VJ, Bates DM, Bolstad B, Dettling M, Dudoit S *et al.* Bioconductor: open software development for computational biology and bioinformatics. Genome Biol 2004; 5(10): R80.

196. Lin K, Kools H, de Groot PJ, Gavai AK, Basnet RK, Cheng F *et al.* MADMAX - Management and analysis database for multiple ~omics experiments. Journal of integrative bioinformatics 2011; 8(2): 160.

197. Dai M, Wang P, Boyd AD, Kostov G, Athey B, Jones EG *et al.* Evolving gene/transcript definitions significantly alter the interpretation of GeneChip data. Nucleic acids research 2005; 33(20): e175.

198.   Bolstad BM, Collin F, Simpson KM, Irizarry RA, Speed TP. Experimental design and low-level analysis of microarray data. International review of neurobiology 2004; 60: 25-58.

199.   Storey JD, Tibshirani R. Statistical significance for genomewide studies. Proceedings of the National Academy of Sciences of the United States of America 2003; 100(16): 9440-9445.

200.   Sartor MA, Tomlinson CR, Wesselkamper SC, Sivaganesan S, Leikauf GD, Medvedovic M. Intensity-based hierarchical Bayes method improves testing for differentially expressed genes in microarray experiments. BMC bioinformatics 2006; 7: 538.

201.   Subramanian A, Tamayo P, Mootha VK, Mukherjee S, Ebert BL, Gillette MA *et al.* Gene set enrichment analysis: A knowledge-based approach for interpreting genome-wide expression profiles. Proceedings of the National Academy of Sciences of the United States of America 2005; 102(43): 15545-15550.

202.   Mootha VK, Lindgren CM, Eriksson KF, Subramanian A, Sihag S, Lehar J *et al.* PGC-1alpha-responsive genes involved in oxidative phosphorylation are coordinately downregulated in human diabetes. Nature genetics 2003; 34(3): 267-273.

203.   Geurts L, Lazarevic V, Derrien M, Everard A, Van Roye M, Knauf C *et al.* Altered gut microbiota and endocannabinoid system tone in obese and diabetic leptin-resistant mice: impact on apelin regulation in adipose tissue. Frontiers in microbiology 2011; 2: 149.

204.   Rajilic-Stojanovic M, Heilig HG, Molenaar D, Kajander K, Surakka A, Smidt H *et al.* Development and application of the human intestinal tract chip, a phylogenetic microarray: analysis of universally conserved phylotypes in the abundant microbiota of young and elderly adults. Environmental microbiology 2009; 11(7): 1736-1751.

205.   Lahti L, Elo LL, Aittokallio T, Kaski S. Probabilistic analysis of probe reliability in differential gene expression studies with short oligonucleotide arrays. IEEE/ACM transactions on computational biology and bioinformatics / IEEE, ACM 2011; 8(1): 217-225.

206.   Braak CJF, Šmilauer, P. Canoco reference manual and user's guide: software for ordination (version 5.0). Ithaca, NH edn, 2012, 118pp.

207.   Goto Y, Obata T, Kunisawa J, Sato S, Ivanov, II, Lamichhane A *et al.* Innate lymphoid cells regulate intestinal epithelial cell glycosylation. Science 2014; 345(6202): 1254009.

208.   Ortega-Cava CF, Ishihara S, Rumi MAK, Aziz MM, Kazumori H, Yuki T *et al.* Epithelial toll-like receptor 5 is constitutively localized in the mouse cecum and exhibits distinctive down-regulation during experimental colitis. Clinical and Vaccine Immunology 2006; 13(1): 132-138.

209.   Gironella M, Iovanna JL, Sans M, Gil F, Penalva M, Closa D *et al.* Anti-inflammatory effects of pancreatitis associated protein in inflammatory bowel disease. Gut 2005; 54(9): 1244-1253.

210.   Zhang H, Kandil E, Lin YY, Levi G, Zenilman ME. Targeted inhibition of gene expression of pancreatitis-associated proteins exacerbates the severity of acute pancreatitis in rats. Scandinavian journal of gastroenterology 2004; 39(9): 870-881.

211.   Closa D, Motoo Y, Iovanna JL. Pancreatitis-associated protein: From a lectin to an anti-infammatory cytokine. World Journal of Gastroenterology 2007; 13(2): 170-174.

212.   Zheng Y, Valdez PA, Danilenko DM, Hu Y, Sa SM, Gong Q *et al.* Interleukin-22 mediates early host defense against attaching and effacing bacterial pathogens. 2008; 14(3): 282-289.

213.   Xu W, Presnell SR, Parrish-Novak J, Kindsvogel W, Jaspers S, Chen Z *et al.* A soluble class II cytokine receptor, IL-22RA2, is a naturally occurring IL-22 antagonist. Proceedings of the National Academy of Sciences 2001; 98(17): 9511-9516.

214.   Pickert G, Neufert C, Leppkes M, Zheng Y, Wittkopf N, Warntjen M *et al.* STAT3 links IL-22 signaling in intestinal epithelial cells to mucosal wound healing. The Journal of experimental medicine 2009; 206(7): 1465-1472.

215.   Grivennikov S, Karin E, Terzic J, Mucida D, Yu GY, Vallabhapurapu S *et al.* IL-6 and Stat3 are required for survival of intestinal epithelial cells and development of colitis-associated cancer. Cancer cell 2009; 15(2): 103-113.

216.   Meng D, Newburg DS, Young C, Baker A, Tonkonogy SL, Sartor RB *et al.* Bacterial symbionts induce a FUT2-dependent fucosylated niche on colonic epithelium via ERK and JNK signaling. American Journal of Physiology-Gastrointestinal and Liver Physiology 2007; 293(4): G780-G787.

217.   Bry L, Falk PG, Midtvedt T, Gordon JI. A model of host-microbial interactions in an open mammalian ecosystem. Science 1996; 273(5280): 1380-1383.

218. Nanthakumar NN, Dai D, Newburg DS, Walker WA. The role of indigenous microflora in the development of murine intestinal fucosyl- and sialyltransferases. FASEB journal : official publication of the Federation of American Societies for Experimental Biology 2003; 17(1): 44-46.

219. Pang KY, Newman AP, Udall JN, Walker WA. Development of gastrointestinal mucosal barrier. VII. In utero maturation of microvillus surface by cortisone. The American journal of physiology 1985; 249(1 Pt 1): G85-91.

220. Shub MD, Pang KY, Swann DA, Walker WA. Age-related changes in chemical composition and physical properties of mucus glycoproteins from rat small intestine. The Biochemical journal 1983; 215(2): 405-411.

221. Derrien M, Collado MC, Ben-Amor K, Salminen S, de Vos WM. The Mucin degrader Akkermansia muciniphila is an abundant resident of the human intestinal tract. Applied and environmental microbiology 2008; 74(5): 1646-1648.

222. Neufert C, Pickert G, Zheng Y, Wittkopf N, Warntjen M, Nikolaev A et al. Activation of epithelial STAT3 regulates intestinal homeostasis. Cell cycle 2010; 9(4): 652-655.

223. Sovran B, Loonen LM, Lu P, Hugenholtz F, Belzer C, Stolte EH et al. IL-22-STAT3 Pathway Plays a Key Role in the Maintenance of Ileal Homeostasis in Mice Lacking Secreted Mucus Barrier. Inflammatory bowel diseases 2015.

224. te Velde AA, de Kort F, Sterrenburg E, Pronk I, ten Kate FJW, Hommes DW et al. Comparative analysis of colonic gene expression of three experimental colitis models mimicking inflammatory bowel disease. Inflammatory bowel diseases 2007; 13(3): 325-330.

225. Miquel S, Martin R, Rossi O, Bermudez-Humaran LG, Chatel JM, Sokol H et al. Faecalibacterium prausnitzii and human intestinal health. Current opinion in microbiology 2013; 16(3): 255-261.

226. Hansen JJ, Huang Y, Peterson DA, Goeser L, Fan T-J, Chang EB et al. The Colitis-Associated Transcriptional Profile of Commensal <italic>Bacteroides thetaiotaomicron</italic> Enhances Adaptive Immune Responses to a Bacterial Antigen. PloS one 2012; 7(8): e42645.

227. Bloom SM, Bijanki VN, Nava GM, Sun L, Malvin NP, Donermeyer DL et al. Commensal Bacteroides species induce colitis in host-genotype-specific fashion in a mouse model of inflammatory bowel disease. Cell host & microbe 2011; 9(5): 390-403.

228. Takaishi H, Matsuki T, Nakazawa A, Takada T, Kado S, Asahara T et al. Imbalance in intestinal microflora constitution could be involved in the pathogenesis of inflammatory bowel disease. International journal of medical microbiology : IJMM 2008; 298(5-6): 463-472.

229. Gophna U, Sommerfeld K, Gophna S, Doolittle WF, Veldhuyzen van Zanten SJO. Differences between Tissue-Associated Intestinal Microfloras of Patients with Crohn's Disease and Ulcerative Colitis. Journal of Clinical Microbiology 2006; 44(11): 4136-4141.

230. Bibiloni R, Mangold M, Madsen KL, Fedorak RN, Tannock GW. The bacteriology of biopsies differs between newly diagnosed, untreated, Crohn's disease and ulcerative colitis patients. Journal of Medical Microbiology 2006; 55(8): 1141-1149.

231. Andoh A, Tsujikawa T, Sasaki M, Mitsuyama K, Suzuki Y, Matsui T et al. Faecal microbiota profile of Crohn's disease determined by terminal restriction fragment length polymorphism analysis. Alimentary pharmacology & therapeutics 2009; 29(1): 75-82.

232. Boulesteix AL, Strimmer K. Partial least squares: a versatile tool for the analysis of high-dimensional genomic data. Briefings in bioinformatics 2007; 8(1): 32-44.

233. Lange K, Hugenholtz F, Jonathan MC, Schols HA, Kleerebezem M, Smidt H et al. Comparison of the effects of five dietary fibers on mucosal transcriptional profiles, and luminal microbiota composition and SCFA concentrations in murine colon. Molecular nutrition & food research 2015.

234. Le Cao KA, Martin PG, Robert-Granie C, Besse P. Sparse canonical methods for biological data integration: application to a cross-platform study. BMC bioinformatics 2009; 10: 34.

235. Gonzalez I, Cao KA, Davis MJ, Dejean S. Visualising associations between paired 'omics' data sets. BioData mining 2012; 5(1): 19.

236. Le Cao KA, Gonzalez I, Dejean S. integrOmics: an R package to unravel relationships between two omics datasets. Bioinformatics 2009; 25(21): 2855-2856.

237. El Aidy S, Derrien M, Merrifield CA, Levenez F, Dore J, Boekschoten MV et al. Gut bacteria-host metabolic interplay during conventionalisation of the mouse germfree colon. The ISME journal 2013; 7(4): 743-755.

238. Hansen J, Gulati A, Sartor RB. The role of mucosal immunity and host genetics in defining intestinal commensal bacteria. Current opinion in gastroenterology 2010; 26(6): 564-571.

239. Schwab C, Berry D, Rauch I, Rennisch I, Ramesmayer J, Hainzl E *et al.* Longitudinal study of murine microbiota activity and interactions with the host during acute inflammation and recovery. The ISME journal 2014; 8(5): 1101-1114.

240. Hammer RE, Maika SD, Richardson JA, Tang JP, Taurog JD. Spontaneous inflammatory disease in transgenic rats expressing HLA-B27 and human beta 2m: an animal model of HLA-B27-associated human disorders. Cell 1990; 63(5): 1099-1112.

241. Rath HC, Herfarth HH, Ikeda JS, Grenther WB, Hamm TE, Jr., Balish E *et al.* Normal luminal bacteria, especially Bacteroides species, mediate chronic colitis, gastritis, and arthritis in HLA-B27/human beta2 microglobulin transgenic rats. J Clin Invest 1996; 98(4): 945-953.

242. Rath HC, Wilson KH, Sartor RB. Differential induction of colitis and gastritis in HLA-B27 transgenic rats selectively colonized with Bacteroides vulgatus or Escherichia coli. Infection and immunity 1999; 67(6): 2969-2974.

243. Ramanan D, Tang MS, Bowcutt R, Loke P, Cadwell K. Bacterial sensor Nod2 prevents inflammation of the small intestine by restricting the expansion of the commensal Bacteroides vulgatus. Immunity 2014; 41(2): 311-324.

244. Chow J, Mazmanian SK. A pathobiont of the microbiota balances host colonization and intestinal inflammation. Cell host & microbe 2010; 7(4): 265-276.

245. Cullen TW, Schofield WB, Barry NA, Putnam EE, Rundell EA, Trent MS *et al.* Antimicrobial peptide resistance mediates resilience of prominent gut commensals during inflammation. Science 2015; 347(6218): 170-175.

246. Gomez CR, Boehmer ED, Kovacs EJ. The aging innate immune system. Current opinion in immunology 2005; 17(5): 457-462.

247. Weng NP. Aging of the immune system: how much can the adaptive immune system adapt? Immunity 2006; 24(5): 495-499.

248. Van der Sluis M, De Koning BAE, De Bruijn ACJM, Velcich A, Meijerink JPP, Van Goudoever JB *et al.* Muc2-Deficient Mice Spontaneously Develop Colitis, Indicating That MUC2 Is Critical for Colonic Protection. Gastroenterology 2006; 131(1): 117-129.

249. Merchant HA, Rabbie SC, Varum FJ, Afonso-Pereira F, Basit AW. Influence of ageing on the gastrointestinal environment of the rat and its implications for drug delivery. European journal of pharmaceutical sciences : official journal of the European Federation for Pharmaceutical Sciences 2014; 62: 76-85.

250. Yu Z, Morrison M. Improved extraction of PCR-quality community DNA from digesta and fecal samples. BioTechniques 2004; 36(5): 808-812.

251. Sovran B, Loonen LM, Lu P, Hugenholtz F, Belzer C, Stolte EH *et al.* IL-22-STAT3 Pathway Plays a Key Role in the Maintenance of Ileal Homeostasis in Mice Lacking Secreted Mucus Barrier. Inflammatory bowel diseases 2015; 21(3): 531-542.

252. Baptista AP, Olivier BJ, Goverse G, Greuter M, Knippenberg M, Kusser K *et al.* Colonic patch and colonic SILT development are independent and differentially regulated events. Mucosal Immunol 2013; 6(3): 511-521.

253. Malmberg EK, Noaksson KA, Phillipson M, Johansson ME, Hinojosa-Kurtzberg M, Holm L *et al.* Increased levels of mucins in the cystic fibrosis mouse small intestine, and modulator effects of the Muc1 mucin expression. American journal of physiology Gastrointestinal and liver physiology 2006; 291(2): G203-210.

254. Randall TD, Carragher DM, Rangel-Moreno J. Development of secondary lymphoid organs. Annual review of immunology 2008; 26: 627-650.

255. Hedlund BP, Gosink JJ, Staley JT. Verrucomicrobia div. nov., a new division of the bacteria containing three new species of Prosthecobacter. Antonie van Leeuwenhoek 1997; 72(1): 29-38.

256. Kang CS, Ban M, Choi EJ, Moon HG, Jeon JS, Kim DK *et al.* Extracellular vesicles derived from gut microbiota, especially Akkermansia muciniphila, protect the progression of dextran sulfate sodium-induced colitis. PloS one 2013; 8(10): e76520.

257. Png CW, Linden SK, Gilshenan KS, Zoetendal EG, McSweeney CS, Sly LI *et al.* Mucolytic bacteria with increased prevalence in IBD mucosa augment in vitro utilization of mucin by other bacteria. The American journal of gastroenterology 2010; 105(11): 2420-2428.

258. Carroll IM, Andrus JM, Bruno-Barcena JM, Klaenhammer TR, Hassan HM, Threadgill DS. Anti-inflammatory properties of Lactobacillus gasseri expressing manganese superoxide dismutase using the interleukin 10-deficient mouse model of colitis. American journal of physiology Gastrointestinal and liver physiology 2007; 293(4): G729-738.

259. Goodman WA, Garg RR, Reuter BK, Mattioli B, Rissman EF, Pizarro TT. Loss of estrogen-mediated immunoprotection underlies female gender bias in experimental Crohn's-like ileitis. Mucosal Immunol 2014; 7(5): 1255-1265.

260. Roth LS, Chande N, Ponich T, Roth ML, Gregor J. Predictors of disease severity in ulcerative colitis patients from Southwestern Ontario. World journal of gastroenterology : WJG 2010; 16(2): 232-236.

261. Lee GJ, Kappelman MD, Boyle B, Colletti RB, King E, Pratt JM *et al.* Role of sex in the treatment and clinical outcomes of pediatric patients with inflammatory bowel disease. Journal of pediatric gastroenterology and nutrition 2012; 55(6): 701-706.

262. Blumenstein I, Herrmann E, Filmann N, Zosel C, Tacke W, Bock H *et al.* Female patients suffering from inflammatory bowel diseases are treated less frequently with immunosuppressive medication and have a higher disease activity: a subgroup analysis of a large multi-centre, prospective, internet-based study. Journal of Crohn's & colitis 2011; 5(3): 203-210.

263. Khalili H, Higuchi LM, Ananthakrishnan AN, Manson JE, Feskanich D, Richter JM *et al.* Hormone therapy increases risk of ulcerative colitis but not Crohn's disease. Gastroenterology 2012; 143(5): 1199-1206.

264. Khalili H, Higuchi LM, Ananthakrishnan AN, Richter JM, Feskanich D, Fuchs CS *et al.* Oral contraceptives, reproductive factors and risk of inflammatory bowel disease. Gut 2013; 62(8): 1153-1159.

265. Hermiston ML, Gordon JI. Inflammatory bowel disease and adenomas in mice expressing a dominant negative N-cadherin. Science 1995; 270(5239): 1203-1207.

266. Gunther C, Martini E, Wittkopf N, Amann K, Weigmann B, Neumann H *et al.* Caspase-8 regulates TNF-alpha-induced epithelial necroptosis and terminal ileitis. Nature 2011; 477(7364): 335-339.

267. Welz PS, Wullaert A, Vlantis K, Kondylis V, Fernandez-Majada V, Ermolaeva M *et al.* FADD prevents RIP3-mediated epithelial cell necrosis and chronic intestinal inflammation. Nature 2011; 477(7364): 330-334.

268. Kaser A, Lee AH, Franke A, Glickman JN, Zeissig S, Tilg H *et al.* XBP1 links ER stress to intestinal inflammation and confers genetic risk for human inflammatory bowel disease. Cell 2008; 134(5): 743-756.

269. Bischoff SC, Barbara G, Buurman W, Ockhuizen T, Schulzke JD, Serino M *et al.* Intestinal permeability--a new target for disease prevention and therapy. BMC gastroenterology 2014; 14: 189.

270. Marshall JK, Thabane M, Garg AX, Clark WF, Moayyedi P, Collins SM *et al.* Eight year prognosis of postinfectious irritable bowel syndrome following waterborne bacterial dysentery. Gut 2010; 59(5): 605-611.

271. Ruigomez A, Garcia Rodriguez LA, Panes J. Risk of irritable bowel syndrome after an episode of bacterial gastroenteritis in general practice: influence of comorbidities. Clinical gastroenterology and hepatology : the official clinical practice journal of the American Gastroenterological Association 2007; 5(4): 465-469.

272. Gwee KA, Leong YL, Graham C, McKendrick MW, Collins SM, Walters SJ *et al.* The role of psychological and biological factors in postinfective gut dysfunction. Gut 1999; 44(3): 400-406.

273. Spiller RC. Postinfectious irritable bowel syndrome. Gastroenterology 2003; 124(6): 1662-1671.

274. Cone RA. Barrier properties of mucus. Advanced drug delivery reviews 2009; 61(2): 75-85.

275. Jager S, Stange EF, Wehkamp J. Inflammatory bowel disease: an impaired barrier disease. Langenbeck's archives of surgery / Deutsche Gesellschaft fur Chirurgie 2013; 398(1): 1-12.

276. Antoni L, Nuding S, Wehkamp J, Stange EF. Intestinal barrier in inflammatory bowel disease. World journal of gastroenterology : WJG 2014; 20(5): 1165-1179.

277. Johansson ME, Gustafsson JK, Holmen-Larsson J, Jabbar KS, Xia L, Xu H *et al.* Bacteria penetrate the normally impenetrable inner colon mucus layer in both murine colitis models and patients with ulcerative colitis. Gut 2014; 63(2): 281-291.

278. Sheth SU, Lu Q, Twelker K, Sharpe SM, Qin X, Reino DC *et al.* Intestinal mucus layer preservation in female rats attenuates gut injury after trauma-hemorrhagic shock. The Journal of trauma 2010; 68(2): 279-288.

279. Babickova J, Tothova L, Lengyelova E, Bartonova A, Hodosy J, Gardlik R *et al.* Sex Differences in Experimentally Induced Colitis in Mice: a Role for Estrogens. Inflammation 2015.

280. Verdu EF, Deng Y, Bercik P, Collins SM. Modulatory effects of estrogen in two murine models of experimental colitis. American journal of physiology Gastrointestinal and liver physiology 2002; 283(1): G27-36.

281. Heijmans J, Wielenga MC, Rosekrans SL, van Lidth de Jeude JF, Roelofs J, Groothuis P *et al.* Oestrogens promote tumorigenesis in a mouse model for colitis-associated cancer. Gut 2014; 63(2): 310-316.

282. Houdeau E, Moriez R, Leveque M, Salvador-Cartier C, Waget A, Leng L *et al.* Sex steroid regulation of macrophage migration inhibitory factor in normal and inflamed colon in the female rat. Gastroenterology 2007; 132(3): 982-993.

283. Gunal O, Oktar BK, Ozcinar E, Sungur M, Arbak S, Yegen B. Estradiol treatment ameliorates acetic acid-induced gastric and colonic injuries in rats. Inflammation 2003; 27(6): 351-359.

284. Harnish DC, Albert LM, Leathurby Y, Eckert AM, Ciarletta A, Kasaian M *et al.* Beneficial effects of estrogen treatment in the HLA-B27 transgenic rat model of inflammatory bowel disease. American journal of physiology Gastrointestinal and liver physiology 2004; 286(1): G118-125.

285. Diebel ME, Diebel LN, Manke CW, Liberati DM. Estrogen modulates intestinal mucus physiochemical properties and protects against oxidant injury. The journal of trauma and acute care surgery 2015; 78(1): 94-99.

286. Ouellette AJ. Paneth cells and innate mucosal immunity. Current opinion in gastroenterology 2010; 26(6): 547-553.

287. Wehkamp J, Salzman NH, Porter E, Nuding S, Weichenthal M, Petras RE *et al.* Reduced Paneth cell alpha-defensins in ileal Crohn's disease. Proceedings of the National Academy of Sciences of the United States of America 2005; 102(50): 18129-18134.

288. Porter EM, Bevins CL, Ghosh D, Ganz T. The multifaceted Paneth cell. Cellular and molecular life sciences : CMLS 2002; 59(1): 156-170.

289. Wilson CL, Ouellette AJ, Satchell DP, Ayabe T, Lopez-Boado YS, Stratman JL *et al.* Regulation of intestinal alpha-defensin activation by the metalloproteinase matrilysin in innate host defense. Science 1999; 286(5437): 113-117.

290. Brandl K, Plitas G, Schnabl B, DeMatteo RP, Pamer EG. MyD88-mediated signals induce the bactericidal lectin RegIII gamma and protect mice against intestinal Listeria monocytogenes infection. The Journal of experimental medicine 2007; 204(8): 1891-1900.

291. Wehkamp J, Fellermann K, Herrlinger KR, Bevins CL, Stange EF. Mechanisms of disease: defensins in gastrointestinal diseases. Nature clinical practice Gastroenterology & hepatology 2005; 2(9): 406-415.

292. Steegenga WT, Mischke M, Lute C, Boekschoten MV, Pruis MG, Lendvai A *et al.* Sexually dimorphic characteristics of the small intestine and colon of prepubescent C57BL/6 mice. Biology of sex differences 2014; 5: 11.

293. Rakoff-Nahoum S, Hao L, Medzhitov R. Role of toll-like receptors in spontaneous commensal-dependent colitis. Immunity 2006; 25(2): 319-329.

294. Vaishnava S, Behrendt CL, Ismail AS, Eckmann L, Hooper LV. Paneth cells directly sense gut commensals and maintain homeostasis at the intestinal host-microbial interface. Proceedings of the National Academy of Sciences 2008; 105(52): 20858-20863.

295. Menendez A, Willing BP, Montero M, Wlodarska M, So CC, Bhinder G *et al.* Bacterial stimulation of the TLR-MyD88 pathway modulates the homeostatic expression of ileal Paneth cell alpha-defensins. Journal of innate immunity 2013; 5(1): 39-49.

296. Rossi O, Karczewski J, Stolte EH, Brummer RJ, van Nieuwenhoven MA, Meijerink M *et al.* Vectorial secretion of interleukin-8 mediates autocrine signalling in intestinal epithelial cells via apically located CXCR1. BMC research notes 2013; 6: 431.

297. Karczewski J, Troost FJ, Konings I, Dekker J, Kleerebezem M, Brummer RJ *et al.* Regulation of human epithelial tight junction proteins by Lactobacillus plantarum in vivo and protective effects on the epithelial barrier. American journal of physiology Gastrointestinal and liver physiology 2010; 298(6): G851-859.

298. Desreumaux P, Dubuquoy L, Nutten S, Peuchmaur M, Englaro W, Schoonjans K *et al.* Attenuation of Colon Inflammation through Activators of the Retinoid X Receptor (Rxr)/Peroxisome Proliferator–Activated Receptor γ (Pparγ) Heterodimer: A Basis for New Therapeutic Strategies. The Journal of experimental medicine 2001; 193(7): 827-838.

299. Bauerl C, Llopis M, Antolin M, Monedero V, Mata M, Zuniga M *et al.* Lactobacillus paracasei and Lactobacillus plantarum strains downregulate proinflammatory genes in an ex vivo system of cultured human colonic mucosa. Genes & nutrition 2013; 8(2): 165-180.

300. Rossi O, Khan MT, Schwarzer M, Hudcovic T, Srutkova D, Duncan SH *et al.* Faecalibacterium prausnitzii Strain HTF-F and Its Extracellular Polymeric Matrix Attenuate Clinical Parameters in DSS-Induced Colitis. PloS one 2015; 10(4): e0123013.

301. Lopez-Otin C, Blasco MA, Partridge L, Serrano M, Kroemer G. The hallmarks of aging. Cell 2013; 153(6): 1194-1217.

302. Chambers SM, Shaw CA, Gatza C, Fisk CJ, Donehower LA, Goodell MA. Aging hematopoietic stem cells decline in function and exhibit epigenetic dysregulation. PLoS biology 2007; 5(8): e201.

303. Sahin E, Depinho RA. Linking functional decline of telomeres, mitochondria and stem cells during ageing. Nature 2010; 464(7288): 520-528.

304. Lindstrom TM, Robinson WH. Rheumatoid arthritis: a role for immunosenescence? Journal of the American Geriatrics Society 2010; 58(8): 1565-1575.

305. Warren LA, Rossi DJ. Stem cells and aging in the hematopoietic system. Mechanisms of ageing and development 2009; 130(1-2): 46-53.

306. Min H, Montecino-Rodriguez E, Dorshkind K. Effects of aging on the common lymphoid progenitor to pro-B cell transition. Journal of immunology 2006; 176(2): 1007-1012.

307. Keren Z, Naor S, Nussbaum S, Golan K, Itkin T, Sasaki Y *et al.* B cell depletion reactivates B lymphopoiesis in the BM and rejuvenates the B lineage in aging. Blood 2011; 117(11): 3104-3112.

308. George AJ, Ritter MA. Thymic involution with ageing: obsolescence or good housekeeping? Immunology today 1996; 17(6): 267-272.

309. Tiihonen K, Ouwehand AC, Rautonen N. Human intestinal microbiota and healthy ageing. Ageing research reviews 2010; 9(2): 107-116.

310. Biagi E, Candela M, Fairweather-Tait S, Franceschi C, Brigidi P. Ageing of the human metaorganism: the microbial counterpart. AGE 2011: 1-21.

311. Candore G, Balistreri CR, Colonna-Romano G, Grimaldi MP, Lio D, Listi F *et al.* Immunosenescence and anti-immunosenescence therapies: the case of probiotics. Rejuvenation research 2008; 11(2): 425-432.

312. Lahtinen SJ, Forssten S, Aakko J, Granlund L, Rautonen N, Salminen S *et al.* Probiotic cheese containing Lactobacillus rhamnosus HN001 and Lactobacillus acidophilus NCFM(R) modifies subpopulations of fecal lactobacilli and Clostridium difficile in the elderly. Age 2012; 34(1): 133-143.

313. Akatsu H, Iwabuchi N, Xiao JZ, Matsuyama Z, Kurihara R, Okuda K *et al.* Clinical effects of probiotic Bifidobacterium longum BB536 on immune function and intestinal microbiota in elderly patients receiving enteral tube feeding. JPEN Journal of parenteral and enteral nutrition 2013; 37(5): 631-640.

314. Perez Martinez G, Bauerl C, Collado MC. Understanding gut microbiota in elderly's health will enable intervention through probiotics. Beneficial microbes 2014; 5(3): 235-246.

315. Spaiser SJ, Culpepper T, Nieves C, Jr., Ukhanova M, Mai V, Percival SS *et al.* Lactobacillus gasseri KS-13, Bifidobacterium bifidum G9-1, and Bifidobacterium longum MM-2 Ingestion Induces a Less Inflammatory Cytokine Profile and a Potentially Beneficial Shift in Gut Microbiota in Older Adults: A Randomized, Double-Blind, Placebo-Controlled, Crossover Study. Journal of the American College of Nutrition 2015: 1-11.

316. Rampelli S, Candela M, Severgnini M, Biagi E, Turroni S, Roselli M *et al.* A probiotics-containing biscuit modulates the intestinal microbiota in the elderly. The journal of nutrition, health & aging 2013; 17(2): 166-172.

317. Sherman PM, Ossa JC, Johnson-Henry K. Unraveling mechanisms of action of probiotics. Nutrition in clinical practice : official publication of the American Society for Parenteral and Enteral Nutrition 2009; 24(1): 10-14.

318. Gill HS, Rutherfurd KJ, Cross ML. Dietary probiotic supplementation enhances natural killer cell activity in the elderly: an investigation of age-related immunological changes. Journal of clinical immunology 2001; 21(4): 264-271.

319. Gill HS, Rutherfurd KJ, Cross ML, Gopal PK. Enhancement of immunity in the elderly by dietary supplementation with the probiotic Bifidobacterium lactis HN019. The American journal of clinical nutrition 2001; 74(6): 833-839.

320. Matsumoto M, Kurihara S, Kibe R, Ashida H, Benno Y. Longevity in mice is promoted by probiotic-induced suppression of colonic senescence dependent on upregulation of gut bacterial polyamine production. PloS one 2011; 6(8): e23652.

321. Vidal K, Benyacoub J, Moser M, Sanchez-Garcia J, Serrant P, Segura-Roggero I et al. Effect of Lactobacillus paracasei NCC2461 on antigen-specific T-cell mediated immune responses in aged mice. Rejuvenation research 2008; 11(5): 957-964.

322. Dollé ME, Kuiper RV, Roodbergen M, Robinson J, de Vlugt S, Wijnhoven SW et al. Broad segmental progeroid changes in short-lived Ercc1−/Δ7 mice. Pathobiology of Aging & Age-related Diseases 2011; 1.

323. Weeda G, Donker I, de Wit J, Morreau H, Janssens R, Vissers CJ et al. Disruption of mouse ERCC1 results in a novel repair syndrome with growth failure, nuclear abnormalities and senescence. Current biology : CB 1997; 7(6): 427-439.

324. Weeda G, Donker I, de Wit J, Morreau H, Janssens R, Vissers C et al. Disruption of mouse ERCC1 results in a novel repair syndrome with growth failure, nuclear abnormalities and senescence. Current Biology 1997; 7(6): 427-439.

325. van Loo PF, Dingjan GM, Maas A, Hendriks RW. Surrogate-light-chain silencing is not critical for the limitation of pre-B cell expansion but is for the termination of constitutive signaling. Immunity 2007; 27(3): 468-480.

326. Daniel C, Repa A, Wild C, Pollak A, Pot B, Breiteneder H et al. Modulation of allergic immune responses by mucosal application of recombinant lactic acid bacteria producing the major birch pollen allergen Bet v 1. Allergy 2006; 61(7): 812-819.

327. Derrien M, Van Baarlen P, Hooiveld G, Norin E, Müller M, de Vos WM. Modulation of mucosal immune response, tolerance, and proliferation in mice colonized by the mucin-degrader Akkermansia muciniphila. Frontiers in Microbiology 2011; 2: 1-14.

328. Ivanovic N, Minic R, Dimitrijevic L, Radojevic Skodric S, Zivkovic I, Djordjevic B. Lactobacillus rhamnosus LA68 and Lactobacillus plantarum WCFS1 differently influence metabolic and immunological parameters in high fat diet-induced hypercholesterolemia and hepatic steatosis. Food & function 2015; 6(2): 558-565.

329. Kleerebezem M, Boekhorst J, van Kranenburg R, Molenaar D, Kuipers OP, Leer R et al. Complete genome sequence of Lactobacillus plantarum WCFS1. Proceedings of the National Academy of Sciences of the United States of America 2003; 100(4): 1990-1995.

330. Marco ML, Peters TH, Bongers RS, Molenaar D, van Hemert S, Sonnenburg JL et al. Lifestyle of Lactobacillus plantarum in the mouse caecum. Environmental microbiology 2009; 11(10): 2747-2757.

331. Meijerink M, Wells JM, Taverne N, de Zeeuw Brouwer ML, Hilhorst B, Venema K et al. Immunomodulatory effects of potential probiotics in a mouse peanut sensitization model. FEMS immunology and medical microbiology 2012; 65(3): 488-496.

332. Snel J, Vissers YM, Smit BA, Jongen JM, van der Meulen ET, Zwijsen R et al. Strain-specific immunomodulatory effects of Lactobacillus plantarum strains on birch-pollen-allergic subjects out of season. Clinical and experimental allergy : journal of the British Society for Allergy and Clinical Immunology 2011; 41(2): 232-242.

333. Foligne B, Nutten S, Grangette C, Dennin V, Goudercourt D, Poiret S et al. Correlation between in vitro and in vivo immunomodulatory properties of lactic acid bacteria. World journal of gastroenterology : WJG 2007; 13(2): 236-243.

334. Bauerl C, Perez-Martinez G, Yan F, Polk DB, Monedero V. Functional analysis of the p40 and p75 proteins from Lactobacillus casei BL23. Journal of molecular microbiology and biotechnology 2010; 19(4): 231-241.

335. Maze A, Boel G, Zuniga M, Bourand A, Loux V, Yebra MJ et al. Complete genome sequence of the probiotic Lactobacillus casei strain BL23. Journal of bacteriology 2010; 192(10): 2647-2648.

336. Hougee S, Vriesema AJ, Wijering SC, Knippels LM, Folkerts G, Nijkamp FP et al. Oral treatment with probiotics reduces allergic symptoms in ovalbumin-sensitized mice: a bacterial strain comparative study. International archives of allergy and immunology 2010; 151(2): 107-117.

337. Clarke TB, Davis KM, Lysenko ES, Zhou AY, Yu Y, Weiser JN. Recognition of peptidoglycan from the microbiota by Nod1 enhances systemic innate immunity. Nat Med 2010; 16(2): 228-231.

338. Hill DA, Siracusa MC, Abt MC, Kim BS, Kobuley D, Kubo M *et al.* Commensal bacteria-derived signals regulate basophil hematopoiesis and allergic inflammation. Nat Med 2012; 18(4): 538-546.

339. Esplin BL, Shimazu T, Welner RS, Garrett KP, Nie L, Zhang Q *et al.* Chronic exposure to a TLR ligand injures hematopoietic stem cells. Journal of immunology 2011; 186(9): 5367-5375.

340. van Hemert S, Meijerink M, Molenaar D, Bron PA, de Vos P, Kleerebezem M *et al.* Identification of Lactobacillus plantarum genes modulating the cytokine response of human peripheral blood mononuclear cells. BMC microbiology 2010; 10: 293.

341. Meijerink M, van Hemert S, Taverne N, Wels M, de Vos P, Bron PA *et al.* Identification of genetic loci in Lactobacillus plantarum that modulate the immune response of dendritic cells using comparative genome hybridization. PloS one 2010; 5(5): e10632.

342. Rakoff-Nahoum S, Paglino J, Eslami-Varzaneh F, Edberg S, Medzhitov R. Recognition of commensal microflora by toll-like receptors is required for intestinal homeostasis. Cell 2004; 118(2): 229-241.

343. Nenci A, Becker C, Wullaert A, Gareus R, van Loo G, Danese S *et al.* Epithelial NEMO links innate immunity to chronic intestinal inflammation. Nature 2007; 446(7135): 557-561.

344. Kollmann TR, Levy O, Montgomery RR, Goriely S. Innate immune function by Toll-like receptors: distinct responses in newborns and the elderly. Immunity 2012; 37(5): 771-783.

345. Claesson MJ, Jeffery IB, Conde S, Power SE, O'Connor EM, Cusack S *et al.* Gut microbiota composition correlates with diet and health in the elderly. Nature 2012; 488(7410): 178-184.

346. Hetz C. The unfolded protein response: controlling cell fate decisions under ER stress and beyond. Nat Rev Mol Cell Biol 2012; 13(2): 89-102.

347. Naidoo N. ER and aging-Protein folding and the ER stress response. Ageing research reviews 2009; 8(3): 150-159.

348. Eri RD, Adams RJ, Tran TV, Tong H, Das I, Roche DK *et al.* An intestinal epithelial defect conferring ER stress results in inflammation involving both innate and adaptive immunity. Mucosal Immunol 2011; 4(3): 354-364.

349. Kibe R, Kurihara S, Sakai Y, Suzuki H, Ooga T, Sawaki E *et al.* Upregulation of colonic luminal polyamines produced by intestinal microbiota delays senescence in mice. Scientific reports 2014; 4: 4548.

350. Bevins CL. Paneth cell defensins: key effector molecules of innate immunity. Biochem Soc Trans 2006; 34(Pt 2): 263-266.

351. Pott J, Hornef M. Innate immune signalling at the intestinal epithelium in homeostasis and disease. EMBO reports 2012; 13(8): 684-698.

352. Hooper LV, Littman DR, Macpherson AJ. Interactions between the microbiota and the immune system. Science 2012; 336(6086): 1268-1273.

353. Ambort D, Johansson ME, Gustafsson JK, Nilsson HE, Ermund A, Johansson BR *et al.* Calcium and pH-dependent packing and release of the gel-forming MUC2 mucin. Proceedings of the National Academy of Sciences of the United States of America 2012; 109(15): 5645-5650.

354. Kim YS, Ho SB. Intestinal goblet cells and mucins in health and disease: recent insights and progress. Current gastroenterology reports 2010; 12(5): 319-330.

355. Corr SC, Gahan CC, Hill C. M-cells: origin, morphology and role in mucosal immunity and microbial pathogenesis. FEMS immunology and medical microbiology 2008; 52(1): 2-12.

356. Neutra MR, Frey A, Kraehenbuhl JP. Epithelial M cells: gateways for mucosal infection and immunization. Cell 1996; 86(3): 345-348.

357. McDole JR, Wheeler LW, McDonald KG, Wang B, Konjufca V, Knoop KA *et al.* Goblet cells deliver luminal antigen to CD103+ dendritic cells in the small intestine. Nature 2012; 483(7389): 345-349.

358. Ivanov I, Atarashi K, Manel N, Brodie EL, Shima T, Karaoz U *et al.* Induction of intestinal Th17 cells by segmented filamentous bacteria. Cell 2009; 139(3): 485-498.

359. Meijerink M, Ferrando ML, Lammers G, Taverne N, Smith HE, Wells JM. Immunomodulatory effects of Streptococcus suis capsule type on human dendritic cell responses, phagocytosis and intracellular survival. PloS one 2012; 7(4): e35849.

360. Hansson GC, Johansson ME. The inner of the two Muc2 mucin-dependent mucus layers in colon is devoid of bacteria. Gut Microbes 2010; 1(1): 51-54.

361. Tanford C, De PK. The unfolding of beta-lactoglobulin at pH 3 by urea, formamide, and other organic substances. The Journal of biological chemistry 1961; 236: 1711-1715.

362. Herskovits TT, Mescanti L. Conformation of Proteins and Polypeptides. Ii. Optical Rotatory Dispersion and Conformation of the Milk Proteins and Other Proteins in Organic Solvents. The Journal of biological chemistry 1965; 240: 639-644.

363. Puchtler H, Waldrop FS, Meloan SN, Terry MS, Conner HM. Methacarn (methanol-Carnoy) fixation. Practical and theoretical considerations. Histochemie Histochemistry Histochimie 1970; 21(2): 97-116.

364. Puchtler H, Waldrop FS, Conner HM, Terry MS. Carnoy fixation: practical and theoretical considerations. Histochemie Histochemistry Histochimie 1968; 16(4): 361-371.

365. Hill RR, Cowley HM, Andremont A. Influence of colonizing micro-flora on the mucin histochemistry of the neonatal mouse colon. Histochem J 1990; 22(2): 102-105.

366. Schwerbrock NM, Makkink MK, van der Sluis M, Buller HA, Einerhand AW, Sartor RB *et al.* Interleukin 10-deficient mice exhibit defective colonic Muc2 synthesis before and after induction of colitis by commensal bacteria. Inflamm Bowel Dis 2004; 10(6): 811-823.

367. Duriancik DM, Hoag KA. The identification and enumeration of dendritic cell populations from individual mouse spleen and Peyer's patches using flow cytometric analysis. Cytometry Part A : the journal of the International Society for Analytical Cytology 2009; 75(11): 951-959.

368. Hamada H, Hiroi T, Nishiyama Y, Takahashi H, Masunaga Y, Hachimura S *et al.* Identification of multiple isolated lymphoid follicles on the antimesenteric wall of the mouse small intestine. J Immunol 2002; 168(1): 57-64.

369. Lorenz RG, Chaplin DD, McDonald KG, McDonough JS, Newberry RD. Isolated lymphoid follicle formation is inducible and dependent upon lymphotoxin-sufficient B lymphocytes, lymphotoxin beta receptor, and TNF receptor I function. J Immunol 2003; 170(11): 5475-5482.

370. Pabst O, Herbrand H, Friedrichsen M, Velaga S, Dorsch M, Berhardt G *et al.* Adaptation of solitary intestinal lymphoid tissue in response to microbiota and chemokine receptor CCR7 signaling. J Immunol 2006; 177(10): 6824-6832.

371. Takahashi N, Vereecke L, Bertrand MJ, Duprez L, Berger SB, Divert T *et al.* RIPK1 ensures intestinal homeostasis by protecting the epithelium against apoptosis. Nature 2014; 513(7516): 95-99.

372. Burger-van Paassen N, Vincent A, Puiman PJ, van der Sluis M, Bouma J, Boehm G *et al.* The regulation of intestinal mucin MUC2 expression by short-chain fatty acids: implications for epithelial protection. The Biochemical journal 2009; 420(2): 211-219.

373. Burger-van Paassen N, Loonen LMP, Witte-Bouma J, Korteland-van Male AM, de Bruijn ACJM, van der Sluis M *et al.* Mucin Muc2 Deficiency and Weaning Influences the Expression of the Innate Defense Genes Reg3β, Reg3γ and Angiogenin-4. PloS one 2012; 7(6): e38798.

374. Amarri S, Benatti F, Callegari ML, Shahkhalili Y, Chauffard F, Rochat F *et al.* Changes of gut microbiota and immune markers during the complementary feeding period in healthy breast-fed infants. Journal of pediatric gastroenterology and nutrition 2006; 42(5): 488-495.

375. Martin HM, Campbell BJ, Hart CA, Mpofu C, Nayar M, Singh R *et al.* Enhanced Escherichia coli adherence and invasion in Crohn's disease and colon cancer. Gastroenterology 2004; 127(1): 80-93.

376. Darfeuille-Michaud A, Boudeau J, Bulois P, Neut C, Glasser AL, Barnich N *et al.* High prevalence of adherent-invasive Escherichia coli associated with ileal mucosa in Crohn's disease. Gastroenterology 2004; 127(2): 412-421.

377. Martinez-Medina M, Aldeguer X, Lopez-Siles M, Gonzalez-Huix F, Lopez-Oliu C, Dahbi G *et al.* Molecular diversity of Escherichia coli in the human gut: new ecological evidence supporting the role of adherent-invasive E. coli (AIEC) in Crohn's disease. Inflammatory bowel diseases 2009; 15(6): 872-882.

378. Baumgart M, Dogan B, Rishniw M, Weitzman G, Bosworth B, Yantiss R *et al.* Culture independent analysis of ileal mucosa reveals a selective increase in invasive Escherichia coli of novel phylogeny relative to depletion of Clostridiales in Crohn's disease involving the ileum. The ISME journal 2007; 1(5): 403-418.

379. Sasaki M, Sitaraman SV, Babbin BA, Gerner-Smidt P, Ribot EM, Garrett N *et al.* Invasive Escherichia coli are a feature of Crohn's disease. Laboratory investigation; a journal of technical methods and pathology 2007; 87(10): 1042-1054.

380. Eaves-Pyles T, Allen CA, Taormina J, Swidsinski A, Tutt CB, Jezek GE *et al.* Escherichia coli isolated from a Crohn's disease patient adheres, invades, and induces inflammatory responses in polarized intestinal epithelial cells. International journal of medical microbiology : IJMM 2008; 298(5-6): 397-409.

381. Smith K, McCoy KD, Macpherson AJ. Use of axenic animals in studying the adaptation of mammals to their commensal intestinal microbiota. Seminars in immunology 2007; 19(2): 59-69.

382. Fagarasan S, Muramatsu M, Suzuki K, Nagaoka H, Hiai H, Honjo T. Critical roles of activation-induced cytidine deaminase in the homeostasis of gut flora. Science 2002; 298(5597): 1424-1427.

383. Bollyky PL, Bice JB, Sweet IR, Falk BA, Gebe JA, Clark AE et al. The toll-like receptor signaling molecule Myd88 contributes to pancreatic beta-cell homeostasis in response to injury. PloS one 2009; 4(4): e5063.

384. Hapfelmeier S, Lawson MAE, Slack E, Kirundi JK, Stoel M, Heikenwalder M et al. Reversible Microbial Colonization of Germ-Free Mice Reveals the Dynamics of IgA Immune Responses. Science 2010; 328(5986): 1705-1709.

385. Linden S, Mahdavi J, Hedenbro J, Boren T, Carlstedt I. Effects of pH on Helicobacter pylori binding to human gastric mucins: identification of binding to non-MUC5AC mucins. The Biochemical journal 2004; 384(Pt 2): 263-270.

386. McGovern DP, Jones MR, Taylor KD, Marciante K, Yan X, Dubinsky M et al. Fucosyltransferase 2 (FUT2) non-secretor status is associated with Crohn's disease. Human molecular genetics 2010; 19(17): 3468-3476.

387. Larsson JM, Karlsson H, Crespo JG, Johansson ME, Eklund L, Sjovall H et al. Altered O-glycosylation profile of MUC2 mucin occurs in active ulcerative colitis and is associated with increased inflammation. Inflammatory bowel diseases 2011; 17(11): 2299-2307.

388. Forni D, Cleynen I, Ferrante M, Cassinotti A, Cagliani R, Ardizzone S et al. ABO histo-blood group might modulate predisposition to Crohn's disease and affect disease behavior. Journal of Crohn's & colitis 2014; 8(6): 489-494.

389. Rausch P, Rehman A, Kunzel S, Hasler R, Ott SJ, Schreiber S et al. Colonic mucosa-associated microbiota is influenced by an interaction of Crohn disease and FUT2 (Secretor) genotype. Proceedings of the National Academy of Sciences of the United States of America 2011; 108(47): 19030-19035.

390. Parmar AS, Alakulppi N, Paavola-Sakki P, Kurppa K, Halme L, Farkkila M et al. Association study of FUT2 (rs601338) with celiac disease and inflammatory bowel disease in the Finnish population. Tissue antigens 2012; 80(6): 488-493.

391. Biagi E, Candela M, Franceschi C, Brigidi P. The aging gut microbiota: new perspectives. Ageing research reviews 2011; 10(4): 428-429.

392. Biagi E, Candela M, Fairweather-Tait S, Franceschi C, Brigidi P. Aging of the human metaorganism: the microbial counterpart. Age 2012; 34(1): 247-267.

393. Corfield AP, Myerscough N, Longman R, Sylvester P, Arul S, Pignatelli M. Mucins and mucosal protection in the gastrointestinal tract: new prospects for mucins in the pathology of gastrointestinal disease. Gut 2000; 47(4): 589-594.

394. Corfield AP. Mucins: a biologically relevant glycan barrier in mucosal protection. Biochimica et biophysica acta 2015; 1850(1): 236-252.

395. Marillier RG, Michels C, Smith EM, Fick LC, Leeto M, Dewals B et al. IL-4/IL-13 independent goblet cell hyperplasia in experimental helminth infections. BMC immunology 2008; 9: 11.

396. Oeser K, Schwartz C, Voehringer D. Conditional IL-4/IL-13-deficient mice reveal a critical role of innate immune cells for protective immunity against gastrointestinal helminths. Mucosal Immunol 2015; 8(3): 672-682.

397. Finkelman FD, Shea-Donohue T, Morris SC, Gildea L, Strait R, Madden KB et al. Interleukin-4- and interleukin-13-mediated host protection against intestinal nematode parasites. Immunological reviews 2004; 201: 139-155.

398. Turner JE, Stockinger B, Helmby H. IL-22 mediates goblet cell hyperplasia and worm expulsion in intestinal helminth infection. PLoS pathogens 2013; 9(10): e1003698.

399. Shimotoyodome A, Meguro S, Hase T, Tokimitsu I, Sakata T. Short chain fatty acids but not lactate or succinate stimulate mucus release in the rat colon. Comparative biochemistry and physiology Part A, Molecular & integrative physiology 2000; 125(4): 525-531.

400. Willemsen LE, Koetsier MA, van Deventer SJ, van Tol EA. Short chain fatty acids stimulate epithelial mucin 2 expression through differential effects on prostaglandin E(1) and E(2) production by intestinal myofibroblasts. Gut 2003; 52(10): 1442-1447.

401. Ferreira TM, Leonel AJ, Melo MA, Santos RR, Cara DC, Cardoso VN et al. Oral supplementation of butyrate reduces mucositis and intestinal permeability associated with 5-Fluorouracil administration. Lipids 2012; 47(7): 669-678.

402. Kaufman RJ, Scheuner D, Schroder M, Shen X, Lee K, Liu CY *et al.* The unfolded protein response in nutrient sensing and differentiation. Nat Rev Mol Cell Biol 2002; 3(6): 411-421.

403. Ron D. Translational control in the endoplasmic reticulum stress response. J Clin Invest 2002; 110(10): 1383-1388.

404. Ellgaard L, Helenius A. Quality control in the endoplasmic reticulum. Nat Rev Mol Cell Biol 2003; 4(3): 181-191.

405. Fonseca SG, Burcin M, Gromada J, Urano F. Endoplasmic reticulum stress in beta-cells and development of diabetes. Current opinion in pharmacology 2009; 9(6): 763-770.

Summary

The use of a multi-disciplinary approach including trancriptomics, microbiota profiling and histology and the use of different mice model such as *Muc2*$Muc2^{-/-}$, $Ercc1^{-/\Delta7}$ and naturally aged C57BL/6 mice, gave insights into the important role played by the mucus in the maintenance of the intestinal barrier and an increased understanding of the effects of barrier dysfunction on microbiota and intestinal physiology.

In Chapter 2, we investigated the effects of the absence of secreted mucus on the small intestinal homeostasis in a MUC2-deficient mouse model. Here we performed transcriptomics, histology, and 16S microbiota profiling on ileal samples from wild-type (WT), $Muc2^{-/-}$, and $Muc2^{+/-}$ mice at 2, 4, and 8 weeks after birth. There were no apparent signs of signs of pathology in the ileum of $Muc2^{-/-}$, although the length of the villi was longer than in WT mice and bacteria were frequently see in contact with the epithelium. Gene set enrichment analysis revealed a down-regulation of TLR, immune, and chemokine signalling pathways compared to WT mice. The predicted effects of enhanced IL-22 signalling were identified in the $Muc2^{-/-}$ transcriptome, as the up-regulation of mucosal defence genes, including *Fut2*, *Reg3β*, *Reg3γ*, *Relmb* and the Defensin *Defb46*. The increased villus length in $Muc2^{-/-}$ mice relative to WT mice was explained by the IL-22 regulator effects on epithelial cell proliferation, altered expression of mitosis and cell cycle control pathways. These findings highlight a role for the IL-22-STAT3 pathway in maintaining ileal homeostasis when the mucus barrier is compromised and its potential as a target for novel therapeutic strategies in IBD.

In Chapter 3, we investigated the effects of absence of secreted mucus (also partial absence) on the colonic homeostasis and microbiota establishment. We took advantage of the $Muc2^{-/-}$ mouse experimental model of colitis, which provides an opportunity to identify microbiota changes and host gene expression before and after the onset of colitis. As in chapter 2, we also performed transcriptomics, histology, and 16S microbiota profiling on colon samples from WT, $Muc2^{-/-}$, and $Muc2^{+/-}$ mice at 2, 4, and 8 weeks after birth. We showed that $Muc2^{-/-}$ mice developed colitis in proximal colon after weaning, resulting in inflammatory and adaptive immune responses, and expression of genes associated with human IBD. $Muc2^{+/-}$ mice did not develop colitis, but produced a thinner mucus layer. The transcriptome of $Muc2^{-/-}$ and $Muc2^{+/-}$ mice revealed differential expression of genes participating in mucosal stress responses and exacerbation of a transient inflammatory state around the time of weaning. At all ages microbiota composition discriminated the groups of mice according to their genotype. Specific bacterial clusters correlated with altered gene expression responses to stress and bacteria, prior to colitis development, including colitogenic members of the genus Bacteroides. The abundance of Bacteroides pathobionts increased prior to histological signs of pathology, suggesting they may play a role in triggering the development of colitis.

In Chapter 4, we investigated effects of ageing on intestinal physiology, including intestinal morphology, mucus barrier properties and bacterial compartmentalization. The aim was to gain a better understanding of the effects of age-related differences on intestinal homeostatic mechanisms and barrier functions, and the impact on diversity and composition of microbiota in the ileum and the colon. We observed in ageing mice an impairment of the intestinal mucus barrier function, associated with bacterial contact with epithelium.

We showed that ageing was associated with increased apoptosis of goblet cells and reduced mucosal thickness in the colon compared to WT mice. Consequently old mice had increased contact between the epithelium and microbiota associated with chronic low-grade mucosal inflammation and a dysbalanced microbiota, all of which are implicated in the pathology of several chronic disorders. Aged mice showed marked changes in intestinal morphology compared to young adult mice. The colonic mucosa was thicker with more immune cell infiltration than in younger mice. Furthermore, the mucus layer was reduced about 6-fold relative to young mice, and more easily penetrable by luminal bacteria. Transcriptomics data indicate a significant down-regulation of innate and adaptive immunity in small and large intestine of old mice. Microbiomics data show a significant decrease in *Akkermansia muciniphilia* and *Lactobacillus gasseri* in old mice.

The deterioration of the mucus barrier was also observed in mice of different gender as well female mice ovariectomized at 15 months (**Chapter 5**) with some notable gender differences. In old females and ovariectomized females the inner mucus layer in the colon was thicker than in old male mice. However, in mice of both genders, the mucus barrier failed to compartmentalize microbiota to the lumen and bacteria were seen in contact with the epithelium.

In Chapter 6, we investigated whether the supplementation of mice with candidate probiotics would ameliorate or exacerbate the mucosal barrier changes observed in Chapter 5. *L. plantarum* WCFS1, *L. casei* BL23, *B. breve* DSM20213 were administered to fast-aging *Ercc1*$^{-/\Delta 7}$ mice by oral gavage over a ten weeks period, respectively.

Supplementation with *B. breve* exacerbated the age-related decline of gut tissue and mucus integrity whereas supplementation with *L. plantarum* ameliorated these effects. In contrast *L. casei* supplementation, had no visible effects on the mucus barrier, but increased inflammatory immune cells and IL-17A production in the spleen. Gut microbiota composition only slightly shifted upon bacterial supplementation, whereas analysis of gene expression corroborated histological findings. We concluded that the *Ercc1*$^{-/\Delta 7}$ model can be used to study the effect of long-term probiotic interventions on ageing. Our data provide an example of how bacterial supplementation can restore age-related decline in intestinal barrier, and highlights the caution needed in the selection of candidate probiotic strains for supplementation to ageing individuals.

In chapter 7, we investigated mucus thickness and permeability throughout the mouse intestinal tract including the Peyer's Patches (PP) in conventional, germ-free and gnotobiotic mice. Sections of the ileal and colonic tissue were fixed or cryopreserved for histology and immunofluorescent histochemistry. A new technique was developed to assess mucus permeability in the small intestine and colon.

This study revealed that the mucus thickness is dependent on the presence of microbiota, as the germ-free mice have a thinner mucus layer than conventional mice. The mucus layer is also thin (or absent) and easily penetrable on top of the dome of PPs, due to the lack of goblet cells in the epithelium of Peyer's patches. *Lactobacillus plantarum* was administered to germ-free mice. Lactobacilli were taken up in the organized lymphoid structures of the small intestine and transported within immune cells to the mesenteric lymph nodes. Sampling of bacteria by PPs is facilitated by the relatively low abundance of goblet cells in the follicular-associated epithelium covering the dome of the PP and a lack of secreted mucus covering the dome.

Chapter 8 summarizes and discusses the key results of the thesis in the context of the wider literature and possible directions for future research.

Keywords: MUC2 knockout mice model, mucus, chronic inflammatory disease, ageing, gender, microbiota, transcriptomics, (immune-) histology

Samenvatting

Door het onderzoek beschreven in dit proefschrift is inzicht verkregen in de rol van mucus in het behoud van de barrièrefunctie van de darm en de relatie van mucus met (dys)functie van microbiota en de darmfysiologie. Dit onderzoek is uitgevoerd door middel van een multidisciplinaire benadering waarin transcriptoom-analyse, microbiota-identificatie en histologie werden gecombineerd met proefdieronderzoek waarin diermodellen zoals de *Muc2* knock-out muis (*Muc2*$^{-/-}$), de snel verouderende muis *Ercc1*$^{-/\Delta7}$ en op natuurlijke wijze verouderde muizen werden gebruikt.

In hoofdstuk 2, is onderzocht wat de afwezigheid van mucus in de darm betekent voor de darmhomeostase in Muc2 deficiënte muizen. We hebben transcriptoom-onderzoek, histologie, en 16S microbiota profilering gebruikt en toegepast op weefsel van het ileum van wild-type, *Muc2*$^{-/-}$ en *Muc2*$^{+/-}$ muizen op 2, 4, en 8 weken na geboorte. Er waren geen zichtbare pathologische afwijkingen in het ileum van de *Muc2*$^{-/-}$ muizen. Er was slechts sprake van iets enigszins verlengde villi en er waren vaker bacteriën te vinden die in contact waren met het epitheel. Analysen van de verrijking in genexpressie toonde een verlaagde expressie aan van TLR, immuun, en chemokine signalerings-pathways wanneer de genepressie vergeleken werd met de wild-type muizen. Een voorspelde verhoging van IL-22 signalering werd gevonden in het *Muc2*$^{-/-}$ transcriptoom tezamen met toegenomen expressie van mucosale verdedigingsgenen zoals *Fut2*, *Reg3β*, *Reg3γ*, *Relmb* en het defensine *Defb46*. De langere villus-lengte in *Muc2*$^{-/-}$ dan in wild-type muizen is geïnterpreteerd als een gevolg van de door IL-22 gereguleerde effecten op epitheel-proliferatie, veranderde expressie van genen die mitose- en celcyclus controleren. De bevindingen suggereren een rol voor het IL-22-STAT3 regelatiemechanisme in behoud van ileum homeostase in de afwezigheid van mucus. Ook lijken onze resultaten een rol voor dit IL-22-STAT3 regulatiemechanismete suggereren als target voor nieuwe therapeutische interventie strategieën voor chronische inflammatoire darmziekten.

In hoofdstuk 3, bestudeerden we de effecten van afwezigheid van mucus (geheel en partieel) op homeostase in de dikke darm. We hebben de *Muc2*$^{-/-}$ muis gebruikt, omdat deze muis van nature colitis ontwikkelt. Dit gaf ons de unieke kans om microbiota- en genen-veranderingen te bestuderen voor en na het ontstaan van colitis. Net als in hoofdstuk 2, hebben we transcriptoom-onderzoek, histologie, en 16S microbiota profilering gebruikt op colonweefsel van wild-type, *Muc2*$^{-/-}$ en *Muc2*$^{+/-}$ muizen op 2, 4, en 8 weken na geboorte. We hebben aangetoond dat *Muc2*$^{-/-}$ muizen direct na geboorte tekenen van colitis ontwikkelen in de proximale colon, dat resulteert in reactie van zowel de aangeboren als adaptieve immuunrespons. Ook werd expressie van genen gevonden die overeenkomsten hebben met humane chronische inflammatoire darmziekten. *Muc2*$^{+/-}$ ontwikkelde geen colitis, maar produceerde een dunnere laag mucus dan wild-type muizen. Het transcriptoom van *Muc2*$^{-/-}$ en *Muc2*$^{+/-}$ muizen vertoonde verschillende

expressieprofielen van genen die geassocieerd zijn met mucosale stress responsen en een matige ontsteking, die reeds ontstaat direct na geboorte. Op alle leeftijden vertoonde de microbiota stereotype verschillen die samenhingen met het genotype van de muizen. Specifieke veranderingen in bacterieclusters correleerden met veranderde genexpressie en stress. Er waren duidelijk, vlak voor ontwikkeling van colitis, bacteriën aanwezig in de colon, die geassocieerd worden met colitis-ontwikkeling zoals Bacteroides. Bacteroides pathobioten waren waarneembaar vlak voordat histologisch colitis kon worden vastgesteld, dat er op wijst dat deze bacteriën een rol kunnen spelen bij de ontwikkeling van colitis.

In hoofdstuk 4, onderzochten we het effect van veroudering op darmfysiologie en -morfologie waarbij eigenschappen van de mucusbarrière en bacteriële compartmentalisatie een hoofdrol speelden. Het doel was om meer inzicht te krijgen in de effecten van veroudering op darmhomeostase en barrièrefunctie, en de impact van veroudering op diversiteit van darmbacteriën in het ileum en colon. We hebben in verouderde muizen een verstoring gevonden van de functie van de darmmucus-barrière, die resulteerde in contact van de darmbacteriën met het epitheel. Verder toonden we aan dat veroudering geassocieerd is met toegenomen apoptose van mucus-producerende cellen en een verminderde dikte van de mucus in het colon. Het gevolg was een toegenomen contact van darmbacteriën met het epitheel met een chronische milde ontsteking tot gevolg. Dit is een beeld dat terug te vinden is in veel menselijke pathologische aandoeningen.

Verouderde muizen hadden ook een andere darmmorfologie. De darmwand was dikker met veel meer immuuncel infiltratie dan in jonge muizen. De mucuslaag was ongeveer zesmaal dunner dan in jonge muizen en meer in verhoogde mate gepenetreerd met bacteriën. Transcriptoom data suggereren een significante verlaging van zowel het aangeboren als adaptieve immuunsysteem in zowel de dunne als dikke darm. De bacteriën *Akkermansia muciniphilia* en *Lactobacillus gasseri* waren verlaagd in oude muizen.

Deze afname in mucus-barrière werd ook waargenomen in muizen van beide geslachten en in vrouwelijke muizen die ovariectomie ondergingen op de leeftijd van 15 maanden (**Hoofdstuk 5**), hoewel er verschillen waren tussen mannelijke en vrouwelijk muizen. In oude vrouwtjes muizen en vrouwtjes die ovariectomie ondergingen was de mucuslaag in het colon dikker dan in oude mannetjes muizen. Niettemin was de mucuslaag in muizen van beide geslachten niet in staat om de microbiota te compartimentaliseren tot het lumen, en werden er bacteriën gezien in direct contact met het colonepitheel.

In **Hoofdstuk 6**, onderzochten we of het toedienen van kandidaat-probiotica aan muizen de verschillen in mucus-barrière, zoals beschreven in hoofdstuk 5, zouden veranderen. *L. plantarum* WCFS1, *L. casei* BL23, en *B. breve* DSM20213 werden toegediend aan de snel

verouderende *Ercc1*^{-/Δ7} muizen door middel gedwongen voeding gedurende tien weken. Toediening van *B. breve* vererergde de leeftijd-gerelateerde afname in de integriteit van de darmwand en mucus, terwijl toediening van *L. plantarum* deze effecten juist verlichtte. Toediening van *L. casei* had geen zichtbaar effect op de mucus-barrière, maar verhoogde wel de productie van ontstekingscellen en IL-17 in de milt. De microbiota van de darm vertoonde slechts kleine afwijkingen na bacterie-toediening, terwijl de analyse van de genexpressie in de darm de histologische bevindingen ondersteunde. We concludeerden dat het *Ercc1*^{-/Δ7} model bruikbaar is om de effecten van langdurige probiotica toediening op veroudering te bestuderen. Onze data geven een voorbeeld hoe de toediening van bacteriën de leeftijd-gerelateerde afname in de functie van de darm-barrière kan bevorderen, maar geven ook aanleiding om voorzichtig om te gaan met de selectie van kandidaat probiotica in het ouder wordende individu.

In **Hoofdstuk 7**, hebben we de dikte en permeabiliteit van de mucuslaag onderzocht, inclusief de Peyerse platen (PP), in conventionele, kiemvrije en gnotobiotisch muizen. Coupes van ileum- en colonweefsel werden gefixeerd of ingevroren voor histologie en immunofluorescente histochemie. Een nieuwe techniek werd ontwikkeld om de permeabiliteit van de mucuslaag te kunnen bepalen in dunne en dikke darm. Deze studie liet zien dat de dikte van de mucuslaag afhankelijk is van de aanwezigheid van microbiota, want kiemvrije muizen hebben een dunnere mucuslaag dan conventionele muizen. De mucuslaag op het oppervlakte van de PP is dun (of afwezig) en gemakkelijk doordringbaar, door de afwezigheid van mucus-producerende cellen in het epitheel van de PP. *Lactobacillus plantarum* werd toegediend aan kiemvrije muizen. Lactobacillen werden opgenomen in de georganiseerde lymfoïde structuren van de dunne darm en binnenin immuuncellen getransporteerd naar de mesenterische lymfeknopen. De opname van bacteriën in de PP wordt vergemakkelijkt door het kleine aantal mucus-producerende cellen in het follikel-epitheel van de PP en het ontbreken van een bedekkende mucuslaag.

Hoofdstuk 8 geeft een samenvatting en bediscussieerd de belangrijkste resultaten, zoals gepresenteerd in dit proefschrift, in het licht van recente literatuur en geeft mogelijke richtingen aan voor vervolgonderzoek.

Trefwoorden: Muc2 knock-out muis model, chronische darmontsteking, mucus, veroudering, sexe, microbiota, transcriptoom-analyse, (immuun-) histologie

Co-author affiliations

Linda MP Loonen,[1,2] Peng Lu,[8,9] Floor Hugenholtz,[1,4] Clara Belzer,[1,4] Ellen H Stolte,[2] Mark V Boekschoten,[1,3] Peter van Baarlen,[2] Michiel Kleerebezem,[1,2,5] Paul de Vos,[1,6] Jan Dekker,[1] Ingrid B Renes,[7,8] Jerry M Wells[1,2], Adriaan A Van Beek[1,10], Katrine Graversen[2], Myrte Huijskes[2], Huub FJ Savelkoul[1,10], Marijke M Faas[1,6], Marlies Elderman[1,6], Ben Meijer[10], Joanne Hoogerland[10], Jan J.H. Hoeijmakers[11], Pieter JM Leenen[12], Rudi W Hendriks[13], Oriana Rossi[2], Wayne Young[14], Nicole Roy[14], Jasper Kamphuis[2], Raymon van Dijk[2]

[1]Top Institute Food and Nutrition, Wageningen, the Netherlands
[2]Host-Microbe Interactomics Group, Animal Sciences Department, Wageningen University and Research Center, Wageningen, the Netherlands
[3]Division of Human Nutrition, Wageningen University and Research Center, Wageningen, the Netherlands
[4]Laboratory of Microbiology, Wageningen University and Research Center, the Netherlands
[5]NIZO food research, Ede, the Netherlands
[6]University Medical Center of Groningen, Groningen, the Netherlands
[7]Nutricia Research, Utrecht, the Netherlands
[8]Department of Pediatrics, Erasmus MC-Sophia, Rotterdam, the Netherlands
[9]Department of Pediatrics, Academic Medical Center, Amsterdam, the Netherlands
[10]Cell Biology and Immunology Group, Wageningen University and Research Center, Wageningen, the Netherlands
[11]Department of Genetics, Erasmus University Medical Center, Rotterdam, the Netherlands
[12]Department of Immunology, Erasmus University Medical Center, Rotterdam, the Netherlands
[13]Department of Pulmonary Medicine, Erasmus University Medical Center, Rotterdam, the Netherlands
[14]Food Nutrition and Health, AgResearch Grasslands, Palmerston North, New Zealand

Acknowledgements

When I decided to come to the Netherlands for a PhD, I had to leave behind me my life in France, my friends and my family. However, since the beginning of my PhD many people became important to making my life in the Netherlands the best possible, despite the weather. Now, as I have enjoyed these past years, I would like to thank them sincerely.

I was lucky to share my working hours with excellent professionals. They helped me stay focussed and enthusiastic throughout my PhD.

First of all, I would like to thank **Jerry Wells**, my promotor. **Jerry**, I thank you for giving me the opportunity to perform my PhD in HMI. You should know that your help and your enthusiasm were essential to me throughout the PhD. I would like to thank you especially for your support and encouragement during the last stretch, when you worked by my side to finish the reading version. You spent evenings and days to read, rewrite and give input on the manuscripts and so I would like to express my sincere gratitude to you. I really enjoyed working with you and hope we will have the opportunity to work together again in the future. **Jan Dekker**, my co-promotor. **Jan**, your considerable knowledge in mucins and gut physiology and your creative ideas have been of great value to me. Thank you for your helpful advice throughout the PhD and your support with revising the manuscripts. **Paul de Vos**, my co-promotor. **Paul**, I would like to thank you for your advice help and support during the PhD and during the writing of the manuscripts and the thesis. Your enthusiasm and leadership helped me to overcome many difficulties throughout my PhD. I am grateful to you also for welcoming me in the TIFN GH002 project, and giving me the chance to attend international conferences where I made valuable contacts to widen my network.

I would like to warmly thank the GH002 team from TIFN, especially **Marlies**, **Elke** and **Adriaan.** It has been a pleasure to work with all of you and I am proud of our collaboration in the past 4 years. Hopefully, we will stay in contact for new collaborations in our respective postdoc projects. **Adriaan,** with whom I spent many mornings sectioning mice at the CKP and collaborated with for the "Ercc1 experiments". I wish you all the best with finishing up your thesis and your future in science. You are a great scientist, I am sure you will succeed in everything you undertake. **Marlies**, thanks for the fun we had at work and during conferences! Good luck with your thesis! **Elke**, it was fun to work with you the first two years. I wish you all the best in your new position.

All my wonderful HMI colleagues, I would like to thank you for the nice times on and off work. **Michiel**, **Peter**, **Annick,** thank you for the constructive discussions we had, your advice and your input in the different studies I performed. **Anja**, **Nico**, **Ellen**, thank you for your technical help; **Ellen**, thanks for all the fun we had ice skating, roller blading and squashing... ☺. It help me a lot releasing my stress. **Anja** in histology and **Ellen** in molecular biology. **Marjolein**, **Linda**, **Rogier**, **Aga**, **Nirupama**, **Soumya**, **Marcela**, **Edo**, **Simon**, **Jori**, and **Nadya**, thank you

for all the fun we shared ! **Loes**, thanks for your help with all bureaucratic affairs, and all the fun we had in coffee breaks. **Oriana** and **Laura**, eventhough you left HMI, we have shared nice moments together at the beginning of my PhD. Thank you for that!

To my office mates, I would like to say that it was fun to share an office with you. **Linda** and **Rogier**, we had a good time together for two years. I miss our conversations, did I talk too much…? ☺ **Linda**, thank you for working with me on the *Muc2*$^{-/-}$ papers. At the end we managed to write a good piece of work. It was fun to be your office mate for 2 years. Besides, I enjoyed going the States with you. We had a lot of fun at Skistone. Hopefully, we will be able to go there again. I wish you the best for the end of your postdoc, and hope we will have the opportunity to stay in contact in the future. **Rogier** (and **Antje**), I wish you and your son **Lasse** all the best for the future. **Edo**, **Marcela** and **Jori**, it was fun to share the second office with you, to complain about the weather, to plan our dinners…☺. Thanks for your support in the last stage of the PhD! **Edo**, good luck with finishing up your PhD and with your defence! **Marcelita**, Oh My God…. ☺, I made it. Thank you so much for bringing entertainment to our office. It was fun to share our frustrations. I wish you all the best in finishing up your PhD, and hope you can get rid of the BD Pathway ASAP…;). **Jori**, good luck with your PhD!

My colleagues from CBI and EZO groups, thank you for all the nice times we had during PhD activities in Winterberg and Belgium. It was fun to have coffee breaks and drink together. I wish you all the best for the future! I would also like to thank the people working at the Animal Facility and particularly **Bert** and **Rene** for their precious help during sectioning days. Thank you!

Of course, a big thank you to all the students who helped me; **Raymon**, **Jasper**, **Katrine** and **Myrte**, you worked hard to get the work done and you did it very well. I wish to all of you the best for the future. **Raymon**, I hope you will find a job soon. **Jasper**, I wish you the best for your PhD thesis at INRA in Toulouse. I am sure you will succeed! **Katrine**, it was a great pleasure to work with you. Please, keep your enthusiasm, and hopefully we will stay in contact for future collaborative work. **Myrte**, I wish you the best for your internship. You worked very hard during your MSc in HMI, so I'm sure you will succeed in your studies and future job.

And then, there is the people with whom I did not work, but were there to be a second family. You made sure I had fun, laughed, played, ate, drank and will hopefully have an epic PhD party.

Thibaut and **Linda,** here I would like to thank you for accepting the difficult task of being my paranymphs. **Linda**, it made sense to ask you to be my paranymph, as our friendship is strong. You have always been there to support me along the PhD and during experiments. We had great fun in the dream team…☺. Dank je wel! **Thibaut**, tu es un super ami, c'est pour cela que je t'ai demander d'être mon paranymph. Les bons diners français, soirées ainsi que nos vacances au ski seront inoubliables ! Merci pour tout ! I would like to say many thanks

to the "Wolfpack": **Danilo**, **Alberto**, **Edo**, **Domenico**. Thanks for all the FIFA nights, for all the nice dinners eating pasta Amatriciana, beers and having fun together...☺. I miss you, but I am happy that our friendship still stands, despite most of you leading your lives outside of Wageningen. My dear friends, **Thibaut**, **Alexia**, **Carla**, **Valentina A.**, **Valentina B.**, **Valentina M.**, **Walter**, **Raffa**, **Niccolò**, **Alessandro**, **Lavinia, Francesco**, **Erika**, **Costas**, **Sourya**, **Arie**, **Martin**, **Eva** and **Elsa**, I would like to thank you for the dinners, beers, festivals and many parties together. I owe special words to **Alexia**: Cela va me manquer nos cafés à nous plaindre de tout! J'espère que ton PhD va continuer à bien se dérouler, je te fais confiance pour cela. J'espère que nous resterons en contact par la suite pour ce faire une petite sortie ski ou autre... ☺. **Rebeca**, **Daniel**, **Leo**, **Zonia, Caro** and **Jose**, I have not known you long, but I am happy to have met you. All the time we spend together helped me feel better during a tough writing period. Muchas gracias!

Amalia, you entered in my life at the complete end of the PhD. Poor you... You had to support my stress during the writing and the final stage of my thesis. Thank you very much for your support every day of the last months! You were inspiring me in the writing and your help has been very precious. I also wish you all the best in your PhD, and I will try to be as supportive as you for your PhD.

Although I have built a good life here, I have not and will not forget the part of me that remains in France. For these people gave me the foundations to be successful as a PhD.

Mes plus sincères remerciements vont à mes parents. **Papa** et **maman**, tout au long de mon cursus, vous m'avez toujours soutenu, encouragé et aidé. Vous avez su me donner toutes les chances pour réussir. Ce travaille représente l'aboutissement de vos efforts ainsi que l'expression de ma plus affectueuse gratitude. Je vous aime fort !

Christophe, mon cher frère, merci pour ton soutien sans limite depuis toutes ses années ! Je te souhaite le meilleur pour ton stage de fin d'études d'ingénieurs et pour ton futur avenir professionnel. Tu peux compter sur moi pour te supporter dans tes futures échéances.

Ma chère **mamie Nanou**, je te remercie du fond du cœur pour tout ce que tu as fait pour moi, ton soutien sans relâche pendant les bons et les mauvais moments. Cette thèse reflète ma reconnaissance et mon amour. J'exprime ma plus profonde gratitude à ma famille qui m'a soutenue pendant toutes ces années. Je voudrais remercier en particulier tontons **Frédéric**, **Pierre** et **Gabriel** pour vos encouragements sans faille. Merci pour tout !Une pensée à toutes les personnes à qui j'aurais voulu montré ma réussite et qui ne sont plus de ce monde : papi **Doro**, tonton **Laurent**, papi **Mario**, mamie **Yvonne**. Cette thèse vous est aussi dédiée. A toute ma famille, que ce travail représente l'accomplissement de tous vos sacrifices et le reflet de mon immense reconnaissance et amour.

I close this book with my deep gratitude for the kindness you have all shown me.

Bruno

Curriculum vitae

Bruno Sovran was born on May 18, 1987 in Toulouse, France. He grew up in a small city called Colomiers where he graduated from high school Lycée Internationnal Victor Hugo, in 2005. He continued his education at the Medical School of Toulouse in 2006 and 2007. In 2007, he joined the Engineer School of Purpan, Toulouse, where graduated Bachelor in Life Sciences in 2009 and *Cum Laude* Master of Science in Life Sciences in 2011. As part of his training he performed an internship at Institut National de la Recherche agronomique (INRA), in the Neurogastroenterology and Nutrition group, in 2009. He worked on understanding the effect of Creeping Fat secretions in colonic paracellular permeability in a colitis mice model, under the supervision of Dr Isabelle Olivier, Dr Vassilia Theodorou and Dr Hélène Eutamène. Also at INRA he followed a second internship on understanding the implication of the cannabinoid receptor-2 in the visceral hyposensitity response induced by PAR-4 activation, under the supervision of Dr Hélène Eutamène. Bruno performed his Master thesis at Nestlé Research Centre in Lausanne, Switzerland, in 2010. He studied the defensin signaling pathways in intestinal epithelial cells upon probiotic treatment, under the supervision of Dr Valérie Petit, Dr Clara Garcia and Dr Gabriela Bergonzelli.

From 2011, Bruno has completed his PhD thesis at the laboratory of Host-Microbe Interactomics of Wageningen University, under the supervision of Professor Jerry M. Wells. The findings of his PhD research can be found in this thesis, entitled "Mucus and Gut Barrier in Health and Disease". This PhD project was a work-package within one of the projects of the Top Institute of Food and Nutrition, Wageningen, the Netherlands (project GH002).

List of publications

Sovran B[*]., Loonen L.M.P[*]., Lu P., Hugenholtz F., Stolte EH., Belzer c., Kleerebezem M., Boekschoten M.V., van Baarlen P., de Vos P., Dekker J., Renes I., Wells J.M., (2015). "IL-22-STAT3 pathway plays a key role in the maintenance of ileal homeostasis in mice lacking secreted mucus barrier." *Inflamm Bowel Dis* 21(3): 531-542.

Sovran B., Lu P., Loonen L.M.P., Hugenholtz F., Stolte EH., Belzer C., Kleerebezem M., Boekschoten M.V., van Baarlen P., de Vos P., Dekker J., Renes I., Wells J.M., (2015). "Identification of commensal species positively correlated with early stress responses to a compromised mucus barrier". *Under review in Inflammatory Bowel Disease*.

Sovran B., Hugenholtz F., Elderman M., Van Beek A.A., Graversen K., Huijskes M., Boekschoten M.V., Kleerebezem M., Savelkoul H.F.J., De Vos P., Dekker J. and Wells J.M., Intestinal barrier impairment in ageing mice predispose to "inflammageing" in the intestinal mucosa. *Submitted*.

Sovran B., Elderman M., Hugenholtz F., Graversen K., Huijskes M., Boekschoten M.V., De Vos P., Dekker J. and Wells J.M., Sexually dimorphic characteristics of the small and large intestine of ageing mice. *Submitted*.

Van Beek A.A **., Sovran B**., Hugenholtz F., Meijer B., Hoogerland J., Boekschoten M.V., Hoeijmarkers J.J.M., De Vos P., Wells J.M., Leenen P.J.M., Hendriks R.W., and Savelkoul H.F.J., Supplementation with *L. plantarum* WCFS1 reverts age-related decline of mucus barrier in fast ageing *Ercc1*[-/Δ7] mice. *Manuscript in preparation*.

Sovran B., Rossi O., Young W., Taverne-Thiele A., Kamphuis J., van Dijk R., de Vos P., Roy N., Dekker J., and Wells J.M., Structure and permeability of mucus in the mouse intestine and its influence on bacterial localization and immune sampling. *Submitted*.

Olivier I., Leveque M., Sovran B., et al., Dual opposite effects of creeping fat on gut barrier function and epithelial cell restitution according to the intestinal inflammatory status. *Submitted*.

* Equally contributed

Overview of completed training activities

Discipline specific activities

<u>Courses</u>

Genetics and physiology of food-associated micro-organisms	2013
Advanced visualization, integration and biological interpretation of ~omics data	2014

<u>Meetings</u>

Keystone Conference, Keystone, Colorado, USA	2012
Cross-Talk Meeting, Paris, France (**Poster Presentation**)	2012
EMIG Conference, Dublin, Ireland	2012
14th Gut Day, Leuven, Belgium (**Poster Presentation**)	2012
Digestive Disease Week 2013, Orlando, USA (**Poster Presentation**)	2013
TIFN annual conference, Amsterdam, the Netherlands (**Poster Presentation**)	2013
Microbiota, Probiota and Host, Seeon, Germany (**Oral Presentation**)	2013
12th International Workshop on Carcinoma-associated Mucins, Cambridge, UK (**Oral Presentation**)	2013
15th Gut Day, Groningen, the Netherlands	2013
Microbiota, Probiota and Host, Seeon, Germany (**Oral Presentation, 1st Price**)	2014
The 9th International Conference of Genomics, Shenzen, China (**Invited Speaker**)	2014
16th Gut Day, Amsterdam, the Netherlands (**Oral Presentation**)	2014
Keystone Conference, Keystone, Colorado, USA (**Poster Presentations**)	2015

General courses

Course on Laboratory Animal Science	2011
Techniques for Writing and Presenting a Scientific Paper	2012
Philosophy and Ethics of Food Science and Technology	2013
TIFN IP-course	2013
Reviewing a scientific paper	2014
Career Perspectives	2015

Optional activities

Preparation of PhD proposal	2011
HMI lab meetings	2011-2015
TIFN research meetings	2011-2015
TIFN expert meetings	2011-2015